

SCANDIUM QUANTIFICATION IN SELECTED INORGANIC AND ORGANOMETALLIC COMPOUNDS

by

Hlengiwe Thandekile Mnculwane

A thesis submitted in fulfilment of the requirements for the degree of
Magister Scientiae

In the Faculty of Natural & Agricultural Sciences
Department of Chemistry
University of the Free State
Bloemfontein

Supervisor: Prof. W. Purcell

Co-Supervisor: Dr. J. Venter

January 2016

Declaration by candidate

I hereby declare that the dissertation submitted here for the degree of Master in Science at the University of the Free State is my own original work and has not been previously submitted for academic examination towards any qualification at any other University. I further declare that all the sources that I have used or quoted have been indicated and acknowledged by means of complete references.

Signature.....

Date.....

Hlengiwe Thandekile Mnculwane

Acknowledgements

I hereby wish to thank God for being with me up to thus far and each and every person who contributed, directly or indirectly, to the completion and success of this study:

Firstly, I am indebted to my supervisor, Prof. W Purcell for giving me the opportunity to further my academic career by accepting me as part of the Analytical chemistry group and for the guidance and patience throughout my study.

To my Co-supervisor, Dr. J. Venter, thank you so much for the review of my work and for the recommendations and suggestions which greatly improved my thesis writing.

To my colleagues, Dr. M. Nete, Dr. T. Chiweshe, S. Xaba, D. Nhlapho, M. Zidge, Dr S. Kumar, G. Malefo, Q. Vilakazi and L. Ntoi, I would like to say thank you very much for being so helpful and for providing such a friendly environment that was also conducive to carry out my project, and to P. Nkoe thank you “skeem” stay cool.

To all my friends, I want to thank you for the love, support and encouragement throughout my studies.

I also wish to express my gratitude to my parents (Mrs T.B. Mnculwane and Mr J.J. Mnculwane), my siblings (Jabulisile, Nonhlanhla, Hlangabeza, Phendukani, Xolile and Sphephelo), and to Mnculwane family as a whole, thank you for the love and support from the onset of my studies.

Special thanks to MINTEK for the financial assistance, you are highly acknowledged.

Hlengiwe Thandekile Mnculwane

TABLE OF CONTENTS

LIST OF FIGURES	viii
LIST OF TABLESxii
LIST OF ABBREVIATIONSxvii
KEYWORDS.....	.xix
Chapter 1: Motivation of the study	1
1.1 Background of scandium	1
1.2 Motivation of this study	7
1.3 Aim of the study	8
Chapter 2: Introduction.....	9
2.1 Introduction	9
2.2 Discovery of scandium.....	9
2.3 Natural occurrence of scandium	11
2.4 Scandium production, market and beneficiation	19
2.4.1 Scandium production.....	19
2.4.2 Scandium market	26
2.4.2 Scandium beneficiation	28
2.5 Applications and uses of scandium.....	32
2.6 Physical and chemical properties	35
2.6.1 Scandium crystallographic structure	37
2.7 Scandium chemistry.....	38
2.7.1 Scandium halides	39
2.7.2 Scandium oxide.....	40
2.7.3 Nitrate and sulphate chemistry of scandium.....	41
2.7.4 Coordination chemistry.....	41
2.8 Conclusion	43
Chapter 3: Analytical techniques for dissolution, quantification and identification of scandium: Literature survey.....	44
3.1 Introduction	44

Table of Contents

3.2 Dissolution and recovery of scandium in different scandium-bearing minerals.....	45
3.2.1 Introduction	45
3.2.2 Conclusion	52
3.3 Analytical techniques for determination of scandium	53
3.3.1 Introduction	53
3.3.2 Spectrophotometric techniques.....	54
3.3.2.1 Ultra Violet-Visible (UV-Vis) spectroscopy.....	54
3.3.3 Inductively coupled plasma techniques.....	60
3.3.3.1 Inductively coupled plasma-optical emission spectrometry	60
3.3.3.2 Inductively coupled plasma-mass spectrometry	65
3.3.4 Atomic absorption spectroscopy and neutron activation analyses	68
3.3.5 Conclusion	69
3.4 Characterization of scandium complexes	70
3.4.1 Infrared (IR).....	70
3.4.2 CHNS micro-elemental analysis.....	75
3.5 Conclusion.....	76
Chapter 4: Selection of analytical techniques	78
4.1 Introduction	78
4.2 Sample dissolution methods.....	78
4.2.1 Open flask acid digestion	79
4.2.2 Microwave-assisted digestion	81
4.2.3 Flux fusion dissolution	84
4.3 Characterization techniques	86
4.3.1 Infrared (IR) spectroscopy.....	87
4.3.2 CHNS micro-analyser.....	89
4.3.3 Melting point determination	91
4.3.4 X-ray crystallography.....	92
4.4 Quantification techniques.....	93
4.4.1 Inductively coupled plasma-optical emission spectrometry.....	94
4.4.1.1 Introduction.....	94
4.4.1.2 Instrumentation and principles of ICP-OES	96
4.5 Separation and purification techniques.....	101

Table of Contents

4.5.1 Magnetic separation	102
4.5.2 Solvent extraction.....	103
4.6 Method validation.....	111
4.6.1 Accuracy	112
4.6.1.1 Absolute error (E)	113
4.6.1.2 Relative error(E_r).....	113
4.6.2 Precision	113
4.6.3 Limit of Detection (LOD).....	114
4.6.4 Limit of Quantification (LOQ).....	114
4.6.5 Specificity and Selectivity	115
4.6.6 Linearity.....	115
4.6.7 Range (w).....	116
4.6.8 Robustness/Ruggedness	116
4.7 Conclusion	117

Chapter 5: Quantification of scandium in different scandium-containing

 matrices and method validation	118
5.1 Introduction	118
5.2 General experimental conditions and procedures.....	119
5.2.1 Preparation of ultra-pure water.....	119
5.2.2 Weighing	119
5.2.3 Micro-pipets.....	120
5.2.4 Glassware	120
5.2.5 Microwave-assisted digestion	120
5.2.6 ICP-OES	121
5.3 Materials and reagents	122
5.4 Experimental procedures for the determination of scandium	122
5.4.1 Preparation of ICP-OES standards	122
5.4.2 Determination of LOD and LOQ's	123
5.5 Quantification of Sc in inorganic compounds	123
5.5.1 Preparation of $ScCl_3 \cdot H_2O$	123
5.5.2 Dissolution of Sc_2O_3 by open-beaker digestion	124
5.5.3 Dissolution of Sc_2O_3 with microwave-assisted digestion in the presence of different acids	125

Table of Contents

5.6 Quantification of Sc in different organometallic complexes.....	126
5.6.1 Introduction	126
5.6.2 General equipment.....	129
5.6.2.1 Melting point apparatus	129
5.6.2.2 IR spectroscopy	129
5.6.2.3 Truspec micro CHNS elemental analyser	130
5.6.3 Materials and solvents.....	131
5.6.3.1 Synthesis of thio-acetylacetone	131
5.6.4 Syntheses of organometallic complexes	132
5.6.4.1 Synthesis of Sc(acac) ₃	132
5.6.4.1.1 Infrared analysis	132
5.6.4.1.2 Elemental analysis	133
5.6.4.1.3 Open-beaker dissolution for Sc(acac) ₃	134
5.6.4.2 Synthesis of Sc(tfac) ₃	134
5.6.4.2.1 Infrared analysis	135
5.6.4.2.2 Elemental analysis	136
5.6.4.2.3 Open-beaker dissolution for Sc(tfac) ₃	136
5.6.4.2.4 Microwave-assisted dissolution for Sc(tfac) ₃	137
5.6.4.3 Synthesis of Sc(btfac) ₃	137
5.6.4.3.1 Infrared analysis	138
5.6.4.3.2 Elemental analysis	138
5.6.4.3.3 Open-beaker dissolution for Sc(btfac) ₃	139
5.6.4.3.4 Microwave-assisted dissolution for Sc(btfac) ₃	139
5.6.4.4 Synthesis of Sc(dbm) ₃	140
5.6.4.4.1 Infrared analysis	140
5.6.4.4.2 Elemental analysis	141
5.6.4.4.3 Open-beaker dissolution for Sc(dbm) ₃	142
5.6.4.4.4 Microwave-assisted dissolution for Sc(dbm) ₃	142
5.6.4.5 Synthesis of Sc(hfac) ₃	143
5.6.4.5.1 Infrared analysis	143
5.6.4.5.2 Elemental analysis	144
5.6.4.5.3 Open-beaker dissolution for Sc(hfac) ₃	144
5.6.4.6 Synthesis of Sc(sacac) ₃	145
5.6.4.6.1 Infrared analysis	145

Table of Contents

5.6.4.6.2 Elemental analysis	146
5.6.4.6.3 X-ray crystallography	147
5.6.4.6.4 Open-beaker dissolution for Sc(sacac) ₃	148
5.7 Digestion and quantification analyses of columbite mineral ore and Ta/Nb residuals	148
5.7.1 General experimental methods	150
5.7.1.1 General procedures, reagents and equipment	150
5.7.1.2 Preparation of standard solutions	151
5.7.2 Experimental procedures for the optimization of the dissolution of the columbite and residue samples	152
5.7.2.1 Dissolution of columbite (Sample A) by NH ₄ F·HF	152
5.7.2.2 Influence of sample:flux ratio and the fusion time on dissolution of columbite ore	154
5.7.3 Application of the optimal conditions for the dissolution of Samples A and B	155
5.7.4 Magnetic removal of Fe and Ti in Samples A and B	156
5.7.4.1 Magnetic susceptibility determinations	156
5.7.4.2 Magnetic separation of Samples A and B	157
5.7.4.3 Quantitative determination of the elements present in the magnetic and in the non-magnetic portions of both samples (A and B)	158
5.7.5 Solvent extraction of tantalum in a columbite mineral (Sample A)	160
5.7.6 Solvent extraction of tantalum and niobium in the non-magnetic portion of Sample A with MIBK	163
5.7.7 Solvent extraction of tantalum and niobium in the non-magnetic portion of Sample A with octan-1-ol and MIAK	165
5.7.8 Solvent extraction of Ta and Nb in the non-magnetic portion of Sample B with MIBK	168
5.8 Results and discussions	169
5.8.1 LOD and LOQ	169
5.8.2 Dissolution and quantification of Sc in inorganic compounds	170
5.8.2.1 ScCl ₃ ·H ₂ O analyses	170
5.8.2.2 Sc ₂ O ₃ analyses	170
5.8.2.2.1 Open-beaker dissolution of Sc ₂ O ₃	170
5.8.2.2.2 Microwave-assisted dissolution of Sc ₂ O ₃	170

Table of Contents

5.8.3 Characterization of organometallic compounds with melting point determination, IR and CHNS micro-element analysis and the quantification of Sc in organometallic compounds using ICP-OES	171
5.8.3.1 Melting point of organometallic compounds.....	171
5.8.3.2 Characterization and quantification of Sc in Sc(acac) ₃	171
5.8.3.2.1 Infrared spectrum of Sc(acac) ₃	171
5.8.3.2.2 CHNS micro-elemental analysis of Sc(acac) ₃	172
5.8.3.2.3 ICP-OES results of Sc(acac) ₃	173
5.8.3.3 Characterization and quantification of Sc in Sc(tfac) ₃	173
5.8.3.3.1 Infrared spectrum of Sc(tfac) ₃	173
5.8.3.3.2 CHNS micro-elemental analysis of Sc(tfac) ₃	174
5.8.3.3.3 Open-beaker and microwave dissolution of Sc(tfac) ₃	174
5.8.3.4 Characterization and quantification of Sc in Sc(btfac) ₃	175
5.8.3.4.1 Sc(btfac) ₃ and btfacH infrared spectra.....	175
5.8.3.4.2 CHNS micro-elemental analysis of Sc(btfac) ₃	175
5.8.3.4.3 Sc recoveries from Sc(btfac) ₃ after open-beaker and microwave dissolution	175
5.8.3.5 Sc(dbm) ₃ characterisation and quantification of Sc	176
5.8.3.5.1 Infrared of dbmH and Sc(dbm) ₃	176
5.8.3.5.2 CHNS micro-elemental analysis of Sc(dbm) ₃	176
5.8.3.5.3 Open-beaker and microwave dissolution of Sc(dbm) ₃	176
5.8.3.6 Sc(hfac) ₃ characterisation and quantification of Sc.....	177
5.8.3.6.1 Infrared of hfach and Sc(hfac) ₃	177
5.8.3.6.2 CHNS micro-elemental analysis of Sc(hfac) ₃	177
5.8.3.6.3 Open-beaker dissolution of Sc(hfac) ₃	177
5.8.3.7 Characterization and quantification of Sc in Sc(sacac) ₃	178
5.8.3.7.1 Infrared of sacacH and Sc(sacac) ₃	178
5.8.3.7.2 CHNS micro-elemental analysis of Sc(sacac) ₃	178
5.8.3.7.3 X-ray crystallography of Sc(sacac) ₃	179
5.8.3.7.4 Quantification of Sc in Sc(sacac) ₃	182
5.8.4 Columbite and Ta/Nb residue or tailings processing	182
5.8.4.1 Dissolution of columbite and the Ta/Nb residue.....	184
5.8.4.1.1 Dissolution of columbite mineral and Ta/Nb residue samples using the NH ₄ F·HF fusion method.....	184

Table of Contents

5.8.4.1.2 Influence of sample:flux ratio and the fusion time on dissolution of columbite ore.....	184
5.8.4.1.3 Application of the optimum conditions for the dissolution of Samples A and B.....	185
5.8.4.2 Magnetic separation of magnetic materials	185
5.8.4.3 Solvent extraction of tantalum in Sample A with MIBK as solvent	186
5.8.4.4 Solvent extraction of tantalum and niobium in the non-magnetic portion of Sample A with MIBK.....	187
5.8.4.5 Evaluation of different extractants on the metal separation process	187
5.8.4.6 Solvent extraction of Ta and Nb in the non-magnetic portion of Sample B with MIBK	188
5.9 Conclusion	188
5.10 Method validation.....	190
5.10.1 Introduction	190
5.10.2 Conclusion	196
Chapter 6: Evaluation of the study and future research	197
6.1 Introduction	197
6.2 Degree of success with regard to the set objectives	197
6.3 Future research	199
Summary	200
Opsomming.....	202

LIST OF FIGURES

Figure 1.1: Mendeleev’s periodic table published in 1860.	2
Figure 1.2: Metallic scandium.	3
Figure 1.3: Worldwide scandium resources.	4
Figure 1.4: Scandium yield strength for different aluminium alloys in ksi (kilopound per square inch).	5
Figure 1.5: The Bayan Obo rare earths mine.	6
Figure 2.1: Swedish chemist Lars Fredrik Nilson.	10
Figure 2.2: Scandium element discovered by Nilson in 1879 in the minerals (a) euxenite and (b) gadolinite, which had not yet been found anywhere except in Scandinavia.	11
Figure 2.3: Locations of significant thortveitite deposits.	15
Figure 2.4: Thortveitite from Norway.	16
Figure 2.5: Spherical ball of kolbeckite.	17
Figure 2.6: Bazzite mineral.	18
Figure 2.7: The Utah region, inserted is kolbeckite ($\text{ScPO}_4 \cdot 2\text{H}_2\text{O}$) from the Little Green Monster Variscite Mine.	20
Figure 2.8: Inner Mongolia region in China where Bayan Obo rare earth mine is situated.	22
Figure 2.9: Bayan Obo deposit image by NASA.	23
Figure 2.10: A scandium-cobalt-nickel deposit near Greenvale in Northern Queensland, Australia	25
Figure 2.11: New South Wales region where the Nyngan scandium project is taking place.	26
Figure 2.12: Sc_2O_3 prices from 1991 to 2013.	28
Figure 2.13: The extraction of scandium from scandium-containing ores.	30
Figure 2.14: The detailed flow diagrams of the beneficiation of scandium in (a) IARED and (b) uranium ores.	31
Figure 2.15: Scandium applications.	33
Figure 2.16: A 40 cell internally-manifolded SOFC stack.	34
Figure 2.17: Hexagonal lattice of scandium metal.	37

Figure 2.18: Hexagonal close-packed crystal structure of scandium metal.	38
Figure 2.19: Scandium oxide powder.....	40
Figure 2.20: Molecular structures of (a) acetylacetonate, (b) tropolonate, (c) oxalate and (d) pyridine-2,6-dicarboxylic acid.....	42
Figure 3.1: p-nitrochlorophosphonazo (CPApN).	56
Figure 3.2: Absorption spectra for reagent blank CPApN (2.12×10^{-6} M) in resin phase against blank resin (1); and Sc-CPApN complex against reagent blank in resin phase in H ₂ SO ₄ (2).....	56
Figure 3.3: A proposed, but unconfirmed (tentative) structure for scandium(III) higher carboxylates.....	71
Figure 3.4: Infrared spectra of Sc(III) complexes of 8-hydroxyquinoline: (A) Pokras and Bernays' compound, (B) compound precipitated from (10 % v/v) aqueous acetone, (C) ScQ ₃ ·H ₂ O, (D) ScQ ₃ ·D ₂ O, and (E) thermal product (heated at 160 °C), ScQ ₃	73
Figure 3.5: Representative structure of the hydrazone complexes prepared by Hegazy and Al-Motawaa.....	74
Figure 4.1: (a) Front view of microwave digester, (b) open view of microwave digester with the rotor and (c) the rotor with reaction vessels.	82
Figure 4.2: Microwave-assisted digestion system: a) single-mode apparatus and b) multi-mode apparatus.....	83
Figure 4.3: A typical high temperature furnace used for flux fusion.	86
Figure 4.4: The electromagnetic spectrum.....	87
Figure 4.5: IR absorption for common functional groups.	88
Figure 4.6: Types of vibrational modes activated by IR.	89
Figure 4.7: Equipment configuration for a CHNS micro-analyser.....	90
Figure 4.8: Melting-point apparatus.	91
Figure 4.9: Bragg's Law for X-ray diffraction.....	93
Figure 4.10: Concentric tube nebulizer.	97
Figure 4.11: (a) Schematic presentation of inductively coupled plasma torch and (b) Typical plasma torch.	98
Figure 4.12: Schematic presentation of sample introduction to ICP-OES.....	99

Figure 4.13: The detection limit ranges for the major atomic spectroscopy techniques.	100
Figure 4.14: Simplified scheme for a liquid–liquid extraction in which the solute’s partitioning depends only on the K_D equilibrium.....	105
Figure 4.15: Scheme for the liquid–liquid extraction of a metal ion, M^{n+}	106
Figure 4.16: Method validation criteria.....	112
Figure 4.17: The determination of LOD and LOQ from the calibration curve.	115
Figure 4.18: A calibration curve showing good linearity with r^2 value close to 1	116
Figure 5.1: Shimadzu (AW320) and Sartorius (CPA26P Series) electronic balance scales.	119
Figure 5.2: Shimadzu ICPS-7510 ICP-OES sequential plasma spectrometer.	121
Figure 5.3: Formation of the acetylacetonate anion.....	127
Figure 5.4: Bidentate ligands (a) acetylacetonate (acacH), (b) 1,1,1-trifluoroacetylacetonate (tfacH), (c) hexafluoroacetylacetonate (hfacH), (d) benzoyl-1,1,1-trifluoroacetylacetonate (btfacH), (e) dibenzoylmethane (dbm) and (f) thioacetylacetonate (sacacH).	127
Figure 5.5: General procedure of synthesis, identification and quantification of different $Sc(acac)_3$ complexes.	128
Figure 5.6: Melting point apparatus used in this study.....	129
Figure 5.7: Infrared spectrometer.....	130
Figure 5.8: Leco CHNS Truspec Micro Series.	130
Figure 5.9: The IR spectra of acetylacetonate and $Sc(acac)_3$	133
Figure 5.10: The IR spectra of tfacH and $Sc(tfac)_3$	135
Figure 5.11: The IR spectra of btfacH and $Sc(btfac)_3$	138
Figure 5.12: The IR spectra of dbmH and $Sc(dbm)_3$	141
Figure 5.13: The IR spectra of hfacH and $Sc(hfac)_3$	144
Figure 5.14: The IR spectra of sacacH and $Sc(sacac)_3$	146
Figure 5.15: Columbite ore (A) and residue (B).	149
Figure 5.16: Thermo Scientific Thermolyne high temperature furnace used in this study	150
Figure 5.17: The % analytes present in Sample A after magnetic separation.....	159
Figure 5.18: The % analytes present in Sample B after magnetic separation.....	160

Figure 5.19: Elemental analysis in the aqueous solution after solvent extraction separation of elements at $[\text{H}_2\text{SO}_4] = 8 \text{ M}$ in Sample A.....	162
Figure 5.20: Elemental analysis in the organic solution after two times solvent extraction separation steps at $[\text{H}_2\text{SO}_4] = 8 \text{ M}$ in Sample A using MIBK.	162
Figure 5.21: % Nb, Ta and Sc extracted with MIBK at different $[\text{H}_2\text{SO}_4]$ concentrations.	164
Figure 5.22: % Nb and % Sc in the aqueous and organic phase after solvent extraction with octan-1-ol at different $[\text{H}_2\text{SO}_4]$	167
Figure 5.23: A proposed structure for $\text{Sc}(\text{acac})_3$	173
Figure 5.24: Molecular structure of $\text{Sc}(\text{tfac})_3$	174
Figure 5.25: The crystal structure of $\text{Sc}(\text{acac})_3$	180
Figure 5.26: Packed unit cell of $\text{Sc}(\text{acac})_3$ along the a-axis.	180
Figure 5.27: Columbite (sample A) processing.	183

LIST OF TABLES

Table 2.1: Abundances for scandium in a number of different environments.....	14
Table 2.2: Minerals containing scandium	16
Table 2.3: Results of microprobe analysis of thortveitite from different locations ..	17
Table 2.4: Chemical composition of a kolbeckite and a bazzite from Switzerland.	18
Table 2.5: Scandium compounds prices from the year 2010 up to 2014.....	27
Table 2.6: Scandium's physical and chemical properties	36
Table 3.1: The fractional content obtained by elution of crude scandium with HEDTA	47
Table 3.2: Effect of acid addition on scandium extraction	52
Table 3.3: Scandium determination at five different concentrations	55
Table 3.4: The Determination of Sc in different metal alloys with UV/Vis spectroscopy.....	57
Table 3.5: Determination of scandium with UV/Vis spectroscopy after complexing with DHNO.....	58
Table 3.6: Sc determination in spiked water and CRM samples	59
Table 3.7: Scandium recovery from acid mine drainage determined with ICP-OES	61
Table 3.8: Scandium determination from different Sc-containing matrices with ICP-OES	62
Table 3.9: Scandium recoveries in river water samples after an on-line pre-concentration method and chemical vapour generation.	64
Table 3.10: Recovery of scandium in river water analyses with ICP-OES after an on-line pre-concentration method (95% confidence interval; n = 6).....	65
Table 3.11: Sc content for the coastal seawater samples determined with ICP-MS.	66
Table 3.12: Scandium concentrations for rock reference materials.....	67
Table 3.13: Concentration of scandium as trace element found in various asbestos samples, (10 replicates).....	69
Table 3.14: IR frequencies of scandium(III) higher carboxylates.....	71
Table 3.15: Selected IR data of Sc hydrazone complexes (cm ⁻¹).....	75

Table 3.16: Elemental analysis data for Sc hydrazone complexes.....	76
Table 4.1: Examples of acids used for wet ashing	80
Table 4.2: Common fluxes used for mineral or metal dissolution	85
Table 4.3: Advantages and disadvantages of ICP-OES.....	101
Table 4.4: Some common extraction solvents.....	110
Table 5.1: Microwave digestion conditions used in this study for digestion of Sc ₂ O ₃ and the Sc organometallic compounds.....	120
Table 5.2: ICP-OES operating conditions.....	122
Table 5.3: Chemicals and reagents used in this study	122
Table 5.4: Calculation of LOD's and LOQ's of Sc in different acids.....	123
Table 5.5: Sc quantification in ScCl ₃ ·H ₂ O by ICP-OES	124
Table 5.6: Quantitative analysis of Sc in Sc ₂ O ₃ by ICP-OES after digestion by open-beaker method.....	125
Table 5.7: Quantitative analysis of Sc in Sc ₂ O ₃ , digested with microwave in the presence of different acids.....	126
Table 5.8: List of materials and solvents	131
Table 5.9: IR stretching frequencies (in cm ⁻¹) for acacH and Sc(acac) ₃	133
Table 5.10: Elemental analysis of Sc(acac) ₃	134
Table 5.11: Quantitative determination of scandium in Sc(acac) ₃ dissolved in HNO ₃	134
Table 5.12: The IR stretching frequencies of tfacH and Sc(tfac) ₃	135
Table 5.13: Elemental analysis of Sc(tfac) ₃	136
Table 5.14: Quantitative determination of scandium in Sc(tfac) ₃ digested by open beaker method.....	136
Table 5.15: Quantitative determination of scandium in Sc(tfac) ₃ digested by the microwave-assisted method	137
Table 5.16: btfacH and Sc(btfac) ₃ IR stretching frequencies	138
Table 5.17: Elemental analysis of Sc(btfac) ₃	139
Table 5.18: Quantitative determination of scandium in Sc(btfac) ₃ after open-beaker digestion.	139
Table 5.19: Quantitative determination of scandium in Sc(btfac) ₃ digested by the microwave-assisted method	140

Table 5.20: IR stretching frequencies of dbmH and Sc(dbm) ₃	141
Table 5.21: Elemental analysis of Sc(dbm) ₃	141
Table 5.22: Quantitative determination of scandium in Sc(dbm) ₃ after open-beaker digestion	142
Table 5.23: Quantitative determination of scandium in Sc(dbm) ₃ dissolved by the microwave-assisted technique.....	143
Table 5.24: IR stretching frequencies of hfachH and Sc(hfac) ₃	144
Table 5.25: Elemental analysis of Sc(hfac) ₃	144
Table 5.26: Quantitative determination of scandium in Sc(hfac) ₃	145
Table 5.27: sacacH and Sc(sacac) ₃ IR stretching frequencies.....	146
Table 5.28: Elemental analysis of Sc(sacac) ₃	146
Table 5.29: The crystal data of Sc(sacac) ₃	147
Table 5.30: Quantitative determination of scandium in Sc(sacac) ₃	148
Table 5.31: Typical chemical compositions of columbite mineral and Ta/Nb residue samples (Sample A and Sample B)	149
Table 5.32: Selected analytical wavelengths, detection limits and quantification limits for the different elements analysed in the columbite and Ta/Nb residue samples	151
Table 5.33: Ammonium bifluoride fusion for Sample A at 1:10 Sample A:NH ₄ F·HF ratio for 30 minutes at 200 °C	153
Table 5.34: Fusion results for Sample A with NH ₄ F·HF at 200 °C.....	154
Table 5.35: Quantitative results obtained after the fusion dissolution of columbite mineral ore (Sample A) and Nb/Ta residue (Sample B) with NH ₄ F·HF (1:10 sample:flux ratio) at 200 °C for 60 min.....	156
Table 5.36: Magnetic susceptibility determinations for the two columbite samples	157
Table 5.37: Mass balance of Samples A and B after magnetic separation	157
Table 5.38: ICP-OES results for the elements contained in the magnetic and the non-magnetic portions of Sample A.....	158
Table 5.39: ICP-OES results for the elements contained in the magnetic and the non-magnetic portions of Sample B.....	159
Table 5.40: Solvent extraction of Ta in Sample A using MIBK after NH ₄ F·HF fusion. [H ₂ SO ₄] varied at 2, 4 and 8 M.	161

Table 5.41: Elemental analysis of the aqueous solution of the non-magnetic portion of Sample A with MIBK at [H ₂ SO ₄] between 4 and 16 M.	163
Table 5.42: Elemental analysis of the organic solution of the non-magnetic portion of Sample A with MIBK at [H ₂ SO ₄] between 4 and 16 M	164
Tables 5.43: Elemental analysis of the aqueous solution of the non-magnetic portion of Sample A with octan-1-ol at [H ₂ SO ₄] between 4 and 16 M	166
Table 5.44: Elemental analysis of the organic solution of the non-magnetic portion of Sample A with octan-1-ol at [H ₂ SO ₄] between 4 and 16 M	166
Tables 5.45: Elemental analysis of the aqueous and organic solutions of the non-magnetic portion of Sample A with MIAK at [H ₂ SO ₄] between 4 and 16 M.....	167
Table 5.46: Elemental analysis of the aqueous and organic solutions of the non-magnetic portion of Sample B with MIBK at [H ₂ SO ₄] = 8 M	169
Table 5.47: Melting points of the different scandium organometallic compounds	171
Table 5.48: Selected bond distances and angles for Sc(acac) ₃ and those of other complexes in the literature	181
Table 5.49: Distribution ratios for elements present in columbite mineral after extraction with MIBK solvent at 8.0 M H ₂ SO ₄	187
Table 5.50: Evaluation of various steps involved in the Sc beneficiation process investigated in this study.....	187
Table 5.51: Validation of Sc determination in ScCl ₃ ·H ₂ O	191
Table 5.52: Validation of Sc determination in Sc ₂ O ₃ dissolved by open-beaker digestion with different acids.....	192
Table 5.53: Validation of Sc determination in Sc ₂ O ₃ dissolved by microwave digestion with different acids.....	192
Table 5.54: Validation of Sc in Sc(acac) ₃	193
Table 5.55: Validation of Sc in Sc(tfac) ₃ dissolved by open-beaker and microwave digestion.	193
Table 5.56: Validation of Sc in Sc(btfac) ₃ dissolved by open-beaker and microwave digestion	194
Table 5.57: Validation of Sc in Sc(dbm) ₃ dissolved by open-beaker and microwave digestion	194
Table 5.58: Validation of Sc in Sc(hfac) ₃	195
Table 5.59: Validation of Sc in Sc(sacac) ₃ /Sc(acac) ₃	195

Table 5.60: Validation of Sc in Columbite and in Ta/Nb residue 196

LIST OF ABBREVIATIONS

Analytical equipment

AAS	Atomic absorption spectroscopy
CHNS micro-analyser	Carbon, hydrogen, nitrogen, sulphur micro-analyser
UV-Vis	Ultraviolet–visible absorption spectrometry
ICP-OES	Inductive coupled plasma-optical emission spectroscopy
ICP-MS	Inductive coupled plasma-mass spectrometry
IR	Infrared
NAAS	Neutron activation analysis spectrometry
PTFE	Polytetrafluoroethylene
MSB	Magnetic susceptibility balance

Ligands and solvents

acacH	acetylacetone
tfacH	1,1,1-trifluoroacetylacetone
btfacH	benzoyl-1,1,1-trifluoroacetylacetone
dbmH	dibenzoylmethane
hfacH	hexafluoroacetylacetone
sacacH	thio-acetylacetone
MIBK	Methyl isobutyl ketone
MIAK	Methyl isoamyl ketone

Units

mmHg	Millimetre of mercury
°C	Degrees Celsius
M	Molar

ppm	Parts per million
ppb	Parts per billion

Miscellaneous terms

REE	Rear earth elements
M_xO_y	Metal oxide
b.p.	Boiling point
M.P.	Melting point

Statistical terms

LOD	Limit of detection
LOQ	Limit of quantitation
R^2	Linear regression line
s	Standard deviation
s_b	Standard deviation of the blank
RSD	Relative standard deviation
m	Slope
H_a	Alternative hypothesis
H_0	Null hypothesis
s_m	Standard deviation of the slope
s_c	Standard deviation of the y-intercept

KEYWORDS

Scandium

Quantitative analysis

Qualitative analysis

1 Motivation of the study

1.1 Background of scandium

In 1860 the Russian chemist Dmitri Mendeleev published the first version of the periodic table (**Figure 1.1**) in which he not only identified the absence or non-discovery of certain elements, but also predicted the chemical properties of these yet to be discovered elements. He predicted that one of these elements should have an atomic weight between calcium (40) and titanium (48)^{1, 2} and he called this missing element ekaboron. It was only in 1879 that Lars Fredrik Nilson discovered a new element while he was attempting to isolate ytterbium from the two rare earth element (REE) minerals gadolinite and euxenite³ which he obtained in Uppsala, Sweden. He synthesized about 2.0 g of this new element (Sc_2O_3) with high purity which he named scandium after the Latin word 'Scanda' meaning Scandinavia, referring to the origin of these rare earth element minerals. After the proper characterisation of this newly discovered element, scientists noted that Nilson's scandium was identical to Mendeleev's ekaboron and it was officially renamed as scandium.² Metallic scandium (**Figure 1.2**) was produced for the first time in 1937.³

¹ Scandium, a rare earth that's really not a rare earth, [Accessed 07-04-2015]. Available from: <http://www.hardassetsinvestor.com/features/2917-scandium-a-rare-earth-thats-not-really-rare.html>

² Scandium, [Accessed 07-04-2015]. Available from: <http://www.molycorp.com/resources/the-rare-earth-elements/scandium/>

³ Scandium Element Facts, [Accessed 17-06-2014]. Available from: <http://www.chemicool.com/elements/scandium.html>

Ueber die Beziehungen der Eigenschaften zu den Atomgewichten der Elemente. Von D. Mendelejeff. — Ordnet man Elemente nach zunehmenden Atomgewichten in verticale Reihen so, dass die Horizontalreihen analoge Elemente enthalten, wieder nach zunehmendem Atomgewicht geordnet, so erhält man folgende Zusammenstellung, aus der sich einige allgemeinere Folgerungen ableiten lassen.

			Ti = 50	Zr = 90	? = 180
			V = 51	Nb = 94	Ta = 182
			Cr = 52	Mo = 96	W = 186
			Mn = 55	Rh = 104,4	Pt = 197,4
			Fe = 56	Ru = 104,4	Ir = 198
		Ni = Co = 59	Pd = 106,6	Os = 199	
		Cu = 63,4	Ag = 108	Hg = 200	
H = 1		Zn = 65,2	Cd = 112		
Be = 9,4	Mg = 24	? = 68	Ur = 116	Au = 197?	
B = 11	Al = 27,4	? = 70	Sn = 118		
C = 12	Si = 28	As = 75	Sb = 122	Bi = 210?	
N = 14	P = 31	Se = 79,4	Te = 128?		
O = 16	S = 32	Br = 80	J = 127		
F = 19	Cl = 35,5	Rb = 85,4	Cs = 133	Tl = 204	
Li = 7	Na = 23	K = 39	Ba = 137	Pb = 207	
		Ca = 40	Sr = 87,6		
		? = 45	Ce = 92		
		?Er = 56	La = 94		
		?Yt = 60	Di = 95		
		?In = 75,6	Th = 118?		

1. Die nach der Grösse des Atomgewichts geordneten Elemente zeigen eine stufenweise Abänderung in den Eigenschaften.
2. Chemisch-analoge Elemente haben entweder übereinstimmende Atomgewichte (Pt, Ir, Os), oder letztere nehmen gleichviel zu (K, Rb, Cs).
3. Das Anordnen nach den Atomgewichten entspricht der *Werthigkeit* der Elemente und bis zu einem gewissen Grade der Verschiedenheit im chemischen Verhalten, z. B. Li, Be, B, C, N, O, F.
4. Die in der Natur verbreitetsten Elemente haben *kleine* Atomgewichte

Figure 1.1: Mendeleev's periodic table published in 1860.⁴

The chemical properties of scandium are very similar to those of the rare earths and it is currently also regarded as one of the rare earth elements. In addition to the similarity of its chemical characteristics with those of the lanthanides, scandium is often found in the same minerals in which the other rare earth metals naturally occur. Scandium is a soft, silvery-white metallic element with an atomic number of 21 and an atomic weight of 44.9559 g/mol (**Figure 1.2**). It easily oxidises and tarnishes to pink or yellow. It is light in weight, like aluminium, but has a much higher melting point (1541 °C) and a boiling point of about 2831 °C.⁵

⁴ 1869 – Mendeleev's Periodic Table, [Accessed 04-05-2014]. Available from: <http://visualoop.com/blog/13817/visualizing-the-periodic-table>

⁵ Scandium, [Accessed 17-06-2014]. Available from: <http://pdfooz.org/k-940576.html>



Figure 1.2: Metallic scandium²

An interesting fact is that scandium is more common in the sun and certain stars than it is on earth and it is the 23rd and 50th most common element in the sun and on earth respectively. The element is widely dispersed in small quantities in more than 800 mineral species in the earth's crust. It is the main component in the mineral thortveitite which contains 44 - 48 % scandium oxide, Sc_2O_3 , and is found in Scandinavia and Madagascar. Recently it was reported that the mineral thortveitite was also found in Kobe, Japan.⁵ Residues or tailings after the extraction of tungsten from Zinnwald's wolframite, and in wiikite and bazzite also have some appreciable amounts of scandium.²

Scandium is commercially mined in a few countries and mostly present in waste material remaining after rare earth mineral mining and processing, in Australia, Norway, Madagascar, Kazakhstan, China, Russia and Ukraine. Australia's scandium resources are mainly contained in the nickel and cobalt deposits in Syerston and Lake Innes in New South Wales. Resources in Norway are distributed in the thortveitite-rich pegmatites of the Iveland-Evje region and a deposit in the northern area of Finnmark. In Madagascar, scandium is found in pegmatites in the Befanamo area. Uranium-bearing deposits are major scandium sources in Kazakhstan. China's resources are in iron, tin, and tungsten deposits found in Fujian while in Russia, resources are located in the Kola Peninsula as apatites. In Ukraine the scandium is

recovered as a byproduct of iron ore processing at Zhelyte Voda.⁶ Geologists believe there are still significant deposits of scandium-bearing minerals yet to be discovered.⁷

Figure 1.3 shows the worldwide occurrence of scandium resources.



Figure 1.3: Worldwide scandium resources

Scandium is extensively used in aluminium-scandium alloy production because it is an effective grain-refining agent for aluminium. Added to aluminium it improves its durability, corrosion resistance, weldability and plasticity.⁸ This soft, light, silvery-white metal is widely used in the aerospace industry (substitutes for aluminium-lithium and aluminium-titanium alloys) due to its higher melting point (it reduces susceptibility to heat-cracking) and lower prices. **Figure 1.4** shows the scandium yield strength for different aluminium-scandium alloys. These alloys are also desirable for their use in sport equipment like baseball bats, lacrosse sticks and bicycle frames.⁵ It is also anticipated that the stronger aluminium-scandium alloys

⁶ Scandium, [Accessed 17-09-2014]. Available from:
<http://minerals.usgs.gov/minerals/pubs/commodity/scandium/mcs-2014-scand.pdf>

⁷ Investing in Scandium, [Accessed 11-02-2015]. Available from:
http://www.elementinvesting.com/investing_in_scandium.htm

⁸ Cote, M., Caudron, Tanguay, J. ORBITE: a strategic scandium producer, version 1, pp. 4-8. (2012).

(0.5 % scandium) could be used to replace entire airline fleets with much cheaper, lighter and stronger aircraft.⁹

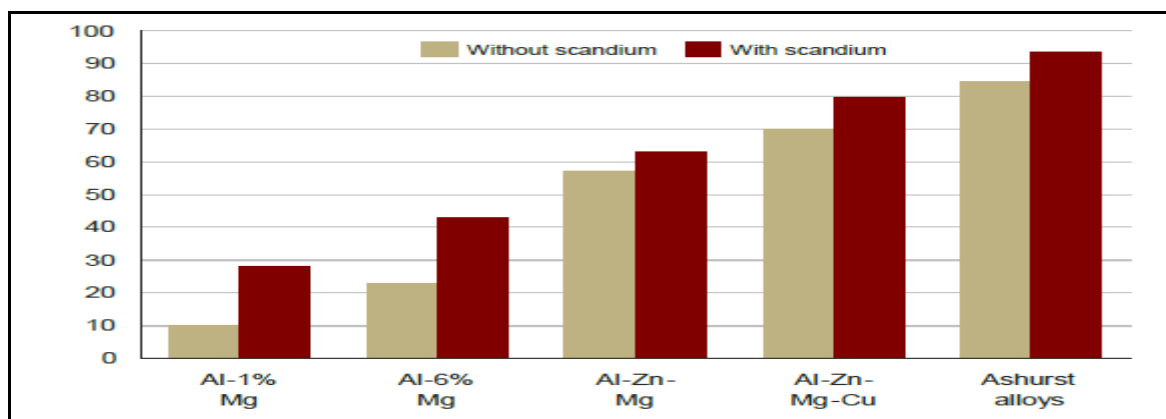


Figure 1.4: Scandium yield strength for different aluminium alloys in ksi (kilopound per square inch).⁷

Sc₂O₃ is used to make scandia-stabilised zirconia (ScSZ) in solid oxide fuel cells that has higher ionic conductivity than other zirconias. Scandium iodide (ScI₃) on the other hand is added to mercury-vapour lamps which produces a highly efficient artificial light source that closely resembles sunlight and allows good colour production. These light sources are widely utilised in household television sets and in large movie screens used in theatres and in sports stadiums. It is estimated that about 80 kg of scandium are used in light bulbs globally per year.⁸

Most of the current scandium supply originates from the former Soviet Union's old weapon stockpiles which are estimated at approximately 400 tonnes. It is estimated that the annual production from other countries is between 1 and 2 tonnes per year. Currently the world's largest scandium producer is the Bayan Obo rare earth element mine in the interior of Mongolia, China (**Figure 1.5**). Additionally, scandium is presently recovered as by-product from uranium mill tailings. Though there are only a few economically viable scandium deposits identified worldwide, their economic exploitation is highly problematic. One of these problems is that rare earth elements mining companies do not usually disclose their actual scandium production, which makes the accurate estimation of the global scandium production testing.

⁹ Scandium, [Accessed 07-03-2015]. Available from: <http://aheadoftheherd.com/Newsletter/2011/Critical-Minerals-and-Materials.htm>



Figure 1.5: The Bayan Obo rare earths mine¹⁰

Financial analysts' however estimates that the worldwide scandium production range between 2 and 10 tonnes per year. It is anticipated that less than half a tonne of scandium is produced through actual mining operations each year, with the largest amount by the Bayan Obo mine and the rest from former Soviet Union stockpiles. The major obstacle with regard to scandium production is that the metal exists in minuscule quantities present in most of minerals. The recovery processes are also complicated due to the similarity of the chemistry to the REE and require numerous separation steps which are not only costly, but also time consuming.

Scandium is usually sold as Sc_2O_3 and then converted to ScF_3 and finally reduced with metallic calcium to metallic scandium. The current scandium oxide price range between 1,000 and 4,500 US\$/kg, although sales contracts, including prices and quantities, normally remain confidential while the high price of scandium may restrict the widespread use of this kind of metal alloys in the Western world.⁸ Demand for the metal is steadily increasing due to its unique mechanical and chemical properties and

¹⁰ TRU Rare Earth Elements, [Accessed 04-05-2015]. Available from: <http://trugroup.com/tru-rare-earth-elements>

is currently extensively used in modern technologies which include the aerospace, electronics, optical and the fuel cells industries (Scandia-stabilised zirconia).¹¹

1.2 Motivation of this study

The biggest challenges to scandium beneficiation remain the low natural abundance of the element in mineral deposits as well as its association with other elements with very similar chemical properties as previous stated. Key to the successful isolation and production of pure scandium is the increase in the quantity of the scandium in the tailings (pre-concentration) and the separation of scandium from the rest of the elements with similar chemical properties. Columbite-tantalite, a niobium rich mineral found in Brazil, is mainly mined and processed for the large amounts of niobium content (31 - 79 % Nb_2O_5) and to a lesser extent the tantalum present in these ores. Chemical characterisation of the mineral also indicate the presence of moderate quantities of iron and titanium, but also small quantities of scandium (0.135 %) and only one other “adopted” rare earth element, yttrium (0.17 %). Characterisation of the process tailings after the removal of the niobium still indicate the presence of large amounts of iron, moderate amounts of tantalum and increased (compared to mineral ore) amounts of scandium (0.996 %) and yttrium (0.38 %).

The presence of only one other rare earth element in these mineral ore/tailings is extremely valuable for the possible isolation of scandium since it may simplify the beneficiation process due to fewer separation steps and impurities in the final product. In addition, the possible isolation of the iron and titanium with magnetic separation and the removal of the tantalum with solvent extraction may proof to be valuable methods to increase the final quantities of scandium in tailings. This opens new opportunities to isolate scandium from this mineral or its tailings and add additional amounts of scandium (Sc_2O_3) to the market. Key to the successful development of a new beneficiation process like this is i) the complete chemical

¹¹ Irvine, J. T. S., Politova, T., Zakowsky, N., Kruth, A., Tao, S., Travis, R., Attia, O., Scandia-Zirconia Electrolytes and Electrodes for SOFCs. In: *Proceedings of the NATO Advanced Research Workshop on Fuel Cell Technologies: State and Perspectives*. Kyiv, Ukrain, pp. 35-47. (2004)

characterisation of the original mineral sample or residue, even with the target elements at very low concentrations ii) the tracing or following of the target element as well as impurities in all the beneficiation steps, iii) the purity of the final product and finally iv) a thorough understanding/knowledge of the inorganic chemistry of the target elements involved in the process.

1.3 Aim of the study

With the above in mind, the following objectives were identified for this study:

- Perform an in-depth literature study of the analytical techniques used in the analysis of scandium compounds
- Develop an analytical procedure that can accurately determine and quantify of scandium in synthetic scandium containing matrices.
- Find an alternative, but effective dissolution method for columbite-tantalite mineral ore and the residue that is friendlier to the environment.
- Develop a method to recover scandium from low grade mineral ores (columbite-tantalite in this case) and residues.
- Study the coordination behaviour of O-O'/O-S bidentate ligands for the possible selective separation of scandium from low grade ores and residues.
- Characterisation of the scandium compounds using different analytical techniques such as ICP-OES, IR and CHNS-micro analysis.
- Validation of the above mentioned methods in accordance with the criteria of the International Standards Organisation (ISO 17025).

2 Introduction

2.1 Introduction

Scandium (Sc) is a silvery-white, low-density, soft and ductile transition metal that oxidizes in air to a yellowish or pinkish colour. The metal has a molar mass of 44.956 g/mol and a melting point of 1541 °C.¹² It was first discovered in the minerals euxenite and gadolinite by Lars Fredrik Nilson in 1879 and has historically been classified as a rare earth element⁵ having chemical and physical properties similar to that of yttrium and the heavy rare earths. Later it was found that scandium exist in more than 800 types of minerals worldwide, but in very minuscule quantities¹² which contribute to a shortage of scandium worldwide.

Metallic scandium was first produced in 1937 and the first pound of 99% pure scandium metal was only produced in 1960. World production of scandium has been estimated to be in the order of 2-5 tons per year, mainly in the form of scandium oxide. Demand for scandium is steadily increasing due to its unique mechanical and chemical properties and it is currently extensively used in aerospace applications, electronics, optical and the fuel cells industries.⁵

2.2 Discovery of Scandium

In a paper published in 1871, Dmitri Ivanovich Mendeleev¹³ (1834 - 1907) not only predicted the existence of a few missing elements, but also their expected properties (as predicted by his periodic laws) on the periodic table. He called them eka-boron,

¹² Scandium, [Accessed 11-01-2015]. Available from:

<http://www.lenntech.com/periodic/elements/sc.htm>

¹³ Horovitz, C.T., (Editor), Gschneidner Jr., K.A., Melson, G.A., Youngblood, D.H. and Schock, H.H., Scandium, its occurrence, chemistry, physics, metallurgy, biology and technology, pp. 1-6, 18-31, 50-57.

eka-aluminium and eka-silicon which fascinated his fellow chemists. These three predicted elements had estimated atomic weights of 45, 68 and 70 g/mol respectively. The periodic table, in which Mendeleev predicted¹⁴ the existence of the element with the atomic weight 45 named eka-boron, is shown in **Section 1.1**, **Figure 1.1**.



Figure 2.1: Swedish chemist Lars Fredrik Nilson

In 1879, a Swedish chemist Lars Fredrik Nilson (**Figure 2.1**) and his co-workers discovered the rare earth elements erbium and ytterbium in the minerals euxenite and gadolinite (**Figure 2.2**) using spectral analysis. While working on the isolation of ytterbium, Nilson also obtain 0.35 g of a new chemical compound (later identified as Sc_2O_3) which was different from the lanthanides due to its basicity, its spectrum analysis and molar mass less than 131 g/mol.⁵

¹⁴ Scandium, [Accessed 12-09-2014]. Available from: <http://www.chemistryexplained.com/elements/P-T/Scandium.html>

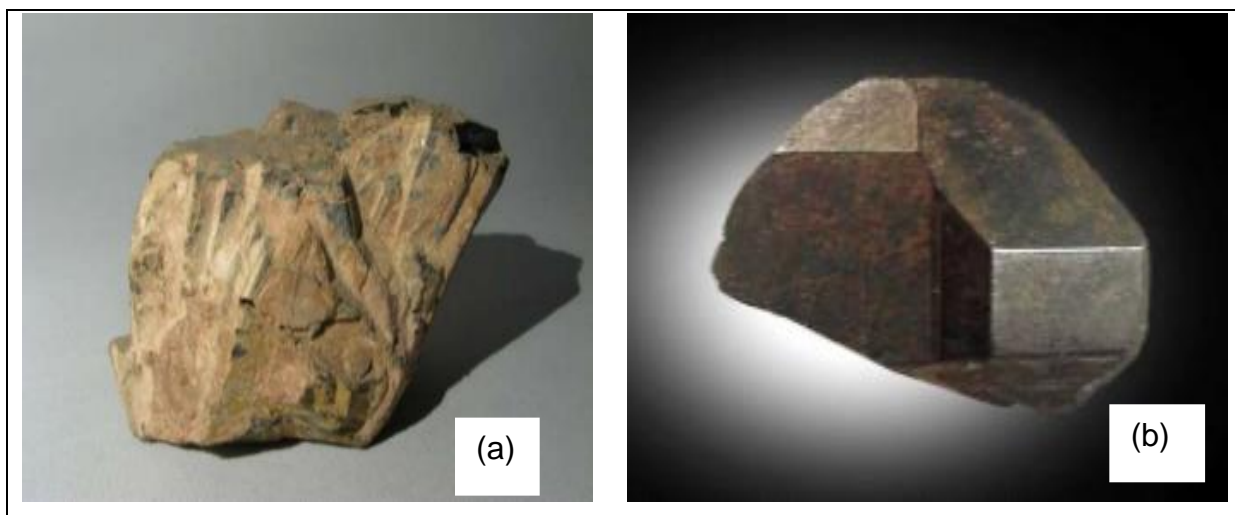


Figure 2.2: The element scandium discovered by Nilson in 1879 in the minerals euxenite (a) and gadolinite (b), which had not yet been found anywhere except in Scandinavia.¹⁵

The newly discovered element was named scandium after Scandinavia (Latin “Scandia”), the location where the two minerals euxenite and gadolinite were discovered at the time.¹³ In the process of isolating the scandium, Nilson and his co-workers were able to produce 2.0 g of pure scandium oxide (Sc_2O_3) from 10 kg of euxenite.⁵ In the same year, another Swedish chemist Per Teodor Cleve also discovered scandium and he is the one who noted, after he did a complete chemical analysis of the compound and the metal it contained, that the newly isolated element was identical to the element eka-boron predicted by Mendeleev.¹⁶

2.3 Natural occurrence of Scandium

An interesting fact is that scandium is more common in the sun (about 23rd most abundant element) and certain stars than on earth where it is about the 50th most common element. Despite the scarcity of isolated scandium, it has a relatively high abundance on earth, but the main obstacle is that it is sparsely distributed in a large number of minerals and occurs only in trace amounts in, e.g. columbite mineral

¹⁵ Skandium - inorganic chemistry, [Accessed 21-07-2014]. Available from: <http://www.slideshare.net/bs3oomusa/skandium-inorganic-chemistry>

¹⁶ Scandium: historical information, [Accessed 21-07-2014]. Available from: <http://www.webelements.com/scandium/history.html>

(0.135 %) as well as in other ores due to its inability to combine with common ore-forming anions.^{5,17} Nilson used the strong lines in the atomic spectrum of scandium to identify the element in his newly isolated products (see **Section 2.2**), and it is also these lines that enabled scientists to predict its relative abundance in stars and in the interstellar medium. In 1908, Sir William Crookes also used these spectra to report that scandium is more abundant in other stars than in our sun.¹⁸

In the work that was done on stellar and other celestial spectra, it was found that in some types of spectra scandium is conspicuously represented by some of its lines. That led Lockyer *et al.* to say that “The prominence of scandium lines in some stellar spectra and particularly in the chromospheric spectrum makes it desirable to give as complete a record of the lines as possible”.¹⁸ Five stellar classes of stars namely, A-, F-, G-, K-, and M-type, in order of decreasing temperature, produce prominent Sc lines in their spectra. In most cases this element occurs as Sc(II) with emission lines at wavelengths ranging from 424.638 – 441.556 nm.^{13,19} Sc lines are also detected at lower wavelengths in peculiar stars. There is not much further information on the abundances of scandium in stars, except for the sun which falls under the G-type of stars which has significant amounts of Sc in its core.¹³

In the first few hundred kilometres of the sun’s chromosphere, strong Sc(II) lines and the strongest Ca(II) lines are observed while ScO absorption lines are observed in the sun’s disk and sunspots light spectrogram.⁵ The scandium abundance in the solar system was found to be 34.2, calculated on the Si scale (which report the relative abundance of scandium to 10 atoms of silicon), and in the solar photosphere to be 3.10 in units numbers of atoms per 10^{12} of hydrogen.²⁰ H.W. Zhang *et al.* in their study of the non-local thermodynamic equilibrium (NLTE) of the sun also

¹⁷ Hedrick, J. B., Scandium Mineral Commodity Summaries 2010, U.S. Geological Survey, pp. 140-141, (2010)

¹⁸ Lockyer N. and Baxandall F.E., The arc spectrum of scandium and its relation to celestial spectra, In: *Proceedings of the Royal Society of London*, London, Vol. 74, pp. 538-541, (1905)

¹⁹ King, A.S., Scandium in the stars, *A paper presented at the Eighty-ninth General Meeting held at Birmingham*, **Journal of the Electrochemical Society**, Vol. 89, issue 1, pp. 301-305, (1946)

²⁰ Horovitz, C.T., Occurrence of Scandium and Yttrium in Nature, *Biochemistry of Scandium and Yttrium*, Part 1: Physical and Chemical Fundamentals, New York, pp. 135-136, (1999).

reported an average scandium value of 3.17 ± 0.10 (in units of numbers of atoms per 10^{12} of hydrogen) that was recorded by N. Gruesse *et al.* as the latest/present-day solar photospheric abundance value. In their paper about the solar chemical composition, they present the current knowledge of the solar chemical composition, based on the recent significant downward revision of the solar photospheric abundances of the most abundant elements. This value is somewhat higher than the meteoritic value, recorded as 3.04 ± 0.04 .^{21,22}

Scandium also occurs in meteorites as a dispersed trace element. One hundred and eighty stony meteorites recovered on earth were analysed by Schmitt *et al.* using neutron activation.²³ They focused on different chondrite classes and also on calcium poor- and rich-achondrites, where they found a Sc content ranging from 24 - 36, 16 - 30 and 53 - 170 atoms/ 10^6 Si for the different chondrite classes, calcium poor- and rich-achondrites respectively. In meteorites the scandium is enriched in calcic pyroxenes within the Ca-rich achondrites and also in the orthopyroxenes of the Ca-poor achondrites.²⁴ Approximate abundances for the concentration of scandium present in the different environments are shown in **Table 2.1**.

Scandium was also recovered from lunar samples collected by Apollo 11 which landed in the Mare Tranquilitas on the 20th of July, 1969. The samples were analyzed using optical spectrographic measurements (using Pd as an internal standard), and indicated the presence of scandium on the moon's surface.^{13,20} These results also indicated that the scandium on the lunar surfaces were more concentrated in the igneous rocks than in basalts, breccias and fines. Surprisingly, samples collected by Apollo 12 and Apollo 14 showed significant different Sc concentrations compared to the samples collected by Apollo 11. One of the noticeable differences was that the Sc

²¹ Zhang, H.W., Gehren, T. and Zhao, G., NLTE study of scandium in the Sun, *Astronomy & Astrophysics manuscript no. 8910*, (2013)

²² Gruesse, N., Asplund, M. and Sauval, A.J., *The solar chemical composition*, *Space Science Review*, 130, pp. 105-114 (2007)

²³ Schmitt, R.A., Goles, G.G., Smith, R.H. and Osborn, T.W., *Elemental abundances in stone meteorites: Meteoritics*, Vol. 7, No. 2, pp. 131-213, (1972)

²⁴ Mason, B., *Data of Geochemistry, Chapter B: Cosmochemistry*, Part 1: Meteorites, 6th Ed., pp. B40-B41, (1979)

content in basalt collected by Apollo 11, 12 and 14 ranged from 96.5 and 40.0 to 22.5 ppm respectively.¹³

Table 2.1: Abundances for scandium in a number of different environments^{25,26}

Location	ppb by weight	ppb by atoms
Universe	30	1
Sun	40	1
Meteorite (carbonaceous)	6,500	2,900
Crustal rocks	26,000	12,000
Sea water	0.0015	0.00021
Human	(no data)	(no data)

Earlier estimates of the abundance of scandium in the earth's crust were made by Walter and Ida Noddack²⁷ and by Goldschmidt²⁸ using data they obtained from the chemical analyses of a large number of minerals. Their calculations indicated the presence of approximately 5 to 6 g Sc/ton of mineral^{13,19} as trace amounts of Sc₂O₃ in the ferromagnesian minerals pyroxene, amphibole-hornblende and biotite. One of the few minerals having notable scandium content is thortveitite with between 44 and 48 % Sc₂O₃ which is mainly found in Norway, the United States and Madagascar. The major scandium containing mineral, thortveitite is a scandium silicate which also contains variable amounts of yttrium and rare earths, iron, aluminium, thorium, zirconium and alkaline earths. It was originally found in a granite pegmatite deposit in southern Norway. It also occurs in befanamites found in Madagascar though its occurrence is very rare.²⁹ The location of the thortveitite in Norway is shown in

Figure 2.3.

²⁵ Scandium: geological information, [Accessed 21-01-2015]. Available from:

<http://www.webelements.com/scandium/geology.html>

²⁶ The element scandium, [Accessed 21-01-2015]. Available from:

<http://www.elementalmatter.info/element-scandium.htm>

²⁷ Noddack, I. and Noddack, W., *Naturwissenschaften*, Vol. 18, p 757, (1930)

²⁸ Goldschmidt, V. M., *The principles of distribution of chemical elements in minerals and rocks*, **Journal of the Chemical Society.**, part 1, pp. 655-673, (1937)

²⁹ Kleber, E.V. and Love B., *The technology of Scandium, Yttrium and the rare earth metals*, pp. 11-13, (1963)

Worldwide, scandium resources are found in Australia, Norway, Madagascar, Kazakhstan, Russia and China. In Australia, scandium is contained in nickel and cobalt deposits in Syerston and Lake Innes, New South Wales. Resources in Norway are distributed in the thortveitite-rich pegmatites of the Iveland-Evje region and a deposit in the northern area of Finnmark. Scandium in Madagascar is found in pegmatites in the Befanamo area. In Kazakhstan, the resource of scandium is in uranium-bearing deposits and in Russia in the Kola Peninsula apatites. China's resources are in tungsten, iron, and tin deposits in Fujian, Guangdong, Guangxi, Jiangxi, and Zhejiang provinces.^{6,7} See **Figure 1.3** for the worldwide scandium sources. Undiscovered scandium resources are thought to be very large and yet to be discovered.

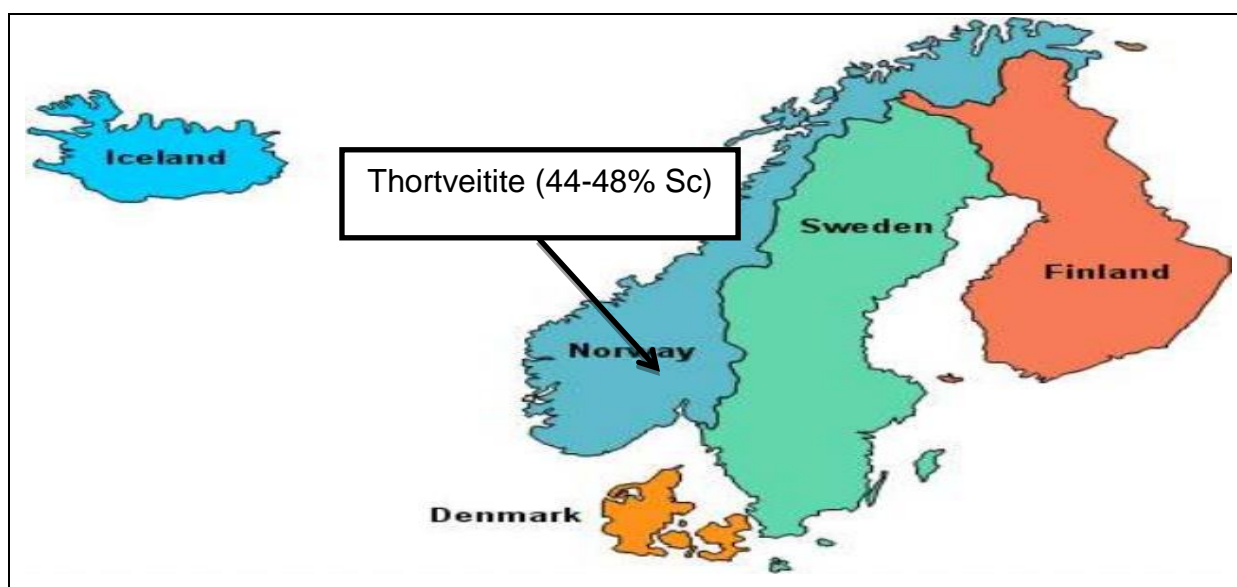


Figure 2.3: Locations of significant thortveitite deposits¹⁵

Other rare minerals which also contain scandium as trace element are bazzite, kolbeckite, magbasite, perrierite-Sc, ixiolite-Sc, rare-earth minerals (such as monazite, bastnasite, and gadolinite), wolframite, columbite, cassiterite, beryl, garnet, muscovite and the aluminium phosphate minerals.^{13,30} Some of the minerals that contain scandium and their chemical formulas are listed in **Table 2.2**. **Table 2.3** shows the analytical results of two thortveitites found in Iveland and in Befanamo.

³⁰ Duyvesteyn, W.P.C. and Putnam, G.F., Scandium, A review of the element, its characteristics, and current and emerging commercial applications, EMC Metals Corporation white paper, (2014)

Table 2.2: Minerals containing scandium

Mineral	Formula
Bazzite	$\text{Be}_3(\text{Sc,Al})_2\text{Si}_6\text{O}_{18}$
Cascandite	$\text{Ca}(\text{Sc,Fe}^{++})\text{Si}_3\text{O}_8(\text{OH})$
Juonniite	$\text{CaMgSc}(\text{PO}_4)_2(\text{OH}) \cdot 4(\text{H}_2\text{O})$
Jervisite	$(\text{Na,Ca,Fe}^{++})(\text{Sc,Mg,Fe}^{++})\text{Si}_2\text{O}_6$
Heftetjernite	ScTaO_4
Pretulite	ScPO_4
Thortveitite	$(\text{Sc,Y})_2\text{Si}_2\text{O}_7$
Scandiobabingtonite	$\text{Ca}_2(\text{Fe}^{++},\text{Mn})\text{ScSi}_5\text{O}_{14}(\text{OH})$
Titanowodginite	$\text{Mn}^{++}(\text{Ti,Ta,Sc})_2\text{O}_8$
Kolbeckite	$\text{ScPO}_4 \cdot 2(\text{H}_2\text{O})$
Magbasite	$\text{KBa}(\text{Al,Sc})(\text{Mg,Fe}^{++})_6\text{Si}_6\text{O}_{20}\text{F}_2$

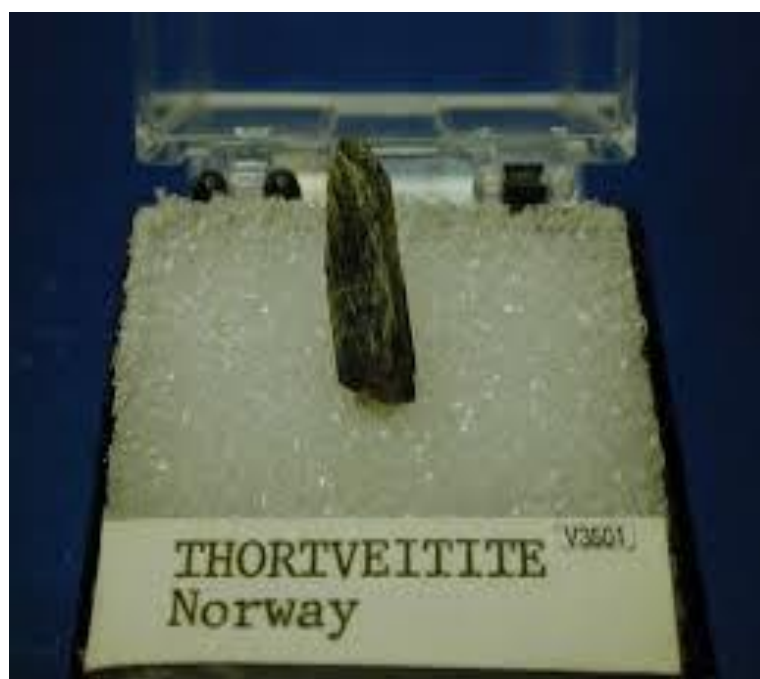


Figure 2.4: Thortveitite from Norway³¹

³¹ Thortveitite from Norway, [Accessed 23-02-2015]. Available from: http://www.beryllen.no/produkter/finn/minerals-from-a-z_thortveitite

Table 2.3: Results of microprobe analysis of thortveitite from different locations¹³

Composition	Iveland, Norway (%)	Befanamo, Malagasy (%)
SiO ₂	46.1	45.5
Sc ₂ O ₃	48.2	44.4
Y ₂ O ₃	2.2	5.1
Fe ₂ O ₃	2.1	2.2
Al ₂ O ₃	0.3	0.3
HfO ₂	–	0.9
ZrO ₂	–	traces

– not detected

Kolbeckite (**Figure 2.5**) is a mineral that also contains scandium in appreciable quantity, is white in colour and usually found in Austria. It was discovered originally at Schmiedeberg, Saxony, Germany in 1926 and it was named after Friedrich L. W. Kolbeck (1860-1943), a mineralogist from the Mining Academy in Freiberg Germany.³² Its chemical composition is presented in **Table 2.4**.



Figure 2.5: Spherical ball of kolbeckite

³² Kolbeckite mineral data, [Accessed 23-02-2015]. Available from: <http://webmineral.com/data/Kolbeckite.shtml#.VRU1nGdxIFo>

Bazzite, (**Figure 2.6**) is a mineral with a blue colour that contains scandium and is found in Switzerland. Its chemical composition is reported in **Table 2.4**.

Table 2.4: Chemical composition of kolbeckite and bazzite samples from Switzerland^{31,32}

Composition	Kolbeckite, Germany (%)	Composition	Bazzite, Switzerland (%)
Sc ₂ O ₃	36.8	SiO ₂	64.8 (29)
V ₂ O ₃	1.28	Sc ₂ O ₃	15.1 (4)
Fe ₂ O ₃	0.9	BeO	13.8 (5)
Al ₂ O ₃	0.3	Fe ₂ O ₃	8.3 (3)
P ₂ O ₅	40.3	Al ₂ O ₃	0.5 (2)
H ₂ O	20.5		

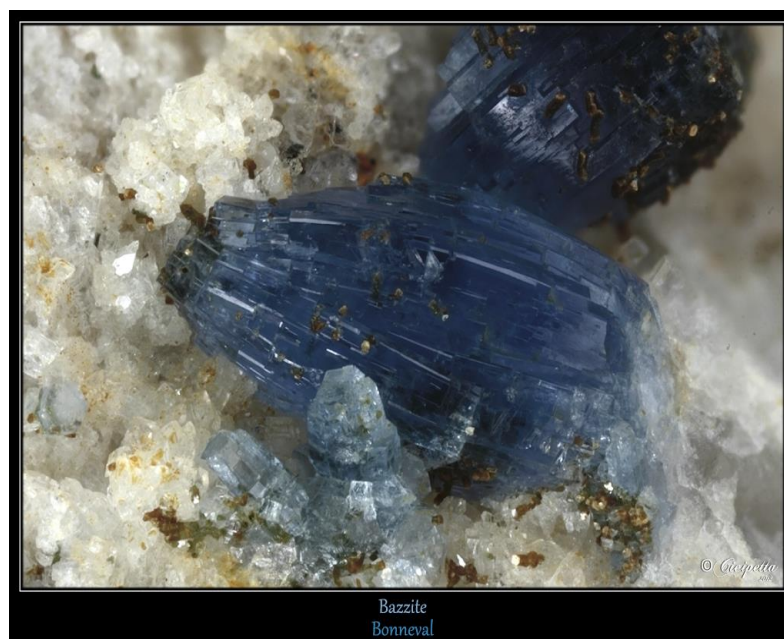


Figure 2.6: Bazzite mineral³³

³³ Bazzite, [Accessed 23-02-2015]. Available from:
<https://mineralogiquementvotre.wordpress.com/tag/bazzite/>

Scandium also occurs in the earth's atmosphere and in natural water bodies in some parts of the world. In the Keiyo industrial area in Japan the mean scandium content of 0.02 µg/mg ash was reported while the soft water from six unnamed rivers in England showed a mean concentration of 17.0 ppb Sc, with large variations ranging from < 0.1 to 28.0 ppb Sc for these water sources.¹³ Analyses for scandium and 13 other elements in seawater samples collected at various locations in the Pacific and Atlantic Oceans were done by Robertson *et al.* (1968).¹³ The scandium concentration determinations indicated a mean of about 0.007 ppb in the Atlantic and Pacific Ocean surface waters along the Central American and Mexican Coasts.^{13, 34}

2.4 Scandium production, market and beneficiation

2.4.1 Scandium production

The production of scandium remained a small scale enterprise from its discovery through the 1970's. In 1940, scandium bearing minerals, which were associated with variscite nodules, were identified. Initially the mineral kolbeckite ($\text{ScPO}_4 \cdot 2(\text{H}_2\text{O})$) was identified as a primary source of scandium production and commercial production and beneficiation began in the 1950's.³⁵ During this time, the Kaweck Chemical Company in the US pursued scandium beneficiation in the phosphate bearing material associated with a variscite mine in Utah (Little Green Monster). The refining of the material however proved to be very challenging.³⁰ It is reported that two samples of phosphate bearing material totalling over 4,300 pounds were shipped to the Kaweck facility and the grades for the two sample batches were reported to average 0.14 % and 0.10 % scandium by weight.^{35,36} These low Sc concentrations and probably the difficulty associated with isolation and purifying the scandium from this material prompted the Kaweck Chemical Company to shut the mine. **Figure 2.7**

³⁴ Amakawa, H., Nomura, M., Sasaki, K., Oura, Y. and Ebihara, M., Vertical distribution of scandium in the north central Pacific, **Geophysical Research Letters**, Vol. 34, pp. 1-4, (2007)

³⁵ EMC signs option agreement to acquire former scandium production site in Utah, USA, [Accessed 22-05-2015]. Available from: <http://www.siliconinvestor.com/readmsg.aspx?msgid=27635631>

³⁶ Frondel, C., Ito, J. and Montgomery, A., Scandium content of some aluminium phosphates, **American Mineralogist**, Vol. 53, pp. 1223-1231, (1968)

shows the Utah region where variscites and kolbeckite were initially mined, with the inserted photo showing a sample of the kolbeckite mineral ($\text{ScPO}_4 \cdot 2\text{H}_2\text{O}$) from the Little Green Monster Variscite Mine, Clay Canyon, Fairfield, Oquirrh Mts, Utah Co., Utah in USA.³⁷

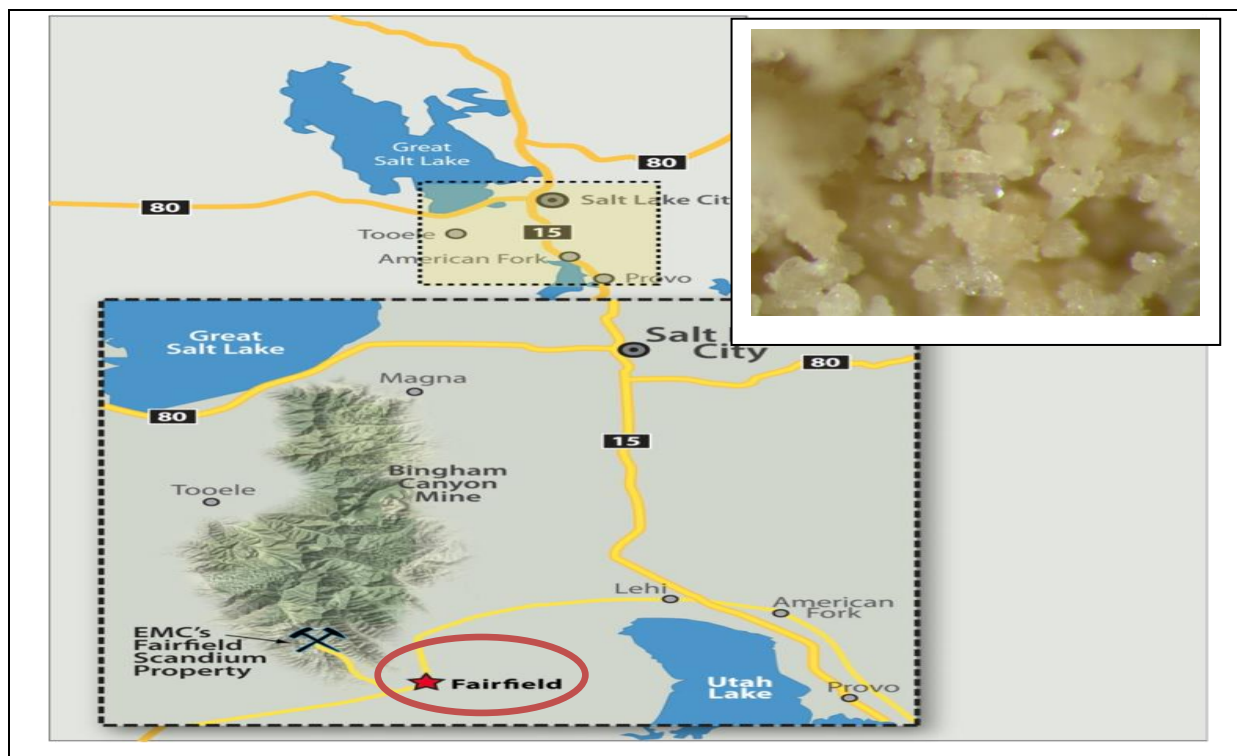


Figure 2.7: The Utah region, inserted is kolbeckite ($\text{ScPO}_4 \cdot 2\text{H}_2\text{O}$) from the Little Green Monster Variscite Mine.

At about the same time, a number of Russian metallurgists were also actively searching for and experimenting with scandium. In Russia, the scandium production began in the Cold War era at the Nova Mine, near the town of Zhovti Vody in the Ukraine, which initially flourished due to the mining of iron and later in the 1950's to the mining of uranium. The 1,000 meters deep Nova mine was known to be a polymetallic resource with large quantities of iron, but it also contained acceptable amounts of scandium, uranium and other radioactive minerals. The scandium resource was estimated to be 7.9 M tonnes with a 105 ppm scandium grade and it was believed to be the only operational scandium mine in the world. Later, the Russians discovered enriched zones in the same area with Sc yields in excess of

³⁷ Kolbeckite, [Accessed 20-05-2015]. Available from: <http://www.mindat.org/photo-132770.html>

100 g/t plus which were then separately mined to produce Sc_2O_3 . The scandium produced from this source was mainly used in the production of the aluminium-scandium (AlMgLi-Sc) master alloy that was used to manufacture the USSR's advanced MiG fighter jets.^{30,38}

At the end of the Cold War, a US metals specialty company called Ashurst Technologies ("Ashurst") formed a joint venture with the Eastern Ore Dressing Kombinat (VostGOK) and the I.N. Frantsevich Institute for Problems of Materials Science to get a controlling share in the Nova mine. Ashurst effectively retained 35% interest in the mine, along with an off-take agreement on all of the scandium products produced. Scandium was recovered and refined at the VostGOK's facilities and the Sc-Al master alloy (2 % Sc content) was also produced and globally sold by Ashurst.^{30,38} During 1996 the Ashurst Company sold about 2 tonnes of the 2 % master alloy, and a similar amount in the first 5 months of year 1997. No commercial data was filed after the 2nd quarter of 1997 and the company ceased trading thereafter. The Nova mine continued to produce Sc_2O_3 for approximately 5 more years, but after a labour strike that took place in 2002, the mine was closed indefinitely and was later flooded with groundwater. In 2003, after attempts to reopen the facility, the mine was permanently closed.³⁰ Stockpiles of scandium oxide and scandium master alloy which was produced in the Cold War era still remains in Russia. How much of the stockpiles remained is unclear, but it is reported that these stockpiles are diminishing gradually as it is been sold in the market today, while the Russian military still buy and uses the master alloy from these stockpiles.³⁸

³⁸ Kaiser, J.A., Recommendation Strategy for EMC Metals Corp, 2014, [Accessed 27-05-2015]. Available from: <http://mininginteractive.com/pdf/KaiserEMCComment20140423.pdf>



Figure 2.8: Inner Mongolia region in China where Bayan Obo rare earth mine is situated.³⁹

China also represents another significant source of scandium deposit and production, the mineral rich Bayan Obo rare earth mine complex (190 known mineral species are present) in Inner Mongolia (**Figure 2.8**), but the scandium production rate from this deposit is unknown (**Figure 2.9**). The various ore types located in this area have different scandium concentrations, ranging from 40 ppm to 169 ppm while the REE tailings also produce scandium waste with high grades, which can reach up to 250 ppm Sc.³⁰

³⁹ Kurt's China photos - Baiyunebo- summer 2004, [Accessed 25-05-2015]. Available from: http://faculty.kutztown.edu/frieauf/china_nei_mengu_2004/baiyunebo.html

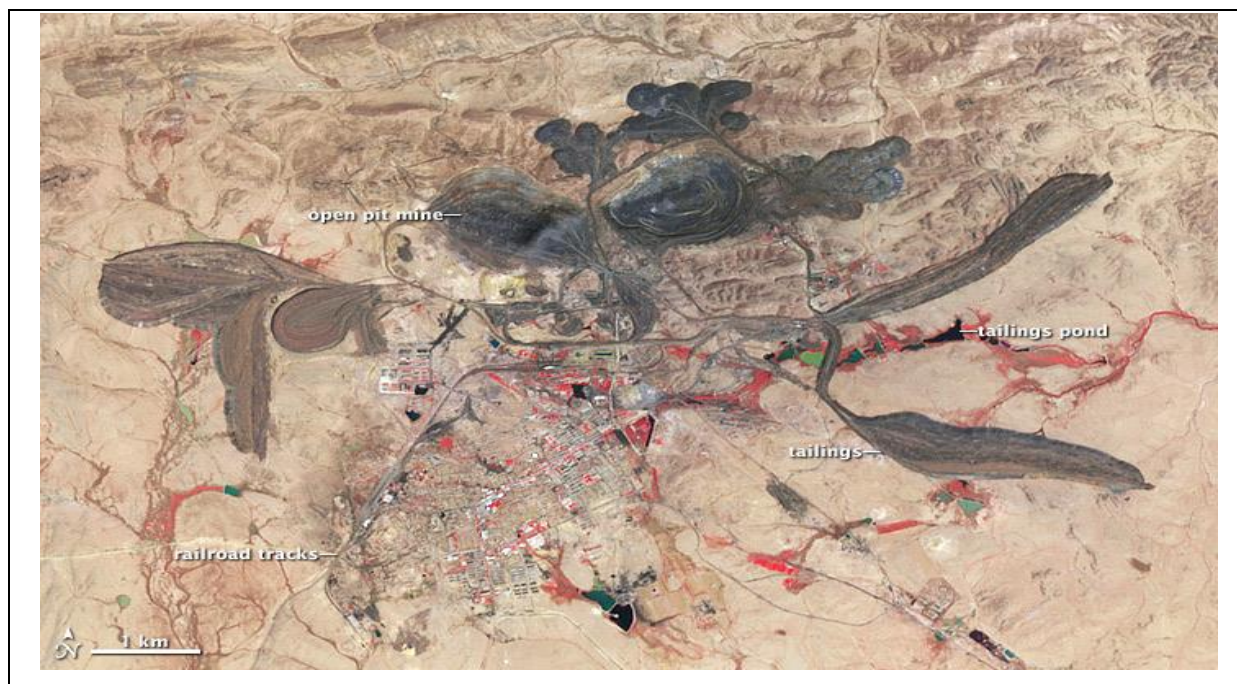


Figure 2.9: Bayan Obo deposit image by NASA⁴⁰

The Minerals Commodity Summary on scandium published by the United States Geological Survey (USGS), estimate the scandium oxide price as US\$5,000/kg for 99.99 % grade (2013), with higher pricing for higher purities.⁴¹ Volumes traded globally are defined as ‘very small’ relative to most other metals with less than 10,000 kg (10 tonnes) traded in that year and it is quoted that the global market for scandia volumes are between 2 and 10 tonnes/year, see **Section 1.2**. Estimations also shows that less than half a tonne is produced through actual mining operations each year, with the major amounts produced by the Bayan Obo deposits and the rest sourced from the former Soviet Union’s stockpiles.

Recently the Russian aluminium producer RUSAL launched a pilot-plant study to produce scandium concentrate from red mud (a residue generated during the production of aluminium). It has been reported that the plant will have the capacity to

⁴⁰ Rare Earth in Bayan Obo, [Accessed 27-05-2015]. Available from:
<http://earthobservatory.nasa.gov/IOTD/view.php?id=77723>

⁴¹ Gambogi, J., Scandium Mineral Commodity Summaries 2015, U.S. Geological Survey, pp. 140-141, (2015)

produce 2.5 tonnes per year of concentrate.^{41,42} The ORBITE Aluminae's pilot-plant in Canada also plans to produce scandium concentrate from red mud and indicated that at current projected production rates, the facility could produce 60 tonnes of scandium annually, which is a relatively large quantity in light of the current market.⁸ The measured and indicated resources of a scandium-cobalt-nickel deposit near Greenvale in Northern Queensland, Australia (**Figure 2.10**) are estimated to include 3,970 tonnes of scandium oxide, using a 1 % nickel-equivalent as cut-off grade. If developed, this deposit can become one of the leading scandium sources worldwide.^{41,43}

⁴² UC RUSAL launches pilot unit at Urals aluminium smelter for the production of scandium concentrate, [Accessed 26-04-2015]. Available from: http://www.rusal.ru/en/press-center/news_details.aspx?id=10866&ibt=13&at=0

⁴³ Scandium, geological survey of Queensland, department of natural resources and mines, [Accessed 16-10-2014]. Available from: https://www.dnrm.qld.gov.au/_data/assets/pdf_file/0019/238114/scandium.pdf

The Scandium International Mining Corporation (SCY), formerly the EMC Metals Corporation and previously part of a joint venture with Jervois Mining Limited of Melbourne, now owns 100 % of the Nyngan Scandium Project (**Figure 2.11**), located in New South Wales in Australia.⁴⁴ Preliminary economic assessments for the production of scandium in October 2014 by SCY advanced this project to a feasibility level with the objective of being the first international company to achieve production from a primary scandium mine. Subject to economic assessment, this company expects to complete the feasibility study late in 2015, with the objective to commence with mine construction in 2016 and the first scandium production in 2017. The assessment concluded that the project has the potential to produce 36 metric tonnes of scandium oxide per year using high pressure acid leaching and solvent extraction as beneficiation techniques.^{38,41,44}

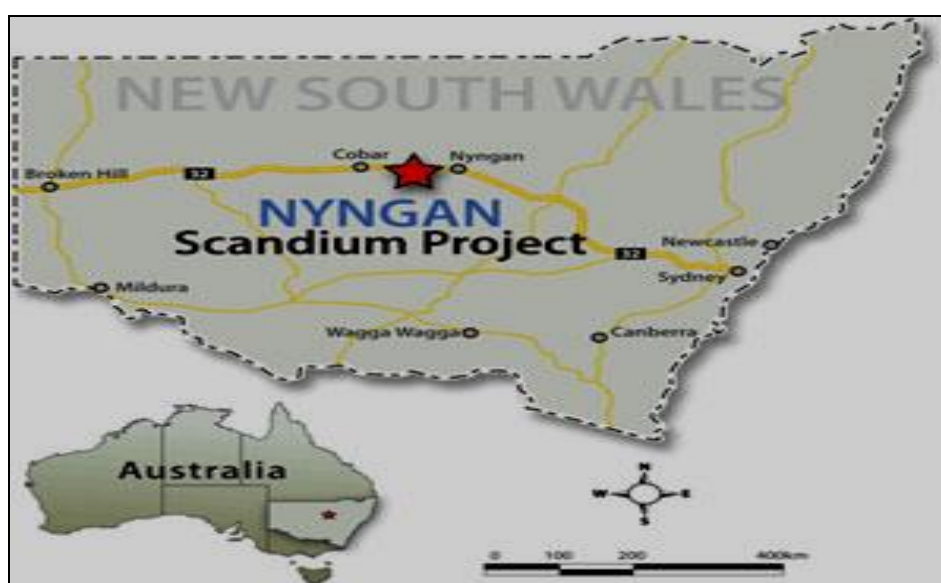


Figure 2.11: New South Wales region where the Nyngan scandium project is taking place⁴⁴

2.4.2 Scandium market

Indications are that China is currently the biggest scandium supplier worldwide. Although sales contracts, including prices and quantities, often remain confidential,

⁴⁴ EMC makes first settlement payment on Nyngan scandium project, controls 100% of project in Australia, [Accessed 16-05-2015]. Available from:

<http://www.scandiummining.com/s/newsreleases.asp?ReportID=590391>

the current price range for scandium is believed to be between US\$1,000/kg and US\$ 4,500/kg.⁸ The potential demand for scandium may greatly exceed current production if prices were lower. Interestingly the USGS reports that most concentrated reserves of scandium remain undiscovered and unexploited due to logistical reasons, difficulties in accessing promising areas, and the generally low concentrations in which scandium occurs. Scandium's potential use in various high technology applications and its current high prices prompted many mining companies to initiate the exploration of new scandium deposits, aiming to uncover scandium resources in significant concentrations.⁴¹ A market study indicated that scandium metal prices increased moderately over the last few years, but the overall market remained very small. The market prices for most of the scandium products including scandium metal (ingot), scandium acetate, scandium chloride and scandium iodide compounds decreased drastically in 2014, see **Table 2.5**. This might be due to the fact that scandium production is increasing thereby resulting in an over-supply on the world market.

Table 2.5: Scandium compound prices from 2010 up to 2014^{41,45}

Prices in US\$/gram					
Compounds	2010	2011	2012	2013	2014
Scandium oxide, 99.99% purity	1.620	4.700	4.700	5.000	NA
Scandium oxide, 99.999% purity	2.540	5.200	5.200	5.000	NA
Scandium oxide, 99.9995% purity	3.260	5.900	5.900	6.000	NA
Scandium acetate, 99.9% purity	47.00	48.40	50.10	51.90	43.00
Scandium chloride, 99.9% purity	62.40	138.00	143.00	148.00	123.00
Scandium fluoride, 99.9% purity	229.00	235.80	244.00	253.00	263.00
Scandium iodide, 99.999% purity	207.00	213.00	220.00	228.00	187.00
Scandium-aluminium alloy	0.074	0.22	0.22	0.155	NA
metal, dendritic	193.00	199.00	206.00	213.00	221.00
metal, ingot	158.00	163.00	169.00	175.00	134.00

NA – Not Available

⁴⁵ Gambogi, J., Scandium Mineral Commodity Summaries 2014, U.S. Geological Survey, pp. 140-141, (2014)

The price for scandium oxide changed little from 2011 through 2013, although prices for the other scandium compounds increased. **Figure 2.12** clearly shows the change in scandium oxide prices from 1991 to 2013.

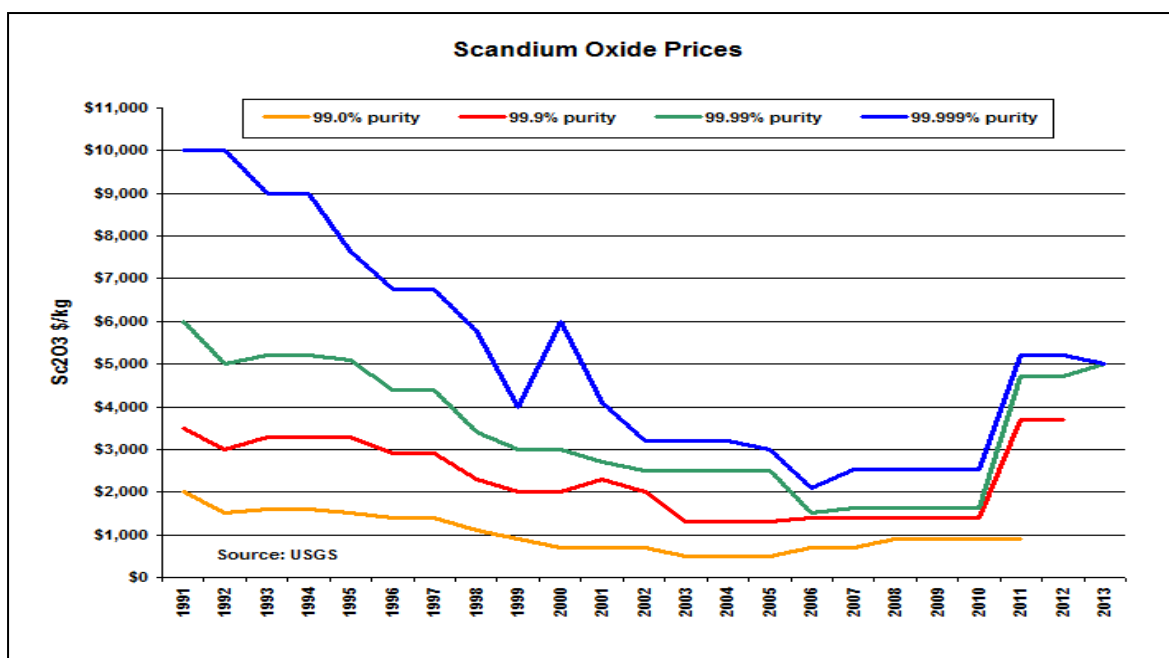


Figure 2.12: Sc₂O₃ prices from 1991 to 2013³⁶

2.4.3 Scandium beneficiation

In most cases scandium is produced as a by-product during the processing of various ores and is found in the enriched slags, residues, tailings and waste liquors of these processes. The easiest method to recover scandium from scandium-containing solutions is by the precipitation of insoluble scandium compounds such as scandium oxalate. However, the co-precipitation of other metals makes it usually difficult and unsuitable for recovery of scandium from solutions that contain large amounts of other impurities.⁴⁶ Currently, hydrometallurgical processes, which mainly involve leaching, solvent extraction and precipitation are commonly used for scandium recovery.

The high scandium content (43 %) in thortveitite and kolbeckite are recovered from the ore by fractional sublimation as ScCl₃. The finely milled ore and coal are heated

⁴⁶ Wang, W., Pranolo Y. and Cheng C.Y., Metallurgical processes for scandium recovery from various resources: A review, **Hydrometallurgy**, Vol. 108, pp. 100–108, (2011)

to 900 - 1000 °C with a current of chlorine gas passing over them. The chlorides of silicon, titanium, aluminium, iron and zirconium are sublimated as their sublimation temperature points are below 350 °C and removed/separated from the Sc. Scandium chloride which sublimate at about 967 °C are deposited in a state of high purity in a zone where the temperature decreased to about 400 °C with yttrium chloride remaining in the residue.

Another thortveitite ore beneficiation process comprises a comminution process of the ore by wet autogenous grinding to substantially liberate the thortveitite contained therein and passing the comminuted ore through a non-uniform magnetic field to produce a concentrate and a tailing, with chemical analysis indicating a substantially higher percentage thortveitite in the concentrate compared to the original ore. In this process the ore is upgraded from approximately 1,050 to 12,050 ppm scandium. If the non-magnetic fraction from such a test is recycled, an additional 2.4 % of the scandium can be recovered yielding a concentrate with about 9,660 ppm scandium.⁴⁷

The beneficiation process for other scandium-containing ores begins with the mining and crushing of the ore, followed by a suitable pre-treatment step to prepare the feedstock for subsequent processing. The ore is then subjected to leaching in order to recover the scandium from it. The leachate is separated from the solids through a solid-liquid separation process and then treated with lime to neutralise its acid content and then disposed of. Meanwhile, the leachate is subjected to solution purification and the pH is adjusted by the addition of base while the recovered solvent is recycled to the leaching step. The scandium is removed by the addition of oxalic acid which precipitates as scandium oxalate. The recovered scandium oxalate is washed with water and subjected to calcination to finally yield the Sc_2O_3 product. The waste water and the solvent recovered from the solid-liquid separation process are then utilised in a reagent recycle, and the recycled reagents are used in further iterations of the ore pre-treatment process.⁴⁸ A detailed flow diagram of the process is presented in **Figure 2.13**.

⁴⁷ Birmingham, S.D., Thortveitite ore beneficiation process, Colo, U.S.P., 5035365. pp. 1–6, (1991)

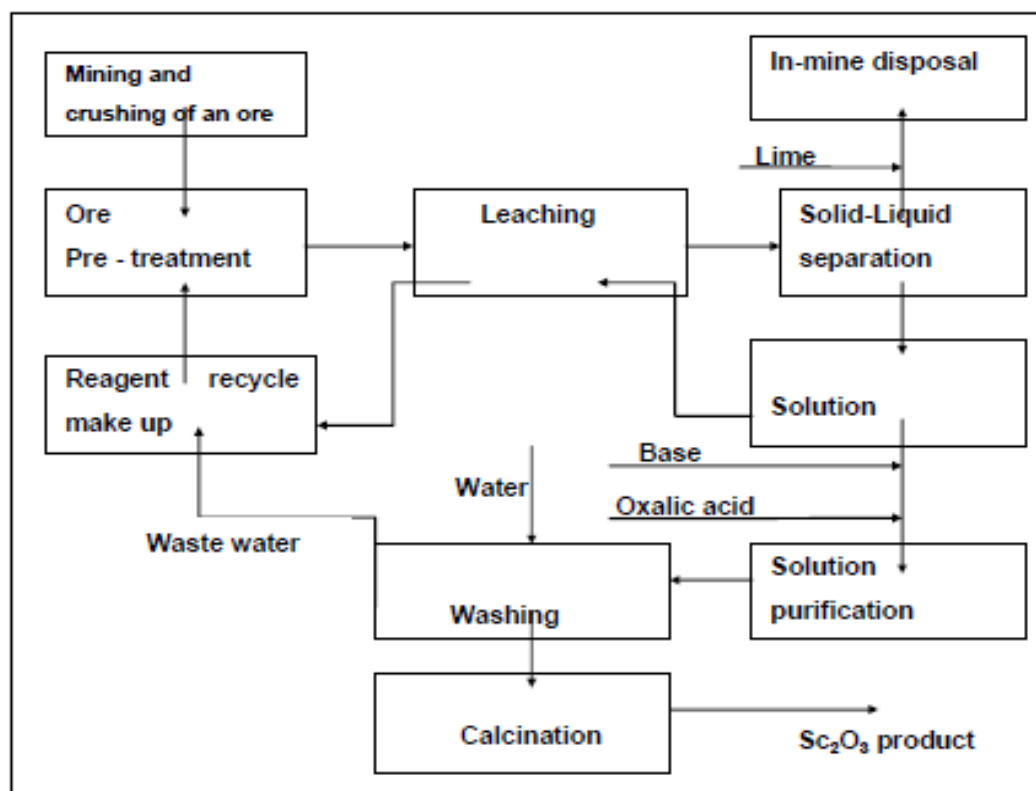


Figure 2.13: The extraction of scandium from scandium-containing ores.⁴⁸

Scandium can also be recovered as a by-product from nickel and cobalt extraction operations. A typical nickel laterite ore contains trace amounts of Sc (0.005 - 0.006 %).⁴⁹ Scandium is leached with sulphuric acid from the nickel laterite ore in the high pressure acid leach (HPAL) process which recover over 94 % of the scandium. After removal of iron and aluminium by neutralisation in the pH range of 2 - 4 (precipitation of the hydroxides) and nickel and cobalt are separated (precipitated) as the sulphides, the scandium is precipitated from the solution by increasing the pH to above 4. Some impurities co-precipitate with scandium and the scandium is separated from these impurities using solvent extraction. Quantitative scandium extraction may be achieved using acidic organo-phosphorus extractants such as di-(2-ethylhexyl) phosphoric acid (HDEHP).⁴⁶

⁴⁸ Duyvesteyn, W.P.C., System and method for recovery of scandium values from scandium-containing ores, Reno, U.S.P., US 2012/0207656 A1. pp. 1-6, (2012)

⁴⁹ Haslam, M. and Arnall, B., An investigation into the feasibility of extracting scandium from nickel laterite ores. In: *Proceeding of ALTA 1999 Nickel/Cobalt Pressure Leaching & Hydrometallurgy Forum. ALTA Metallurgical Services, Perth, Australia, (1999)*

Several mining companies are developing plants for scandium recovery from nickel laterites and are expected to produce scandium oxides in large amount. The Nyngan project for example plans to construct a hydrometallurgical plant which is designed to produce 28,000 kg of Sc_2O_3 /year.⁴⁴ The Ni-Co-Sc laterite processing plant will involve a high atmospheric acid leach process that is being developed for the NORNICO project near Greenvale, Queensland (see **Section 2.5.1**). High-purity scandium oxide production from this is estimate to be 10,000 – 40,000 kg/year.^{43,46}

Rare earth deposits and uranium ores are also very important sources of scandium. **Figure 2.14** details two flow diagrams **(a)** and **(b)** for scandium beneficiation using ionic-adsorption as separation technique involving rare earth deposits (IARED) and uranium ores respectively.

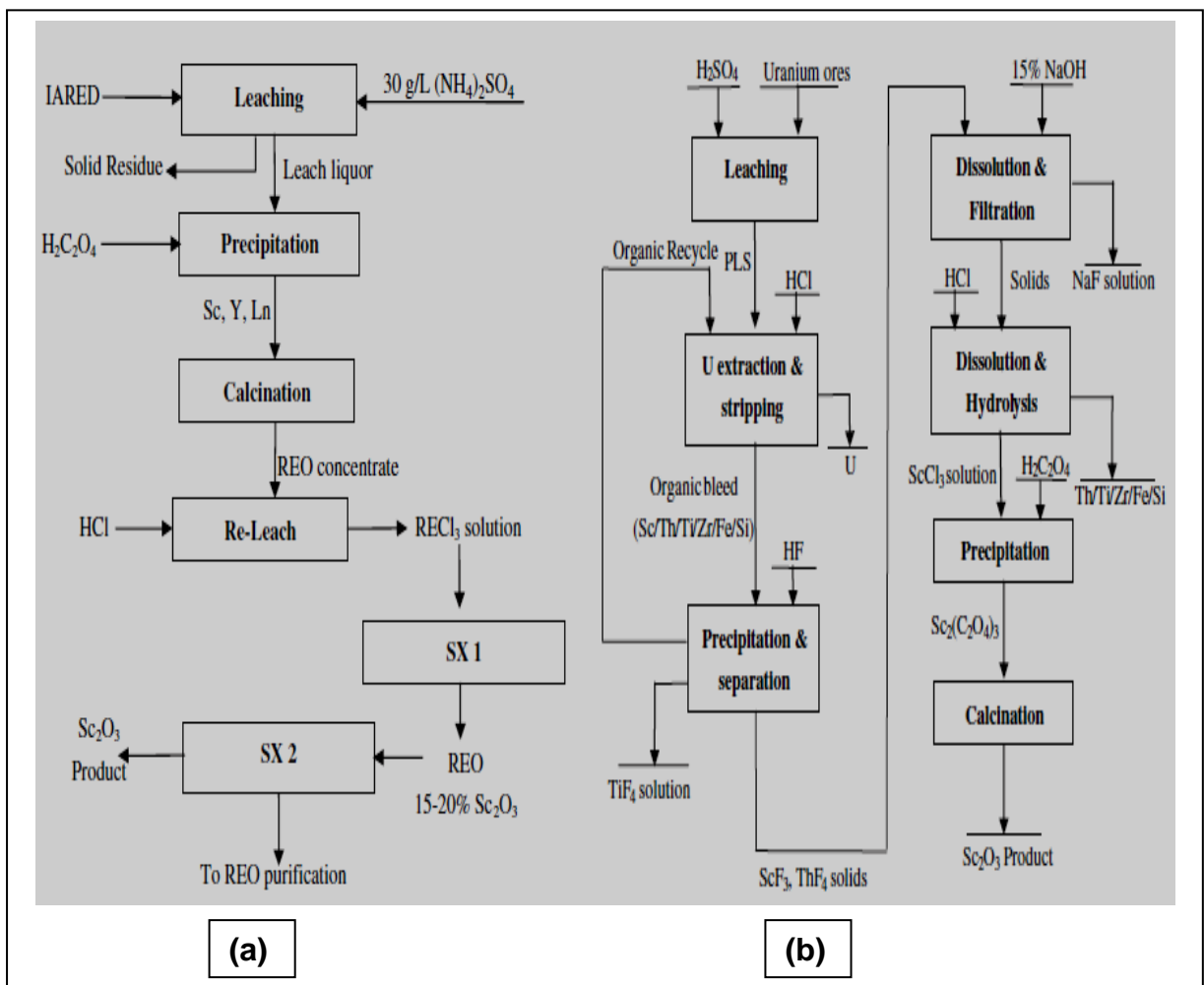


Figure 2.14: The detailed flow diagrams of the beneficiation of scandium in IARED (a) and uranium ores (b).⁴⁶

Further steps are taken to prepare pure scandium metal from scandium oxide. Scandium fluoride (ScF_3) is first prepared by heating Sc_2O_3 in a platinum boat under an anhydrous HF-Ar gas mixture at 600 - 750 °C for 16 hours. Scandium fluoride is then reduced with metallic calcium to produce pure scandium metal (**Equations 2.1 and 2.2**).¹³



2.5 Applications and uses of scandium

Scandium has a number of interesting applications in industry, ranging from the manufacturing of sports equipment, aluminium-scandium master alloys, lighting, to fuel cell technology. Scandium is widely used in the aerospace industry due to its strength-to-weight benefits and is used as substitutes for aluminium-lithium and aluminium-titanium alloys due to its higher melting point (it reduces susceptibility to heat-cracking) and lower prices. These Al-Sc master alloys typically contain only 2 % Sc. The minute amounts of scandium in these aluminium alloys has an effect of refining the grain size during casting and welding which increases its superplastic properties, inhibiting recrystallisation, increasing the strength of aluminium and enhancing its fatigue resistance (see **Section 1.1**).⁵⁰ Some of these alloys are also used in sporting equipment. These light, high strength alloys are mainly used in high performance sporting equipment such as baseball bats, bicycle frames, lacrosse sticks or golf clubs.⁵¹ Scandium alloy is also used to produce/manufacture high strength hand gun frames for the same reason due to its weight and strength properties, while Russia uses the scandium-aluminium alloy in the production of their MiG fighter aircrafts.^{8,30} **Figure 2.15** shows some of the scandium applications.

⁵⁰ Wang, W. and Cheng, C.Y., Separation and purification of scandium by solvent extraction and related technologies: A review, **Journal of Chemical Technology and Biotechnology**, Vol. 86, Issue 10, pp. 1237–1246, (2011)

⁵¹ Gongyi, G., YuH, C. and Yu, L., Solvent Extraction of Scandium from Wolframite Residue, **Journal of Metals**, Vol. 40, Issue 7, pp. 28-31, (1988)



Figure 2.15: Scandium applications.⁵²

⁵² Scandium, [Accessed 13-06-2015]. Available from: <http://www.reehandbook.com/scandium.html>

The element scandium is also used to synthesize scandium iodide which is added to mercury vapour lamps to produce a highly efficient light source that resembles sunlight. This 'daylight' effect is desirable for camera lighting, as well as movie and television studio lights. In Solid Oxide Fuel Cells (SOFC's), **Figure 2.16**, scandia can substitute yttria as a stabilizing agent for the solid electrolyte (typically scandia-stabilised zirconia (ScSZ)) in the fuel cell to produce more efficient cells at lower temperatures which provide more efficient on-site electricity and heating.^{30,53}



Figure 2.16: A 40 cell internally-manifolded SOFC stack³⁰

Scandium is also used in the electronics industry for the manufacturing or preparation of the laser material $Gd_3Sc_2Ga_3O_{12}$, gadolinium scandium gallium garnet (GSGG) while ferrites and garnets containing scandium are primarily used in switches in computers.⁴³ Scandium compounds are also used as hosts for phosphorus or as the activator ion in TV or computer monitors with Sc_2O_3 and $ScVO_4$ typical the host materials. In ceramics, the addition of about 20 % scandium carbide to titanium carbide results in a doubling of the hardness to about 50 GPa for the mixed Ti-Sc carbide, second only to diamonds in hardness.^{30,54} The current cost of scandium however dictates the use of the element in other materials.

⁵³ Onghena, B. and Binnemans, K., Recovery of Scandium(III) from Aqueous Solutions by Solvent Extraction with the Functionalised Ionic Liquid Betainium Bis(trifluoromethylsulfonyl)imide, **Ind. Eng. Chem. Res.**, Vol. 54, pp. 1887-1898, (2015)

⁵⁴ Zhang, P., You, S., Zhang, L., Feng, S. and Hou, S., A solvent extraction process for the preparation of ultrahigh purity scandium oxide, **Hydrometallurgy**, Vol. 47, pp. 47-56, (1997)

2.6 Physical and chemical properties

Scandium is a soft, silvery-white metallic element with an atomic number of 21, and is technically regarded as one of the earlier transition metals. The metal exhibit some characteristics that are similar to the rare-earth elements (lanthanides), and is often classified along with yttrium as a member of the REE group. The smaller size of scandium's ion allows it to react chemically with elements like aluminium, magnesium and zirconium. Scandium exists in nature in its oxide form, and tarnishes to pink or yellow. It is very difficult to reduce it to its pure elemental state. Scandium's reduction equation is $\text{Sc}^{3+} + 3\text{e} \rightarrow \text{Sc}$, with a standard reduction potential of $E^\circ = -2.03 \text{ V}$.⁵⁵

⁵⁵ Bard, A.J., Parsons, R. and Jordan, J., Standard Potential in Aqueous Solution, p. 585, (1985)

Table 2.6: Scandium's physical and chemical properties^{56,57,58}

Property	Value	Property	Value
Appearance	Silvery-white	Electronegativity	1.36 (Pauling scale)
Element category	Transition metal	Ionisation energy (1 st , 2 nd , 3 rd)	633.1, 1,235.0, 2,388.6 kJ/mol
Group, period, block	3,4,d	Atomic radius	162 pm
Standard atomic weight	44.955912(6) g/mol	Covalent radius	170±7 pm
Electron configuration	[Ar]3d ¹ 4s ²	Van der Waals radius	211 pm
Electrons per shell	2,8,9,2	Crystal structure	Hexagonal
Phase	Solid	Magnetic ordering	Paramagnetic
Density	2.985 g/cm ³	Electrical resistance	(r.t) 562 nΩ.m
Melting point	1,814 K	Thermal conductivity	(300 K) 15.8 W/m.K
Boiling point	3,109 K	Young's modulus	74.4 GPa
Heat of fusion	14.1 kJ/mol	Shear modulus	29.1 GPa
Heat of vaporisation	377.8 kJ/mol	Bulk modulus	56.6 GPa
Specific heat capacity	(25 °C) 25.52 J/mol.K	Poisson ratio	0.279
Oxidation states	3, 2, 1(amphoteric)	Brinell hardness	750 MPa

⁵⁶ Neikov, O.D., Naboychenko S.S. and Dowson G., Handbook of non-ferrous metal powders, Technologies and applications, 1st Ed., p. 524, (2005)

⁵⁷ Scandium, [Accessed 28-05-2015]. Available from: <http://www.rsc.org/periodic-table/element/21/scandium>

⁵⁸ Scandium, [Accessed 28-05-2015]. Available from: <http://www.americanelements.com/sc.html>

Naturally occurring scandium consists of only one stable isotope, ^{45}Sc which has a nuclear spin of $7/2$. There are 13 known radioisotopes of scandium that have been characterised with the most stable being ^{46}Sc with a half-life of 83.8 days, ^{47}Sc and ^{48}Sc with half-lives of 3.35 days and 43.7 hours respectively. The remaining radioactive isotopes have half-lives that are less than 4 hours. The Sc isotopes range from ^{36}Sc to ^{60}Sc and the primary decay mode results in masses lower than the only stable isotope.⁵⁹

2.6.1 Scandium crystallographic structure

Figure 2.17 represents the scandium crystallographic structure with space group: P63/mmc and cell parameters:

- a : 330.9 pm
- b : 330.9 pm
- c : 527.33 pm
- α : 90.000°
- β : 90.000°
- γ : 120.000°

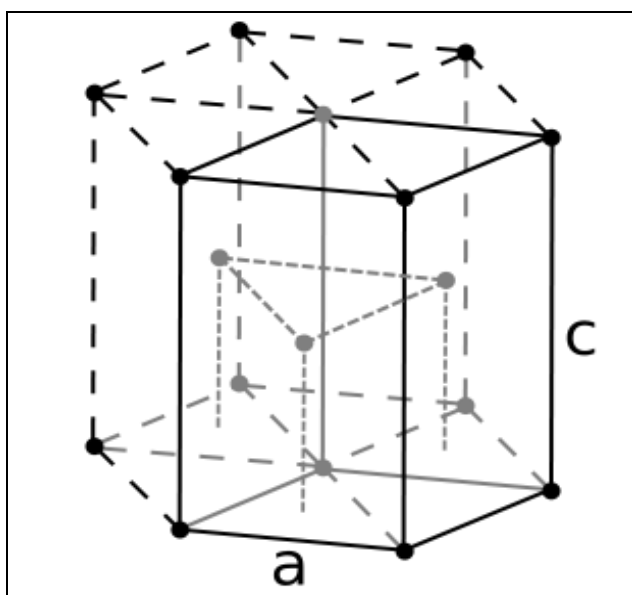


Figure 2.17: Hexagonal lattice of scandium metal⁶⁰

⁵⁹ Meierfrankenfeld, D., Bury, A. and Thoennesen, M., Discovery of Scandium, Titanium, Mercury, and Einsteinium Isotopes, *Preprint submitted to Atomic Data and Nuclear Data Tables*, pp. 4-9, (2010)

⁶⁰ Holgate, S.A., *Understanding Solid State Physics*, p. 43, (2009)

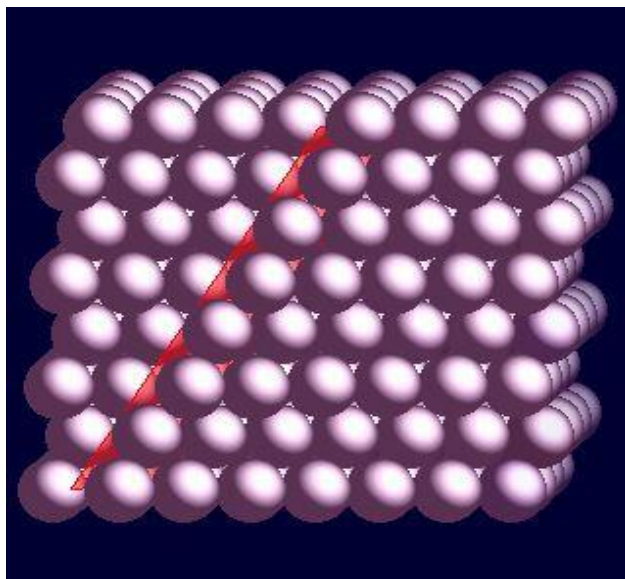


Figure 2.18: Hexagonal close-packed crystal structure of scandium metal⁶¹

2.7 Scandium chemistry

Scandium is a member of the 3d-block of elements and has an electronic configuration of $[\text{Ar}]3d^14s^2$. Scandium cannot form an ion with an incomplete 3d sub-shell and is therefore regarded as not a true transition element. Scandium's chemistry is determined solely by the formation of compounds in its +3 oxidation state. This element does form many complexes, complexes with oxidation states ranging from +2 and +1, though not as many as other transition metals. Most scandium compounds and complex ions (where Sc only exhibits a +3 oxidation state) are white or colourless. The lack of scope for a variety of coloured compounds arises from the fundamental electronic configuration of the Sc^{3+} ion, namely $[\text{Ar}]3d^0$, giving a completely empty 3d sub-shell and no electron that can be promoted to a higher level when the 3d sub-shell is split when the central metal ion interacts with the different ligands. The aqueous octahedral hexa-aqua ion of scandium, $[\text{Sc}(\text{H}_2\text{O})_6]^{3+}$ is therefore colourless and with no other oxidation state.

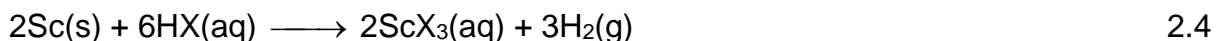
⁶¹ Scandium crystal structure, [Accessed 29-05-2015]. Available from:
https://www.webelements.com/scandium/crystal_structure.html

2.7.1 Scandium halides

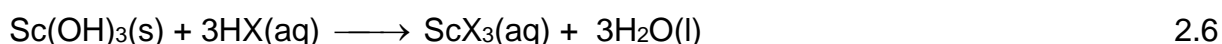
Scandium's chemistry is dominated by the +3 oxidation state (Sc^{3+}) as a result of losing its outer 3d and 4s electrons and is likely to form the typical series of binary compounds with non-metals e.g. ScCl_3 . Scandium is very reactive towards fluorine, chlorine, bromine and iodine, and burns to form the trihalides, scandium(III) fluoride (ScF_3), scandium(III) chloride (ScCl_3), scandium(III) bromide (ScBr_3) and scandium(III) iodide (ScI_3) respectively. The general equation for the reaction is shown in **Equation 2.3**.



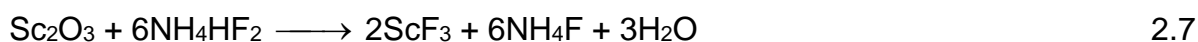
Scandium also dissolves in acids like HCl and HBr to form the different scandium halide salts, ScCl_3 and ScBr_3 respectively (**Equation 2.4**) Scandium however does not dissolve in diluted hydrofluoric acid (HF) because of the formation of a protective trifluoride layer that prevents the further reaction. Scandium oxide also dissolves in acids like HCl to form colourless solutions of scandium halide salts (**Equation 2.5**).



The non-amphoteric scandium hydroxide Sc(OH)_3 also dissolves in acids HX (X = Cl, Br, F) to form scandium halides, see **Equation 2.6**.



ScF_3 is also formed during the extraction from the ore like thortveitite by the reaction of Sc_2O_3 with ammonium bifluoride at high temperature according to **Equation 2.7**.



All the halides, except for ScF_3 ($X = \text{Cl}, \text{Br}, \text{I}$) are very soluble in water. Most of the halides are Lewis acids; e.g. ScF_3 dissolves in a solution containing excess fluoride ion to form $[\text{ScF}_6]^{3-}$. The coordination number of Sc(III) is typical 6 and the ionic field strength of scandium is in complete agreement with its ability to form salts containing water of crystallisation.

2.7.2 Scandium oxide

Scandium is fairly stable in air but will slowly change its colour from silvery white to a yellowish appearance because of the formation of Sc_2O_3 on the surface. The white basic oxide (**Figure 2.19**) is obtained via **Equation 2.8**.



Figure 2.19: Scandium oxide powder.⁶²

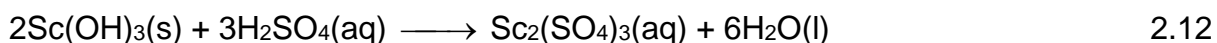
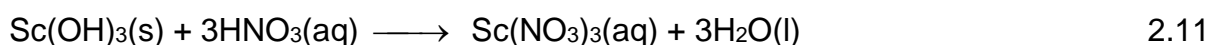
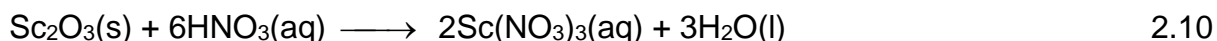
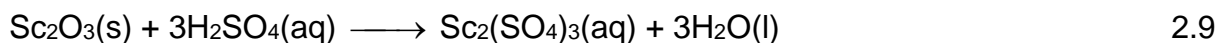
Scandium oxide has a high melting point of 2,485 °C and is the primary product produced by the mining industry, making it the starting point for all scandium chemistry and is used in the preparation of numerous other scandium compounds as well as in high-temperature systems (due its resistance to heat and thermal shock). Metallic scandium is produced by the reduction of scandium oxide, converted to

⁶² Scandium oxide (Sc_2O_3) powder, [Accessed 29-05-2015]. Available from: <http://www.topmetalmaterial.com/products/ScandiumOxide.html>

scandium fluoride followed by a reduction with metallic calcium. Scandium oxide adopts a cubic crystal structure containing 6-coordinate metal centres⁶³ and is an insulator with a band gap of 6.0 eV.⁶⁴ This oxide is insoluble in water and soluble in hot acids.

2.7.3 Nitrate and sulphate chemistry of scandium

Scandium nitrates and sulphates are readily prepared by the addition of nitric and sulphuric acid to pure scandium metal, scandium oxide or scandium hydroxide. Some of the reactions that take place are shown below in **Equations 2.9 to 2.12**.



2.7.4 Coordination chemistry

The coordination chemistry of Sc complexes has been a fertile area of research for many decades and is applicable to many biological and industrial processes. The chemistry is almost completely dominated by the trivalent ion, Sc^{3+} with the ionic radius of 0.745 Å (for 6 coordination). It is the largest of the metals in its period and

⁶³ Scandium oxide (Sc_2O_3), [Accessed 15-06-2015]. Available from:

<http://www.samaterials.com/scandium/723-scandium-oxide-evaporation-materials.html>

⁶⁴ Emeline, A. V., Kataeva, G. V., Ryabchuk, V. K. and Serpone, N., "Photostimulated Generation of Defects and Surface Reactions on a Series of Wide Band Gap Metal-Oxide Solids". **The Journal of Physical Chemistry**, B, No.103, Vol. 43 pp. 9190–9199, (1999)

the coordination number depends on the relative size of the atoms or ions.⁶⁵ Scandium forms stable complexes with O and N donor ligands such as acetylacetonate, tropolonate, oxalate and pyridine-2,6-dicarboxylic acid. **Figure 2.20** shows the molecular structures of some ligands with which Sc^{3+} readily react.

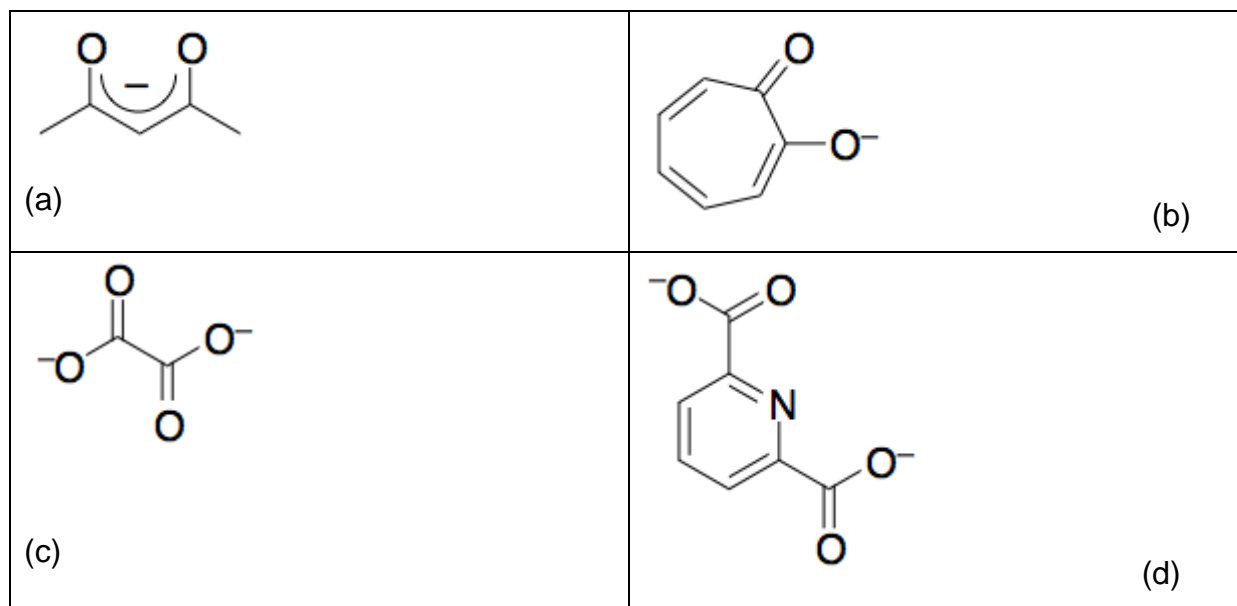
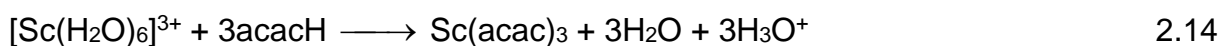


Figure 2.20: Molecular structures of (a) acetylacetonate, (b) tropolonate, (c) oxalate and (d) pyridine-2,6-dicarboxylic acid

Acetylacetonates are a source of great interest for researchers studying rare-earth elements, including scandium, especially due to their unique spectral characteristics and also due to the fact that they crystallise without water and are slightly soluble in organic solvents. Acetylacetonate (acac^-) has a single negative charge but possesses two donor atoms and is therefore a potential bidentate ligand i.e. the two donor atoms will occupy two adjacent coordination positions around the metal ion. Sc^{3+} normally react with acetylacetonate with the slow mixing of an ammonium acetylacetonate solution with a scandium chloride solution at a pH barely lower than that at which the hydroxides of scandium precipitate. After some time the formation of the crystalline acetylacetonates is complete. The proposed reactions of the formation

⁶⁵ Sulyanova, E.A., Molchanov, V.N., Sorokin, N.I., Karimov, D.N., Sulyanov, S.N. and Sobolev, B.P., Defect Structure and Ionic Conductivity of $\text{Ca}_{1-x}\text{Sc}_x\text{F}_{2+x}$ ($0.02 \leq x \leq 0.15$) Single Crystals, **Crystallography Reports**, Vol. 54, No. 4, pp. 572–58, (2009)

of the scandium acetylacetonate complex ([Sc(acac)₃]) are demonstrated in **Equations 2.13** and **2.14**.



Sc has a general coordination number of 6 and has an octahedral geometry. Scandium oxalate, Sc₂(C₂O₄)₃·5H₂O, may be precipitated from an aqueous solution of a scandium salt by the addition of oxalic acid, and when air-dried, it forms a white, crystalline powder.⁶⁶ It also forms complex oxalates of the type M₃[Sc(C₂O₄)₃] and they are sufficiently stable to be resolved into optical antipodes thus proving their octahedral configuration.⁶⁷ Scandium oxalate dissolves slowly in potassium or sodium oxalate, and on cooling, forming double oxalates of the type Sc₂(C₂O₄)₃·3M₂C₂O₄·10H₂O, or M₃[Sc(C₂O₄)₃]·5H₂O.

2.8 Conclusion

Regardless of its historically lamentable supply, scandium has a latent potential as a very useful metal in many applications and is already in demand. Scandium and its chemical compounds have found applications in optical, aeronautical, electronics, automotive and transportation industries but the absence of reliable, secure, stable and long term production supplies has limited the commercial applications of scandium. Despite this low level of usage, scandium offers significant commercial benefits and increases in supply may lead to lower prices, more research in its application in technology and eventually to wider and more useful applications.

⁶⁶Scandium oxalate, Sc₂(C₂O₄)₃, [Accessed 14-06-2015]. Available from:
http://scandium.atomistry.com/scandium_oxalate.html

⁶⁷ Grinberg, A.A., The chemistry of complex compounds, p. 325, (1962)

3 Analytical techniques for dissolution, quantification and identification of scandium:

Literature survey

3.1 Introduction

Scandium is almost exclusively produced as a by-product during the processing of various ores and mine tailings due to its dispersed nature and resulting low concentrations in many mineral and ore deposits. However, the metal is found in appreciable quantity in only a few minerals such as thortveitite and wolframite. Since Sc minerals contain a wide variety of other elements, numerous sample preparation methods exist which include acid digestion (especially when silica is absent) and salt or flux fusions. The aim of this chapter is to review some of the research that has been done up to now on the different processes for the beneficiation of scandium from various mineral ores and synthetic Sc-containing matrices. In this chapter, discussions on digestion techniques of four of the main Sc containing minerals namely thortveitite, tantalite-columbite, uranium ores and wolframite (out of more than 800 minerals) as well as the recovery processes of the metal from these minerals will be covered. Different analytical techniques used during the quantification of scandium in these natural and synthetic Sc-containing matrices will also be discussed.

3.2 Dissolution and recovery of scandium in different scandium-bearing minerals

3.2.1 Introduction

The decomposition or dissolution step in the recovering of scandium from its bearing ores is very important since this step not only liberate the scandium and all the other elements from the mineral matrix, but it also allow for the accurate quantification of the elements (complete chemical characterisation) and also for its isolation and separation in a hydrometallurgical process. Recent research concentrated on the development of successful dissolution methods for Sc-containing matrices and also the beneficiation of the element from its containing matrices. The only step as part of the purification process of the elements that does not require complete solubilisation of the primary material is the removal of iron and titanium by magnetism prior to dissolution.^{68,69}

Thortveitite is one of the minerals which is known to contain an appreciable amount of scandium, but it is quite rare and only found in a few locations worldwide. Scandium is extracted from thortveitite by several methods but the mineral acid dissolution of this mineral is complicated by its high silica content. One dissolution method involves the heating of the ore with charcoal (carbon) at 1800 °C to form a mixture of metal carbides. These carbides are then further decomposed with hydrochloric acid to form soluble chlorides with the residue consisting of silica, silica carbide and carbon.⁷⁰ Vickery⁷¹ describes a method which involves the chlorination of a mixture of thortveitite and carbon in the presence of chlorine gas at 800 - 850 °C to

⁶⁸ Birmingham S.D., Thortveitite ore beneficiation process, United States Patent No. 5035365, (1991)

⁶⁹ Nete M., Separation and purification of niobium and tantalum from synthetic and natural compounds, PhD. Thesis, Bloemfontein: University of the Free State, (2013)

⁷⁰ Iya V.K., Preparation of pure scandium, Comptes Rendus Academy Science, Paris, Volume 236, pp. 608–610, (1953)

⁷¹ Vickery R.C., The extraction and purification of scandium, **Journal of the Chemical Society**, pp. 245-251, (1955)

form scandium chloride which is then leached with HCl.⁷² Scandium is subsequently recovered by the addition of ammonium oxalate or tartrate to the solution to produce a scandium precipitate (scandium oxalate or scandium ammonium tartrate). This precipitate is filtered, washed and decomposed by ignition at 900 °C. This process yields a product of Sc₂O₃ with (98 %) purity. Ion exchange is then used for further purification.

Spedding *et al.*⁷³ developed a method for the extracting of scandium from thortveitite which involves the use of fluoride ions in the process. This research group heated a mixture of thortveitite and ammonium bifluoride NH₄HF₂ (25 % excess) at a temperature of 400 °C in a stream of dry air. SiO₂ was removed as SiF₄ and the metal fluorides, including ScF₃, were then mixed with calcium and heated to 1400 °C in a tantalum crucible. The product was dissolved in HCl and the scandium was purified by thiocyanate extraction and ion exchange (elution with N-hydroxyethylethylenediaminetriacetic acid, HEDTA, buffered to a pH of 7.4 - 7.6 with ammonium hydroxide). No visible band fronts were visible during the extraction process and the collection of samples commenced immediately after the elution process begun (**Table 3.1**). This process recovered 94.38 % Sc₂O₃ present in the mineral. In another study, Adamoli⁷⁴ mixed the thortveitite ore with MgF₂ and then added a mixture of HCl and KCl. This mixture was heated at low temperature to form MgCl₂ and a water soluble ScF₆⁻ complex. The scandium was then precipitated as Sc(OH)₃. No further purification steps were discussed in this article.

⁷² Maxwell D.K., Final summary report of mineral industry processing wastes , pp. 3-20 – 3-24, (1988)

⁷³ Spedding G.H., Powell J.E., Daane A.H., Hiller M.A. and Adams W.H., Methods for preparing pure scandium oxide, **Journal of the Electrochemical Society**, Volume 105, pp. 683-686, (1958)

⁷⁴ Adamoli C., Process for the extraction of bases of rare elements contained in ores and rocks, United States Patent No. 2250851, (1941)

Table 3.1: The fractional content obtained by elution of crude scandium with HEDTA⁷³

Sample no.	Volume (mL)	Solution colour	Oxide colour	Weight of oxide (g)	Composition
1 – 3	60	Colourless	Brown	0.17	Fe, Ca
4	4	Yellow	Tan	0.07	Fe, Ca
5	12	Yellow	Brown	1.83	Sc with Fe
6	6	Yellow	Tan	4.10	Sc with Fe
7	10	Light yellow	Cream	7.20	Sc, Fe , Y
8	7.5	Pale yellow	Yellowish	5.13	Sc, Fe , Y
9	10	Colourless	Yellowish	7.02	Sc, Fe , Y, Lu, Yb
10	10	Colourless	White	8.13	Sc, Y, Lu, Yb
11	10	Colourless	White	8.36	Sc, Y, Lu, Yb
12	10	Colourless	White	9.41	Sc, Y, Lu, Yb
13	10	Colourless	White	8.43	Sc, Y, Lu, Yb
14	10	Colourless	White	5.11	Sc, Y, Lu, Yb
15	20	Colourless	White	6.35	Sc, Y, Lu, Yb
16	10	Colourless	White	2.94	Sc, Y, Lu, Yb
17	10	Colourless	White	6.26	Sc, Y, Lu, Yb
18	15	Colourless	Dirty white	2.64	Sc, Y, Lu, Yb
19	13	Colourless	Tan	3.00	Sc, Y, REE, Mn
20	12	Pink	Brown	1.35	Sc, Y, Mn, REE*
21	15	Colourless	Tan	0.12	
Total				84.00	

Bold – trace amounts, *REE – other rare earth elements

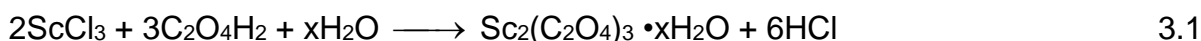
Marble and Glass⁷⁵ decomposed thortveitite that contained 45.79 % SiO₂ and 34.32 % Sc₂O₃ by three prolonged fusions with sodium carbonate. Hydrofluoric acid was added to the melt and evaporated repeatedly to remove silica. The insoluble fluorides were dissolved with nitric acid. The rare-earth group was repeatedly precipitated with oxalic acid in a slightly acidic environment free from ammonium salts. All other ions were left in solution. The oxalates were then converted to nitrates by the addition of HNO₃, and after removal of thorium (as peroxynitrate), the rest of the elements were converted to fluorides by the use of HF. Scandium was finally removed in a slightly acidic and warm ammonium fluoride solution as the double acid ammonium fluoride. Three replicates gave a mean recovery of 99.99 % Sc₂O₃.

Scandium is also found in the tantalum-niobium mineral ores called columbite or tantalite. In the processing of these ores to isolate the tantalum and niobium, a variety of residual compounds are generated. This residue which is normally in the presence of a high fluoride content also contains residual tantalum and niobium as well as scandium and other minerals such as uranium, thorium, zirconium and hafnium. In a study done by Black *et al.*⁷⁶, they mixed the dried composite material (residue) with concentrated H₂SO₄ and then calcined it at 500 °C for 1 hour to remove the excess fluoride as HF gas. The sulfated solids were then leached with water at 90 °C during which the water-soluble sulfates, namely the bulk of the Sc, Zr, Ta, Nb and U and also significant portions of Th and Ti contained in the residue, dissolved. Phosphoric acid was then added to precipitate the low soluble phosphate compounds which consisted mostly of Ta, Nb, Sc, Th and Zr. These phosphates were then reacted with 30 - 40 % H₂SO₄ to selectively dissolve scandium and thorium and leaving Ta, Nb, Zr and Hf as the solid phosphate residue. The filtrate was then mixed with an immiscible extraction solvent mixture with 5 - 10 % trialkylphosphine oxides and 5 - 10 % 2-ethylhexyl 2-ethylhexylphosphonic acid (PC-88A). In this process the Sc is extracted into the organic layer. In the next step 1.0 M

⁷⁵ Marble J.P. and Glass J.J., Some new data on thortveitite, *American Mineralogist*, Volume 27, pp. 696-698, (1942)

⁷⁶ Black, W.D., Tierney D.R. and Notz-Loiselle H., Process for recovering tantalum and/or niobium compounds from composites containing a variety of metal compounds, United States Patent No. 5787332, (1998)

HF is added to the organic layer to strip the scandium fluoride compounds from the solvent. The next step in this process involved the addition of NaOH to the HF strip solution with heating to precipitate scandium hydroxide. This was then followed by HCl digestion at a pH of 4.0, the heating of the solution at 100 °C to separate any impurities and finally the addition of oxalic acid to precipitate scandium oxalate according to **Equation 3.1**. The scandium oxalate was finally calcined at 750 °C and converted to scandium oxide to yield a 100 % Sc₂O₃ (95 % purity) recovery.



Dobretsov and Pokhilenko⁷⁷ digested or fused a niobium ore that contains 0.1 - 0.3 % Sc₂O₃, and 10 % REE oxides with 45 % NaOH to convert the rare-earths to hydroxides⁷⁸. The scandium in the hydroxide cake was dissolved with HCl leaving most of the niobium and titanium in the solid phase. The scandium in the leach liquor was then completely extracted and separated from other rare earth elements, alkali-earth elements and aluminium with 80% TBP (tributyl phosphate) in a counter-current SX circuit. The co-extracted iron and uranium were removed by selective stripping with different concentrations of HCl. Scandium was precipitated by ethane diacid, and the residue was washed and ignited. Results indicated that a recovery of 82 % of scandium oxide was obtained with a purity of 99.9 %.

In another study done by Odekirk and Harbuck^{79,80} tantalum sulphate tailings were leached with water and a leach liquor containing scandium and over 20 other elements in significant quantities were obtained. The scandium was completely extracted from the H₂SO₄ solution (50 - 200 g/L) with an organic system containing

⁷⁷ Dobretsov N.L. and Pokhilenko N.P., Mineral resources and development in the Russian Arctic, Russia, Geology, Geophysics, pp. 98–111, (2010)

⁷⁸ Kuz'min V.I., Lomaev V.G., Pashkov G.L., Ovchinnikov S.V., Kuz'mina V.N. and Dorokhova L.I., Dressing ores from weathered carbonatites as a future of the Russian rare-metal production, **Non Ferrous Metal**, Volume 12, pp. 62–68, (2006)

⁷⁹ Odekirk M.D. and Harbuck, D.D., Scandium solvent extraction from liquors produced by leaching sulfated tantalum tailings. *Proceedings of EPD Congress 1993, Denver, Colorado, US*, pp. 83–98, (1993)

⁸⁰ Odekirk M.D., Separation of scandium from tantalum residue using fractional liquid–liquid extraction, United States Patent No. 5492680, (1996)

phosphoric acid (di-(2-ethylhexyl)phosphoric acid or HDEHP) and phosphonic acid (PC-88A). Impurities such as Nb, Ta, Y and Fe were effectively separated from the scandium, but significant amounts of Zr, Hf, Ti, Th and U were co-extracted in this process. The organic solution was then scrubbed by 350 g/L H₂SO₄ solution to remove the Th, and then again scrubbed by 0.1 M HF to remove some of the co-extracted elements such as Zr, Hf, Ti and U. Results however indicated that not all the impurities were removed in this step. Finally HF solutions (0.5 - 5 M) were used to strip the loaded metals that were still present in the organic phase in the following order: Th>Ti>Zr>Hf>Sc>U. The main disadvantage of this process was the use of large amounts of HF solutions which contribute to environmental and personal risks.

Trace amounts of scandium are found in most uranium ores and are recovered as by-product when processing these ores as a significant source of scandium raw material. Lash and Ross⁸¹ crushed and ground the uranium ores and then leached it with sulphuric acid. Results indicated that leach liquor contained up to 1 mg/L Sc₂O₃. The uranium was completely extracted with dodecyl phosphoric acid (0.1 M) from the sulphuric acid leach solution but with scandium, thorium and titanium as co-extractants. The uranium was finally stripped with 10 M HCl while the Sc and Th were recovered by the stripping with HF. The obtained Sc-Th fluoride cake was digested with a 15 % NaOH solution at a temperature of 75 - 90 °C, resulting in the precipitation of scandium hydroxide. After filtration, HCl was added to the Sc(OH)₃ precipitate, the pH was adjusted to 4 and then heated to 100 °C to hydrolyse any impurities (Ti, Zr, Fe and Si). Scandium was then precipitated with oxalic acid to ensure the separation from any co-dissolved U and Fe. The scandium oxalate obtained was calcined at 700 °C to yield scandium oxide with a purity of 99.5 %. Disadvantages of this process include multiple precipitation and dissolution steps and the use of HF.

In another method, developed by Ross and Schack⁸², 98 % of the scandium present in the mineral was extracted from a uranium plant raffinate solution. Scandium was

⁸¹ Lash L.D. and Ross J.R., Scandium recovery from uranium solutions, **Journal of Metals**, Volume 13, No. 8, pp. 555-558, (1961)

⁸² Ross and Schack C.H., recovery of scandium from uranium plant iron sludge and from wolframite concentrates, U.S., Bur. Mines Rept. Inv. 6580, p. 22, (1965)

extracted along with uranium from a H_2SO_4 solution using HDEHP as extraction solvent. After extraction, the organic phase was stripped with Na_2CO_3 and an iron sludge containing 0.14 % Sc, Th, Fe, Ti and U precipitated. This sludge was calcinated at 250 °C and then dissolved in H_2SO_4 before scandium was extracted by a mixture of long-chain primary aliphatic amines (Primene JM-T) dissolved in kerosene. In a study done by Canning⁸³, uranium was extracted from a sulphate solution containing Sc, Fe, Al, Ti, Y, Th and the lanthanides by ion exchange. The iron in solution was reduced to the ferrous state using metallic iron while the scandium was extracted or separated along with Al, Ti, Y, Th into the HDEHP-kerosene solution. The lanthanides remained with iron in aqueous solution. The metals noted above were stripped from the organic phase with 4.5 M H_2SO_4 leaving scandium in the organic phase which was then stripped from organic solution using 2.5 M NaOH. He mentioned that 90 % pure scandium was obtained with no further processing attempted.

Wolframite minerals are also important sources of scandium. Ross and Schack⁸² extracted scandium from wolframite with H_2SO_4 (6 M) at 90 °C. Iron was reduced to the ferrous state by SO_2 and activated carbon as catalyst before scandium was extracted by a mixture of Primene JM-T in kerosene. A scandium concentrate was obtained from the two stripping steps of the organic solution by HNO_3 (2 M) and was purified on a strong anion exchange resin. Scandium was separated from the rest of the impurities such as Ti, Mn and Th by a thiocyanate extraction. The elements were stripped with a H_2SO_4 solution and the aqueous solution was again extracted with a Primene JM-T-kerosene mixture to remove the scandium. The scandium was finally stripped with HNO_3 and precipitated with oxalic acid producing scandium oxalate that was calcined at 850 °C to obtain a Sc_2O_3 (99.99 % pure) recovery of 83 %.

⁸³ Canning R. G., The recovery and separation of scandium, yttrium, thorium and lanthanides by solvent extraction, *Australasian Institute Mining and Metallurgy Proceedings*, No. 198, p. 113-146, (1961)

Navtanovich *et al.*⁸⁴ leached wolframite with concentrated HCl and extracted scandium with octyl hydrogen phosphate. The scandium was stripped with HF after the majority of the metallic impurities from the organic phase were removed with HCl and H₂SO₄. The ScF₃ precipitate was first converted to Sc(OH)₃ and then dissolved in HCl. Oxalic acid was then added to precipitate the scandium oxalate which was then filtered and ignited at a temperature of 800 °C to give 99 % pure Sc₂O₃. Gongyi *et al.*⁸⁵ decomposed a wolframite residue with HCl and extracted scandium from the resultant leach liquor with HDEHP in kerosene. In their study they pointed out that acid addition and the ratio of liquid to solid during leaching had a significant impact on the scandium recovery (**Table 3.2**). Results indicated that both an increase in acid ratio as well as liquid:solid ratio impacted the scandium recovery.

Table 3.2: Effect of acid addition on scandium extraction⁸⁵

Residue to acid ratio	Liquid to solid ratio	Temperature (°C)	Time (hrs.)	Scandium extraction (%)
1:0.7	2.55:1	100	2	71.14
1:1	2.35:1	100	2	66.89
1:1.5	2.55:1	100	2	72.49
1:2	2.55:1	100	2	95.31
1:2.5	2.58:1	100	2	96.10

3.2.2 Conclusion

The precipitation of insoluble scandium compounds from scandium-containing solutions is by far the easiest method to recover scandium. However, co-precipitation of other metals makes it less suitable for recovery from solutions which also contain large amounts of other metal impurities. Currently, hydrometallurgical processing,

⁸⁴ Navtanovich M. L., Chernyak A. S. and Sutyryn Y.E., The selective extraction of scandium with alkyl hydrogen phosphates, **Journal of Applied Chemistry** of the U.S.S.R., (English translation of Zhurnal Prikladnoi Khimii, Volume 38, No. 2, pp. 341—344, (1965)

⁸⁵ Gongyi G., YuH C and Yu L., Solvent extraction of scandium from wolframite residue, **Journal of metals**, pp. 28-31, (1988)

which mainly involve leaching, solvent extraction and precipitation are most commonly used for scandium recovery. The main disadvantages of the HCl-leach method are the evaporation of HCl and the formation of toxic compounds, leading to an increase in operating costs and pollution. The H₂SO₄ leach method also offers high scandium leaching efficiencies, but without the formation of harmful chlorine gas. Xu and Li⁸⁶ reported that under optimised conditions, about 94.9 % scandium can be leached with concentrated H₂SO₄ at high temperatures from a wolframite ore containing Sc (0.04 %), W (69.3 %), Fe (11.6 %) and Mn (4.8 %).

3.3 Analytical techniques for determination of scandium

3.3.1 Introduction

The next step in the analytical process is the accurate determination of the target element/s at concentration levels ranging from macro to sub-micro. The analytical techniques available to the analyst range from classical techniques such as titrimetric and gravimetric methods to modern techniques which include ICP-OES/MS, AA and neutron activation.

The scandium concentration levels, as previously discussed, are usually very low in almost all its mineral ore sources which complicate its analyses, and therefore require the more sensitive type of analytical techniques for its accurate quantification. In this respect neutron activation analysis (NAA) and inductively coupled plasma optical emission spectrometry (ICP-OES) are very suitable methods for Sc determination in these types of matrices. Some of these processes may be costly while other may require pre-concentration before analysis. While a method such as electrothermal atomic absorption spectrometry (AAS) is also frequently used, it is a method such as UV/Vis which is still very popular due to its accuracy, inexpensive

⁸⁶ Xu S., and Li S., Review of the extractive metallurgy of scandium in China (1978–1991), **Hydrometallurgy**, Volume 42, pp. 337–343, (1996)

instrumentation required, simple operation, and widespread availability. This method however, suffer from a lack of selectivity and sensitivity.^{87,88}

3.3.2 Spectrophotometric techniques

3.3.2.1 Ultra Violet Visible (UV-Vis) Spectroscopy

A sensitive and selective spectrophotometric method for the trace amounts of scandium was developed by Bashir and Sarsam.⁸⁹ In their method, scandium (range of 0.1 - 3 μg / 25 mL) was reacted with 1 mL of 5×10^{-4} M Eriochrome Cyanine R (ECR), 1 mL of 1×10^{-3} M cetylpyridinium chloride (CPC) surfactant, 2 mL buffer solution with a pH of 4.1 and then diluted to 25.0 mL. A violet-blue Sc(III)-ECR-CPC chelate with an absorption maximum at 595 nm was produced in this process. Beer's law was obeyed in the 0.004 - 0.12 ppm concentration range with $R^2 = 0.9991$, a molar absorptivity of $1.3 \times 10^5 \text{ L}\cdot\text{mol}^{-1}\cdot\text{cm}^{-1}$ and a Sandell's sensitivity of $0.45 \text{ ng}\cdot\text{cm}^{-2}$. The accuracy and precision are shown in **Table 3.3**. The method has been successfully applied to determine the scandium in various water samples and synthetic alloys.

In another study, Hsu *et al.*⁹⁰ developed a spectrophotometric method for the determination of scandium in metal alloy and low-alloy steel samples with p-nitrochlorophosphonazo (CPApN) as reagent (Figure 3.1). Scandium forms a blue complex with CPApN in acidic medium. He reported that both the CPApN and the

⁸⁷ Cerutti S., Escudero L.A., Gasquez J.A., Olsina R.A. and Martinez L.D., On-line pre-concentration and vapor generation of scandium prior to ICP-OES detection, **Journal of Analytical Atomic Spectrometry**, Volume 26, No. 12, pp. 2428–2433, (2011)

⁸⁸ Eberle A.R. and Lerner M.W., Separation and determination of scandium spectrophotometric method using Alizarin red S, **Analytical Chemistry**, Volume 27, Issue 10, pp. 1551–1554, (1955)

⁸⁹ Bashir W.A. and Sarsam L.A., Spectrophotometric determination of scandium (III) with eriochrome cyanine R and cetylpyridinium chloride – Application to waters and synthetic alloys, **Rafidain Journal of Science**, Volume 20, No.3, pp. 48- 65, (2009)

⁹⁰ Hsu C., Xu Q. and Pan J., Determination of trace scandium by ion-exchanger phase spectrophotometry with p-Nitrochlorophosphonazo, **Mikrochimica Acta**, Volume 126, pp. 83-86, (1997)

Sc-CPApN complex can be adsorbed on an anion-exchange resin (**Figure 3.2**). Curve 1 is for CPApN adsorbed onto the resin and shows the maximum absorbance

Table 3.3: Scandium determination at five different concentrations⁸⁹

Sc(III) taken, (μg)	Recovery, %*	RSD, %
0.3	100.0	± 6.1
0.5	100.0	0.0
1.0	100.0	± 0.75
2.0	104.0	± 0.6
3.0	100.0	± 1.1

*- Five determinations

at 560 nm, while Curve 2 shows the two absorption peaks at 635 and 689 nm for the complex in the resin. A wavelength range of 689 - 800 nm was selected for the measurements of absorbance of the complex since that is where the complex in the resin gives the maximum absorbance and the reagent blank in resin absorbance is weak and therefore it will minimize the effect of the resin.

The linear calibration range was determined to be 1 - 8 μg of scandium in 50 mL of solution, using 0.8 g of resin to concentrate scandium. The straight line equation by least squares treatment ($n = 8$) was $\Delta A = 0.0614 + 0.0637C$, where C is micrograms of scandium in 50 mL of solution and the correlation coefficient $R^2 = 0.996$, with a calculated molar absorptivity of $2.76 \times 10^5 \text{ L}\cdot\text{mol}^{-1}\text{cm}^{-1}$ and Sandell's sensitivity of $0.16 \text{ ng}\cdot\text{cm}^{-2}$ of scandium. Ten replicates containing 2.0 μg of scandium gave a coefficient of variation (CV) of 2.2%. They also mentioned that aluminium and the presence of rare earth elements in reasonable amounts did not interfere in the recovery of the scandium. This method was successfully applied to the determination of scandium in alloys, with relative standard deviations reported to be 2 – 4 %. Hsu *et al.*⁹⁰ also prepared synthetic samples by adding known amounts of scandium to solutions of standard samples. Samples of copper, zinc, magnesium alloys and low-alloy steel were decomposed by heating each of them with 10 mL of aqua regia

before they were spiked with known amounts of scandium. To a scandium-containing sample solution, 2 mL of 3 M H₂SO₄ and 3.5 mL of 0.02 % CPApN solution were added and diluted to a volume of 50 mL with water and mixed well. The mixture was left to stand for 10 min for full colour development and 0.8 g of resin (for concentrating scandium) was added and stirred for 25 min. The absorbance of the resin was then measured against a reagent blank resin (prepared in the same manner as that for the sample solution but without the addition of scandium). The recoveries of scandium obtained ranged from 97.9 to 103 % (Table 3.4).

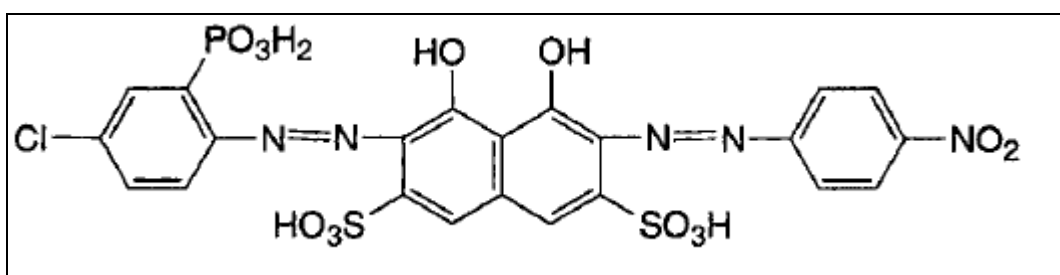


Figure 3.1: p-nitrochlorophosphonazo (CPApN)⁹⁰

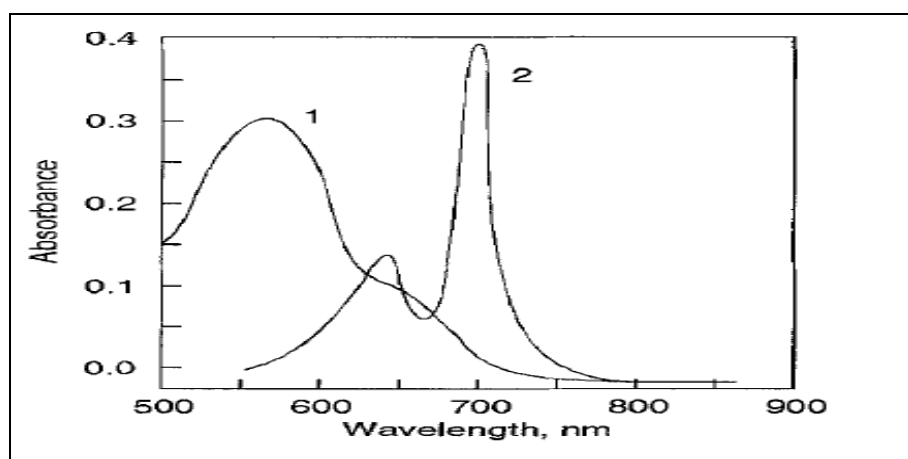


Figure 3.2: Absorption spectra for reagent blank CPAPN (2.12×10^{-6} M) in resin phase against blank resin (1); and Sc-CPAPN complex against reagent blank in resin phase in H₂SO₄ (2).⁹⁰

Table 3.4: The determination of Sc in different metal alloys with UV/Vis spectroscopy⁹⁰

Sample ^a	Scandium (10 ⁻³ %)		CV (%)	Recovery (%)
	Content	Found ^b		
Al-brass	2.42	2.37	2.78	97.9
Mn-brass	3.20	3.28	3.45	103
Zn alloy	3.11	3.05	2.88	98.0
Low-alloy steel	2.41	2.43	4.14	101
Mg alloy	3.90	3.82	2.09	97.9

^a Standard sample compositions (%): Al-brass: Cu(57.66), Al(3.46), Ni(2.50), Fe(0.43), Pb(0.076), Bi(0.0023), Sb(0.0040), P(0.0080). Mn-brass: Cu(57.09), Mn(3.23), Al(1.18), Fe(0.98), Pb(0.18), Bi(0.0017), Sb(0.0044), P(0.013). Low-alloy steel: C(0.087), Si(0.360), Mn(1.033), P(0.0123), Cr(0.033), Ni(0.350), V(0.231), Mo(0.152), Ti(0.150), Cu(0.435), Al(0.106).

^b Mean of five determinations.

Beaupré and Holland⁹¹ reported another spectrophotometric method for the determination of scandium with disodium 3-hydroxy-4-[(6-methyl-2-pyridyl)azo]-2,7-naphthalene disulfonate N-oxide (DHNO) as reagent. In this method the Sc is mixed with HCl or NaOH in order to have a final pH of 0.8 - 0.9, 5.0 mL of reagent DHNO is added and the mixture is diluted to 25 mL with distilled water. The highly coloured Sc-chelate has an absorption maximum at 555 nm with molar absorptivity of $1.55 \times 10^4 \text{ L.mol}^{-1}.\text{cm}^{-1}$. Results indicated small absorbance increases as the sample is exposed to light. The absorption maxima stabilised after 30 - 60 sec and a linear graph was obtained over the concentration range 0.4 - 2.8 ppm of Sc. Method validation which included precision and accuracy were studied by analyzing aliquots containing known amounts of Sc and the results are summarised in **Table 3.5**. Selectivity was studied by the addition of a number of diverse ions and no appreciable change in Sc recovery was observed for any elements that were added. An error of only ± 2 % in the absorbance reading was observed using this method.

⁹¹ Beaupré P.W. and Holland W.J., The spectrophotometric determination of scandium with disodium 3-hydroxy-4-[(6-methyl-2-pyridyl) azo]-2,7-naphthalenedisulfonate N-oxide, **Mikrochimica Acta**, pp. 419-422, (1982)

They also mentioned that the use of cupferron as extractant (used to eliminate the interference from Fe^{3+} , V^{5+} and Cu^{2+}) prior to analysis, improved the selectivity of the method.

Table 3.5: Determination of scandium with UV/Vis spectroscopy after complexing with DHNO⁹¹

Sc added (ppm)	Sc found ^a (ppm)	Relative error (%)	Standard deviation (ppm)
0.813	0.813	0.0	0.01
1.22	1.23	+ 0.82	0.01
1.63	1.63	0.0	0.02

^a Mean of ten separate analyses

Shahida *et al.*⁹² described a robust analytical method that consists of a flow injection-spectrophotometric system to determine the scandium in simple Sc-containing matrices such as tap water, ground water as well as in more complex matrices such as mock sea water and a CRM lake sediment called IAEA-SL-1. A mini-column containing XAD-4 resin impregnated with nalidixic acid (HNA) was used for the pre-concentration of the samples, before the determination of scandium. An aqueous sample solution containing scandium was adjusted to a pH of 4.5 with NaOH or HCl and was retained in the mini-column at a flow rate of 11.8 mL.min⁻¹ as scandium-nalidixic acid complex. This scandium complex was desorbed from the resin by 0.1 M HCl and mixed with the chromogenic reagent arsenazo-III solution. The absorbance was then measured at a wavelength of 640 nm on a spectrophotometer. A pre-concentration time of 60 seconds was used and a calibration curve with good linearity in the range 25 - 125 $\mu\text{g.L}^{-1}$ was obtained. The linear equation was reported as $A = 0.0007C + 0.0004$ with a correlation coefficient $R^2 = 0.9994$ (for 15 readings), where A was the maximum absorbance and C the concentration of Sc(III) in $\mu\text{g.L}^{-1}$.

⁹² Shahida S., Ali A. and Khan M.H., On-line spectrophotometric determination of scandium after pre-concentration on XAD-4 resin impregnated with nalidixic acid, **Iranian Chemical Society**, Volume 10, pp. 461–470, (2013)

The detection limit corresponding to 3 x SD of the blank was found to be 1.4 µg.L⁻¹. The pre-concentration or enrichment factor was calculated to be 35. Ten replicate determinations of 100 µg.L⁻¹ Sc(III) solutions gave a mean absorbance of 0.069 with a relative standard deviation of 1.6 %. They also observed for the pre-concentration time of 300 seconds that the straight line with a Sc range of 5 - 25 µg.L⁻¹ had the following equation: $A = 0.0031C + 0.0009$, with a correlation coefficient $R^2 = 0.9996$ (for 15 readings). The detection limit for this set of standards was calculated as 0.32 µg.L⁻¹ and the pre-concentration factor was 155. Ten replicate determinations of 20 µg.L⁻¹ Sc(III) solutions gave a mean absorbance of 0.063 with a relative standard deviation of 2.2 %. This exceptionally good/low detection limit (0.32 µg.L⁻¹) indicated that the method is suitable to detect very low Sc(III) concentrations.

This method was then successfully applied to the determination of scandium in spiked water samples and in the CRM sample to validate the method for Sc quantification in different matrices. The results are presented in **Table 3.6**.

Table 3.6: Sc determination in spiked water and CRM samples⁹²

Sample	Sc added (µg.L ⁻¹)	Sc found ^a (µg.L ⁻¹)	± Deviation (%)
Tap water	10	10.2 ± 2.1	2.0
	20	20.6 ± 1.5	3.0
Well water	10	10.3 ± 2.0	3.0
	20	21.0 ± 1.4	5.0
Mock sea water	10	10.5 ± 2.2	5.0
	20	19.1 ± 1.6	-4.5
CRM ^b	17 ^c	16.7 ± 1.2	-1.76

^a Mean for three determinations ^b CRM values in units of µg.g⁻¹ ^c Certified value for CRM

Good recoveries were obtained by this method and it is considered as one of the best methods to determine scandium with UV-visible spectrophotometry due to its very low detection limits. However, the purification of the XAD-4 resin, the impregnation of XAD-4 resin with HNA, the desorption of HNA from the XAD-4 resin

and the pre-concentration steps made this method pretty time-consuming. Shahida *et al.*⁹² mentioned that this study demonstrated that the active ingredients of cheap pharmaceutical drugs can be successfully used for the pre-concentration of metal ions prior to their determination by UV–visible spectrophotometry.

3.3.3 Inductively coupled plasma techniques

3.3.3.1 Inductively coupled plasma - optical emission spectrometry

Jerez *et al.*⁹³ reported the use of an on-line flow injection system and a packed mini-column associated with ICP-OES to determine the scandium concentration in acid mine drainage samples from La Carolina, an abandoned mine located approximately 80 km north of San Luis city, situated at the bottom of the Tomolasta hills. 25 mL of an aqueous scandium-containing sample at a pH of 1.5 was passed through the Ox-CNTs mini-column and the retained metal was eluted with 30 % (v/v) (maximum of 12 mL) nitric acid at a flow rate of 1.5 mL.min⁻¹, directly into the ICP-OES. The optimal operating conditions were established and the Sc determination was carried out. Results indicated that an enhancement factor of 225-fold can be obtained for a pre-concentration time of 300 s. Ten replicates gave a relative standard deviation (RSD) of 5 %. Linear calibration with a correlation coefficient (R^2) of 0.9996 using the pre-concentration system for scandium was obtained at levels near the detection limits, to concentrations of 10 mg/L. The detection limit was calculated as 4 ng/L. After optimisation of the whole process, 10 portions of 25 mL each of acid mine drainage sample were collected for the study. The proposed pre-concentration method was applied to six diluted portions and the average quantity of scandium obtained was taken as a base value. Then, known amounts of scandium were added to the other four aliquots of samples and after pre-concentration, scandium was determined by ICP-OES (**Table 3.7**). These results demonstrated the possibility to quantify the retaining/pre-concentrating Sc without the need of any complexing agent, making the method simpler and more economical.

Table 3.7: Scandium recovery from acid mine drainage determined with ICP-OES⁹³

Aliquots	Quantity of Sc added ($\mu\text{g/L}$)	Quantity of Sc found ^a ($\mu\text{g/L}$)	Recovery ^b (%)
1-6	0.0	1.5 \pm 0.1	–
7	2.0	3.4	95.0
8	4.0	5.5	100.0
9	6.0	7.7	103.3
10	8.0	9.4	98.8

^a Mean for three determinations ^b $100 \times [(\text{found} - \text{base}) / \text{added}]$

G.V. Ramanaiah⁹⁴ described a method for the rapid determination of yttrium, scandium, and other rare earth elements (REEs) in uranium-rich geological samples (containing more than 0.1% U) and in pitch blende type of samples by ICP–OES. Uranium was separated by the selective precipitation of all the other analytes as the hydroxides using a $\text{H}_2\text{O}_2\text{:NaOH}$ mixture in the presence of iron as carrier, while the U-peruranate complex remained in solution. The precipitated rare earth hydroxides (including Y and Sc) were filtered and dissolved in HCl. The concentrations of elements were measured at different interference free wavelengths and the results obtained were used as a single point calibration method. The method was also compared with the well-established cation exchange separation procedure reported by Crock *et al.*⁹⁵ It was also evaluated using the international reference standards SY-2 and SY-3 as well as the in-house pitch blende sample. Since these reference standards do not contain uranium, an amount of 200 mg of uranium was doped into the samples and then decontaminated by selective precipitation of the other analytes

⁹³ Jerez J., Isaguirre A.C., Bazán C., Martínez L.D. and Cerutti S., Determination of scandium in acid mine drainage by ICP-OES with flow injection on-line pre-concentration using oxidized multiwalled carbon nanotubes, **Talanta**, Volume 124, pp. 89–94, (2014)

⁹⁴ Ramanaiah G.V., Determination of yttrium, scandium and other rare earth elements in uranium-rich geological materials by ICP–AES, **Talanta**, Volume 46, pp. 533–540, (1998)

⁹⁵ Crock J. G., Lichte F. E., Riddle G. O. and Beech C. L., Separation and pre-concentration of the rare-earth elements and yttrium from geological material by ion-exchange and sequential acid elution, **Talanta**, Volume 33, p. 601, (1986)

as the hydroxides using a H₂O₂:NaOH mixture. Sc values obtained with this method are reported in **Table 3.8**. This method is simple, rapid, precise and accurate. It is important to note that the separation of the analytes from the U-matrix is essential prior to elemental quantification with ICP–OES, due to the spectral interferences on many of the REE emission lines.

Table 3.8: Scandium determination from different Sc-containing matrices with ICP-OES⁹⁴

Sample	Scandium ^a , µg/g	(% R.S.D.)	Ion exchange method, µg/g
Pitch blende	5.2	5.8	6.0
CCRMP standard reference sample SY-2	7.31	5.5	7.0
CCRMP standard reference sample SY-3	7.0	5.5	-
Geological samples			
4595	4.8	4.2	4.9
4596	1.3	7.1	1.4
4597	20.3	4.0	20.2
4598	3.3	6.1	3.8
4605	3.5	5.7	4.1
4606	2.6	6.9	3.5

^a Average of five values

In another study, by Ochsenkühn-Petropulu *et al.*⁹⁶, red mud was digested by borate/carbonate fusion and the sample solution was passed through the ion exchanger Dowex 50W-X8. The elements Fe, Al, Ca, Si, Ti, Na, Ni, Mn, Cr and V were removed by elution with 1.75 M HCl while Sc, Y and the lanthanides were quantitatively obtained by a subsequent elution with 6 M HCl. Scandium was then selectively extracted with di(2-ethylhexyl)phosphoric acid in hexane while yttrium and the other lanthanides remained in the aqueous phase. After back-stripping from the organic phase, the scandium was quantitatively recovered in high purity in the aqueous phase and the scandium determination was done with ICP-OES at wavelengths of 361.384 nm and 363.074 nm. A bauxitic reference sample BX-N from the “Association Nationale de la Recherche Technique”, France (ANRT) was used for evaluating this method and the procedure was also applied to the red mud samples from a Greek alumina production site. The Sc recovery for the whole separation procedure for the above-mentioned samples gave an average recovery of 93 % with a standard deviation of ± 5 %, while the concentrations of the other elements in the backstripping solution were below the detection limits. The obtained scandium detection limits were 10 ng/g at 361.348 nm and 15 ng/g at 363.074 nm, allowing the determination of very low levels of scandium in complex matrices. It was noted that the detection limits can be improved by further enrichment of Sc in the organic phase.

Cerutti *et al.*⁸⁷ did a study of an on-line scandium pre-concentration system followed by chemical vapour generation and finally elemental quantification with ICP-OES. Trace amounts of scandium in river water samples were pre-concentrated by the sorption of the scandium in a mini-column packed with activated carbon at a pH 7.0. The analyte retained was then eluted with 10 % (v/v) HCl mixed with a solution of tetrahydroborate(III) in a continuous flow system to generate volatile species of scandium (scandium borohydride). The gaseous Sc sample was then introduced to the ICP-OES and a detection limit of 4.0 $\mu\text{g/L}$ was obtained. The precision (RSD) for ten replicate determinations was 4.0 %. Potential interfering effects on the Sc signal were also examined. Recovery studies on real samples demonstrated that this

⁹⁶ Ochsenkühn-Petropulu M., Lyberopulu Th. and Parissakis G., Selective separation and determination of scandium from yttrium and lanthanides in red mud by a combined ion exchange/solvent extraction method, **Analytica Chimica Acta**, Volume 315, pp. 231-237, (1995)

method is adequate for the scandium determination with recoveries obtained in the 96.2 - 100.3 % range (**Table 3.9**).

Table 3.9: Scandium recoveries in river water samples after an on-line pre-concentration method and chemical vapour generation⁸⁷

Aliquots	Sc added, µg/L	Sc found ^a , µg/L	Recovery ^b (%)
1-6	0.0	ND ^c	–
7	50.0	48.1	96.2
8	75.0	73.2	97.6
9	100.0	100.3	100.3
10	200.0	200.0	100.0

^a Mean for six determinations ^b $100 \times [(found - base) / added]$ ^c ND: Not detected

In another study, Cerutti *et al.*⁹⁷ developed an on-line scandium pre-concentration method followed by a scandium determination system using ICP-OES, which was associated with a flow injection system (FI) utilizing a knotted reactor with an ultrasonic nebulization system (USN). 30 mL of aqueous sample solution containing scandium and 5-bromo-2-pyridylazo)-5-diethylaminophenol (5-Br-PADAP) (1×10^{-4} M) buffered at pH 9.5 were mixed on-line to form the Sc-(5-Br-PADAP) complex. This mixture was then loaded on the knotted reactor for 300 s, and the retained metal complex was directly eluted with 30 % (v/v) HNO₃ into the ultrasonic nebulizer and ICP-OES. The standard solutions used to perform the calibration curve were also passed through the knotted reactor. A linear calibration curve with a correlation coefficient (R^2) of 0.9996 at levels near the detection limits up to at least 50 µg/L for scandium was obtained. The detection limit for the pre-concentration was 0.45 ng/L

⁹⁷ Cerutti S., Salonia J.A., Gasqu ez J.A., Olsina R.A. and Martinez L.D., Determination of scandium in river water by ICP-OES with flow-injection on-line pre-concentration using knotted reactor and ultrasonic nebulization, **Journal of Analytical Atomic Spectrometry**, Volume 18, pp. 18, 1198–1201, (2003)

and the RSD was 3.5 %. This method was also successfully applied to the determination of scandium in river water samples (**Table 3.10**).

Table 3.10: Recovery of scandium in river water analyses with ICP-OES after an on-line pre-concentration method (95 % confidence interval; n = 6)⁹⁷

Aliquots	Base value, ng/L	Sc added, ng/L	Sc found, ng/L	Recovery ^a (%)
1	–	0.00	4.1 ± 0.2	–
2	4.1	2.0	6.0	95.0
3	4.1	4.0	8.1	100.0
4	4.1	6.0	10.0	98.3
5	4.1	8.0	12.2	101.2

^a 100 x [(found - base)/ added]

3.3.3.2 Inductively coupled plasma – mass spectrometry

Duan *et al.*⁹⁸ performed a study on the effective removal of high-salinity matrices through polymer-complexation-ultrafiltration and detecting/evaluating the trace levels of rare earth elements (REEs) using ICP-MS after the filtration process. The REEs were converted into the REE-polymer complexes using a water-soluble polymer namely polyacrylic acid (PAA) at a pH of 7.5 which were retained for 40 min at room temperature on the ultrafiltration membrane of a centrifugal filter. The complexes were finally eluted using 3 % (v/v) HNO₃ to separate them from the matrices with relatively high levels of sodium, potassium, calcium, magnesium, and chloride ions. Standard addition was chosen in this study to validate the adaptability of the method for samples with relevant matrices. Artificial seawater samples spiked with REE standard solutions at a range between 0.00 - 1.00 µg/L were prepared and analysed

⁹⁸ Duan H., Lin J., Gong Z., Huang J. and Yang S., Removal of high-salinity matrices through polymer-complexation–ultra filtration for the detection of trace levels of REEs using inductively coupled plasma mass spectrometry, *Talanta*, Volume 143, pp. 287–293, (2015)

to investigate recoveries. For scandium, a relative standard deviation of 1.99 % for five replicates was obtained. A linear regression line with the correlation coefficient (R^2) of 0.9926 and the mean recovery of 89.4 % for Sc was reported and the limit of quantification was calculated as 0.0026 $\mu\text{g/L}$. This method was successfully applied for the determination of trace levels of dissolved Sc, Y, and lanthanides in six coastal seawater samples from the Xiamen Bay, PR China. The results for the Sc content in the seawater samples found, using the standard calibration method and the standard addition method are presented in **Table 3.11**, with the results obtained by the two methods in good agreement.

Table 3.11: Sc content for the coastal seawater samples determined with ICP-MS⁹⁸

Sample ID	Sample salinity	^a Standard calibration method, $\mu\text{g/L}$	Standard addition method, $\mu\text{g/L}$
A	0.0	0.91 \pm 0.06	0.98
B	10.4	0.65 \pm 0.06	0.58
C	15.0	0.70 \pm 0.07	0.52
D	19.6	0.42 \pm 0.03	0.49
E	25.4	0.27 \pm 0.03	0.36
F	30.2	0.20 \pm 0.08	0.28

^a The uncertainty was determined by performing 3 replicates.

Robinson *et al.*⁹⁹ used high resolution inductively coupled plasma-mass spectrometry (HR-ICP-MS) for the direct determination of Sc, Y and REE in different international certified reference materials (CRMs) namely i) basalts (BCR-1, BHVO-1, BIR-1, DNC-1), ii) andesite (AGV-1) and iii) ultramafics (UB-N, PCC-1 and DTS-1). HF-HNO₃ decomposition was used for the basalt and andesite AGV-1 samples where powdered samples of the CRMs (100 mg) were weighed and moistened with water.

⁹⁹ Robinson P., Townsend A.T., Yu Z. and Münker C., Determination of scandium, yttrium and rare earth elements in rocks by High Resolution Inductively Coupled Plasma-Mass Spectrometry, **Geostandards Newsletter**, Volume 23, pp. 43-51, (1998)

HF (2 mL) and HNO₃ (0.5 mL) were then added to the samples and heated on a hotplate at 130 °C for 48 hours. The mixtures were then evaporated to incipient dryness re-dissolved with the addition of HNO₃, followed by the addition of 10 - 20 mL H₂O and indium internal standard. These solutions were then transferred into 100 mL volumetric flasks to give a final concentration of 10 ng/mL. Ultramafic and other basaltic samples were digested using HF-HClO₄ acid decomposition in the same manner as the HF-HNO₃ method. Standard solutions covering the concentration range 0 - 50 ng/mL were used for external calibration and this method gave calibration curves with correlation coefficients in excess of 0.995. The Sc detection limit was found to be 0.0139 ng/mL. Sc results obtained for a range of international rock RMs are presented in **Table 3.12** where they are also compared with the results obtained by Govindaraju¹⁰⁰.

Table 3.12: Scandium concentrations for rock reference materials⁹⁹

Sample name	Sc found, µg/g	RSD (%)	Sc found ^a , µg/g
BCR-1	32.3	1.7	32.6
BHVO-1	31.9	1.8	31
BIR-1	42	3.1	44
DNC-1	30.5	2.7	31
AGV-1	12.4	0.8	12.2
UB-N	11.4	1.6	13
PCC-1	8	4.2	8.4
DTS-1	3.16	2.2	3.5

^a Govindaraju (1994)

¹⁰⁰ Govindaraju K., 1994 Compilation of working values and sample description for 383 geostandards, Geostandards Newsletter, 18 (Special Issue), p. 158, (1994)

3.3.4 Atomic absorption spectroscopy and neutron activation analyses

Liang *et al.*¹⁰¹ described a method for determining trace amounts of scandium (0.4 to 40 ppb) using a spectrophotometric technique (with Arsenazo III) and an electrothermal AAS technique after the enrichment of aqueous solutions by means of an adsorptive bubble technique. Sc(III) and FeCl₃ were added to 250 mL of water while stirring. The pH of the solution was adjusted to 7 with the addition of NH₄OH and immediately a yellowish brown precipitate was formed. Sodium oleate solution (1.5 mL) was added to this precipitate and after stirring for 10 min, CTAB solution (1.0 mL) was also added. A nitrogen gas stream was passed through the mixture and the obtained froth was then dissolved in HCl. For electrothermal AAS, this solution was further diluted before the analyses. The mean of 12 parallel runs was calculated to be 92.3 % and the standard deviation of ± 3.6 and relative standard deviation of 3.9 % were obtained using this method.

A study done by Teherani¹⁰² demonstrated the determining of Sc, As, Cr, Co and Ni in various chrysolite-asbestos samples from Canada, Russia and Italy using the neutron activation analysis (NAA) technique. The dried and weighed asbestos samples (0.1 to 0.15 g) were sealed in quartz ampoules and irradiated in a thermal neutron flux for 24 h. All the samples were quantified with a Canberra 4000-channel analyzer connected to an 80 cm³ Ge/Li - detector with a resolution of 1.7 keV at 1332 keV. The Sc results are presented in **Table 3.13**.

¹⁰¹ Liang S., Zhong Y. and Wang Z., Enrichment of traces of scandium from aqueous solutions by means of flotation, **Fresenius' Zeitschrift für analytische Chemie**, Volume 318, Issue 1, pp. 19-21, (1984)

¹⁰² Teherani D.K., Determination of arsenic, scandium, chromium, cobalt and nickel in asbestos by neutron activation analysis, **Journal of Radioanalytical and Nuclear Chemistry**, Letters, Volume 95, No. 3, pp. 177-184, (1985)

Table 3.13: Concentration of scandium as trace element found in various asbestos samples, (10 replicates) as determined by NAA.¹⁰²

Sample	A	B	C	D	E	F	G
Sc conc. (µg/g)	4.95	11.07	11.00	6.38	14.51	5.84	6.84
	5.31	9.73	11.01	5.52	14.24	6.24	5.25
	4.40	9.32	9.57	6.23	13.85	6.21	5.14
	4.75	9.48	11.41	6.41	14.24	6.24	5.25
	5.36	11.92	12.05	6.54	13.47	6.22	5.33
	6.21	11.05	11.60	6.39	15.69	6.53	5.52
	5.87	11.02	10.43	6.26	15.45	6.43	5.60
	5.75	10.06	10.98	6.25	15.39	6.60	5.84
	5.70	10.76	11.67	6.33	15.19	6.53	5.44
	5.56	10.90	11.50	6.19	15.48	6.53	5.54
Mean	5.37	10.53	11.12	6.25	14.80	6.30	5.56
SD	0.56	0.84	0.71	0.28	0.76	0.27	0.61

A = Canadian Chrysolite-Asbestos - 180 kg/m³

B = Russian Chrysolite-Asbestos - 360 kg/m³

C = Russian Chrysolite-Asbestos - 240 kg/m³

D = Asbestos Plate

E = Italian Asbestos

F = Asbestos dry manufactured

G = Asbestos wet manufactured

3.3.5 Summary

UV-Visible, ICP-OES, ICP-MS, AAS and NAA techniques proved to be better techniques for the determination of scandium, judging by the relatively high percentage recoveries. However, separation and pre-concentration of this metal in many of the methods is required before the analyses.

3.4 Characterisation of scandium complexes

The proper characterisation of newly synthesized complexes is also extremely important to ensure that the quantitative results and the empirical formula for these complexes collaborate. Methods of characterisation of these new complexes include the establishment of purity of sample, determination of physical properties, the determination of elementary composition, empirical formula and elucidation of structural formula. IR spectroscopic and elemental analyses are extensively used to characterise Sc compounds (inorganic and organometallic).

3.4.1 Infrared (IR)

Anhydrous scandium(III) carboxylates of general composition $\text{Sc}(\text{O}_2\text{CR})_3$ (where R = $\text{C}_{11}\text{H}_{23}$, $\text{C}_{13}\text{H}_{27}$, $\text{C}_{15}\text{H}_{31}$, $\text{C}_{17}\text{H}_{35}$ and $\text{C}_{21}\text{H}_{43}$) were synthesized by Parashar and Rai¹⁰³. An aqueous solution of scandium chloride was added dropwise with constant stirring to a ca. 0.1 M ethanolic solution of the sodium salt of the corresponding carboxylic acid (prepared by titrating the carboxylic acid against 0.1 M NaOH solution using phenolphthalein as indicator). The isolated product was warmed, filtered and repeatedly washed with hot water, then with ethanol and finally dried before the infrared spectra of the products were recorded. **Table 3.14** reports some important IR frequencies of these complexes.

¹⁰³ Parashar G.K. and Rai A. K., Synthesis, molecular weights and infrared spectra of some scandium(III) higher carboxylates, **Transition Metal Chemistry**, Volume 3, pp. 49-50, (1978)

Table 3.14: IR frequencies of scandium(III) higher carboxylates¹⁰³

Compound	$\nu_{\text{asym}}(\text{COO})$	$\nu_{\text{sym}}(\text{COO})$	Δ^a	$\nu(\text{Sc-O})$
NaO_2CCH_3	1578	1414	164	–
$\text{Sc}(\text{O}_2\text{CC}_{11}\text{H}_{23})_3$	1535	1460	75	510
$\text{Sc}(\text{O}_2\text{CC}_{13}\text{H}_{27})_3$	1535	1465	70	520
$\text{Sc}(\text{O}_2\text{CC}_{15}\text{H}_{31})_3$	1530	1465	75	500
$\text{Sc}(\text{O}_2\text{CC}_{17}\text{H}_{35})_3$	1535	1455	75	520
$\text{Sc}(\text{O}_2\text{CC}_{21}\text{H}_{43})_3$	1530	1460	70	530

^a $\Delta = \nu_{\text{asym}}(\text{COO}) - \nu_{\text{sym}}(\text{COO})$

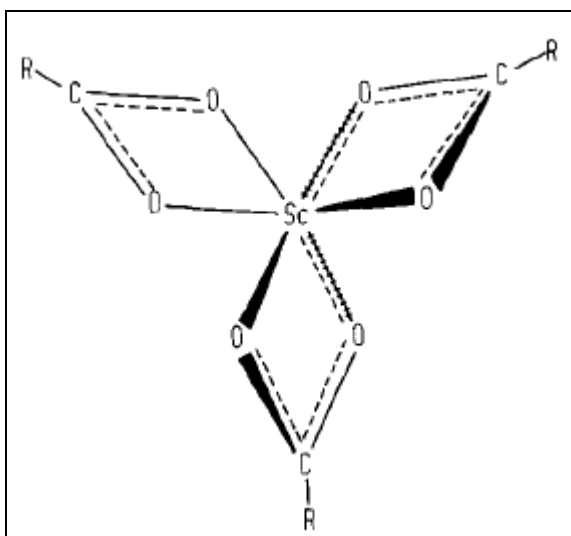


Figure 3.3: A proposed, but unconfirmed (tentative) structure for scandium(III) higher carboxylates¹⁰³

Parashar and Rai¹⁰³ reported that the characteristic free carboxylic acid vibrations were completely absent from the spectra of all the derivatives as indicated by the absence of the strong bands at 3600 - 3200, ca. 1708 cm^{-1} and ca. 935 cm^{-1} regions which are normally assigned to $\nu(\text{OH})$, $\nu(\text{C}=\text{O})$ and $\nu(\text{OH})$ deformation vibrations respectively. The strong bands for newly synthesized compounds at ca. 1535 and ca. 1460 cm^{-1} were assigned to the $\nu_{\text{asym}}(\text{COO})$ and $\nu_{\text{sym}}(\text{COO})$ vibrations respectively

and the stretching frequencies at ca. 510 cm^{-1} to $\nu(\text{Sc-O})$ vibrations. These results indicate that the C=O groups were involved in coordination with the metal ion and thus absent from the IR spectra. The low Δ values of the scandium(III) carboxylates (**Table 3.14**) suggest the bidentate character of the carboxylate groups in these derivatives.

Corsini *et al.*¹⁰⁴ prepared scandium(III) complexes of 8-hydroxyquinoline (QH) and its derivatives ($\text{Sc}(\text{C}_9\text{H}_6\text{NO})_3 \cdot \text{H}_2\text{O}$) and they characterized the complexes using IR and elemental analysis. The buffered QH solution (in acetic acid) was added with constant stirring to a warm Sc solution. The resultant suspension was stirred for 1 hr. The lemon-yellow precipitate was filtered from the hot mother solution and then washed with 100 mL of hot water. The product was then dried *in vacuo* and the elemental analysis performed. The above procedure was repeated using deuterated reagents and D_2O as solvent, dried at $100\text{ }^\circ\text{C}$ and characterised with IR. In a follow-up study, this procedure was modified by precipitating the compound from a mixed aqueous/organic solvent in which the final precipitation medium was 10 % (v/v) H_2O :acetone. Infrared spectra for all compounds prepared are shown in **Figure 3.4**. Pokras and Bernays¹⁰⁵ also reported the IR spectrum for the same compound prepared in the same way as the above mentioned method.

¹⁰⁴ Corsini A., Toneguzzo F. and Thompson M., Scandium(III) complexes of 8-hydroxyquinoline and derivatives, **Canadian Journal of Chemistry**, Volume 51, pp. 1248-1256, (1973)

¹⁰⁵ Pokras L. and Bernays P.M., Determination of scandium with 8-quinolinol, **Analytical Chemistry**, Volume 23, pp. 757-759, (1951)

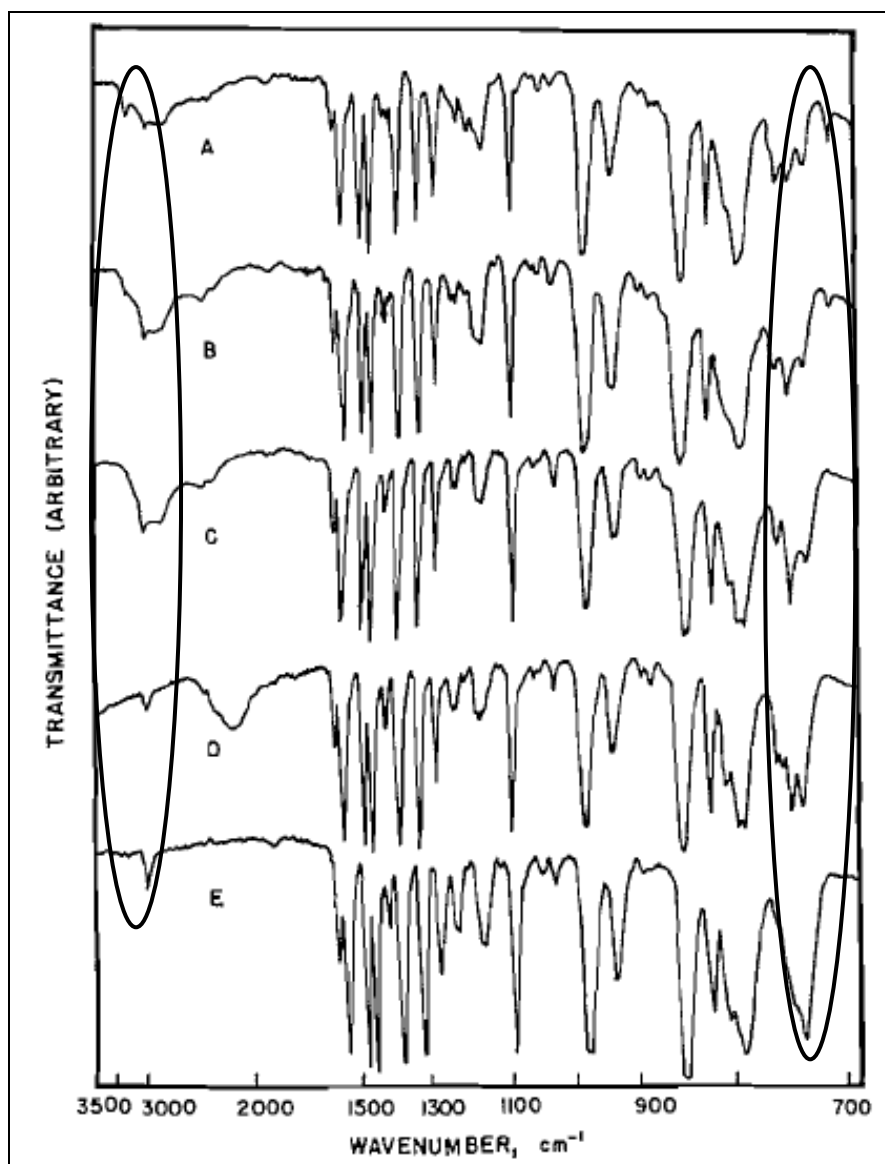


Figure 3.4: Infrared spectra of Sc(III) complexes of 8-hydroxyquinoline: (A) Pokras and Bernays' compound, (B) compound precipitated from (10 % v/v) aqueous acetone, (C) $\text{ScQ}_3 \cdot \text{H}_2\text{O}$, (D) $\text{ScQ}_3 \cdot \text{D}_2\text{O}$, and (E) thermal product (heated at 160°C), ScQ_3 .¹⁰⁴

The three spectra A, B and C are very similar except that the weak bands at 3330 and 710 cm^{-1} in spectrum A are reduced in intensity in spectrum B (relative to other bands in the spectrum), and are absent in spectrum C. These bands are likely reduced due to a contaminating reagent, meaning that that the complex represented by spectrum A was contaminated. A broad band at approximately 2900 cm^{-1} is present in all three spectra. The spectrum D of the complex precipitated from D_2O solution shows the 2900 cm^{-1} band shifted to 2150 cm^{-1} , proving that the absorption

is protonic and this band is absent in spectrum E after the compound has been dried at 160 °C in *vacuo* to remove any/all the H₂O.

In another study Hegazy and Al-Motawaa¹⁰⁶ prepared a series of β -diketone hydrazone derivatives through the condensation of β -diketone with aromatic aldehydes followed by the reaction with phenylhydrazine. They also synthesized new complexes of trivalent Sc, Y, La and Ce with these hydrazone ligands. In a solution containing 5 mmol of the ligand ($L_1 = C_{24}H_{23}N_4F$, $L_2 = C_{24}H_{23}N_4Cl$, $L_7 = C_{29}H_{23}N_4Br$, $L_9 = C_{34}H_{27}N_4F$ or $L_{12} = C_{34}H_{27}N_5O_2$) in 40 cm³ ethanol, a solution of 7 mmol of Sc(III), Y(III), La(III), and Ce(III) nitrates was added and refluxed for about 12 h after adjusting the pH to be basic using ammonia. The mixture was cooled to room temperature, filtered, washed with ethanol and water, then recrystallised from ethanol and dried in air. The prepared complexes were stable in air and room temperature. The structures of the products (**Figure 3.5**) were then confirmed through elemental and IR analyses. The IR frequencies of Sc complexes prepared are listed in **Table 3.15**.

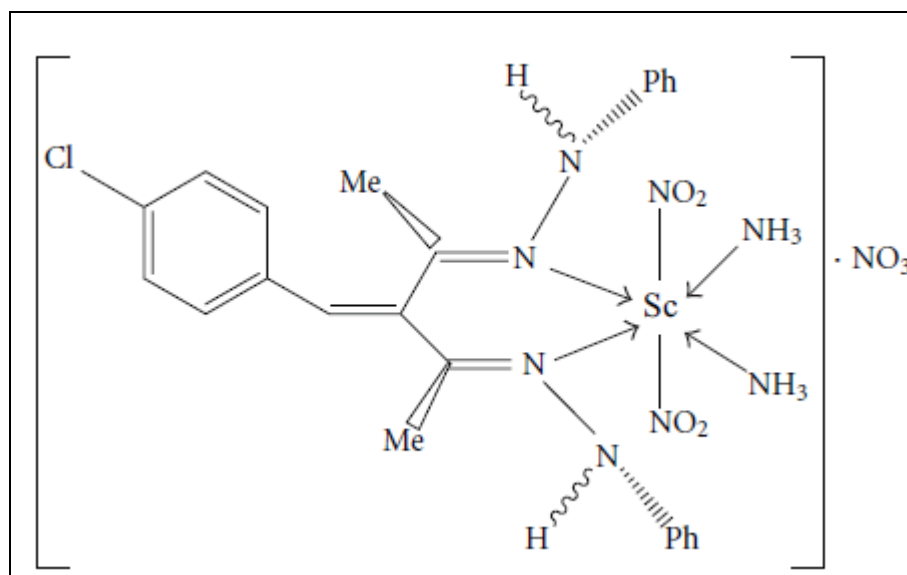


Figure 3.5: Representative structure of the hydrazone complexes prepared by Hegazy and Al-Motawaa.¹⁰⁶

¹⁰⁶ Hegazy W.H. and Al-Motawaa I.H., Lanthanide complexes of substituted β -diketone hydrazone derivatives: synthesis, characterisation, and biological activities, *Bioinorganic Chemistry and Applications*, pp. 1-10, (2011)

Table 3.15: Selected IR data of the Sc hydrazone complexes (cm⁻¹)¹⁰⁶

Complex	$\nu(\text{O-H})$	$\nu(\text{N-H})$	$\nu(\text{C=N})$	$\nu(\text{C-N}) + \delta(\text{N-H})$	$\nu(\text{N=N})$	$\delta(\text{N-H})$	$\nu(\text{N-N})$
Sc- <i>L</i> ₁	3425	overlap	1598	1503	1365	1225	1079
Sc- <i>L</i> ₂	3445	3208	1613	1493	1360	1281	1067
Sc- <i>L</i> ₇	3450	3331	1596	1490	1382	1235	1072
Sc- <i>L</i> ₉	3500	3448	1617	1492	1365	1242	1113
Sc- <i>L</i> ₁₂	3435	Overlap	1594	1491	1360	1290	1067

Sc-*L*₁ product = Sc[C₂₄H₂₅N₇O₁₀F]

Sc-*L*₂ product = Sc[C₂₄H₂₉N₈O₆Cl]NO₃

Sc-*L*₇ product = Sc[C₂₉H₃₁N₅O₆Br]NO₃

Sc-*L*₉ product = Sc[C₃₄H₃₅N₄O₄F](NO₃)₃·7H₂O

Sc-*L*₁₂ product = Sc[C₃₄H₃₅N₅O₆](NO₃)₃·H₂O

The spectra of the complexes were carefully compared with those of the ligands and the researchers mentioned that the shifts observed suggest coordination through the two lone pairs of electrons of the two sp² nitrogen atoms of the hydrazone which acts as a bidentate ligand to form stable six-membered rings.

3.4.2 CHNS-elemental analysis

Schumann *et al.*¹⁰⁷ successfully complexed ScCl₃ with 1 equivalent of K[(*S*)-C₅H₄CHPhCH₂NMe₂] or K[C₅H₄CH₂CH₂NMe₂] followed by 2 equivalents of Me₃SiCH₂Li to yield the complexes [(*S*)-C₅H₄CHPhCH₂NMe₂]Sc(CH₂SiMe₃)₂ or (C₅H₄CH₂CH₂NMe₂)Sc(CH₂SiMe₃)₂, respectively. To a stirred suspension of ScCl₃(THF)₃ in THF, K[(*S*)-C₅H₄CHPhCH₂NMe₂] was added in small portions at room temperature and after 30 min of stirring the mixture, the solvent was evaporated under vacuum. The residue was suspended in diethyl ether and was then reacted with LiCH₂SiMe₃. The mixture was stirred for 12 hr and after removal of the solvent under vacuum, the oily residue was washed and then extracted with *n*-hexane. The resulting hexane solution was concentrated and after cooling to -28 °C colourless crystals of [(*S*)-C₅H₄CHPhCH₂NMe₂]Sc(CH₂SiMe₃)₂ were obtained. The same procedure was followed for the preparation of (C₅H₄CH₂CH₂NMe₂)Sc(CH₂SiMe₃)₂.

¹⁰⁷ Schumann H., Herrmann K. and Erbstein F., Organometallic compounds of the lanthanides 169. Lanthanidocene complexes containing chiral nitrogen-functionalised cyclopentadienyl ligands, Z. Naturforsch, 58b, pp. 832-837, (2003)

Elemental analysis data for the two synthesized complexes were as follows (%): for [(S)-C₅H₄CHPhCH₂NMe₂]Sc(CH₂SiMe₃)₂ calculated C 63.99, H 9.34, N 3.24; found C 62.64, H 8.92, N 2.51; for (C₅H₄CH₂CH₂NMe₂)Sc(CH₂SiMe₃)₂, calculated C 57.42, H 10.20, N 3.94; found C 57.45, H 10.60, N 3.56.

Corsini *et al.*¹⁰⁴ prepared scandium(III) complexes of 8-hydroxyquinoline (QH), Sc(C₉H₆N₀)₃·H₂O and derivatives as described in the above section and they also characterised the complexes with elemental analysis. The results were as follows (%): calculated C 65.46, H 4.07, N 8.48; found C 65.84, H 4.00, N 8.75.

The scandium complexes prepared by Hegazy and Al-Motawaa¹⁰⁶ (**Table 3.15**) were also characterised by elemental analysis and the results are presented in **Table 3.16**.

Table 3.16: Elemental analysis data for Sc hydrazone complexes¹⁰⁶

Complex	C (%)	H (%)	N (%)
Sc[C ₂₄ H ₂₅ N ₇ O ₁₀ F]	46.27 (45.35)	3.70 (3.93)	15.14 (15.43)
Sc[C ₂₄ H ₂₉ N ₈ O ₆ Cl]NO ₃	44.06 (43.14)	5.13 (4.34)	18.26 (18.87)
Sc[C ₂₉ H ₃₁ N ₅ O ₆ Br]NO ₃	46.92 (44.54)	4.74 (4.23)	11.35 (12.48)
Sc[C ₃₄ H ₃₅ N ₄ O ₄ F](NO ₃) ₃ ·7H ₂ O	42.15 (43.46)	5.31 (5.22)	10.70 (10.44)
Sc[C ₃₄ H ₃₅ N ₅ O ₆](NO ₃) ₃ ·H ₂ O	48.22 (47.57)	3.86 (4.38)	13.05 (14.31)

(Calculated)

3.5 Conclusion

The discussion in the above sections revealed that most scandium containing mineral matrices are digested by flux fusion followed by dissolving the melt in acids. Other Sc-containing matrices are leached with acids and good metal recoveries were obtained. Industrial processing used for scandium recovery is dominated by hydrometallurgical processes, which mainly involve leaching, solvent extraction and precipitation. However, most of the techniques discussed above utilises HF as solvent which liberate HF gas during the process that needs to be eliminated or

reduced due to its ecological detrimental properties. Quantification of Sc is mainly done by using ICP-OES, ICP-MS and UV/Vis in various Sc containing matrices due to several equipment and method advantages. IR and CHNS elemental analysis are widely used for the characterisation of Sc complexes owing to their simplicity.

4 Selection of analytical techniques

4.1 Introduction

An in-depth literature study on the possible analytical techniques for the identification and accurate quantification of scandium analysis in different scandium containing matrices was done. The complete and accurate chemical characterisation of any chemical compound depends on the three important processes which include i) the digestion (complete dissolution) of the sample, ii) qualitative analysis and lastly iii) quantitative analysis of the elements present in the sample. The sample dissolution techniques can include open flask acid digestion, microwave digestion or flux fusion. Different characterisation techniques such as IR, melting point determination and CHNS microanalysis can be used to characterise the different samples. Quantification can be done with UV/Visible, AAS, ICP-OES or ICP-MS.

This chapter will therefore deal with these three analytical principles namely dissolution, characterisation and the quantification. The chapter will also discuss the most important principle theory of the equipment used throughout this study and validation parameters which are applicable to this study.

4.2 Sample dissolution methods

The overall success of any analytical procedure depends heavily on the complete digestion of the sample. Proper analytical characterisation and complete quantification require the complete dissolution of the sample as first step in the whole

process. Sample digestion or decomposition is needed to release and solubilise all the elements in the mineral to enable complete quantification.¹⁰⁸

Sample dissolution is normally one of the biggest challenges facing the analytical chemist, because most mineral samples consist of a number of unknown compounds with unknown chemical behaviour which are also in their most stable oxidation states. The main aim of sample dissolution is to totally convert a solid or non-aqueous liquid sample quantitatively into a homogeneous aqueous solution for subsequent analyses. The main techniques for sample decomposition are flux fusion, acid dissolution or wet ashing and microwave digestion. These techniques were used in this study for sample dissolution and will be discussed in detail.

4.2.1 Open flask acid digestion

The most common digestion technique involves the use of acids, either singly or in combination with other acids. These are usually fairly simple, yet effective techniques. Difficulties often arise when the acid(s) will digest the matrix but adversely react with the elements of interest. Some elements of interest can be lost due to precipitation while other elements may be lost due to volatilisation. Usually in case of organic matrices, an oxidizing mixture is used to destroy the entire organic matrix and solubilise it. Additionally, safety considerations must be taken into account prior to the use of specific acids. For example, perchloric acid (HClO_4) is excellent for digesting certain matrices, but has been known to react violently and may even explode. The different mineral acids with their typical uses are reported in **Table 4.1**. Nitric acid (HNO_3) is often used because it doesn't lead to formation of insoluble salts as might happen with the use of HCl and H_2SO_4 as acids. Hydrofluoric acid is another dangerous acid which is frequently used. It is well known for its effective digestion of silicates, but can be extremely dangerous or toxic for the analyst.¹⁰⁹

¹⁰⁸ Poykio R. and Peramaki P., Acid dissolution methods for heavy metals determination in pine needles, *Environmental Chemistry Letters* 1, pp. 191-195, (2003)

¹⁰⁹ Mitra S., *Sample preparation techniques in analytical chemistry*, pp. 229-237, (2003)

Table 4.1: Examples of acids used for wet ashing¹¹⁰

Acid	Typical Uses
Hydrofluoric acid, HF	Digest silicates and dissolves oxides of Nb, Ta, Ti, and Zr ores.
Hydrobromic acid, HBr	Distillation of bromides (e.g., As, Sb, Sn, Se).
Hydrochloric acid, HCl	Dissolves carbonates, oxides, hydroxides, phosphates, borates, sulphides and cement.
Sulphuric acid, H ₂ SO ₄	Dissolves oxides, hydroxides, carbonates, and various sulphide ores; hot concentrated acid oxidizes most organic compounds.
Nitric acid, HNO ₃	Oxidizes many metals and alloys to soluble nitrates; organic material oxidized slowly.
Phosphoric acid, H ₃ PO ₄	Dissolves Al ₂ O ₃ , chrome ores, iron oxide ores and slag.
Perchloric acid, HClO ₄	Extremely strong oxidizer; reacts violently and attacks nearly all metals.
<i>Aqua regia</i> (1 HCl:3 HNO ₃)	Digest various apatites

Acid digestion or wet ashing is done in an open beaker, where suitable acids are added to the sample on a hotplate with stirring capacity and a watch glass to prevent spills. The sample is normally heated to increase the dissolution process. Some of these acids, such as HNO₃, achieve dissolution through an oxidation-reduction process that leaves the constituent elements in a more soluble form. In acid/base reactions the acids react with the metal oxides in a neutralisation reaction to produce soluble metal ions and water as products.

¹¹⁰ Kenkel J., Analytical chemistry for technicians, 3rd edition, pp. 26-28, (2002)

4.2.2 Microwave-assisted digestion

Microwave digestion is a relatively new dissolution technique with enormous potential. Microwave energy as a heat source for sample digestion was first described in the mid 1970's.¹¹¹ Currently it is widely recognized as the leading technique for the digestion of different kinds of samples due to the fact that it operates at high temperature and pressure, is faster, cleaner, more reproducible, and more accurate than traditional hotplate digestion. Microwave digestion can be applied to a much wider range of samples, producing a clear solution for most sample types. With microwave digestion, the samples are enclosed and cross contamination and loss of volatiles can be eliminated.

The microwave digestion technique is depending on the direct coupling of electromagnetic radiation with the reagents¹¹² and make use of electromagnetic radiation with frequencies between 300 MHz and 300 GHz.¹¹³ Microwaves cannot rupture molecular bonds directly because the corresponding energy is too low to excite electronic or vibrational states. Rotational excitation of dipoles and molecular motion associated with the migration of ions are the only processes that take place in the "microwave-assisted" digestion.¹¹⁴

The microwave-assisted digestion is usually preferred to conventional heating and the process makes use of the conductive properties of the container to conduct heat to actively heat the chemical content. Microwave digestion eliminates conductive heating and convection, it heats uniformly and saves digestion time because of quick heat generation compared to conventional heating.¹¹⁵ The multi-mode microwave

¹¹¹ Abu-Samra, A., Morris, J.S., and Koirtyohann, S.R., "Wet ashing of some biological samples in a microwave oven," **Analytical Chemistry**, Volume 47, Issue 8, pp. 1475-1477, (1975)

¹¹² Abu-Samra A., Morris J. S and Koirtyohann S. R., **Trace Substitution Environmental Health**, Volume 9, pp. 297-299, (1975)

¹¹³ Kingston H.M. and Jassie L.B., Introduction to microwave sample preparation theory and practice, USA. American Chemical Society, p. 8, (1988)

¹¹⁴ Nadkarni R. A., Applications of microwave oven sample dissolution in analysis, **Analytical Chemistry**, Volume 56, Issue 12, pp. 2233-2237, (1984)

¹¹⁵ Theron T.A., Quantification of tantalum in series of tantalum-containing compounds, M.Sc. Thesis, Bloemfontein: University of the Free State, (2009)

instrumentation used in this project is presented in **Figure 4.1**. The instrument is fitted with a rotor that ensures the uniform heating of all samples. The employed vessels used in this equipment must be resistant to acid attack and are made of teflon or quartz glass to ensure both chemical as well as temperature stability.



Figure 4.1: (a) Front view of microwave digester, (b) open view of microwave digester with the rotor and (c) the rotor with reaction vessels.

Modern microwave digestion systems are equipped to monitor both temperature and pressure during the digestion procedure to control the whole process as well as to

prevent any accidental explosion. The digestion time and oven power can also be programmed and controlled to ensure reproducibility.¹⁰⁹

The microwave apparatus can be classified as single-mode or multi-mode. The feature of a single-mode apparatus is its ability to create a standing wave pattern, which is generated by the interference of electronic fields that have the same amplitude but different oscillating directions. This interface generates an array of nodes where the microwave energy intensity is zero, and an array of antinodes where the magnitude of microwave energy is at its highest.¹¹⁶ This allows a more homogenous energy distribution and higher power densities than the multi-mode apparatus. The single-mode apparatus design is governed by the distance of the sample from the magnetron (**Figure 4.2 a**). An advantage of a single-mode apparatus is their high rate of heating while a major disadvantage is that only one vessel can be irradiated at a time.¹¹⁷

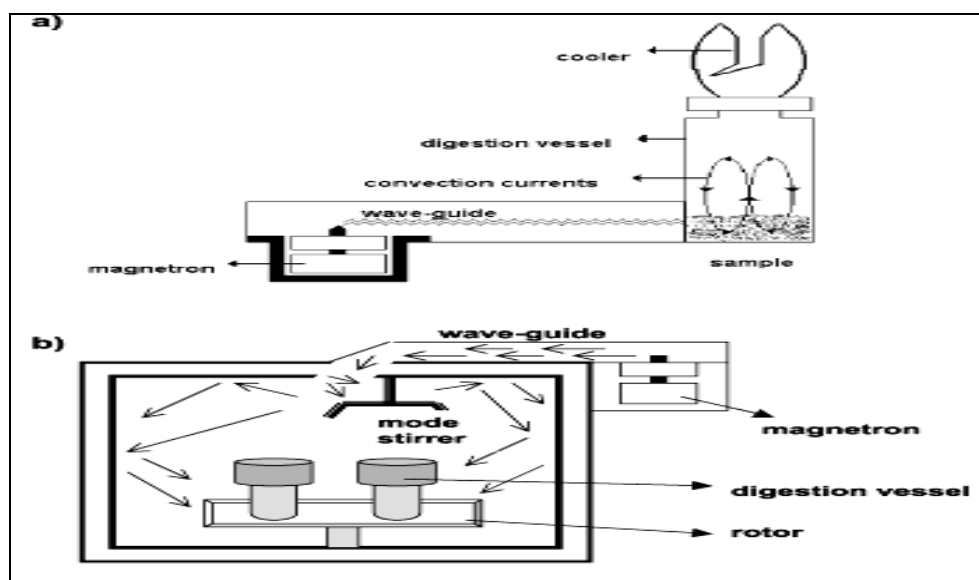


Figure 4.2: Microwave-assisted digestion system: a) single-mode apparatus and b) multi-mode apparatus¹¹⁸

¹¹⁶ Taylor M., Singh Atri B. and Minhas S., Developments in microwave chemistry, Evalueserve, pp. 5-18, (2005)

¹¹⁷ Angela, M. and Meireles, A., Extracting bioactive compounds for food products: Theory and Applications, pp. 168-169, (2009)

¹¹⁸ Elisabeth de Oliveira, Sample Preparation for Atomic Spectroscopy: Evolution and Future Trends, **Journal of the Brazilian chemical Society**, Volume. 14, No. 2, pp. 174-182, (2003)

Heating samples in multi-mode are not governed by the distance of samples from the magnetron but utilise large chamber microwaves which are generated by a magnetron. These microwaves are large enough to propagate multiple modes of microwave energy which interact with each other constructively and destructively to generate “hot spots” and “cold spots”. The main goal of a multi-mode apparatus is to generate as much chaos as possible inside the apparatus. The greater the chaos, the higher is the dispersion of radiation, which then increases the effective heating area inside the apparatus. Homogenous heating is obtained by the mode stirrer (rotor) and a major advantage of a multi-mode microwave heating apparatus is that a number of samples can be heated simultaneously.¹¹⁶

4.2.3 Flux fusion dissolution

Flux fusion is normally used for samples that are difficult to dissolve in acids, which include samples such as silicates, refractory materials, some mineral oxides and alloys. Flux fusion involves the heating of a homogenous mixture containing an excess of salt (flux) and the sample at temperatures which exceed the melting point of the flux salt. Crucible selection is important in this technique since the flux mixture can react with the crucible itself. Types of crucibles include those made of Pt, Ni, Zr and quartz. The sample in the flux or ionic liquid reacts with a flux to form products that are soluble in water, in bases or acids. High temperatures which are usually required can be achieved by flame, hotplate or high temperature ovens (furnace), see **Figure 4.3**. Types of fluxes include carbonates (Na_2CO_3), borates (LiBO_2), hydroxides (KOH or NaOH) or fluorides (NaF or NH_4HF_2). In this study, the NH_4HF_2 flux was used for the digestion of some of the mineral samples. Some examples of fluxes are presented in **Table 4.2**.

Table 4.2: Common fluxes used for mineral or metal dissolution^{119,120,121,122}

Flux	Melting point (°C)	Crucible type for fusion	Substance type digested
Na ₂ CO ₃	851	Pt	Silicates and Si-containing, alumina-containing samples, sulphates and phosphates
LiBO ₂	849	Pt, Au, glassy carbon	Most minerals, ceramics, slags and silicates
NaOH or KOH	320-380	Ni, Ag, Au	Silicates, silicon carbide and certain minerals
K ₂ S ₂ O ₇	300	Pt, porcelain	Slightly soluble oxides and oxide-containing samples
Na ₂ O ₂	Decomposes	Fe, Ni	Acid-insoluble alloys of Fe, Ni, Cr, Mo, W and Li; platinum alloys; Sn, Cr and Zr minerals and sulphides
NH ₄ HF ₂ or NaF	200-900	Pt	Si-containing minerals, silicates, rare earth minerals and the oxides of Nb, Ta, Ti, and Zr

Decomposition of the sample matrix depends on relatively high temperatures to melt the flux salt to produce an ionic liquid with a relative high flux:mineral/sample ratios. After the reaction is completed, the melt is allowed to cool and then dissolves in a suitable medium. The disadvantages of this method are the risk of contamination due to possible impurities in the fluxes, loss of important elements due to volatilisation and the high salt content in the resulting solution.¹¹

¹¹⁹ Alfassi Z.B., Instrumental Multi-Element Chemical Analysis, Glasgow, (1998)

¹²⁰ Kahn B., Radioanalytical Chemistry, New York, p. 71, (2007)

¹²¹ Pradyot P., Handbook of Inorganic Chemicals, New York, pp. 26-27, (2002)

¹²² Bock R., A Handbook of Decomposition Methods in Analytical Chemistry, Halsted Press, John Wiley and Sons, New York, (1979)

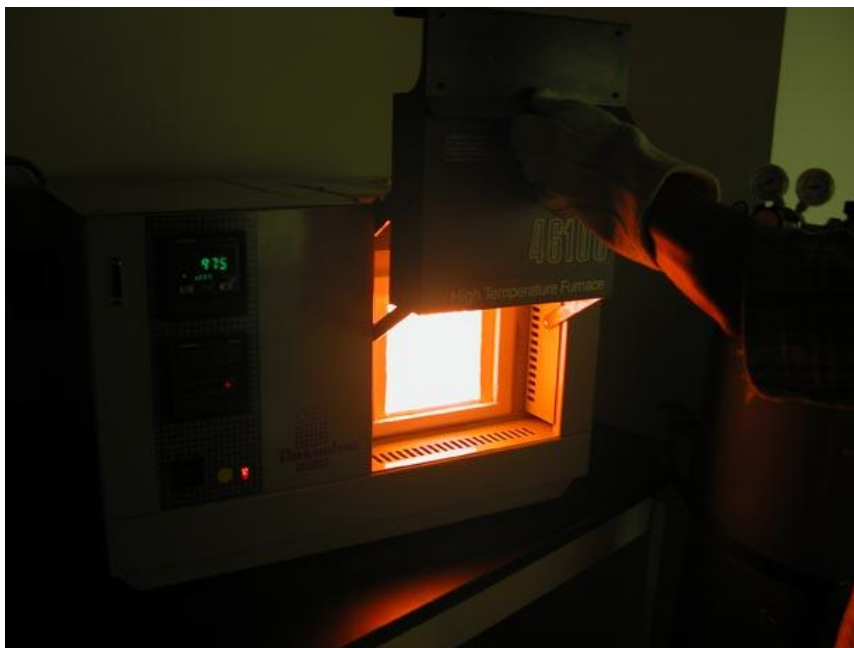


Figure 4.3: A typical high temperature furnace used for flux fusion

4.3 Characterisation techniques

The accepted requirements for full characterisation of an organic or organometallic compound include the establishment of the purity of sample, the determination of physical properties such as melting point, boiling point, index of refraction and colour, determination of empirical or molecular formula as well as functional groups present in the compound.¹²³ There are a number of different analytical techniques available that can be used for the characterisation of compounds, some of which are more effective than others and the choice of criteria and procedural steps is often dependent on availability of the equipment. In this study, infrared spectroscopy (IR), CHNS elemental analysis and melting point techniques were used for the characterisation of the synthesized compounds.

¹²³ Peck R.L. and Gale P.H., Characterisation of organic compounds, **Analytical Chemistry**, Vol. 24, Issue 1, pp. 116-120, 1952

4.3.1 Infrared (IR) spectroscopy

Infrared spectroscopy is an important tool in chemistry to characterise or identify the synthesized compounds, especially for the organic and organometallic chemists. This quick and easy technique can be used to assess the purity of a compound and gather the information about the structure of a compound.¹²⁴ From the electromagnetic spectrum (**Figure 4.4**), infrared is the region between the visible and microwave regions and itself is further divided into three regions, namely near-IR, middle-IR and far-IR as shown in **Figure 4.4**. The middle IR region is of greatest practical use to the organic chemist.

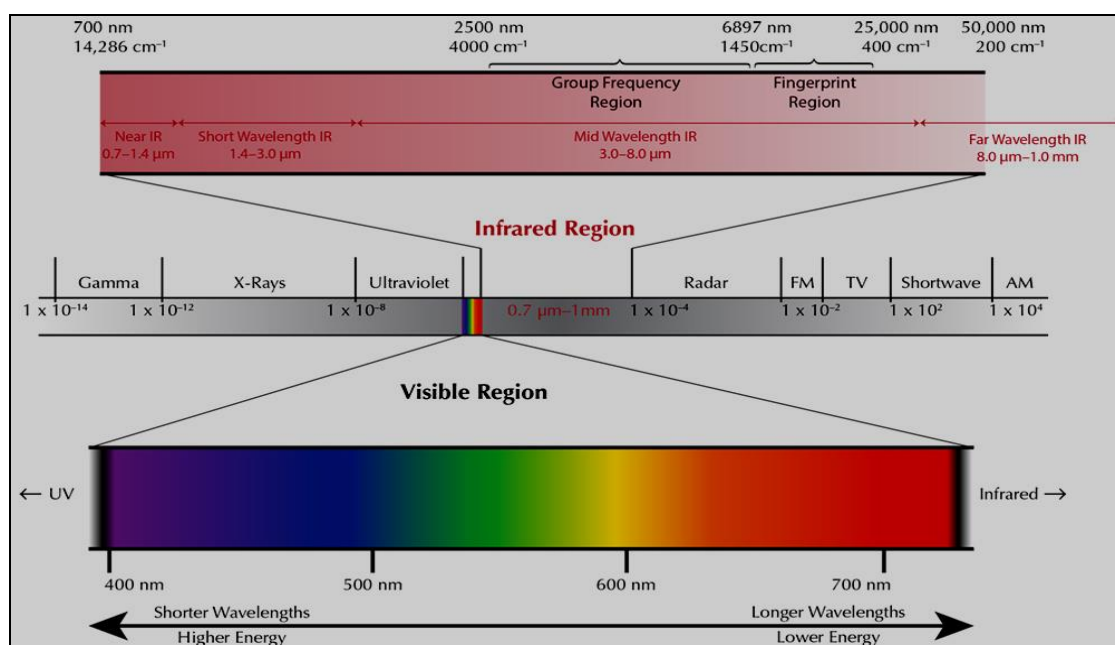


Figure 4.4: The electromagnetic spectrum.¹²⁵

During the exposure of a molecule to infrared radiation, the infrared radiation or energy is absorbed and converted to molecular vibration energy and when the absorbed energy matches the energy of a specific molecular vibration, absorption within the molecule occurs which is recorded as peaks (stretching frequencies) in the

¹²⁴ Chapter 15, Infrared Spectroscopy: Theory, [Accessed 12-07-2015]. Available from: <http://orgchem.colorado.edu/Spectroscopy/irtutor/IRtheory.pdf>

¹²⁵ The electromagnetic spectrum, [Accessed 12-07-2015]. Available from: <http://www.lotusgemology.com/images/library/articles/gemologyarticles/ftir-intrigue/infrared-spectrum.jpg>

IR spectrum.¹²⁴ These frequencies at which the molecule absorbs the radiation produce information on the type of functional groups present in the molecule. Tables indicating the correlation of frequencies (usually expressed as wavenumbers) with functional groups are readily available and of great help for analysing a spectrum of a newly synthesized compound, **Figure 4.5**.

Type of bond	Wavenumber (cm ⁻¹)	Intensity
C≡N	2260–2220	medium
C≡C	2260–2100	medium to weak
C=C	1680–1600	medium
C=N	1650–1550	medium
	~1600 and ~1500–1430	strong to weak
C=O	1780–1650	strong
C—O	1250–1050	strong
C—N	1230–1020	medium
O—H (alcohol)	3650–3200	strong, broad
O—H (carboxylic acid)	3300–2500	strong, very broad
N—H	3500–3300	medium, broad
C—H	3300–2700	medium

Figure 4.5: IR absorption for common functional groups.¹²⁶

For a molecule to be IR active, a vibration must cause a change in the dipole moment of the molecule. Molecular vibrations are divided into two categories namely stretching and bending vibrations. The stretching vibrations can be either symmetric or asymmetric; while bending vibrations mainly consist of scissoring, rocking, wagging and twisting as shown in **Figure 4.6**. Symmetric stretch allows a molecule to move in space while asymmetric stretching leads to an increase or decrease in bond length. Bending vibrations leads to changes of the angle between atoms.¹²⁴

¹²⁶ IR spectrum table functional groups, [Accessed 12-07-2015]. Available from: <http://gallery4share.com/i/ir-spectrum-table-functional-groups.html>

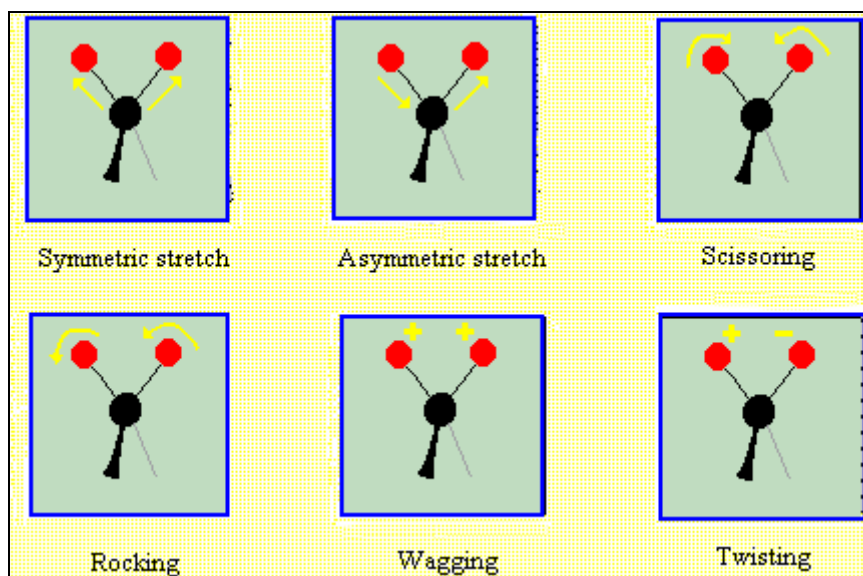


Figure 4.6: Types of vibrational modes activated by IR.¹²⁷

4.3.2 CHNS micro-analyser

CHNS elemental analyses provide a convenient way to determine the % of carbon, hydrogen, nitrogen and sulphur in organic type matrices to determine the molecular or empirical formula of a compound or its purity. A large variety of sample types which include solids, liquids, volatile and viscous samples (may be important to the fields of pharmaceuticals, polymers, fine chemicals, environment, food and energy) can be analysed with this method.

This simultaneous CHNS analyser combusts small amounts of a sample in an oxygen-rich environment at high temperature (950 °C). Catalysts are often added to the combustion tube to aid the conversion.¹²⁸ In the process, the elements C, H, N and S are converted into gaseous oxidation products, CO₂, H₂O, as well as a mixture of N₂ + NO_x and SO₂.¹²⁹

¹²⁷ IR spectroscopy vibrational modes, [Accessed 12-07-2015]. Available from:

<http://gallery4share.com/i/ir-spectroscopy-vibrational-modes.html>

¹²⁸ Thompson M., CHNS Elemental Analysers, *AMC technical briefs No. 29*, Volume 4, **The Royal Society of Chemistry**, 2008

¹²⁹ Rouessac, F. and Rouessac, A., *Chemical Analysis: Modern Instrumentation Methods and Techniques*, 2nd Edition, pp. 356–360, 441–447, (2007)

The CHNS microanalyser is illustrated in **Figure 4.7**, which was used for the quantitative determination of carbon, hydrogen, nitrogen and sulphur atoms present in the organometallic compounds that were prepared in this study. The combustion products are transported or swept out of the combustion chamber by helium as carrier gas and passed over high purity heated copper turnings. The copper removes any oxygen that was not consumed in the initial combustion zone and to convert any oxides of nitrogen to nitrogen gas. The gases are then passed through to thermal conductivity detectors which quantify the amount of N₂, CO₂ and SO₂ and convert that back to % N, C, O and S.^{128,129} The equipment requires calibration for each element by using high purity 'micro-analytical standard' compounds such as EDTA, 3,5-dinitrobenzoic acid and sulfamethazine. This technique has the major advantage of the simultaneous determination of C, H, N and S, being quick and applicability to a variety of sample types.

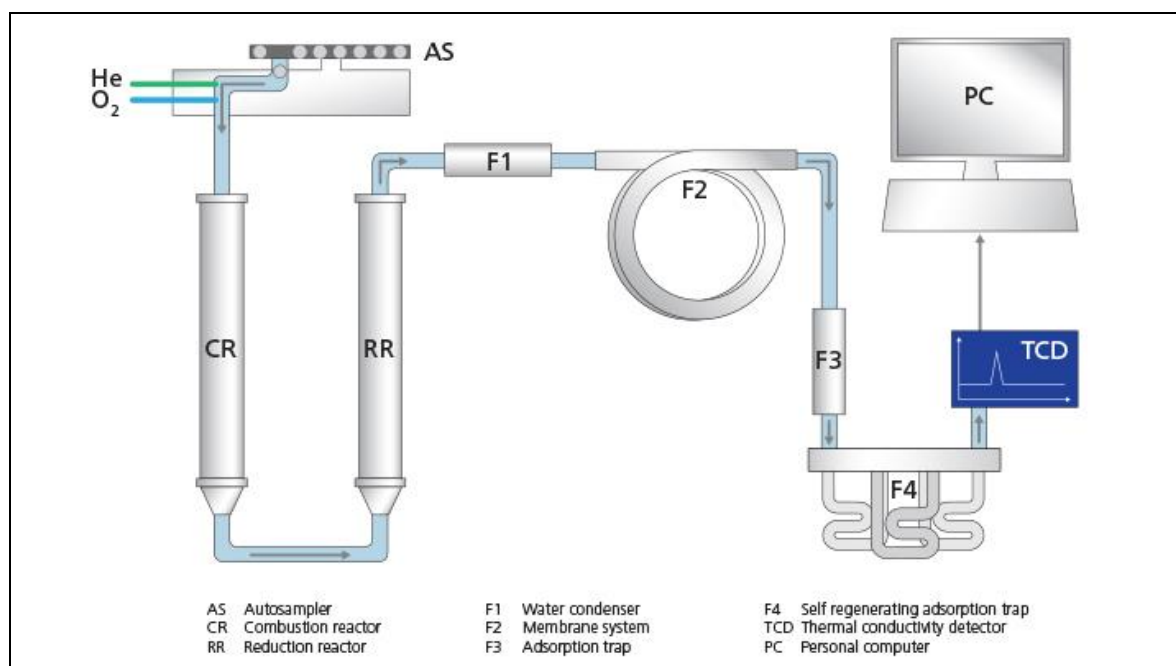


Figure 4.7: Equipment configuration for a CHNS microanalyser¹³⁰

¹³⁰ Chemical analysis, [Accessed 19-07-2015]. Available from: <http://www.foss.co.jp/industry-solution/products/dumatec/>

4.3.3 Melting point determination

The melting point of a solid is defined as the temperature at which the solid and liquid are in equilibrium at a pressure of 1 atm. Volume changes during the melting process is very small and is practically independent of any normal pressure fluctuation.¹³¹ The melting point of a solid can easily and accurately be determined using small amounts of material, and is therefore a fundamental physical property which can be used in chemical identification and characterisation, and as a criterion of the purity of the synthesized compounds.^{131,132}

Several methods can be used to measure melting point. In this study the capillary method was chosen, which depends mainly upon how much material is available. In this technique a small amount of the compound investigated is placed in a thin walled capillary tube which is closed at one end and which has an inside diameter of 1 mm. The melting-point apparatus used in this study is shown in **Figure 4.8**. The sample is compacted in the capillary tube and then introduced into the equipment. A suspended thermometer is used to monitor the temperature range over which the sample melts is observed and is recorded as the melting point. It is important that the thermometer and sample are at the same temperature while the sample melts and the rate of heating must be decreased as the melting point of the sample is approached (about 1 °C/min.).



Figure 4.8: Melting-point apparatus

¹³¹ Melting Point Determination, [Accessed 26-06-2015]. Available from:
http://www.chem.wisc.edu/courses/342/Fall2004/Melting_Point.pdf

¹³² Katritzky A. R., Jain R., Lomaka A., Petrukhin R., Maran U. and Karelson M., Perspective on the relationship between melting points and chemical structure, pp. 262-265, (2001)

The purity of a compound can also be determined using the melting point technique. A sharp melting point (a melting range of less than about 1°C) is often taken as a proof that the sample is fairly pure, and a wide melting range is evidence that it is not pure due to the influence of impurities present in the compound (impurities increase the melting point). The melting point technique can be used for the identification and characterisation of compounds provided that the melting point of that particular compound is known. Unfortunately this applies only to pure substances, and ignoring that some substances can exist in different crystalline forms that have different melting points.¹³¹

4.3.4 X-ray crystallography

X-rays are a form of electromagnetic radiation situated in the higher energy side in the electromagnetic spectrum (**Figure 4.4**). Although X-rays had been discovered in 1895 by C.W. Röntgen, it was only in 1912 that Max von Laue discovered the diffraction of X-rays by crystals. This property of X-rays allows for the determination of the exact configuration and chemical formulation of previously unknown chemical compounds to be determined and is currently one of the most powerful tools to characterise newly synthesized compounds in the solid state.¹³³

Lawrence and William Henry Bragg first proposed the mathematical formula for X-ray diffraction in 1913 in response to their discovery that crystalline solids produced surprisingly systematic patterns of reflected X-rays. Bragg found that these crystals produce peaks of varied intensities due to the reflected radiation at certain specific wavelengths and incident angles.¹³⁴ Following this, the fundamental law of X-ray diffraction (Bragg's Law) was constructed and is presented in **Equation 4.1**.

$$n\lambda = 2d\sin\theta \quad 4.1$$

¹³³ Kojić-Prodić B., A century of X-ray crystallography and 2014 international year of X-ray crystallography, **Macedonian Journal of Chemistry and Chemical Engineering**, Volume 34, No. 1, pp. 19-32, (2015)

¹³⁴ The History of X-Ray Crystallography, [Accessed 01-11-2015]. Available from: <http://arts.leeds.ac.uk/museum-of-hstm/research/william-thomas-astbury/the-history-of-x-ray-crystallography/>

where n is an integer determined by the given order or reflection integer, λ is the wavelength of the X-ray, d is the distance between each plane in the set and θ is the angle between the plane and the incident X-rays as demonstrated in **Figure 4.9**.

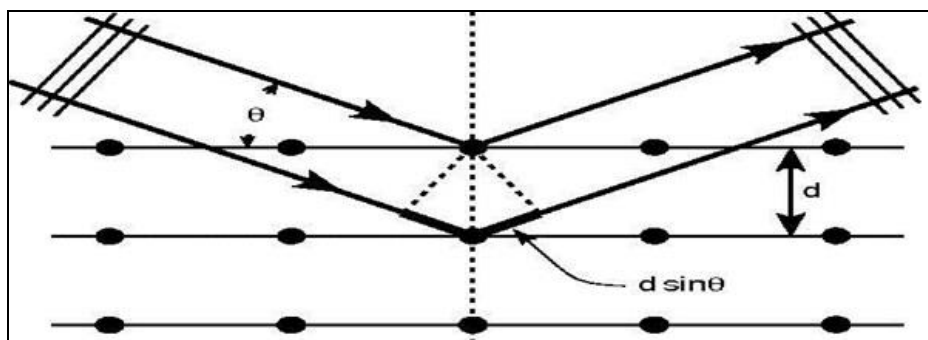


Figure 4.9: Bragg's Law for X-ray diffraction¹³⁴

X-ray crystallography involves the exposure of newly isolated single crystals to X-rays which then produces a very unique diffraction pattern. Data obtained from this diffraction pattern with the associated intensities are then mathematically manipulated which then presents detailed atomic information of the chemical compound within the crystal structure.

4.4 Quantification techniques

The next step in the analytical procedure involves the quantification of the target element or elements. Once the sample preparation is complete (complete dissolution), quantification analysis is carried out by an instrument of choice. A variety of instruments are used for different types of analysis, depending on the information which is required. Spectrometric methods are by far the most popular techniques for the quantification of the majority of the elements on the periodic table due to advantages such as easy and rapid qualitative analysis, simultaneous multi-element analysis, low running cost, low detection limits and minimised chemical interferences. Spectrometric methods are a large group of analytical methods that are based on atomic and molecular spectroscopy. These methods deal with the interactions of various types of radiation (mainly electromagnetic radiation) with matter. Examples of

spectrometric methods are atomic absorption spectroscopy (AAS), inductively coupled plasma optical emission spectrometry (ICP-OES) and inductively coupled plasma mass spectrometry (ICP-MS). These analytical techniques measure a physical property which is directly related to the concentration of chemical elements in a sample. When elements are transformed into atomic vapour at high temperatures for example, absorption or emission of light may occur and can be accurately measured at a certain wavelength. Importantly, the emission or absorption is characteristic of individual elements concerned (finger-printing of elements). In this study ICP-OES was utilised for quantification of elements in different samples. This technique will be discussed in detail in the following sections.

4.4.1 Inductively coupled plasma optical emission spectrometry (ICP-OES)

4.4.1.1 Introduction

The best tool for chemical analyses in the mid-20th century was quantitative arc and spark spectroscopy. Sample preparation techniques which were able to analyse relatively low concentration for a wide variety of elements were however difficult and/or time-consuming. At about the same time, flame emission spectrometry, also known as flame photometry, was extensively used for the determination of the alkali metals and other easily excited elements (EIE's).¹³⁵ The atomic spectra emitted from flames had the advantage of being simpler than those emitted from arcs and sparks due to the fact that flames are just not energetic enough to produce more emissions from higher energy level lines for the same element. However, the main limitation of the technique was that the temperatures produced by flames were not high enough to affect emission (activate electrons) for many of the other elements on the periodic table. Flame and arc/spark optical emission spectrometry's popularity faded in the 1960's and 1970's and many of the chemical analyses that were performed using optical emission were increasingly performed using atomic absorption spectrophotometry (AAS). The need for very high temperatures to populate excited

¹³⁵ Charles B. B. and Kenneth J. F., Concepts, instrumentation and techniques in inductively coupled plasma optical emission spectrometry, 2nd Edition, pp. 1-8 – 3-4, (1997)

states of atoms was no longer a limitation in the industry and the spectral interferences which afflicted arc/spark emission techniques were also greatly reduced by atomic absorption techniques. AAS technique is still widely used and provides excellent means of trace elemental analysis. However most atomic absorption instruments still suffer from the fact that it can measure only one element at a time and the operating conditions may require changing (hollow cathode) lamps or using different furnace parameters for each element to be determined.¹³⁵

In 1964 Greenfield *et al.*¹³⁶ published a paper on the use of atmospheric pressure inductively coupled plasma (ICP) for elemental analysis *via* optical emission spectrometry (OES) in which he highlighted the advantages of this technique over flames and arc/spark. Some of the advantages include the high degree of stability of the plasma source, the ability to overcome interferences, the capability of exciting several elements that were not excited in flames, as well as increased sensitivity of detection (over flame photometry). As with most new techniques, the original optical emission results using ICP sources were not spectacular although the technique proved to be better than flame atomic absorption. The ICP equipment configuration was refined to make it practical for the analyses of nebulized solutions by OES, the sources of noise were eliminated and some components and settings were optimised.

Equipment that was produced to the market in 1973, proved to be free of chemical interferences, had low detection limits and long linear working ranges which clearly proved that ICP was a better emission source than those previously used in analytical optical emission spectrometry. This rapid multi-element ICP-OES was first commercialised in 1974 and 18 years later, more than 9000 units had been sold. From 1983 to 2013, approximately 48,000 ICP-OES systems have been installed. Another most popular type of ICP equipment is ICP-MS. This method or equipment also permits multi-element determination with high accuracy and precision for most

¹³⁶ Greenfield S., Jones I. L. I. and Berry C. T., High pressure plasmas as spectroscopic emission sources, *Analyst*, No. **89**, pp. 713-720, (1964)

elements, rapid analysis, reduced interferences and low detection limits, as well as the quantification of elemental isotopes.¹³⁷

4.4.1.2 *Instrumentation and principles of ICP-OES*

ICP-OES is based on atomic emission spectroscopy, where the sample is exposed to high plasma temperatures which range between 6000 and 10000 K during which the sample is converted to free, excited or ionized ions. The excited electron emits radiation ($h\nu$) when it returns to its ground state and the emitted characteristic radiation (unique for each element) and intensities are measured optically by detectors.

The first process that takes place in the ICP is called nebulization where the liquid sample is converted to a fine spray called an aerosol.¹³⁸ Different kinds of nebulizers are available and the most commonly used nebulizer for ICP-OES is a concentric tube nebulizer (**Figure 4.10**). In this nebulizer the sample is sucked into the capillary tube by a high pressure stream of argon gas which flows around the tip of the tube. This high pressure Ar breaks the liquid into fine droplets of various sizes (aerosol) which are then introduced into the spray chamber. The nebulization process is one of the critical steps in ICP-OES. The sample introduction system where the sample is delivered to the plasma will be in a form that the plasma could reproducibly desolvate, vaporise, atomise and ionise and excite the different elements in the samples.

¹³⁷ The Evolution of Inductively Coupled Plasma - Optical Emission Spectroscopy (ICP-OES), [Accessed 02-08-2015]. Available from: http://cdn2.hubspot.net/hub/132427/file-2384562830-pdf/Evolution_of_ICP_Series.pdf?t=1432144873695

¹³⁸ Inductively Coupled Plasma Optical Emission Spectrometry (ICP-OES), [Accessed 30-07-2015]. Available from: <http://www.chemiasoft.com/chemd/node/52>

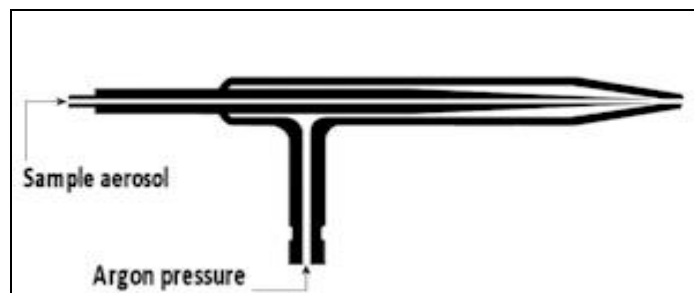


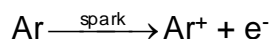
Figure 4.10: Concentric tube nebulizer¹³⁸

Once the sample aerosol is created by the nebulizer, it is transported to the torch by the Ar gas and is injected into the plasma through the spray chamber. A spray chamber is placed between the nebulizer and the torch to remove large droplets from the aerosol (only very small droplets in the aerosol are suitable for injection into the plasma) and to smooth out pulses that occur during nebulization, often due to irregular pumping of the solution. About 1 - 5% of the sample which is initially introduced to the nebulizer is transported to the plasma while the rest of the sample is drained into a waste container.¹³⁹

By definition, plasma is a conducting (ionic) gaseous mixture containing a significant concentration of ions and electrons. In the argon environment, argon ions and electrons are the conducting species. Once these ions are formed in the plasma, they are capable of absorbing sufficient power from an external source (ICP in this case) to maintain the temperature at high levels. **Figure 4.11 (a)** is a schematic presentation of a typical inductively coupled plasma torch and **(b)** a photo of a typical plasma torch. The torch consists of three concentric quartz tubes through which argon gas flow at the total rate of 11 to 17 L/min. The diameter of the largest tube is often about 2.5 cm. A water-cooled induction coil that is powered by a radio-frequency (RF) generator surrounds the top of this tube.^{138,139} Ionisation of the flowing argon is initiated by a spark from a Tesla coil, which initialise the plasma (**Equation 4.2**). The resulting ions and electrons within the plasma interact with the fluctuating magnetic field produced by the induction coil and are accelerated (in opposite directions) by the RF field which causes further ionisation to produce the

¹³⁹ Skoog D.A., West D.M., Holler F.J. and Crouch S.R., Fundamentals of analytical chemistry, 9th Edition, pp. 776-781, (2014)

plasma with high temperatures (6000 - 10000 K). **Figure 4.12** is a schematic presentation of the major components and configuration of a typical ICP-OES instrument.



4.2

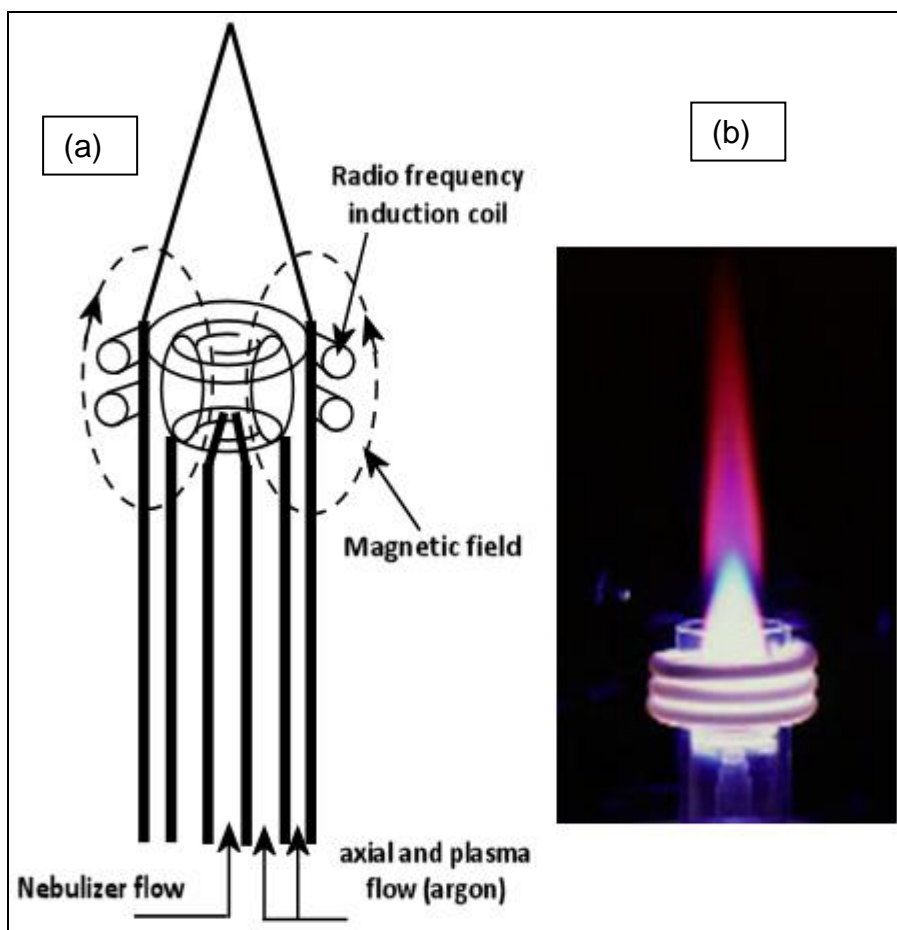


Figure 4.11: (a) Schematic presentation of an inductively coupled plasma torch and (b) Photograph of a typical plasma torch¹³⁸

The high temperature generated by the plasma activates the valence electrons of the elements present in the sample to higher vacant orbitals. Energy in the form of photons at specific wavelengths is released when these activated electrons return to their respective ground states. The emitted light is collected by a grating monochromator and only a specific wavelength passes to the photomultiplier detector. The emitted radiation from the plasma is then measured by an array detector and converted into signals that can be used for identification (unique for

each element) or quantification (emission intensity is directly proportional to concentration of element). Plasmas have high flame stability and are also considered to generate an inert environment with low chemical interferences which make the ICP-OES a technique which produce better qualitative and quantitative analytical data.¹³⁹

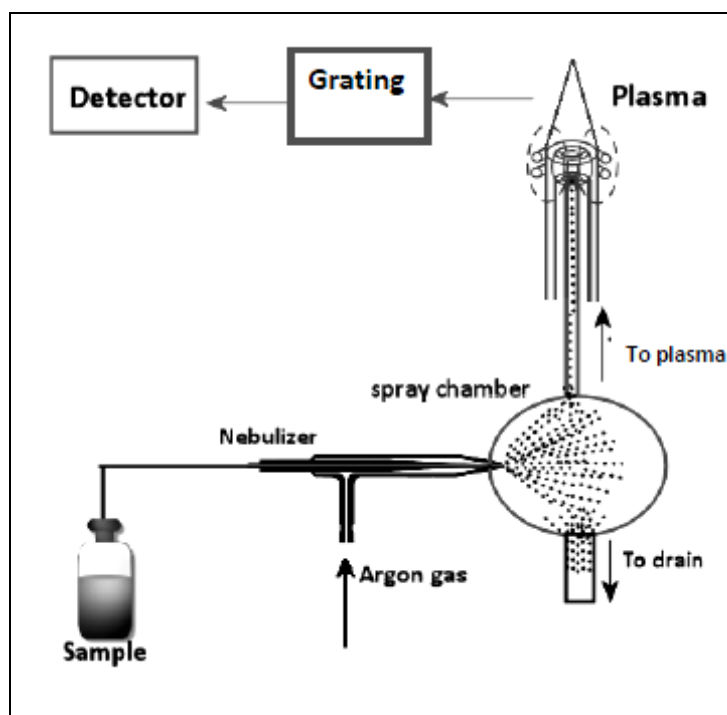


Figure 4.12: Schematic presentation of the major components and sample introduction of a typical ICP-OES instrument.¹³⁸

When selecting an analytical technique, the sensitivity of an instrument, or how low it can detect the presence of the element of interest is very important. From **Figure 4.13**, it is clear that the ICP-MS technique has detection limits that are very impressive compared to the other techniques and ICP-OES has typically two to three orders of magnitude poorer detection limits than ICP-MS. Other spectrometers have been improved with configurations that use an axially viewed ICP, although this view has problematic matrix interferences. It should be noted, however, that some

common lighter elements (e.g., S, Ca, Fe, K and Se) have more interferences in ICP-MS, and this degrades the detection limits considerably.¹⁴⁰

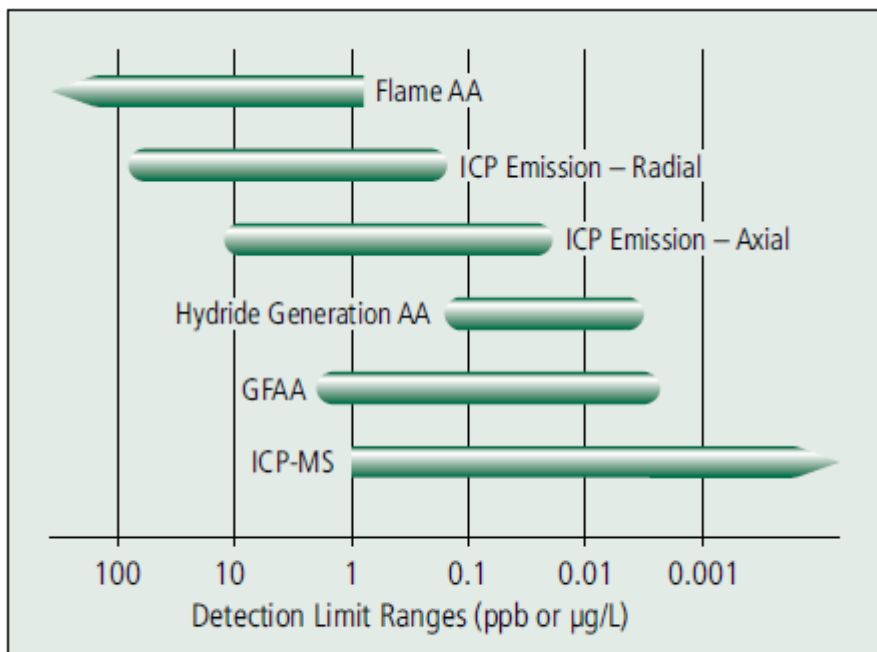


Figure 4.13: The detection limit ranges for the major atomic spectroscopy techniques.¹⁴¹

ICP-OES does have its limitations with spectral interferences, matrix effects and ionisation (interference from easily ionizable elements).¹⁴⁰ **Table 4.3** lists the advantages and disadvantages of the ICP-OES technique.

¹⁴⁰ Tyler G., ICP-OES, ICP-MS and AAS techniques compared, ICP-MS instruments at work, Varian, (1994)

¹⁴¹ Thomas R., Determining elemental impurities in pharmaceutical materials: How to choose the right technique, **Spectroscopy**, Volume 30, Issue 3, (2015)

Table 4.3: Advantages and disadvantages of ICP-OES¹⁴²

Technique	Advantages	Disadvantages
ICP-OES	Low detection limits	Relatively expensive to run but cheaper with respect to ICP-MS
	Multiple element analysis	Wet analysis only
	Limited spectral interferences	Poor tolerance of plasma to organic solvents
	Fairly simple to run the instrument	High capital costs
	Good accuracy and precision	

4.5 Separation and purification techniques

Hydrometallurgy is the process of separation and purification of elements in a complex matrix in an aqueous medium. Analytical chemistry is often used to facilitate decision making in the development of such a hydrometallurgical process. Decisions such as the choice of the most effective dissolution process depend on the composition and quantity of the different elements present in such a mineral matrix, which rely like the efficiency of separation steps and purity of the final products, all heavily on analytical chemistry.

It is also important to identify the most important physical properties of these minerals in order to utilise any significant difference to separate some elements prior to complete dissolution to simplify down-stream separation and purification processes. These physical properties may include density difference or magnetic properties.

¹⁴² Scott R. A. and Lukehart C. M., Applications of physical methods to inorganic and bioinorganic chemistry, p. 206, (2007)

Chemical separation techniques include selective precipitation, solvent extraction and ion exchange.

4.5.1 Magnetic separation

The origin of magnetism in minerals lies in the orbital and spin motions of valence electrons of the elements present as well as electrons interacting with one another. It is well known that most of the transition elements have paramagnetic properties. There is a direct and sometimes very sensitivity relationship between the magnetic properties of the different elements or minerals and the number of unpaired electrons present in the metal ions. These unpaired electrons (negatively charged) are sensitive to their orientations in an external magnetic field. Aligned orientation in this magnetic field ensures that these ions or minerals become magnetised or polarised themselves and this property is called magnetic susceptibility. It is therefore accepted that the elements with the largest number of unpaired electrons will be magnetically the strongest or easily polarised. Magnetic separation is a process in which the best magnetically susceptible elements are separated from the other mineral components by the application of an external magnetic field. There are three magnetic properties, namely diamagnetic, paramagnetic and ferromagnetic, and minerals normally fall into one of them.¹⁴³

Ferromagnetic minerals are strongly attracted to magnetic fields and retain their magnetic properties even after the externally applied field has been removed (magnetisation does not return to zero unlike the paramagnetic and diamagnetic minerals). They have the ability to record the direction of an applied magnetic field. Metals with ferromagnetic properties include Fe and Ni. The magnetism remains locked in the minerals unless they are subsequently heated above a temperature called the Curie point (the temperature at which all materials lose their magnetism).¹⁴⁴

¹⁴³ Rock Magnetism, [Accessed 21-07-2015]. Available from:

http://gravmag.ou.edu/mag_rock/mag_rock.html

¹⁴⁴ Classes of Magnetic Materials, [Accessed 21-07-2015]. Available from:

http://www.irm.umn.edu/hg2m/hg2m_b/hg2m_b.html

The presence of certain element combinations, normally in close proximity of Fe²⁺ or Fe³⁺, reacts to an applied magnetic field. The difference in the way the different elemental combinations in a mixture react or respond to an applied external field makes it possible for magnetism to be employed as separation technique. The magnetic portion (paramagnetic and ferromagnetic materials) can be separated, or rather be extracted from the non-magnetic portion (diamagnetic material). However, it is important to note that slight elemental combination differences (in the presence of larger amounts of Mn²⁺ in a mineral for example) may have a negative effect on the total removal of the magnetic elements in the sample. **Equation 4.3**⁶⁹ shows how magnetic susceptibility is calculated in the presence of an applied magnetic field (for magnetic separation process).

$$\chi_g = \frac{C_{\text{bal}} \times l \times (R - R_0)}{(10^9 \times m)} \quad 4.3$$

where: χ_g = mass magnetic susceptibility

C_{bal} = balance calibration constant

l = sample length (cm)

R = reading from the digital display for the tube plus sample

R_0 = reading from the digital display for the empty tube

m = sample mass (g)

This method of separation has an advantage of being relatively cheap, it needs no chemicals and a variable electromagnet with power supply or a permanent magnet can be used for separation. However, samples have to be crushed to very small (finely) particles before magnetic separation is attempted to ensure that the magnetic particles are free to react with the external magnetic field.

4.5.2 Solvent extraction

Although solvent extraction (liquid-liquid extraction) as a separation method has long been known to chemists, it is only in recent years that it has achieved recognition among analysts as a powerful separation technique. This method involves a process

in which a solute of interest transfers between two immiscible liquids.¹⁴⁵ It is quite a simple process with the two immiscible solvents shaken vigorously together and left to separate. This process either dissolves or extracts the solute of interest into the organic phase, leaving undesirable substances in the aqueous phase or by the extraction of the undesirable substances into the organic phase, leaving the desirable solute in the aqueous phase.¹⁴⁶ This is one of the most extensively studied and most widely used techniques for the separation and purification of elements due to the development of selective chelating agents for metal separation.¹⁴⁶ With a proper choice of extracting agents, this technique can achieve group separation or selective elements separation with high degrees of efficiency.

The success of any extraction of a solute is determined by the distribution of the solute between the two immiscible solvents (constant K_D), the chemical transformations to produce extractable species, the extraction ratio, d and the separation factor α .¹⁴⁷ The ratio between two essentially immiscible solvents at constant temperatures is a constant (distribution constant K_D). Provided that there is no solute involvement in chemical interactions in either solvent phase, the distribution constant can be presented according to **Equation 4.4** for the reaction illustrated in **Figure 4.14**.¹⁴⁸

$$K_D = \frac{[S_{org}]}{[S_{aq}]} \quad 4.4$$

In this equation, S is a solute distributed between the two immiscible solvents. A large value for K_D indicates that the solute's extraction into the organic phase is favourable.

¹⁴⁵ Solvent extraction, [Accessed 25-07-2015]. Available from:

<http://www.gonuke.org/acad/Solvent%20extraction.pdf>

¹⁴⁶ Rydberg J., Choppin G.R., Musikas C. and Sekine T., Solvent Extraction Equilibria, (1992),

[Accessed 25-07-2015]. Available from:

http://ww2.araku.ac.ir/~g_azimi/Solvent_extraction/solv_ext_ch4.pdf

¹⁴⁷ Fraiser H., Separations processes in analytical chemistry, The industrial environment- its evaluation and control, U.S. Department of health and human services, Chapter 18, pp. 207-222, (1973)

¹⁴⁸ Liquid-Liquid Extractions, [Accessed 28-07-2015]. Available from:

http://chemwiki.ucdavis.edu/Analytical_Chemistry/Analytical_Chemistry_2.0/07%3A_Collecting_and_Preparing_Samples/7G%3A_Liquid%E2%80%93Liquid_Extractions

To evaluate the efficiency of an extraction, the solute's total concentration (when S can exist in more than one chemical form) in each phase is considered and this is defined as the distribution ratio, D.

$$D = \frac{[S_{\text{org}}]_{\text{tot}}}{[S_{\text{aq}}]_{\text{tot}}} \quad 4.5$$

The distribution constant and the distribution ratio are identical if the solute has only one chemical form in each phase.

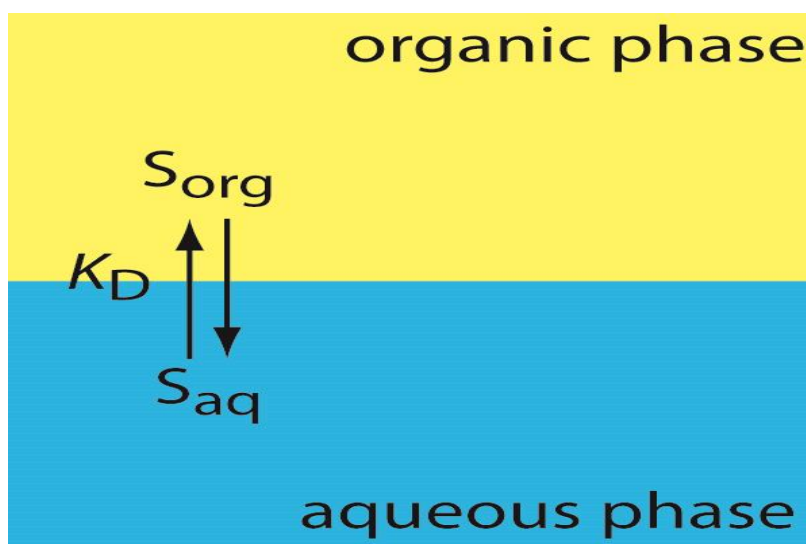


Figure 4.14: Simplified scheme for a liquid-liquid extraction in which the solute's partitioning depends only on the K_D equilibrium.

Using this technique, metal ions can be separated in a number of different ways including the extracting of the metal in an anion-associated complex (the metal ion reacts or bonds with the anion to form a new chelate complex which may now have organic type of character which will facilitate its extraction into the organic layer). The chelates are often insoluble in water and will precipitate but they are soluble in organic solvents such as chloroform or carbon tetrachloride.¹⁴⁹ The general extraction process of the metal ion from the aqueous phase into the organic layer is shown in **Figure 4.15**. The neutral chelate metal complex is transferred from the water layer to the immiscible organic layer by the mixing of the two solvents.

¹⁴⁹ Christian G.D., Analytical Chemistry, pp. 92-97, (1971)

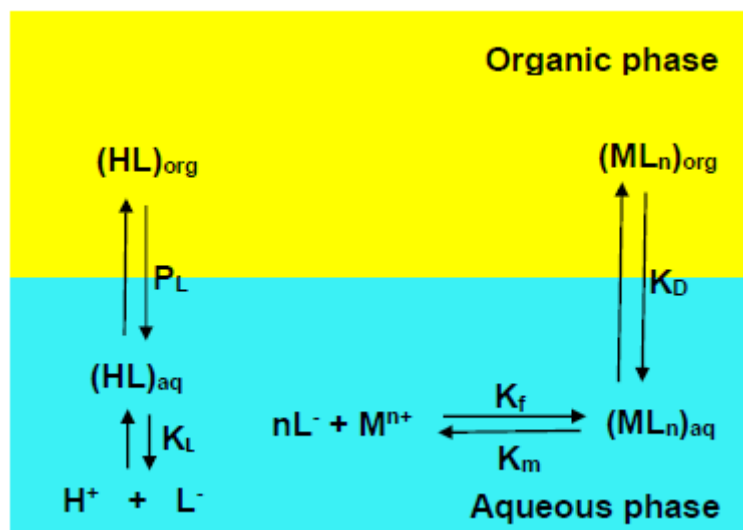
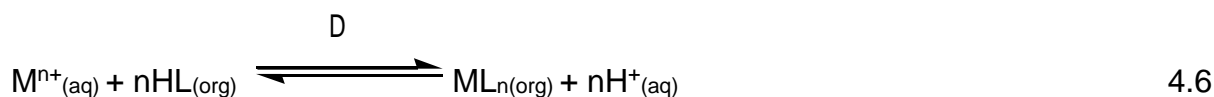


Figure 4.15: Scheme for the liquid-liquid extraction of a metal ion, M^{n+} .

The solvent extraction of metal chelates can be described in general as follows: the metal ion M^{n+} reacts with the organic reagent HL, giving a neutral complex ML_n which is distributed between two phases according to **Equation 4.6**.



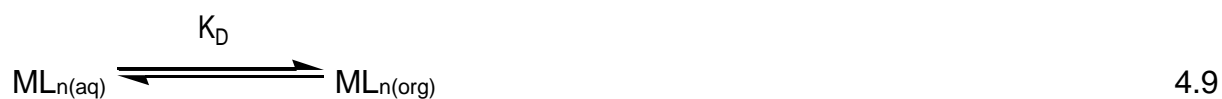
with

$$D = \frac{[ML_n]_{org}[H^+]_{aq}^n}{[M^{n+}]_{aq}[HL]_{org}^n} \quad 4.7$$

D can also be presented as a combination of the individual processes indicated in **Figure 4.15** with

$$D = \frac{K_D K_L^n}{K_m P_L^n} \quad 4.8$$

The four equilibrium steps involved in the extraction process (**Figure 4.15**) with their equilibrium constants are indicated by **Equations 4.9** to **4.16**:



with

$$K_D = \frac{[ML_n]_{org}}{[ML_n]_{aq}} \quad 4.10$$

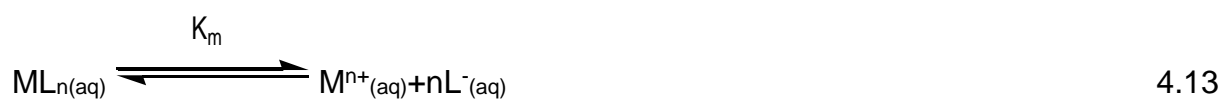
where K_D is the distribution constant of the metal chelate between the two immiscible layers.



with

$$P_L = \frac{[HL]_{org}}{[HL]_{aq}} \quad 4.12$$

where P_L is the distribution constant of the chelating agent between the two immiscible layers.



with

$$K_m = \frac{[M^{n+}]_{aq}[L^{-}]_{aq}^n}{[ML_n]_{aq}} \quad 4.14$$

where K_m is the dissociation constant of the metal chelate in the aqueous phase.



with

$$K_L = \frac{[H^+]_{aq}[L^-]_{aq}}{[HL]_{aq}} \quad 4.16$$

where K_L is the dissociation constant of the chelating agent in the aqueous layer.

When dividing **Equations 4.10** by **4.14** and Equation **4.16** by **4.12**, the two following expressions are obtained:

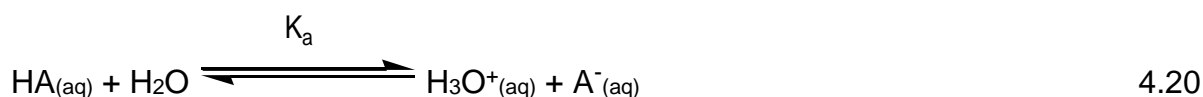
$$\frac{[ML_n]_{org}}{[M^{n+}]_{aq}} = \frac{K_D}{K_m} [L^-]_{aq}^n \quad 4.17$$

$$[L^-]_{aq} = \frac{K_L}{P_L} \times \frac{[HL]_{org}}{[H^+]_{aq}} \quad 4.18$$

Substitution of **Equation 4.18** into **4.17** and solving further gives **Equation 4.7**, mentioned previously which can also be expressed as:

$$D = \frac{[ML_n]_{org}[H^+]_{aq}^n}{[M^{n+}]_{aq}[HL]_{org}^n} = K_D \frac{[H^+]_{aq}^n}{[HL]_{org}^n} \quad \text{where } K_D = \frac{[ML_n]_{org}}{[ML_n]_{aq}} \quad 4.19$$

because $[M^{n+}]_{aq}$ and $[ML_n]_{aq}$ both represents the aqueous phase of the metal in solution. Another way to determine the relationship between D and K_D of an acid is as follows:



with

$$K_a = \frac{[H_3O^+]_{aq}[A^-]_{aq}}{[HA]_{aq}} \quad 4.21$$

where K_a is the dissociation constant of the acid. **Equation 4.21** can be rearranged to:

$$[A^-]_{aq} = \frac{K_a[HA]_{aq}}{[H_3O^+]_{aq}} \quad 4.22$$

The total amount of A in the aqueous layer is given by $[HA]_{(aq)}^T$ (**Equation 4.23**):

$$[HA]_{(aq)}^T = [HA]_{(aq)} + [A^-]_{(aq)} \quad 4.23$$

The distribution ratio D as a measure of the total concentration in each phase is given by **Equation 4.24**:

$$D = \frac{[HA]_{org}}{[HA]_{aq} + [A^-]_{aq}} \quad 4.24$$

Substituting **Equation 4.22** into **4.23**, rearranging with **Equation 4.4** for K_D and substituting into **Equation 4.24** gives **Equation 4.25**.⁴⁰

$$D = K_D \left(\frac{1}{1 + \frac{K_a}{[H_3O^+]}} \right) \quad 4.25$$

From **Equation 4.25** it can be seen that D is directly proportional to the $[H_3O^+]$ (when $[H_3O^+] \gg K_a$, $D \cong K_D$).

Since solvent extraction is used for the separation of different elements and species from each other, it becomes necessary to introduce a term to describe the effectiveness of separation of two solutes. A measure of the ability of the system to separate two solutes is determined by the separation factor α (**Equation 4.26**)¹⁵⁰ which is the ratio of the distribution coefficient of A to the distribution coefficient of B.

¹⁵⁰ Liquid-liquid extraction basic principles, [Accessed 06-09-2015]. Available from: http://www.academia.edu/3641270/Liquid-Liquid_Extraction_Basic_Principles

The separation of the different metal species is only viable when $\alpha > 1$. A large value of α indicates the potential for a high degree of separation in a small number of extraction stages.^{147,148}

$$\alpha_{A,B} = \frac{K_{D(A)}}{K_{D(B)}} \quad 4.26$$

Factors that need to be considered when choosing the extracting solvent include selectivity, distribution coefficient, solubility of solvent in H₂O, recoverability of solute from solvent, density difference between liquid phases, chemical reactivity, cost effectiveness, viscosity, vapour pressure, flammability and toxicity.¹⁵¹ Common extraction solvents are listed in **Table 4.4**.

Table 4.4: Some common extraction solvents¹⁵²

Solvent	Density, g/ml	Solubility in H ₂ O
Hexane	0.695	0.014 % at 20°C
Toluene	0.867	0.05 % at 25C
Dichloromethane	1.325	1.60 % at 20°C
Chloroform	1.492	0.815 % at 20°C
MIBK	0.802	1.90 % at 20 °C
1-octanol	0.819	0.096 % at 25 °C

The advantages of the solvent separation technique include its applicability to trace and macro levels, relatively low solvent usage and excellent extraction efficiency. A further advantage of the solvent extraction method lies in the convenience of subsequent analysis of the extracted species. If the extracted species are coloured, as is the case with many chelates, spectrophotometric methods can be employed. Alternatively, the solution may be aspirated for atomic absorption or ICP-emission spectrometric analysis. There are however disadvantages to this technique in that it may be time consuming (18 - 24 hours), very volatile compounds can be lost, labour-

¹⁵¹ Ashall P., (2007), Liquid-liquid separation principles, [Accessed 28-07-2015]. Available from: <http://eleceng.dit.ie/gavin/Bioprocess%20SC/Liquid-liquid%20extraction%20principles.ppt>

¹⁵² Properties of organic solvents, [Accessed 04-09-2015]. Available from: <http://murov.info/orgsolvents.htm>

intensive, sample pre-concentration is often required, the process is not easily automated and sometimes it is associated with high cost.¹⁵³

4.6 Method validation^{154,155,156,157}

The final step in the analytical process is the validation of the results that were obtained. The validation process is intended to verify if the analytical procedure employed for a specific analysis is suitable for its intended use. Various validation parameters need to be determined during the validation process and the results from this process can be used to judge the quality, reliability and consistency of analytical results while it is also an integral part of any good analytical practice. **Figure 4.16** shows the validation parameters.

¹⁵³ Principle of extraction (overview), [Accessed 09-08-2015]. Available from:

http://www.chemistry.sc.chula.ac.th/course_info/2302548/Wk3.pdf

¹⁵⁴ Skoog D.A., West D.M., Holler F.J. and Crouch S.R., Fundamentals of analytical chemistry, 9th Edition, pp. 43-50, (2014)

¹⁵⁵ Kalra K. (2011), Method development and validation of analytical procedures, Quality control of herbal medicines and related areas, [Accessed 09-08-2015]. Available from:

<http://www.intechopen.com/books/quality-control-of-herbal-medicines-and-related-areas/methoddevelopment-and-validation-of-analytical-procedures>

¹⁵⁶ Assay Validation Methods - Definitions and Terms, [Accessed 09-08-2015]. Available from:

<http://www.fws.gov/aah/PDF/QI-Terms%20and%20Defs.pdf>

¹⁵⁷ Selecting an Analytical Method, [Accessed 09-08-2015]. Available from:

http://chemwiki.ucdavis.edu/Analytical_Chemistry/Analytical_Chemistry_2.0/03_The_Vocabulary_of_Analytical_Chemistry/3D%3A_Selecting_an_Analytical_Method

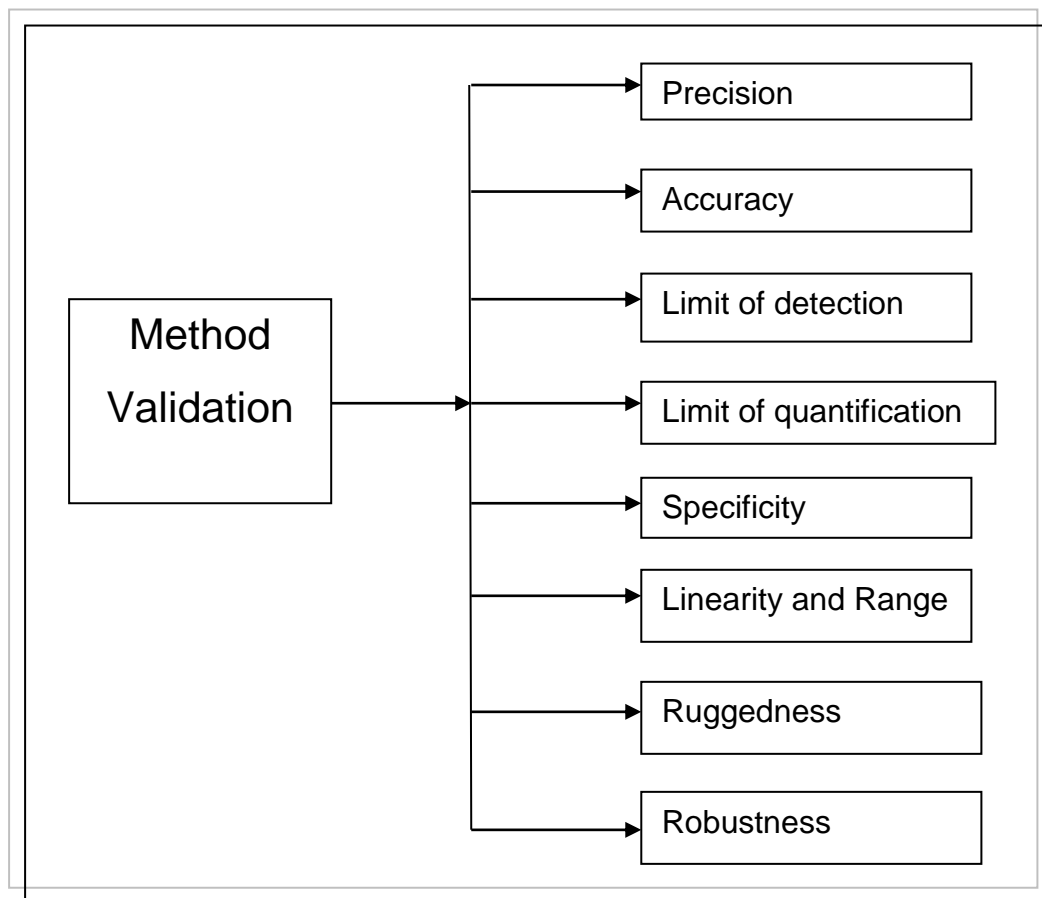


Figure 4.16: Method validation criteria

4.6.1 Accuracy

Accuracy is how closely the result of an experiment agrees with the “true” or expected result, taking into account systematic method and laboratory error. Accuracy, or more correct traceability, is ideally determined using Certified Reference Materials (CRMs) when available. Traceability also includes the use of reference methods, collaborative studies or comparison with other methods. If certified reference materials or control samples are not available, a blank sample matrix of interest can be spiked with a known concentration by weight or volume of the element in question. Other samples valid to determine traceability include pure compounds with known metal concentrations (from X-ray diffraction). A measure of accuracy is obtained using the student t-test at appropriate confidence levels. Accuracy is normally indicated with the absolute or relative error of the obtained results, compared to the expected value.

4.6.1.1 Absolute error (E)

The absolute error in the measurement of a quantity x is expressed as the difference between the obtained average and the true value as shown in **Equation 4.27** where \bar{x} is the mean or average and x_t is the true or expected value.

$$E = \bar{x} - x_t \quad 4.27$$

4.6.1.2 Relative error (E_r)

The relative error E_r is more useful than the absolute error and is the percentage relative error as expressed in **Equation 4.28**.

$$E_r = \frac{\bar{x} - x_t}{x_t} \times 100 \% \quad 4.28$$

4.6.2 Precision

This analytical parameter expresses the closeness or agreement (degree of scattered results) between a series of measurements obtained from multiple sampling (normally triplicates) of the same homogeneous sample under the prescribed conditions. The closer the agreement between individual analyses, the more precise or smaller the standard deviation between the results. Precision may be considered at three levels: repeatability (expresses the precision under the same operating conditions over a short interval of time), intermediate precision (expresses within-laboratory variations e.g. different days, different analysts) and reproducibility (expresses the precision between laboratories). The precision of an analytical procedure is usually expressed as the standard deviation (s), variance (s^2) or coefficient of variation (CV). **Equations 4.29, 4.30** and **4.31** show the how the latter three expressions of precision are calculated respectively.

$$s = \sqrt{\frac{\sum_{i=1}^N (x_i - \bar{x})^2}{N-1}} \quad 4.29$$

$$s^2 = \frac{\sum_{i=1}^N (x_i - \bar{x})^2}{N-1} \quad 4.30$$

$$CV = \frac{s}{\bar{x}} \times 100 \% \quad 4.31$$

N represents the number of measurements while x_i is the value of the i -th measurement. The lower these values are, the more precise (closeness) the set of measurements. CV can also be expressed as the relative standard deviation (RSD) or as % RSD when the value is multiplied by 100 where $RSD = \frac{s}{\bar{x}}$ or

$$\% RSD = \frac{s}{\bar{x}} \times 100$$

4.6.3 Limit of Detection (LOD)

The limit of detection of an analytical procedure is also a very important quantity which is the smallest amount of analyte concentration present in a sample which can unequivocally be detected by the analysis method. The LOD is calculated by **Equation 4.32**, where s_b is the standard deviation of the blank solution and m (also expresses sensitivity of the method) is the slope of the calibration curve.

$$LOD = \frac{3 \times s_b}{m} \quad 4.32$$

The value 3 corresponds to a confidence interval of 99.7 %.

4.6.4 Limit of Quantitation (LOQ)

The limit of quantitation (LOQ) of an analytical procedure is related to the LOD and is the lowest amount of analyte in a sample which can confidently be quantified with suitable precision and accuracy. This parameter is normally for the quantification of low levels of analytes in sample matrices, and is particularly useful for the determination of impurities. The LOQ is calculated according to **Equation 4.33** and are illustrated in **Figure 4.17**.

$$\text{LOQ} = 10 \times \text{LOD}$$

4.33

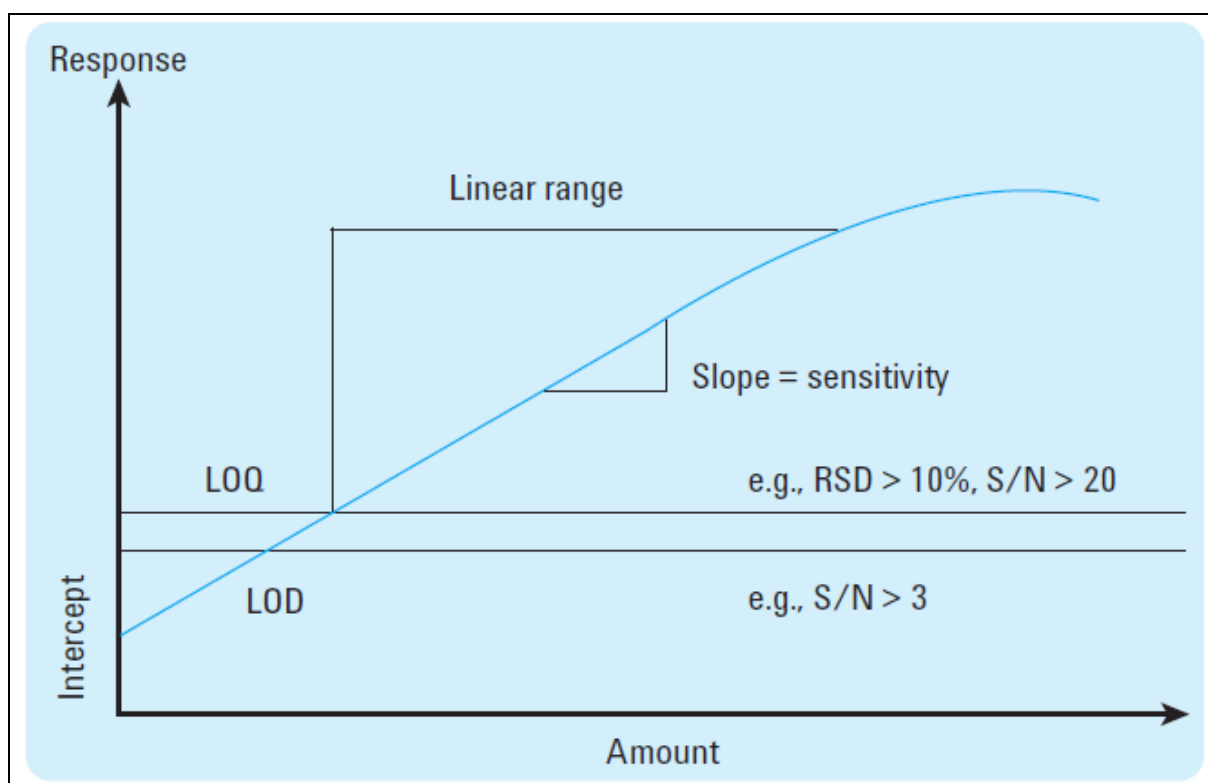


Figure 4.17: The determination of LOD and LOQ from the calibration curve

4.6.5 Specificity and Selectivity

Specificity and selectivity are often used interchangeably and both are parameters that measure the reliability of measurements or analyses in the presence of the interferences. Specificity is the ability to assess unequivocally the analyte in the presence of compounds that are expected to be present. Selectivity is the ability of a method to differentiate and quantify the analyte in the presence of other components in the sample.

4.6.6 Linearity

An analytical procedure is described as linear when there is a directly proportional relationship (within a given range) between the method response and concentration of the analyte in the sample. Usually, measurements using standards with known concentrations are used to determine a calibration curve to demonstrate linearity.

Acceptance criteria involve a good-fit of a straight line through the points and are reflected by the correlation coefficient R^2 of the linear regression line. This line should have a value close to 1 as illustrated in **Figure 4.18**. The y-intercept should not differ significantly from zero (this value describes the background) as this indicates that there is little or no matrix interfering.

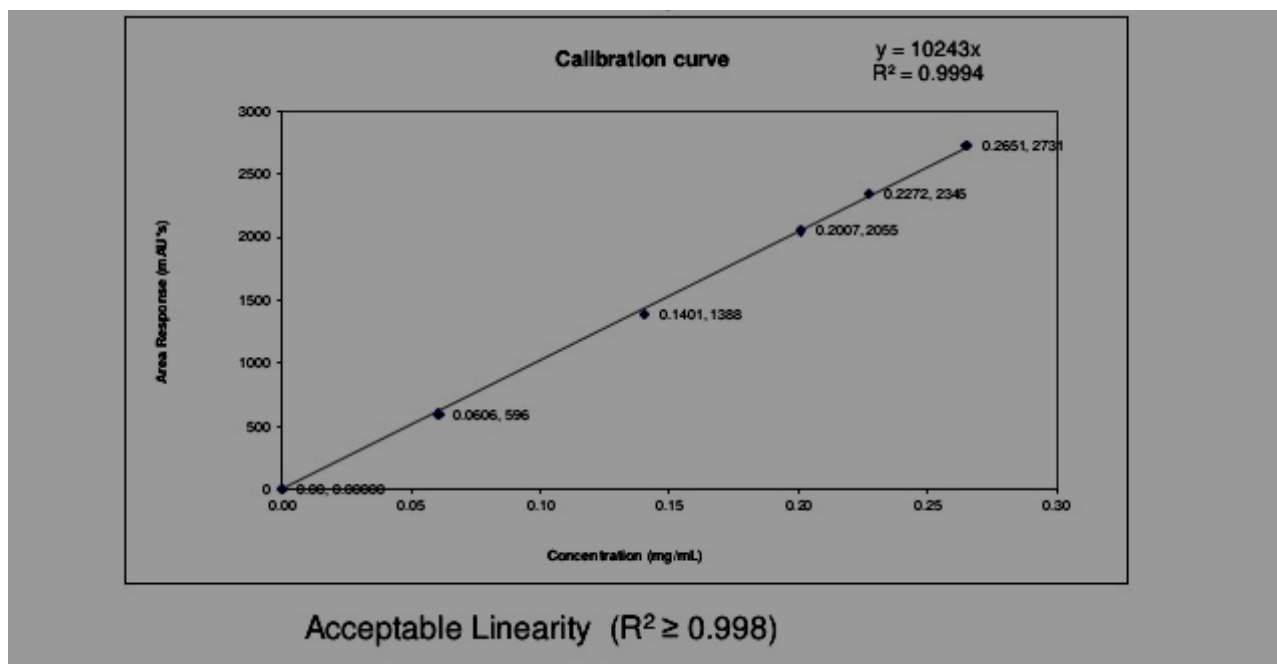


Figure 4.18: A calibration curve showing good linearity with R^2 value close to 1.

4.6.7 Range (w)

The range of an analytical method is defined as the concentration range of the analyte which can be analyzed accurately on a calibration curve and is dependent on the set of standards. Protocol dictate that analyses should be performed within the range (above the lowest concentration and below the highest concentration), but preferably in the middle of the calibration range.

4.6.8 Robustness/Ruggedness

Robustness or ruggedness is a measure of how capable an analytical procedure is to remain unaffected by small but deliberate variations in the method parameters and provides valuable information about the reliability of the method during its normal

usage. A method which is relatively free from chemical interferences can normally be used on a wide variety of analytes covering a wide variety of sample matrices. A rugged method is relatively insensitive to changes in experimental conditions such as acidity or temperature. These properties should be explored during the development of the method and the actual method validation will ensure that the final, chosen ranges are robust.

4.7 Conclusion

Open beaker, microwave and furnace techniques for digestion were attempted in this study. For identification of synthesized complexes, IR, melting point and CHNS elemental analysis techniques were used and due to the advantages of ICP-OES, it was used for the quantification of scandium. The above mentioned validation parameters all prove to be useful to ensure the quality of the developed method in this study.

5 Quantification of scandium in different scandium-containing matrices and method validation

5.1 Introduction

The biggest challenges to scandium beneficiation remain its low natural abundance in different mineral deposits as well as its association with other elements with very similar chemical properties as discussed in **Chapter 1**. The pre-concentration of scandium before extraction is a key step in the successful isolation (from the rest of the elements with similar chemical properties) and production of pure scandium metal or products. Scandium has been successfully quantified in different scandium-containing samples, but low percentage recoveries were obtained for some of the methods described in **Chapter 3** while other methods proved to be environmental unfriendly.

The main objective of this study was to do an in-depth study to accurately determine and quantify scandium in different matrices including inorganic compounds and organometallic complexes as well as columbite mineral, using ICP-OES. Different dissolution methods including open-beaker dissolution, microwave-assisted dissolution and flux fusion were employed in this study for sample dissolution. Different techniques such as melting point measurements, IR spectroscopy and CHNS-micro analysis were used for the proper identification of the newly synthesized complexes while ICP-OES was used for the quantification of Sc in the different matrices. Optimum conditions for both sample preparation and quantification of scandium in mineral ore were investigated and employed in other scandium-containing matrices in this study. Validation parameters such as precision, accuracy,

linearity, etc., were also determined for the methods (**Chapter 4**) in this study to ensure the newly devised method adhere to sound analytical chemistry principles.

5.2 General experimental conditions and procedures

5.2.1 Preparation of ultra-pure water

The ultra-pure water that was used for all the analytical solution preparations was prepared in the laboratory using an ultra-reverse osmosis system from AJD Traders. The quality of the pure and ultra-pure water was measured as 0.02 and 0.00 $\mu\text{S}/\text{cm}$ respectively using a Hanna DIST 3 (HI98304S) conductivity meter.

5.2.2 Weighing

All the samples were accurately weighed to 0.1 mg at 20 ± 3 °C using a Shimadzu (AW320) electronic balance calibrated under ISO 9001. A much more sensitive balance, Sartorius CP Series, Model CPA26P was also used to accurately measure masses less than 0.01 g (accurate to 0.01 mg). Analytical samples and reagents used in the study were all weighed by adding a sample in a pre-weighed glass vial or a tin capsule.



Figure 5.1: Shimadzu (AW320) and Sartorius (CPA26P Series) electronic balance scales

5.2.3 Micro-pipets

An adjustable-volume Gilson Pipetman (100 μL - 1000 μL) and Brand Transferettes (1 mL - 10 mL) micro-pipettes were used to accurately transfer solutions.

5.2.4 Glassware

The glassware (beakers and volumetric flasks) used for all the elemental analysis in this study was of Schott Duran, grade (A) type. The glassware were first soaked in 55 % HNO_3 for about 24 hours and rinsed 2 - 3 times with ultra-pure water and dried prior to use.

5.2.5 Microwave-assisted digestion

Acid assisted microwave digestion of Sc_2O_3 and the Sc organometallic complexes were performed with an Anton Paar Perkin & Elmer Multiwave 3000 microwave digestion system equipped with an 8SXF 100 rotor and eight polytetrafluoroethylene (PTFE) reaction vessels (**Figure 4.2**). An internal program optimised for the digestion of the platinum group metals (PGM XF100-8) was selected and used during the digestion process and are reported in **Table 5.1**.

Table 5.1: Microwave digestion conditions used in this study for digestion of Sc_2O_3 and the Sc organometallic compounds

Parameter	Condition
Power	600 Watts
Ramp	15 minutes
Holding Time	45 minutes
Pressure rate	0.5 bar/sec
Infra-red (IR)	240 °C
Pressure	60 bar
Volume of the acid	8.0 mL
Reagent	65 % HNO_3 , 32 % HCl , 98 % H_2SO_4

5.2.6 ICP-OES

A Shimadzu ICPS-7510 ICP-OES sequential plasma spectrometer controlled by a computer (**Figure 5.2**) was used for the qualitative and quantitative analysis of Sc in the inorganic and organometallic compounds, as well as for the elemental composition of the columbite which also indicated the presence of Nb, Ti, Sn, W, Si, Ta, Zr, Y, Fe, Al, Mn, U and Th in the solutions. The operating conditions used during this study are given in **Table 5.2**. The average values (for three replicates) for the results in this chapter are reported, based on the standard deviations to indicate the uncertainty in the last digit of the value.



Figure 5.2: Shimadzu ICPS-7510 ICP-OES sequential plasma spectrometer

Table 5.2: ICP-OES operating conditions

Parameter	Condition
RF power	1.2 kW
Coolant gas flow	14.0 L/min
Plasma gas flow	1.2 L/min
Carrier gas flow	0.7 L/min
Sample uptake method	Peristaltic pump
Spray chamber	Glass cyclonic
Type of nebuliser	Concentric

5.3 Materials and reagents

All chemicals, reagents and samples (with their known purity) which were used during the entire study are listed in **Table 5.3** and were all used without further purification. An ICP standard solution containing 1000 mg/L Sc was bought from Merck.

Table 5.3: Chemicals and reagents used in this study

Chemical	Formula	Purity/grade	Supplier
Acids			
Nitric acid	HNO ₃	55 %	Merck
Nitric acid	HNO ₃	65 %	Merck
Hydrochloric acid	HCl	32 %	Merck
Sulphuric acid	H ₂ SO ₄	95 - 99 %	Merck
Reagents			
Scandium chloride	ScCl ₃ ·H ₂ O	99.9 %	Sigma-Aldrich
Scandium oxide	Sc ₂ O ₃	99.9 %	Sigma-Aldrich

5.4 Experimental procedures for the determination of scandium

5.4.1 Preparation of ICP-OES standards

Three sets of calibration standard solutions for ICP-OES analysis were prepared from the 1000 mg/L Sc ICP-OES standard solution by adding the appropriate volumes in different 100.0 mL volumetric flasks to obtain 0.5, 1.0, 3.0, 5.0 and 10.0 mg/L concentrations. To the first set, 65 % HNO₃ (5.0 mL) was added to each flask (to ensure matrix matching) and then the volumetric flasks were filled to the mark with ultra-pure water. To the second set of standards, 32 % HCl (5.0 mL) was added to ensure acid matrix matching and to the third set 95 - 99 % H₂SO₄ (5.0 mL) was added. Blanks were prepared by diluting 5.0 mL of each acid to 100.0 mL in volumetric flasks. The prepared standard solutions were homogenized and left to stand for 5 hours before use. Quantitative analyses were performed at a Sc wavelength of 361.384 nm.

5.4.2 Determination of LOD and LOQ's

The LOD and the LOQ were determined by measuring the intensities of the blank solutions for each acid (10 replicates for these calculations). The standard deviation (s_b) of a blank solution and the slope (m) of the calibration curve for each acid was determined and used as shown in **Chapter 4, Equations 4.9, 4.12 and 4.13**. **Table 5.4** reports the LOD and LOQ values obtained for Sc in the different mineral acids.

Table 5.4: Calculation of LOD's and LOQ's of Sc in different acids

Acid	Standard deviation (s_b)	Slope (m)	LOD (ppm)	LOQ (ppm)
HNO ₃ (65 %)	0.004675	14.1560	0.0009907	0.009907
HCl (32 %)	0.006280	9.8852	0.001906	0.01906
H ₂ SO ₄ (95 - 99 %)	0.004828	13.3450	0.001085	0.01085

5.5 Quantification of Sc in inorganic compounds

5.5.1 Preparation of ScCl₃·H₂O

Three samples with masses of approximately 0.07 g of ScCl₃·H₂O (accurately weighed to 0.1 mg) were dissolved in a minimum amount of ultra-pure water then quantitatively transferred to 100.0 mL volumetric flasks after which the flasks were filled to the mark. These solutions were further diluted by pipetting 2.0 mL of the stock solution into 100.0 mL flasks and 5.0 mL 65 % HNO₃ was added to each before the flasks were filled to the mark with ultra-pure water. The solutions were left to stand for at least 5 hours before they were analysed with ICP-OES. Results are shown in **Table 5.5**.

Table 5.5: Sc quantification in ScCl₃·H₂O by ICP-OES

Sample	Analysis No.	Mass weighed (g)	Theoretical Sc conc. (ppm)	Actual Sc conc. (ppm)	Sc Recovery (%)	Ave. % Recovery (s)	RSD (%)
ScCl ₃ ·H ₂ O	1	0.0747	4.4389	4.4294	99.79	99.71(7)	0.075
	2	0.0755	4.4864	4.4729	99.70		
	3	0.0760	4.5161	4.4998	99.64		

5.5.2 Dissolution of Sc₂O₃ by open-beaker digestion

Three Sc₂O₃ samples (for each acid) of approximately 0.01 g portions (accurately weighed to 0.1 mg) were quantitatively transferred to 50.0 mL glass beakers and 6 mL portions of different mineral acids (32 % HCl, 65 % HNO₃ or 95 - 99 % H₂SO₄) were added to each glass beaker. The mixtures were then heated to 60 °C with continuous stirring for 40 min in a fume hood to try and dissolve the Sc₂O₃. Visual inspection indicated that Sc₂O₃ were completely dissolved by both HCl and HNO₃ while the presence of some Sc₂O₃ after this time indicated the incomplete dissolution in H₂SO₄. The H₂SO₄ mixtures were filtered after which all the solutions were transferred to 100.0 mL volumetric flasks. Further dilution was done by pipetting 10.0 mL into other 100.0 mL volumetric flasks and 5.0 mL of different acids were added to ensure matrix matching with the standards prepared in **Section 5.4.1**. The solutions

were then analysed with ICP-OES for Sc content and the results are given in **Table 5.6**.

Table 5.6: Quantitative analysis of Sc in Sc_2O_3 by ICP-OES after digestion by open-beaker method.

Sample	Analysis No.	Mass weighed (g)	Theoretical Sc conc. (ppm)	Actual Sc conc. (ppm)	Sc Recovery (%)	Ave. % Recovery (s)	RSD (%)
Sc_2O_3 in HCl	1	0.0101	6.5848	6.5315	99.19	98.9(3)	0.25
	2	0.0103	6.7152	6.6420	98.91		
	3	0.0104	6.7804	6.6916	98.69		
Sc_2O_3 in HNO_3	1	0.0102	6.6500	6.6021	99.28	99.2(4)	0.43
	2	0.0103	6.7152	6.6830	99.52		
	3	0.0100	6.5196	6.4342	98.69		
Sc_2O_3 in H_2SO_4	1	0.0100	6.5196	2.9508	45.26	44.7(7)	1.46
	2	0.0102	6.6500	2.9253	43.99		
	3	0.0104	6.7804	3.0437	44.89		

5.5.3 Dissolution of Sc_2O_3 with microwave assisted digestion in the presence of different acids

The low Sc recovery with H_2SO_4 in the previous study prompted the investigation into the use of microwave digestion in the presence of the different acids. Three Sc_2O_3 samples (for each acid) of approximately 0.02 g portions were weighed (accurately to 0.1 mg) and quantitatively transferred to clean microwave polytetrafluoroethylene (PTFE) vessels. 8 mL of 65 % HNO_3 , 32 % HCl or 95 - 99 % H_2SO_4 was added to each vessel and the mixtures were digested under the microwave conditions listed in **Table 5.1**. In this case visual inspection indicated that all the samples in the different acids were completely dissolved. The resulting solutions were quantitatively transferred to 250.0 mL volumetric flasks and filled to the mark with ultra-pure water. New solutions were prepared from these stock solutions by pipetting 4.0 mL into 100.0 mL volumetric flasks and 5.0 mL acids were added to each volumetric flask to match the acid conditions with those of the Sc standards prepared in **Section 5.4.1**. The volumetric flasks were filled to the mark with ultra-pure water. The solutions were

then analysed with ICP-OES for Sc concentrations and the results are presented in **Table 5.7**.

Table 5.7: Quantitative analysis of Sc in Sc₂O₃, digested with microwave in the presence of different acids

Sample	Analysis No.	Mass weighed (g)	Theoretical Sc conc. (ppm)	Actual Sc conc. (ppm)	Sc Recovery (%)	Ave. % Recovery (s)	RSD (%)
Sc ₂ O ₃ in HCl	1	0.0200	2.0863	2.0921	100.3	100.1(3)	0.27
	2	0.0197	2.0550	2.0499	99.75		
	3	0.0200	2.0863	2.0890	100.1		
Sc ₂ O ₃ in HNO ₃	1	0.0205	2.1384	2.1264	99.44	99.8(3)	0.32
	2	0.0202	2.1073	2.1062	99.95		
	3	0.0204	2.1301	2.1282	99.91		
Sc ₂ O ₃ in H ₂ SO ₄	1	0.0226	2.3571	2.3515	99.75	101(1)	1.16
	2	0.0219	2.2842	2.3280	101.9		
	3	0.0227	2.3681	2.3691	100.04		

5.6 Quantification of Sc in different organometallic complexes

5.6.1 Introduction

One of the objectives of this study was also to develop an analytical method for scandium quantification in different organometallic complexes. The different organometallic complexes investigated in this study were all synthesized using ScCl₃·H₂O and different acetylacetonate ligands in basic solution as starting compounds. The different acetylacetonate ligands, such as 2,4-pentanedione, acacH, (or acetyl acetone), react with a base or alkali according to **Figure 5.3** to form the acetylacetonate anion, acac.

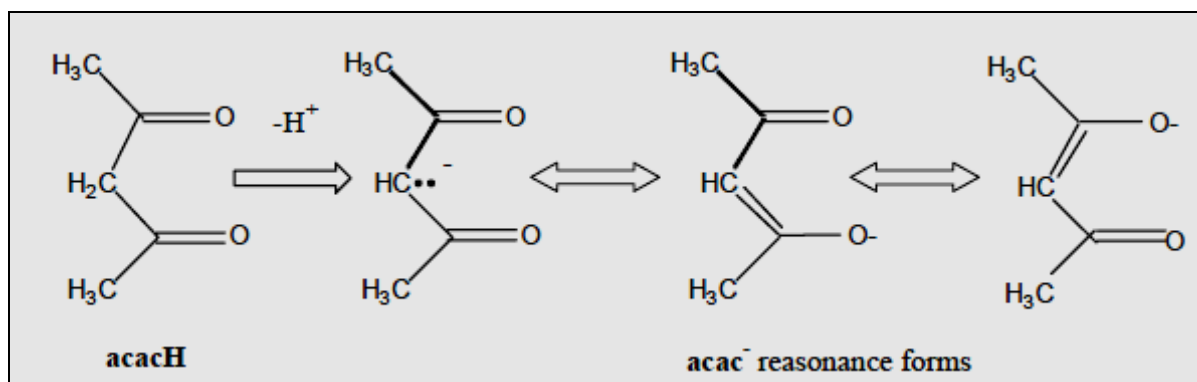


Figure 5.3: Formation of the acetylacetonate anion

The hydrogen atoms on α -carbon atoms that are adjacent to carbonyl, $\text{C}=\text{O}$, groups are relatively acidic¹⁵⁸ and it is relatively easy for alkalis to remove or deprotonate the proton. These ligands have the potential to act as bidentate ligands which can bond to a metal via both oxygen atoms or oxygen and sulphur atoms, depending on the type of acetylacetonate starting material. The bidentate ligands used in this study are presented in **Figure 5.4**.

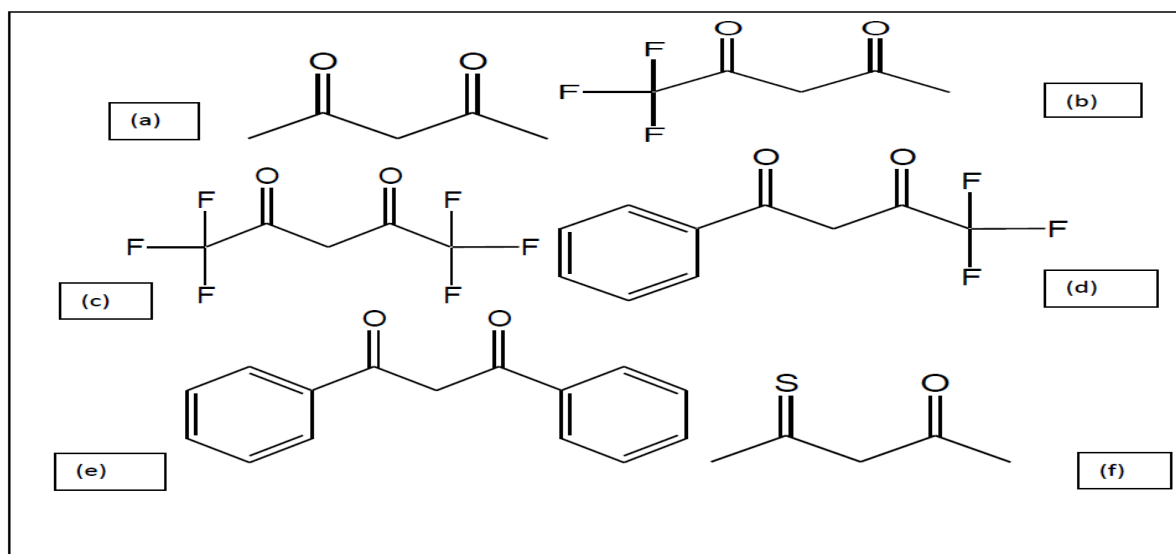


Figure 5.4: Bidentate ligands (a) acetylacetone (acacH), (b) 1,1,1-trifluoroacetylacetone (tfacH), (c) hexafluoroacetylacetone (hfacH), (d) benzoyl-1,1,1-trifluoroacetylacetone (btfacH), (e) dibenzoylmethane (dbm) and (f) thioacetylacetone (sacacH)

¹⁵⁸ Synthesis of metal acetylacetonates: Preparation of Tris(2,4-pentanedionato)chromium(III), [Accessed 12-09-2015]. Available from: <http://www.colby.edu/chemistry/Grants/lab2ch141spring04.pdf>

A summary of the process that was followed in the syntheses of the different scandium complexes, the characterisation and the quantification techniques used in this study is shown in **Figure 5.5**.

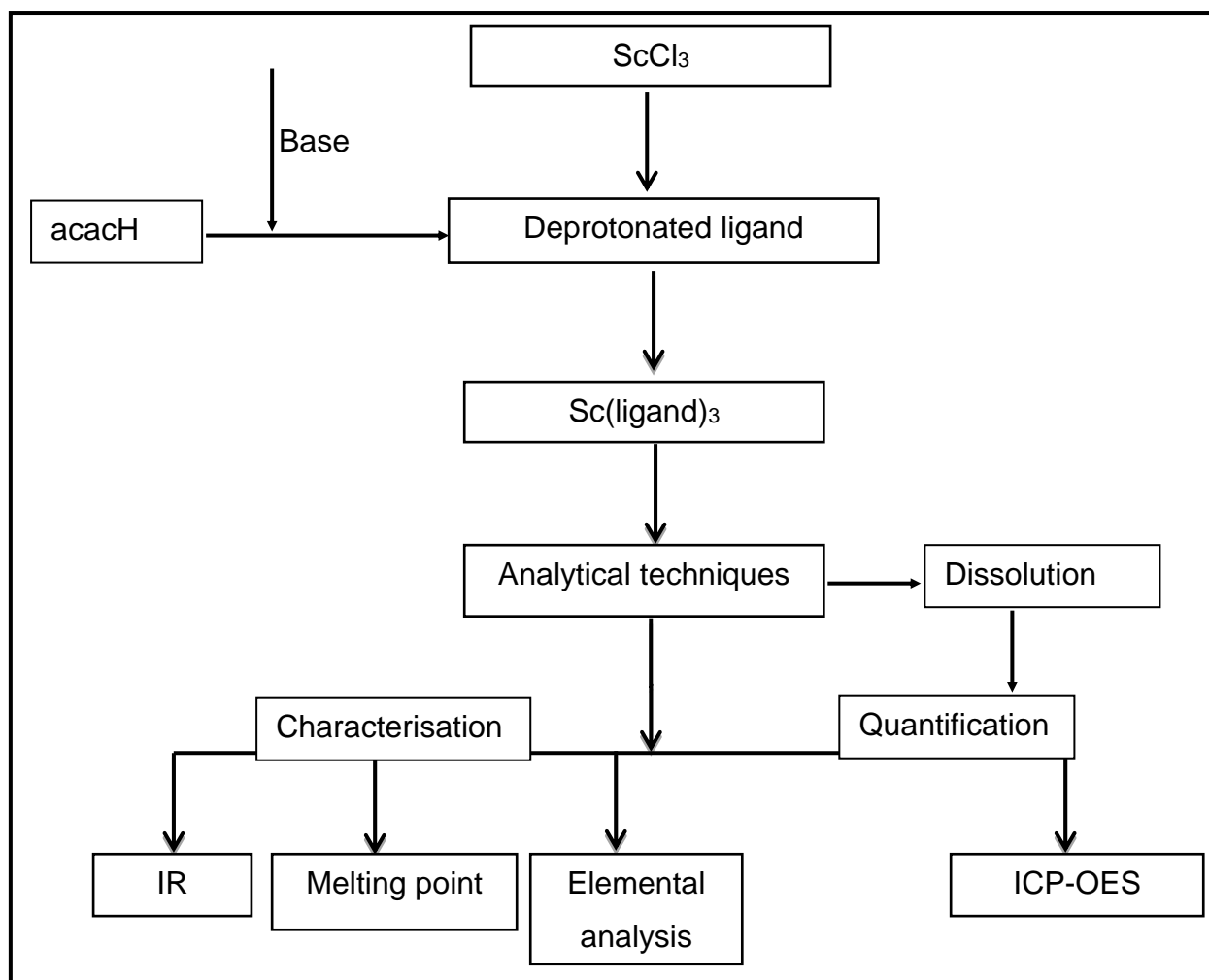


Figure 5.5: General procedure of the synthesis, identification and quantification of different $\text{Sc}(\text{acac})_3$ complexes

The synthesized Sc complexes were characterised using melting point, IR and the CHNS micro-element analysis techniques. Open beaker and microwave-assisted digestion methods were used for digesting the samples prior to the ICP-OES quantitative analyses. The experimental conditions for the ICP-OES in **Table 5.2** were applied to quantify the Sc in the different organometallic complexes.

5.6.2 General equipment

5.6.2.1 *Melting point apparatus*

Melting points for the synthesized complexes were obtained with a Gallenkamp melting point apparatus which is shown in **Figure 5.6**.



Figure 5.6: Melting point apparatus used in this study

5.6.2.2 *IR spectroscopy*

A Digilab Scimitar Series infrared spectrometer (**Figure 5.7**) was used for the recording of the IR spectra for the synthesized Sc complexes.

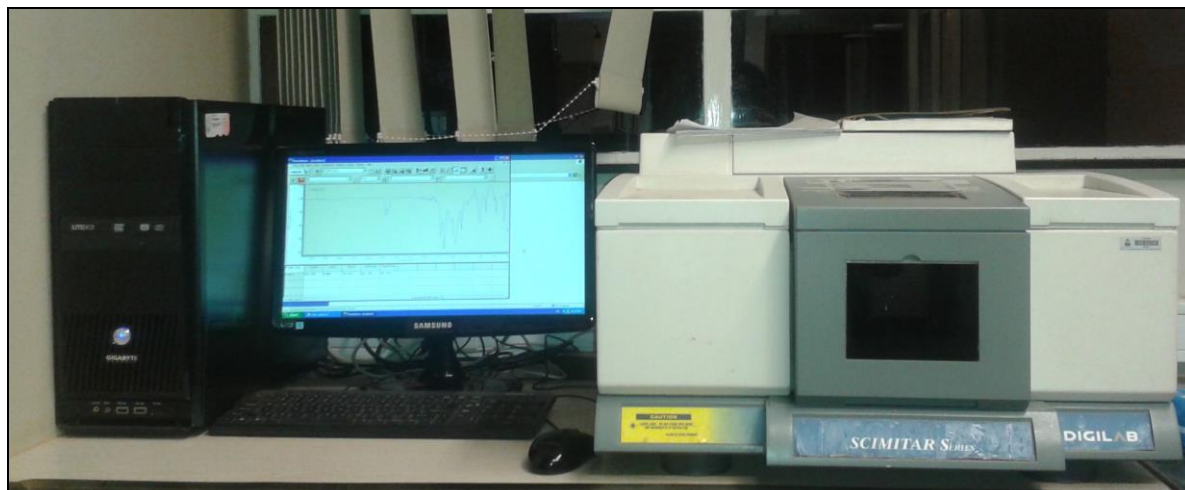


Figure 5.7: Infrared spectrometer

5.6.2.3 *Truspec micro CHNS elemental analyser*

A TruSpec Micro CHNS (**Figure 5.8**) micro-element analyser bought from LECO was used for the determination of elemental carbon, hydrogen, nitrogen and sulphur content and hence the empirical formulas of the newly synthesized complexes.



Figure 5.8: Leco CHNS Truspec Micro Series

5.6.3 Materials and solvents

All chemicals and reagents were bought from different commercial suppliers and used without further purification. The chemical, their purity and the suppliers are listed in **Table 5.8**.

Table 5.8: List of materials and solvents

Chemical	Formula	Purity	Supplier
Ligand			
Acetylacetone (acacH)	C ₅ H ₈ O ₂	99.5 %	Riedel-deHaën
1,1,1-trifluoroacetylacetone (tfacH)	C ₅ H ₅ F ₃ O ₂	98 %	Sigma-Aldrich
Benzoyl-1,1,1-trifluoroacetone (btfacH)	C ₁₀ H ₇ F ₃ O ₂	–	Riedel-deHaën
Dibenzoylmethane (DBM)	C ₁₅ H ₁₂ O ₂	≥ 98 %	Sigma-Aldrich
Hexafluoroacetone (hfacH)	C ₅ H ₂ F ₆ O ₂	98 %	Sigma-Aldrich
Thio-acetylacetone (sacacH)	C ₅ H ₂ SO	–	Synthesized*
Base			
Ammonium hydroxide	NH ₄ OH	25 %	Merck
Sodium carbonate	Na ₂ CO ₃	99 %	Riedel-deHaën
Solvent			
Benzene	C ₆ H ₆	–	American Burdick & Jackson
Chloroform	CHCl ₃	99 %	Merck
Diethyl ether	C ₄ H ₁₀ O	–	Merck
Heptane	C ₇ H ₁₆	–	Merck
Hexane	C ₆ H ₁₄	–	Merck

* - Synthesis in Section 5.6.3.1,

– Not supplied

5.6.3.1 Synthesis of thio-acetylacetone

Acetylacetone (50 mL, 0.5 mol) and morpholine (4.3 g, 0.05 mol) was mixed in a long cylindrical container. Small H₂S gas bubbles were introduced for 180 min at the bottom of the container with the aid of a long glass pipe and a sinter glass frit to ensure effective gas to solution mass transfer. The unreacted H₂S gas was removed by bubbling the spent gas through a concentrated NaOH solution. The container was sealed and left overnight at room temperature. The mixture was subsequently

washed with 100 mL of petroleum ether (b.p. 80 - 100 °C) and then with 3 M HCl. The crude product was dried over anhydrous Na₂SO₄ and concentrated with reduced pressure. The final gold-yellow product was obtained by fractional distillation at 40 °C and 5 mmHg. Yield: 71%.

5.6.4 Syntheses of organometallic complexes

5.6.4.1 Synthesis of Sc(acac)₃¹⁵⁹

Scandium chloride (0.3025 g, 0.002 mol) was dissolved in 10 mL of water and then added to a mixture (pH 7) of acetylacetone (acacH) (0.008 mol, 1 mL) and concentrated aqueous ammonia (2 mL). The mixture was continuously stirred and turned milky. A white precipitate was obtained by the slow addition of additional aqueous ammonia (2 mL, 0.1 M). The obtained precipitate was filtered, air dried and recrystallised from a mixture of benzene and acetylacetone (10:1, v:v). Yellow needle-like crystals were collected (68.39 % yield), M.P. in the range of 183 - 184.7 °C.

5.6.4.1.1 Infrared analysis

The Sc(acac)₃ complex and the ligand acetylacetone infrared spectra were recorded with a Digilab Scimitar Series spectrometer and the spectra are shown in **Figure 5.9** and their stretching frequencies are listed in **Table 5.9**.

¹⁵⁹ Garon S., Novel organic materials for organic Electroluminescent Devices and Organic photovoltaic devices, p. 90, (2006)

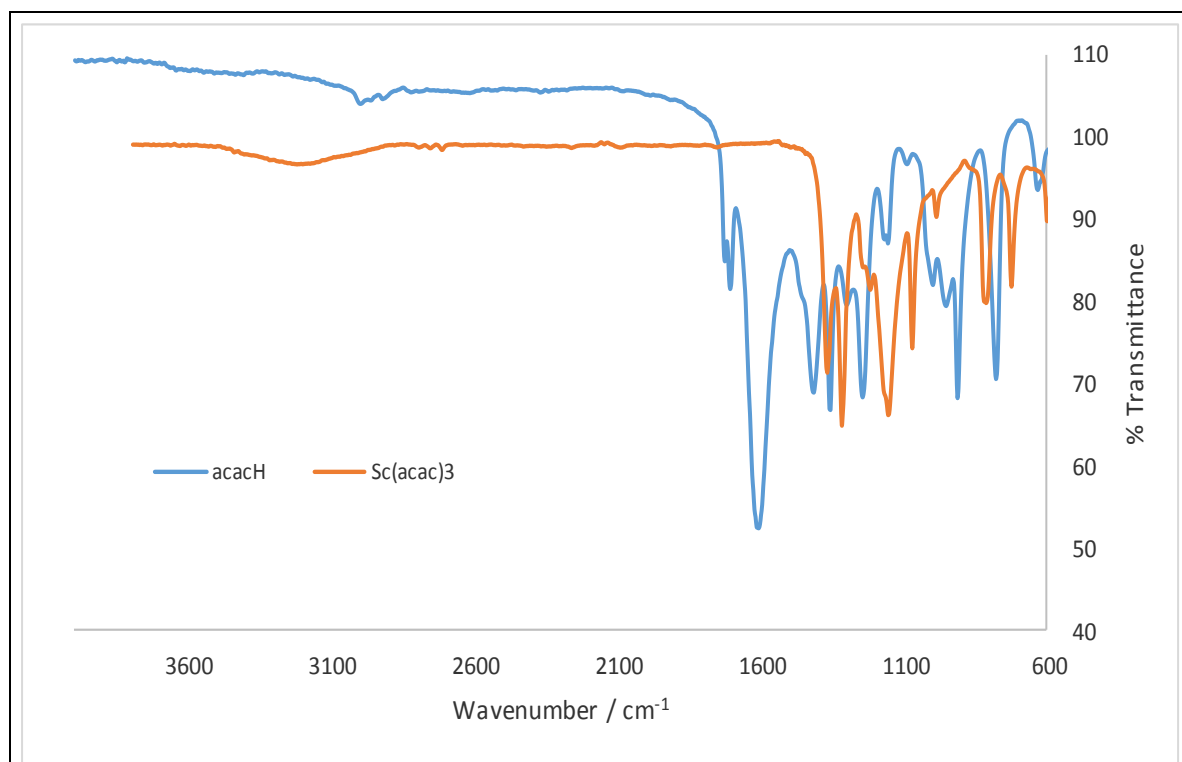


Figure 5.9: The IR spectra of acetylacetonone and $\text{Sc}(\text{acac})_3$.

Table 5.9: IR stretching frequencies (in cm^{-1}) for acacH and $\text{Sc}(\text{acac})_3$

Compound	$\nu(\text{C}=\text{O})^{\text{a}}$	$\nu(\text{C}=\text{O})^{\text{b}}$	$\nu(\text{C}=\text{C})$	$\nu(\text{C}=\text{O}) + \delta(\text{C}-\text{H})$	$\delta(\text{CH}_3)$
acacH	1708.5	1610.3	-	1417.5	1359.7
$\text{Sc}(\text{acac})_3$	-	1570.7	1519.0	1421.7	1356.3

^a – keto form, ^b – enol form

5.6.4.1.2 Elemental analysis

Approximately 2.0 mg of the $\text{Sc}(\text{acac})_3$ complex was accurately weighed with a sensitive Sartorius (CPA26P Series) electronic balance (**Figure 5.1**) to 0.01 mg in tin capsules and analysed for C and H content using the LECO CHNS analyser. The results are presented in **Table 5.10**.

Table 5.10: Elemental analysis of Sc(acac)₃

Molecular formula	Empirical formula	% C*		% H*	
		Calculated	52.64	Calculated	6.18
Sc(acac) ₃	ScC ₁₅ H ₂₁ O ₆	Found	54.75	Found	5.19

* Average of three replicates

5.6.4.1.3 Open-beaker dissolution for Sc(acac)₃

The Sc(acac)₃ complex prepared in **Section 5.6.4.1** was weighed (0.0100 – 0.0103 g) and dissolved in 5 mL of 65 % HNO₃. Visual inspection indicated complete dissolution and these solutions were then transferred to 100.0 mL volumetric flasks and filled to the mark with ultra-pure water and left to stabilise for 4 hours. These solutions were analysed for Sc content using ICP-OES and the results are presented in **Table 5.11**.

Table 5.11: Quantitative determination of scandium in Sc(acac)₃ dissolved in HNO₃

Sample No.	Sample mass weighed (g)	Theoretical metal concentration (ppm)	Actual concentration (ppm)	Sc Recovery (%)
1	0.0101	13.266	13.219	99.65
2	0.0100	13.134	13.100	99.74
3	0.0103	13.528	13.357	98.73
Average recovery (%) (s)				99.4(6)
RSD (%)				0.56

5.6.4.2 Synthesis of Sc(tfac)₃

A solution of scandium chloride (0.1398 g, 0.001 mol) in 10 mL of ultra-pure water was added to a mixture of 1,1,1-trifluoroacetylacetone (tfacH) (0.004 mol, 1.5 mL) and concentrated aqueous ammonia to a pH of 8. An orange precipitate was formed with continuous stirring for an hour. The precipitate obtained was filtered, dried on air and recrystallised from a mixture of benzene and 1,1,1-trifluoroacetylacetone (10:1

v:v). Shiny but very small yellow crystals were obtained (45.07 % yield), M.P. in the range of 97.3 - 98.3 °C.

5.6.4.2.1 Infrared analysis

The IR spectra of the Sc(tfac)₃ complex and the tfacH ligand were recorded with a Digilab Scimitar Series spectrometer and are shown in **Figure 5.10** with their most important stretching frequencies listed in **Table 5.12**.

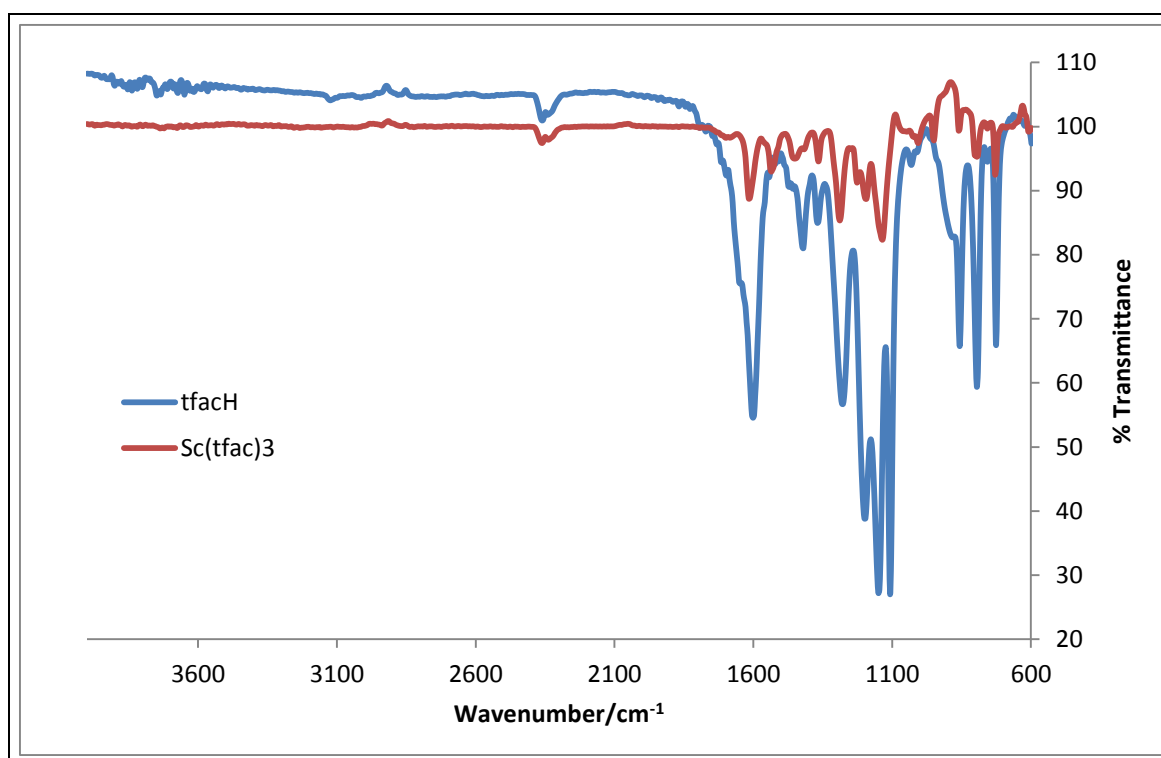


Figure 5.10: The IR spectra of tfacH and Sc(tfac)₃.

Table 5.12: The IR stretching frequencies of tfacH and Sc(tfac)₃

Compound	$\nu(\text{C=O}) / \text{cm}^{-1}$	$\nu(\text{C=C}) / \text{cm}^{-1}$	$\nu(\text{C=O}) + \delta(\text{C-H}) / \text{cm}^{-1}$
tfacH	1600.9	-	1416.9
Sc(tfac) ₃	1614.5	1534.7	1450.5

5.6.4.2.2 Elemental analysis

Portions (2.0 mg) of the $\text{Sc}(\text{tfac})_3$ complex prepared in **Section 5.6.4.2** were accurately weighed (0.01 mg) in tin capsules and analysed using the LECO CHNS micro-element analyser. The results for the elemental analysis are presented in **Table 5.13**.

Table 5.13: Elemental analysis of $\text{Sc}(\text{tfac})_3$

Molecular formula	Empirical formula	% C*		% H*	
		Calculated	35.73	Calculated	2.40
$\text{Sc}(\text{tfac})_3$	$\text{ScC}_{15}\text{H}_{12}\text{F}_9\text{O}_6$	Found	34.22	Found	2.47

* Average of two replicates

5.6.4.2.3 Open-beaker dissolution for $\text{Sc}(\text{tfac})_3$

Three portions of the $\text{Sc}(\text{tfac})_3$ complex prepared in **Section 5.6.4.2** were accurately weighed (0.0101 - 0.0106 g) and dissolved in 5 mL of 65 % at 60 °C on a hotplate. Visual inspection indicated the incomplete dissolution of these portions and an oily substance was visible floating on top of the aqueous solution. The Sc mixtures were then filtered and the filtrates transferred to 100.0 mL volumetric flasks, filled to the mark with ultra-pure water and left to stabilise for 4 hours. The solutions were analysed for their Sc concentration using ICP-OES and the results are presented in **Table 5.14**.

Table 5.14: Quantitative determination of scandium in $\text{Sc}(\text{tfac})_3$ digested by the open beaker method.

Sample No.	Sample mass weighed (g)	Theoretical metal concentration (ppm)	Actual concentration (ppm)	Sc Recovery (%)
1	0.0103	9.184	5.411	58.92
2	0.0101	9.005	5.183	57.56
3	0.0106	9.451	5.424	57.39
Average recovery (%) (s)				58.0(8)
RSD (%)				1.45

5.6.4.2.4 Microwave-assisted dissolution for $\text{Sc}(\text{tfac})_3$

Three 8 mL volumes of 65 % HNO_3 were added to three different $\text{Sc}(\text{tfac})_3$ portions (0.0117 - 0.0118 g), transferred to clean microwave PTFE vessels and dissolved by applying the microwave conditions cited in **Table 5.1**. Visual inspection indicated the complete dissolution of the solid samples. The solutions were quantitatively transferred to 50 mL beakers and heated on a hotplate to concentrate them to a volume of 5 mL. The latter solutions were quantitatively transferred to 100.0 mL volumetric flasks using a micropipette and filled to the mark with ultra-pure water. These solutions were then left for 5 hours to stabilise and analysed for Sc content using ICP-OES. The results are presented in **Table 5.15**.

Table 5.15: Quantitative determination of scandium in $\text{Sc}(\text{tfac})_3$ digested by the microwave-assisted method.

Sample No.	Sample mass weighed (g)	Theoretical metal concentration (ppm)	Actual concentration (ppm)	Sc Recovery (%)
1	0.0102	9.095	8.814	96.91
2	0.0101	9.005	8.699	96.60
3	0.0102	9.095	8.717	95.85
Average recovery (%) (s)				96.5(6)
RSD (%)				0.57

5.6.4.3 Synthesis of $\text{Sc}(\text{btfac})_3$

Benzoyl-1,1,1-trifluoroacetone (btfacH) (0.8647 g, 4 mmol) was mixed with a solution of sodium carbonate to deprotonate the benzoyl-1,1,1-trifluoroacetone which was added until the oily liquid disappeared. A scandium chloride solution (0.08121 g, 0.5 mmol) was added to the ligand solution mixture (pH 7). A sticky orange precipitate formed with continuous stirring for an hour. The solution was filtered, the precipitate was dried in air and recrystallised from a solution of benzoyl-1,1,1-trifluoroacetone in benzene (0.01 g in 10 mL). A salmon-pink precipitate (57.98 % yield) was obtained with a M.P. in the range of 107.2 - 108.1 °C.

5.6.4.3.1 Infrared analysis

The $\text{Sc}(\text{btfac})_3$ complex synthesized in **Section 5.6.4.3** as well as the btfacH ligand were characterised by infrared spectroscopy. The spectra are shown in **Figure 5.11**. The stretching frequencies of both the ligand and the resulting complex are listed in **Table 5.16**.

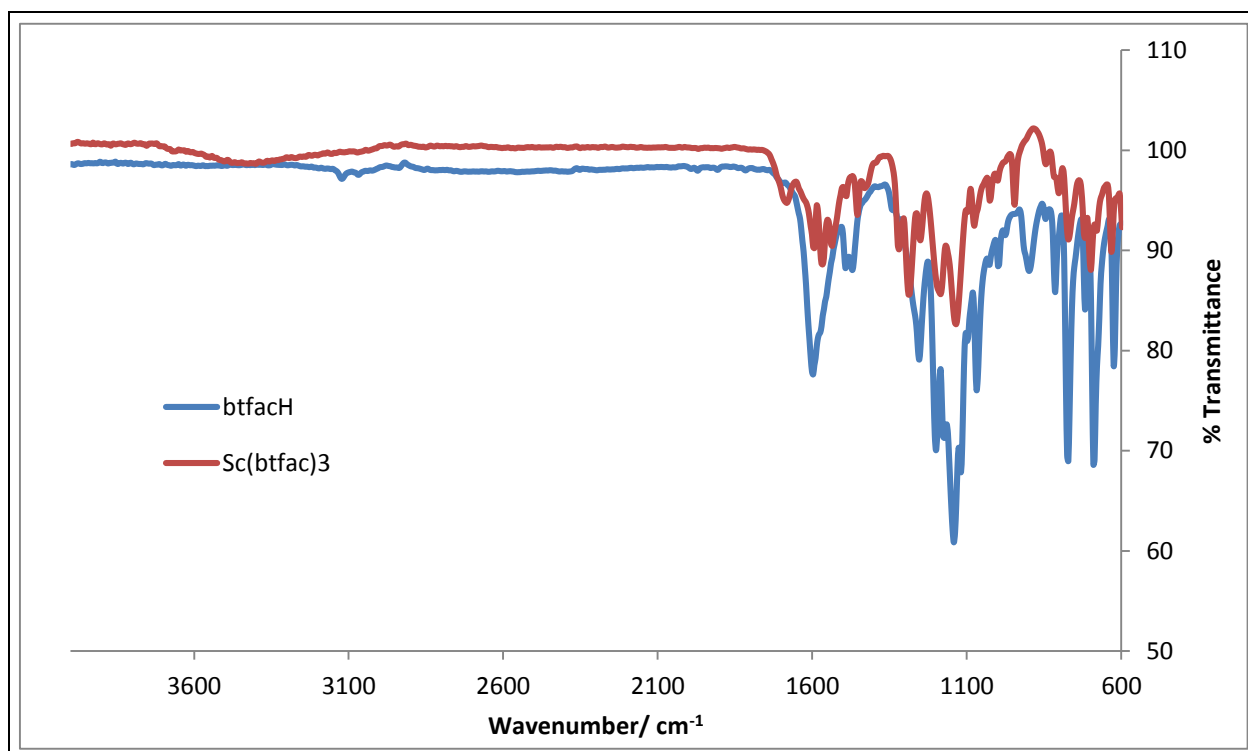


Figure 5.11: The IR spectra of btfacH and $\text{Sc}(\text{btfac})_3$.

Table 5.16: btfacH and $\text{Sc}(\text{btfac})_3$ IR stretching frequencies

Compound	$\nu(\text{C}=\text{O}) / \text{cm}^{-1}$	$\nu(\text{C}=\text{C}) / \text{cm}^{-1}$	$\nu(\text{C}=\text{O}) + \delta(\text{C}-\text{H}) / \text{cm}^{-1}$
btfacH	1598.0	-	1491.5
$\text{Sc}(\text{btfac})_3$	1592.5	1567.6	1454.1

5.6.4.3.2 Elemental analysis

Approximately 2.0 mg of the $\text{Sc}(\text{btfac})_3$ complex was accurately weighed (0.01 mg) in tin capsules and analysed using the LECO CHNS analyser. The results are presented in **Table 5.17**.

Table 5.17: Elemental analysis of Sc(btfac)₃

Molecular formula	Empirical formula	% C*		% H*	
		Calculated	52.19	Calculated	2.63
Sc(btfac) ₃	ScC ₃₀ H ₁₈ F ₉ O ₆	Found	51.81	Found	2.62

* Average of three replicates

5.6.4.3.3 Open-beaker dissolution for Sc(btfac)₃

The Sc(btfac)₃ complex (0.0600 - 0.0601 g) was accurately weighed (0.1 mg) and dissolved in 5 mL of 65 % HNO₃. Visual inspection indicated incomplete dissolution. The mixtures were then filtered and the filtrates were transferred to 100.0 mL volumetric flasks and filled to the mark with ultra-pure water. The stock solutions were further diluted by the transfer of 10 mL to 100.0 mL volumetric flasks and the flasks were filled to the mark with ultra-pure water after the addition of 5 mL 65 % HNO₃ to match the standard prepared in **Section 5.4.1**. These diluted solutions were analysed for their Sc concentration using ICP-OES and the results are presented in **Table 5.18**.

Table 5.18: Quantitative determination of scandium in Sc(btfac)₃ after open-beaker digestion.

Sample No.	Sample mass weighed (g)	Theoretical metal concentration (ppm)	Actual concentration (ppm)	Sc Recovery (%)
1	0.0600	3.907	1.019	26.08
2	0.0601	3.913	1.073	27.42
3	0.0600	3.907	1.036	26.52
Average recovery (%) (s)				26.7(7)
RSD (%)				2.56

5.6.4.3.4 Microwave-assisted dissolution for Sc(btfac)₃

Sc(btfac)₃ portions (0.0100 - 0.0101 g) were accurately weighed and quantitatively transferred to clean microwave PTFE vessels containing 8 mL of 65 % HNO₃. Dissolution was afforded with the microwave with conditions listed in **Table 5.1**.

Visual inspection indicated the complete dissolution of the complex. The solutions were quantitatively transferred into 50 mL beakers and heated on a hotplate to concentrate them to a volume of 5 mL. The latter solutions were quantitatively transferred to 100.0 mL volumetric flasks using a micropipette and filled to the mark with ultra-pure water and left to stabilise. The Sc content was determined using ICP-OES and the results are presented in **Table 5.19**.

Table 5.19: Quantitative determination of scandium in $\text{Sc}(\text{btfac})_3$ digested by the microwave-assisted method.

Sample No.	Sample mass weighed (g)	Theoretical metal concentration (ppm)	Actual concentration (ppm)	Sc Recovery (%)
1	0.0100	6.512	6.000	92.14
2	0.0101	6.577	6.248	95.00
3	0.0101	6.577	6.482	98.57
Average recovery (%) (s)				95(3)
RSD (%)				3.38

5.6.4.4 Synthesis of $\text{Sc}(\text{dbm})_3$

Dibenzoylmethane (dbmH) (4 mmol) was dissolved in 10 ml of chloroform with constant stirring and 3 ml of 1 M aqueous NH_4OH solution was added (pH 7). ScCl_3 (1 mmol, 0.3031 g) dissolved in water (5 ml) was added drop-wise to the above solution and allowed to react for 2 hours. During this process, a light-yellow precipitate of $\text{Sc}(\text{dbm})_3$ formed in the solution. The precipitate was collected by filtration, dried in the oven at 100 °C and then recrystallised in benzene. The shiny, fine yellow powder (84.76 % yield) had a M.P. in the range of 87.5 - 90 °C.

5.6.4.4.1 Infrared analysis

The IR of the $\text{Sc}(\text{dbm})_3$ complex and the dbmH ligand were recorded with a Digilab Scimitar Series spectrometer. Their spectra are shown in **Figure 5.12** and the most important stretching frequencies are listed in **Table 5.20**.

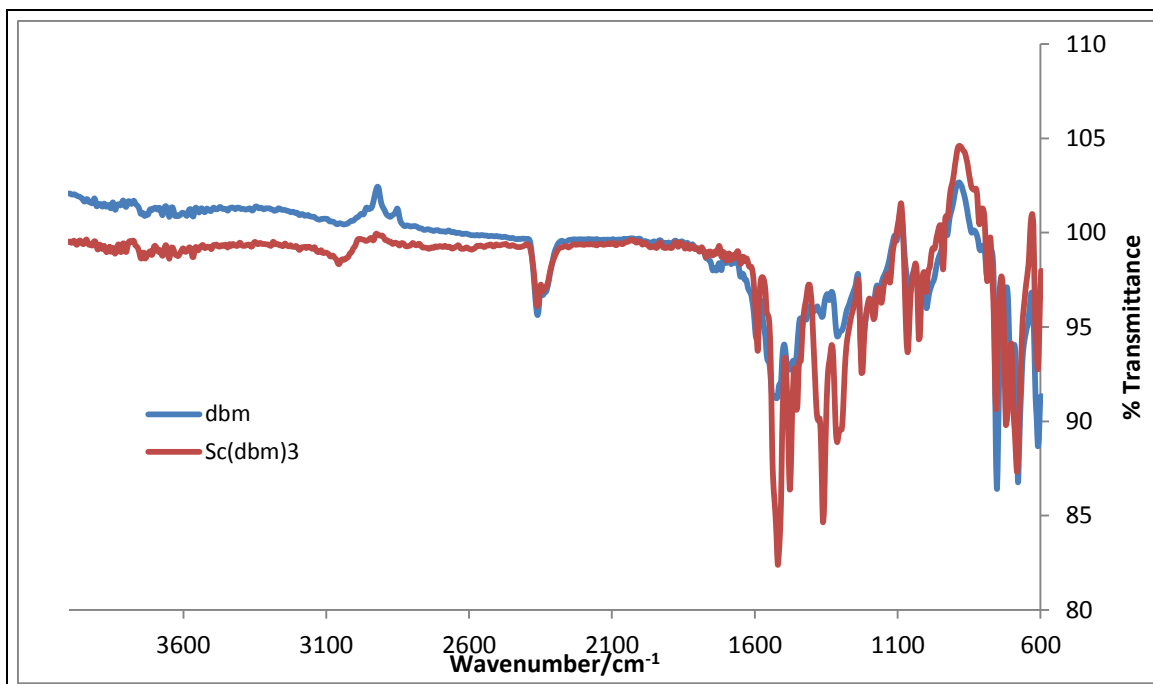


Figure 5.12: The IR spectra of dbmH and Sc(dbm)₃.

Table 5.20: IR stretching frequencies of dbmH and Sc(dbm)₃

Compound	$\nu(\text{C=O}) / \text{cm}^{-1}$	$\nu(\text{C=C}) / \text{cm}^{-1}$	$\nu(\text{C=O}) + \delta(\text{C-H}) / \text{cm}^{-1}$
dbmH	1590.9	1523.9	1474.9
Sc(dbm) ₃	1586.9	1517.5	1478.2

5.6.4.4.2 Elemental analysis

Portions of the Sc(dbm)₃ complex were accurately weighed (approximately 2.0 mg) in tin capsules and analysed for their C and H content. The results are presented in **Table 5.21**.

Table 5.21: Elemental analysis of Sc(dbm)₃

Molecular formula	Empirical formula	% C*		% H*	
		Calculated	75.63	Calculated	4.65
Sc(dbm) ₃	ScC ₄₅ H ₃₃ O ₆	Found	85.63	Found	4.26

* Average of three replicates

5.6.4.4.3 Open-beaker dissolution for $\text{Sc}(\text{dbm})_3$

Portions of the $\text{Sc}(\text{dbm})_3$ complex (0.0091 - 0.0094 g) were accurately weighed (to 0.1 mg) and dissolved in 5 mL of 65 % HNO_3 for 10 min. Visual inspection indicated poor dissolution. The solutions were filtered and the filtrates were transferred to 100.0 mL volumetric flasks and filled to the mark with ultra-pure water. These solutions were allowed to stabilise and then analysed for their Sc concentration. The results are presented in **Table 5.22**.

Table 5.22: Quantitative determination of scandium in $\text{Sc}(\text{dbm})_3$ after open-beaker digestion

Sample No.	Sample mass weighed (g)	Theoretical metal concentration (ppm)	Actual concentration (ppm)	Sc Recovery (%)
1	0.0091	5.724	3.968	69.32
2	0.0094	5.913	3.907	66.07
3	0.0092	5.787	3.820	66.01
Average recovery (%) (s)				67(2)
RSD (%)				2.82

5.6.4.4.4 Microwave-assisted dissolution for $\text{Sc}(\text{dbm})_3$

65 % HNO_3 (8 mL) were added to $\text{Sc}(\text{dbm})_3$ portions (0.0129 - 0.0131 g) and quantitatively transferred to clean microwave PTFE vessels. Microwave dissolution was done applying the microwave conditions in **Table 5.1**. Visual inspection indicated complete dissolution of the solid samples. The solutions were quantitatively transferred into 50 mL beakers and heated on a hotplate to reduce the volume to 5 mL. The latter solutions were quantitatively transferred into 100.0 mL volumetric flasks and filled to the mark with ultra-pure water and left to stabilise. The Sc recoveries are presented in **Table 5.23**.

Table 5.23: Quantitative determination of scandium in $\text{Sc}(\text{dbm})_3$ dissolved by the microwave-assisted technique

Sample No.	Sample mass weighed (g)	Theoretical metal concentration (ppm)	Actual concentration (ppm)	Sc Recovery (%)
1	0.0131	8.240	7.572	91.89
2	0.0130	8.177	7.857	96.08
3	0.0129	8.115	7.850	96.74
Average recovery (%) (s)				95(3)
RSD (%)				2.77

5.6.4.5 Synthesis of $\text{Sc}(\text{hfac})_3$

A solution containing hexafluoroacetylacetonone (hfacH) (0.016 mol, 1.5 mL) and concentrated aqueous ammonia (≈ 2 mL) was added to a scandium chloride solution (0.1398 g, 0.004 mol) (pH = 8). A white precipitate immediately formed. The precipitate was filtered, dried in air and recrystallised from heptane. A white precipitate was obtained (40.72 % yield, M.P. in the range of 99.22 - 99.9 °C).

5.6.4.5.1 Infrared analysis

The IR of both the $\text{Sc}(\text{hfac})_3$ complex and the hfacH ligand were recorded with the Digilab Scimitar Series spectrometer (**Figure 5.13**). The most important stretching frequencies of the two compounds are listed in **Table 5.24**.

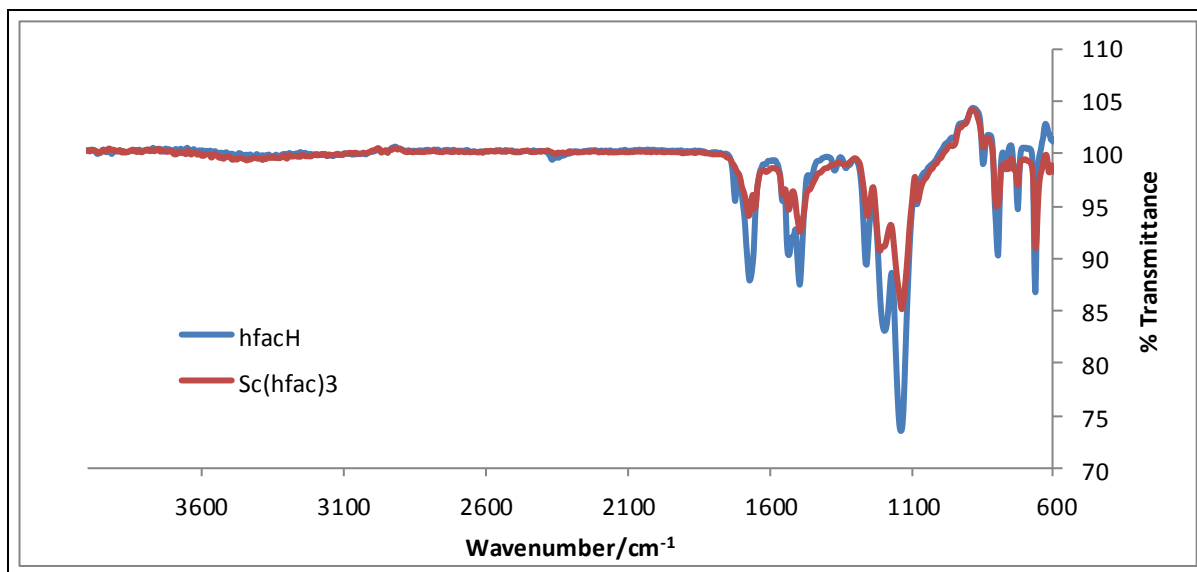


Figure 5.13: The IR spectra of hfach and Sc(hfac)₃.

Table 5.24: IR stretching frequencies of hfach and Sc(hfac)₃

Compound	$\nu(\text{C=O}) / \text{cm}^{-1}$	$\nu(\text{C=C}) / \text{cm}^{-1}$	$\nu(\text{C=O}) + \delta(\text{C-H}) / \text{cm}^{-1}$
hfach	1718.2	1669.0	1535.3
Sc(hfac) ₃	1672.8	1646.2	1528.5

5.6.4.5.2 Elemental analysis

Approximately 2.0 mg portions of the Sc(hfac)₃ complex were accurately weighed in tin capsules and analysed for C and H content. The results for the elemental analysis are presented in **Table 5.25**.

Table 5.25: Elemental analysis of Sc(hfac)₃

Molecular formula	Empirical formula	% C*		% H*	
		Calculated	27.05	Calculated	0.45
Sc(hfac) ₃	ScC ₁₅ H ₃ F ₁₈ O ₆	Found	23.02	Found	0.56

* Average of three replicates

5.6.4.5.3 Open-beaker dissolution for Sc(hfac)₃

Portions of the Sc(hfac)₃ complex (0.0100 - 0.0102 g) were weighed and dissolved in 5 mL of 65 % HNO₃ and visual inspection indicated complete dissolution. The

solutions were transferred to 100.0 mL volumetric flasks and filled to the mark with ultra-pure water. These solutions were stabilised and then analysed for their Sc content using ICP-OES and the results are presented in **Table 5.26**.

Table 5.26: Quantitative determination of scandium in $\text{Sc}(\text{hfac})_3$

Sample No.	Sample mass weighed (g)	Theoretical metal concentration (ppm)	Actual concentration (ppm)	Sc Recovery (%)
1	0.0102	6.884	5.508	80.02
2	0.0100	6.749	5.433	80.50
3	0.0101	6.817	5.501	80.70
Average recovery (%) (s)				80.4(4)
RSD (%)				0.44

5.6.4.6 Synthesis of $\text{Sc}(\text{sacac})_3$

An aqueous solution (5 mL H_2O) of scandium chloride (0.1563 g, 0.002 mol) was added to a mixture of thio-acetylacetonone (sacacH) (0.008 mol, 1.2 mL) and concentrated aqueous ammonia (2 mL) (pH 8). The mixture was thoroughly stirred for 24 hours and a dark-brown precipitate was obtained after this period. The precipitate was filtered and dried in air. Recrystallisation from a mixture of hexane and diethyl ether yielded light orange needle-like crystals, suitable for X-ray analysis (85.32 % yield), M.P. in the range of 172 - 173.8 °C.

5.6.4.6.1 Infrared analysis

Both the $\text{Sc}(\text{sacac})_3$ complex and the sacacH ligand were characterised with a Digilab Scimitar Series IR spectrometer. The spectra are shown in **Figure 5.14** and the most important stretching frequencies are listed in **Table 5.27**.

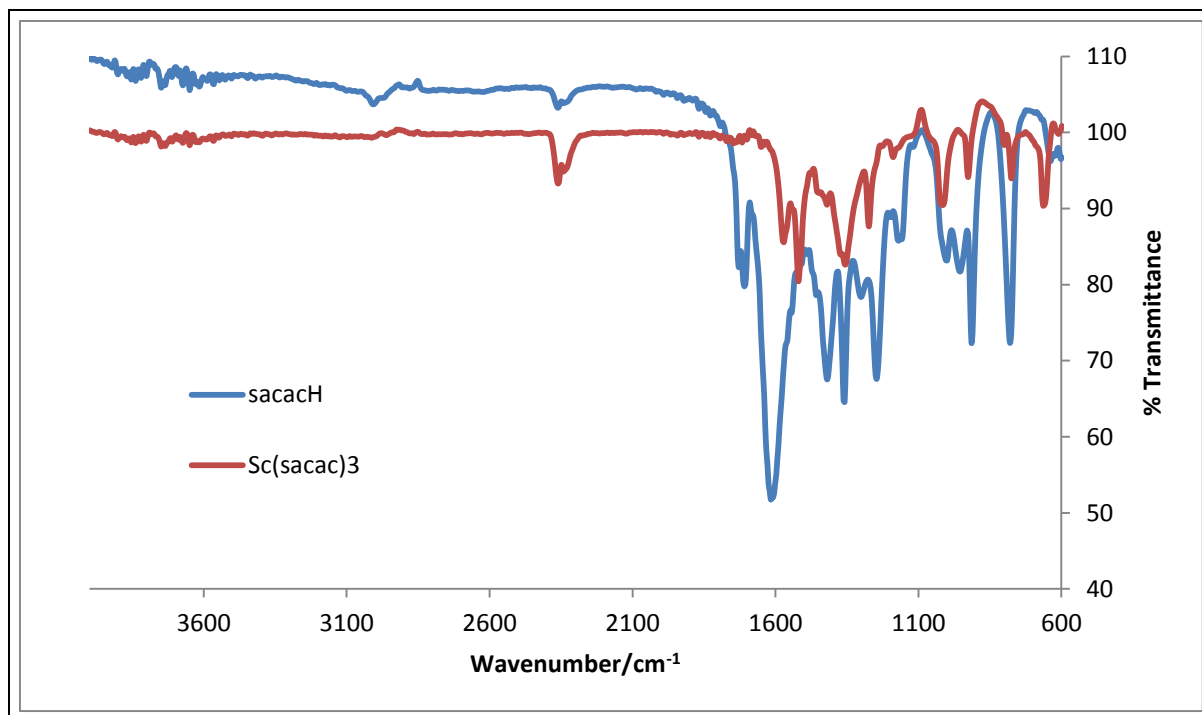


Figure 5.14: The IR spectra of sacacH and Sc(sacac)₃.

Table 5.27: sacacH and Sc(sacac)₃ IR stretching frequencies

Compound	$\nu(\text{C}=\text{O})^{\text{a}}$	$\nu(\text{C}=\text{O})^{\text{b}}$	$\nu(\text{C}=\text{C})$	$\nu(\text{C}=\text{O}) + \delta(\text{C}-\text{H})$	$\delta(\text{CH}_3)$
sacacH	1703.5	1615.0	–	1418.8	1359.2
Sc(sacac) ₃	–	1570.5	1517.2	1417.2	1350.8

5.6.4.6.2 Elemental analysis

Portions of the Sc(sacac)₃ complex were accurately weighed (approximately 2.0 mg) in tin capsules and analysed for their C, H and S content. The results for the elemental analysis are presented in **Table 5.28**.

Table 5.28: Elemental analysis of Sc(sacac)₃

Molecular formula	Empirical formula	% C*		% H*		% S*	
		Calculated	Found	Calculated	Found	Calculated	Found
Sc(sacac) ₃	ScC ₁₅ H ₂₁ O ₃ S ₃	Calculated	46.14	Calculated	5.42	Calculated	24.64
		Found	46.12	Found	4.35	Found	1.61

* Average of three replicates

5.6.4.6.3 X-ray crystallography

A single crystal of Sc(sacac)₃ was selected for X-ray diffraction data collection which was performed by the Inorganic chemistry laboratory of the UFS. The crystal structure data is reported in **Table 5.29**.

Table 5.29: The crystal data of Sc(sacac)₃

Empirical formula	C ₁₅ H ₂₁ O ₆ S ₀ Sc
Formula weight (g mol ⁻¹)	342.28
Crystal system	Orthorhombic
Space group	<i>Pbca</i>
<i>a</i> (Å)	13.535(3)
<i>b</i> (Å)	15.292(3)
<i>c</i> (Å)	16.576(3)
α (°)	90
β (°)	90
γ (°)	90
Volume (Å ⁻³)	3430.9(12)
Z	8
P_{calc} (g cm ⁻³)	1.325
Absorption coefficient (mm ⁻¹)	0.453
F (000)	1440
θ range (°)	2.355 - 27.988
Index ranges	-15 ≤ <i>h</i> ≤ 17 -18 ≤ <i>k</i> ≤ 18 -21 ≤ <i>l</i> ≤ 21
Reflections collected	57938
Independent reflections	3889
R _{int}	0.0587
Completeness to theta (°, %)	25.242, 99.7
Data/restraints/parameters	3889/0/218
Goof	1.040
R[<i>I</i> >2σ(<i>I</i>)]	R ₁ = 0.0397 wR ₂ = 0.1094
R(all data)	R ₁ = 0.0475 wR ₂ = 0.1187
Extinction coefficient	0.0016 (4)
Largest diff. peak and hole (e.Å ⁻³)	0.378 and -0.529

5.6.4.6.4 Open-beaker dissolution for Sc(sacac)₃

Portions of approximately 0.005 g of the Sc(sacac)₃ complex was accurately weighed and dissolved in 5.0 mL of concentrated H₂SO₄. Visual inspection indicated complete dissolution. The solutions were transferred to 100.0 mL volumetric flasks and filled to the mark with ultra-pure water. These solutions were allowed to stabilise for 3 hours and then analysed for their Sc content. The results are presented in **Table 5.30**.

Table 5.30: Quantitative determination of scandium in Sc(sacac)₃

Sample No.	Sample mass weighed (g)	Theoretical metal concentration (ppm)	Actual concentration (ppm)	Sc Recovery (%)
1	0.0054	6.2170	6.1303	98.61
2	0.0053	6.1019	6.1131	100.2
3	0.0053	6.1019	6.1459	99.08
Average recovery (%) (s)				99.3(8)
RSD (%)				0.82

5.7 Digestion and quantification analyses of columbite mineral ore and Ta/Nb residuals

In this study two different scandium containing mineral samples were studied in order to develop a dissolution method for the Sc minerals, quantify the elemental content and possibly develop beneficiation methods for scandium in these samples. The first sample that was investigated (Sample A) is a columbite mineral ore originating from Brazil and the second one (Sample B) is the residue that remained after the columbite ore sample was chemically treated and the Ta and Nb removed, **Figure 5.15**. The typical chemical composition of the two ore samples are given in **Table 5.31**.



Figure 5.15: Columbite ore (A) and residue (B)

Table 5.31: Typical chemical compositions of columbite mineral and Ta/Nb residue samples (Sample A and Sample B)¹⁶⁰

Analyte	Average concentration (%)	
	Sample A	Sample B
Nb ₂ O ₅	43.74	3.89
Fe ₂ O ₃	29.49	39.93
TiO ₂	10.63	1.58
Al ₂ O ₃	0.89	4.01
Mn ₃ O ₄	2.10	0.26
SnO ₂	1.42	2.45
U ₃ O ₈	<0.05	0.19
ThO ₂	<0.055	0.18
WO ₃	0.81	0.31
Ta ₂ O ₅	4.51	0.35
ZrO ₂	0.64	1.38
SiO ₂	1.63	1.18
Y ₂ O ₃	0.15	0.38
Sc ₂ O ₃	0.135	0.795

This part of the study comprises of two subdivisions, namely (i) the optimisation and application of the developed dissolution methods on the two samples and (ii) pre-concentration of the minerals in order to develop the beneficiation methods for scandium contained in the two samples. The results in **Table 5.31** indicate that the main difference between the two samples are the Nb and Ta content, the high Fe₂O₃

¹⁶⁰ London and Scandinavian Metallurgical Co Limited (LSM) analytical services

and Sc_2O_3 contents in Sample B compared to Sample A and also the low TiO_2 content in Sample B compared to that in Sample A.

5.7.1 General experimental methods

5.7.1.1 General procedures, reagents and equipment

Two different samples namely a columbite sample and a Ta/Nb residue sample labelled as Sample A and Sample B which originate from Brazil, were supplied by the London and Scandinavian Metallurgical Co. Limited. Methyl isoamyl ketone (MIAK) ($\geq 98\%$) and H_2SO_4 (95 - 97 %) were bought from Merck while 1-octanol (99.5 %) was obtained from Associated Chemical Enterprises and methyl isobutyl ketone (MIBK) (99 %) from Saarchem. Ammonium bifluoride ($\text{NH}_4\text{F}\cdot\text{HF}$) and ICP standard solutions containing 1000 mg/L Nb, Ti, Sn, W, Si, Ta, Y as well as a multi-element (32 elements) standard containing 1000 mg/L each of Mn, Al, Fe and other elements were also bought from Merck. ICP standard solutions containing 1000 mg/L Th and U were bought from De Bruyn Spectroscopic and an ICP standard solution containing 100 mg/L Sc was bought from Spectrascan. The ICP standard solution containing 100 mg/L Zr was from Sigma-Aldrich. Ultra-pure water was used throughout the study. A high temperature furnace (**Figure 5.16**) was used for the fusion digestion method.



Figure 5.16: Thermo Scientific Thermolyne high temperature furnace used in this study

5.7.1.2 Preparation of standard solutions

A set of calibration standards for ICP-OES analysis was prepared from the 1000 mg/L Nb, Ti, Si, Ta, Mn, Al, Fe, Th and U ICP-OES standard solutions by adding the appropriate volumes in 100.0 mL volumetric flasks to prepare 0.5, 1.0, 3.0, 5.0 and 10.0 mg/L concentrations. From the 1000 mg/L Sc, Y, Sn, W and Zr ICP-OES standard solutions calibration standards were prepared by adding the appropriate volumes of the standard solutions in 100.0 mL volumetric flasks to prepare 0.1, 0.3, 0.5, 0.7 and 1.0 mg/L concentrations. To each volumetric flask, 10 mL 95 - 97 % H₂SO₄ was added before they were filled up to the mark with ultra-pure water. The blank solutions were prepared by diluting 10 mL H₂SO₄ to the 100.0 mL volumetric flasks and were used for background corrections. All prepared standard solutions were homogenised and left to stand for 5 hours before use. Quantitative analyses were performed using the ICP-OES conditions in **Table 5.2** at the selected wavelengths listed in **Table 5.32**.

Table 5.32: Selected wavelengths, detection limits and quantification limits for the different elements analysed in the columbite and Ta/Nb residue samples¹⁶¹

Element	Wavelength/ nm	LOD/ ppm	LOQ / ppm
Nb	309.418	0.01045	0.1045
Fe	238.204	0.008456	0.08456
Ti	336.121	0.005836	0.05836
Al	394.403	0.05595	0.5595
Mn	279.482	0.005360	0.05360
Sn	189.989	0.0001192	0.001192
U	385.958	0.2307	2.307
Th	283.730	0.04792	0.4792
W	220.448	0.08220	0.8220
Ta	228.916	0.07768	0.7768
Zr	357.247	0.001909	0.01909
Si	252.851	0.2203	2.203
Y	371.029	0.001444	0.01444
Sc	357.252	0.0008518	0.008518

¹⁶¹ Winge R.K., Fassel V.A., Peterson V.J. and Floyd M.A., Inductively Coupled Plasma-Atomic Emission Spectroscopy, an atlas of spectral information, Volume 20, pp. 262 – 286, (1985)

5.7.2 Experimental procedures for the optimisation of the dissolution of the columbite and residue samples

Sample A was chosen to optimise the experimental conditions and these conditions were then used for the dissolution of Sample B.

5.7.2.1 Dissolution of columbite (Sample A) by $\text{NH}_4\text{F}\cdot\text{HF}$ fusion

Approximately 0.05 g of Sample A was weighed (accurately to 0.1 mg) in a platinum crucible and thoroughly mixed with approximately 0.5 g of $\text{NH}_4\text{F}\cdot\text{HF}$ flux (1:10 sample:flux ratio). The mixture was then fused at 200 °C for 30 min in a high temperature oven and a white amorphous solid melt was obtained. The melt was then dissolved in ultra-pure water and the solution was magnetically stirred for 5 min. Some of the solid sample remained undissolved. The residue was then filtered and the filtrate was quantitatively transferred into 100.0 mL volumetric flasks and filled to the mark with ultra-pure water. A 10.0 mL sample of the solution was pipetted into a 100.0 mL volumetric flask and 10 mL 95 - 97 % H_2SO_4 was added. The solution was left to cool down and then filled to the mark with ultra-pure water for quantitative analysis using ICP-OES. The results are reported in **Table 5.33** as the equivalent oxides of the most stable oxidation state of the elements for comparison purposes with previously reported results in **Table 5.31**.

Table 5.33: Ammonium bifluoride fusion for Sample A at 1:10 Sample A:NH₄F·HF ratio for 30 minutes at 200 °C

Analyte	Quantity (%) Expected*	Quantity (%) Found
Nb ₂ O ₅	43.74	36.24
Fe ₂ O ₃	29.49	26.12
TiO ₂	10.63	9.63
Al ₂ O ₃	0.89	5.09
Mn ₃ O ₄	2.10	1.14
SnO ₂	1.42	3.94
U ₃ O ₈	<0.05	<0.00
ThO ₂	<0.055	<0.00
WO ₃	0.81	0.65
Ta ₂ O ₅	4.51	3.81
ZrO ₂	0.64	0.34
SiO ₂	1.63	64.31
Y ₂ O ₃	0.15	0.050
Sc ₂ O ₃	0.135	0.066

* - From the results reported by the London and Scandinavian Metallurgical Co Limited (LSM) analytical services in **Table 5.31**

The incomplete sample dissolution and low recoveries compared to their expected content values in **Table 5.31** prompted a further investigation to optimise the experimental conditions for the dissolution method of this mineral sample. The Al₂O₃ results were found to be highly inaccurate as a result of the presence of the residual fluoride from ammonium bifluoride. The SiO₂ results are highly inaccurate and this can be due to the fact that when silica reacts with ammonium bifluoride, an ammonium hexafluorosilicate forms, which according to the literature¹⁶² can damage the glass surface as it is also used in the etching of glass.¹⁶³ In this case the ICP-OES nebulizer is made of glass and hence this may have led to the inaccurate results.

¹⁶² Timokhin, A. R. and Komarova, L. A., 1986, "Chemical reaction of ammonium bifluoride with quartz glass" pp. 267–269, [Accessed 24-10-2015]. Available from: http://download.springer.com/static/pdf/837/art%253A10.1007%252FBF00697937.pdf?auth66=1353397748_24e33c0ab6ff5c533fd24ef3dd809d02&ext=.pdf

¹⁶³ Indian standard, ammonium bifluoride specification, [Accessed 24-10-2015]. Available from: <https://law.resource.org/pub/in/bis/S02/is.13119.1991.html>

5.7.2.2 Influence of sample:flux ratio and the fusion time on dissolution of columbite ore

Three portions of Sample A (approximately 0.05 g) were weighed (accurately to 0.1 mg) in three different platinum crucibles. To the 1st crucible, Sample A was mixed with NH₄F·HF flux in ratio of 1:20 (sample:flux) and fused for 30 min at 200 °C. The 2nd and the 3rd portions were mixed with NH₄F·HF flux in ratio of 1:10 (sample:flux) and fused at 200 °C for 60 min and for 90 min respectively. The obtained melts were allowed to cool to ambient temperature and were then dissolved in water. Visual inspection indicated that small portions of the sample had not dissolved in the mixtures. The undissolved solids were removed by filtration and the solutions were quantitatively transferred to 100.0 mL volumetric flasks and filled to the mark with ultra-pure water. A 10.0 mL aliquot of each solution was transferred to another 100.0 mL volumetric flask and 10 mL 95 - 97 % H₂SO₄ was added to each volumetric flask. The solutions were left to cool down and then filled to the mark with ultra-pure water for quantitative analysis using ICP-OES. The obtained results are given in **Table 5.34**.

Table 5.34: Fusion results for Sample A with NH₄F·HF at 200 °C

Analyte	Quantity (%) Found			Quantity (%) Expected
	1:20, 30 min	1:10, 60 min	1:10, 90 min	
Nb ₂ O ₅	39.85	42.12	45.32	43.74
Fe ₂ O ₃	26.98	29.23	29.51	29.49
TiO ₂	10.31	10.45	10.36	10.63
Mn ₃ O ₄	1.19	1.66	1.69	2.10
SnO ₂	4.19	4.29	4.86	1.42
U ₃ O ₈	0.00	0.00	0.01	<0.05
ThO ₂	0.00	<0.01	0.01	<0.055
WO ₃	0.76	0.58	0.51	0.81
Ta ₂ O ₅	4.83	4.09	5.82	4.51
ZrO ₂	0.34	0.18	0.05	0.64
Y ₂ O ₃	0.039	0.036	0.09	0.15
Sc ₂ O ₃	0.075	0.134	0.133	0.135

5.7.3 Application of the optimal conditions for the dissolution of Samples A and B

From the results obtained in the above sections, a 60 min digestion at 200 °C at a 1:10 sample:flux ratio was selected as optimum conditions (comparing the recovery of the major elements such as Nb and Fe, as well as the element of interest namely Sc). The $\text{NH}_4\text{F}\cdot\text{HF}$ fusion and dissolution procedures were then repeated for Sample A and also applied to Sample B. Approximately 0.05 g (accurately weighed to 0.1 mg) of each mineral sample was thoroughly mixed with 0.5 g of $\text{NH}_4\text{F}\cdot\text{HF}$ in platinum crucibles and fused at 200 °C for 60 min. The obtained melts were cooled to room temperature and dissolved in water. Visual inspection indicated that small amounts of the sample did not dissolve. After filtering, the filtrates were quantitatively transferred to 100.0 mL volumetric flasks and filled to the mark with ultra-pure water and allowed to stabilise for 4 hours. These were further diluted by pipetting a 10.0 mL aliquot of each solution and quantitatively transfer it to a 100.0 mL volumetric flask. 10 mL 95 – 97 % H_2SO_4 was added and the solutions were allowed to cool to room temperature before filling them to the mark with ultra-pure water. The ICP-OES analysis of the two samples are reported in **Table 5.35**.

Table 5.35: Quantitative results obtained after the fusion dissolution of the columbite mineral ore (Sample A) and Nb/Ta residue (Sample B) with $\text{NH}_4\text{F}\cdot\text{HF}$ (1:10 sample:flux ratio) at 200 °C for 60 min

Analyte	Concentration (%)			
	Sample A		Sample B	
	Found*	Expected	Found*	Expected
Nb_2O_5	42.14	43.74	3.51	3.89
Fe_2O_3	28.86	29.49	34.02	39.93
TiO_2	10.34	10.63	0.93	1.58
Mn_3O_4	1.74	2.10	0.29	0.26
SnO_2	4.85	1.42	0.33	2.45
U_3O_8	0.002	<0.05	0.00	0.19
ThO_2	0.00	<0.055	0.00	0.18
WO_3	0.77	0.81	0.07	0.31
Ta_2O_5	4.61	4.51	0.53	0.35
ZrO_2	0.06	0.64	0.17	1.38
Y_2O_3	0.09	0.15	0.03	0.38
Sc_2O_3	0.14	0.135	0.51	0.795

* - Average of three replicates

In the process of beneficiating the scandium in the samples, several methods were implemented to try and remove the dominating elements in the samples. Magnetic separation, which involves the separation of some particles that are magnetic in the sample using a permanent magnet, as well as solvent extraction were implemented.

5.7.4 Magnetic removal of Fe and Ti in Samples A and B

In an attempt to remove the majority of Fe and Ti in both the samples to concentrate the scandium in the remaining solid, magnetic separation was chosen, but the magnetic susceptibility of both samples was first determined.

5.7.4.1 Magnetic susceptibility determinations

The magnetic susceptibility of samples A and B were determined with a Sherwood Scientific magnetic susceptibility balance (MSB) at 25 °C. The MSB balance was reset to zero and the empty capillary tube was weighed and then placed into the

balance to determine the R_0 value. After this the capillary tube was refilled with sample to a height between 2.6 cm and 3.1 cm. The capillary tube with the sample was re-weighed and the R value was recorded. The mass susceptibility (χ_g) of these samples was calculated using **Equation 4.3** and the results are reported in **Table 5.36**.

Table 5.36: Magnetic susceptibility determinations for the two columbite samples

Sample	Mass m (g)	Length l (cm)	R_0	R	C_{bal}	$10^6 \chi_g$ (cm ³ .g ⁻¹)
Sample A	0.5168	2.6	0.8316	965	1.003918	1.301
Sample B	0.1237	3.1	0.8316	186	1.003918	0.0713

5.7.4.2 Magnetic separation of Samples A and B

Portions of about 1.0 g (Samples A and B) were weighed (accurately to 0.1 mg) and transferred to a piece of paper. The magnetic particles were manually removed (using a permanent magnet) by moving/rotating a permanent (household) magnet that was held below the paper with the sample, to attract and collect the magnetic material. The magnet was subsequently moved to the side of the paper with the collected magnetic material. The magnet was then removed from the paper and returned to the sample to collect the next batch of magnetic material. This procedure was repeated until visual inspection indicated that all the magnetic material were collected. The collected magnetic and non-magnetic portions were then re-weighed to determine the amount of mass lost due to the adherence of small amounts of the finely ground mineral sample to the paper surfaces used during the separation process. Their respective masses are reported in **Table 5.37**.

Table 5.37: Mass balance of Samples A and B after magnetic separation

Sample	Replicate	Total mass (g)	Magnetic mass (g)	Non-magnetic mass (g)
Sample A	1	0.1185	0.0436	0.0617
	2	0.1080	0.0412	0.0480
Sample B	1	0.1002	0.0474	0.0426
	2	0.1027	0.0364	0.0546

5.7.4.3 Quantitative determination of the elements present in the magnetic and in the non-magnetic portions of both samples (A and B)

The different portions were accurately weighed (0.1 mg) and quantitatively transferred to platinum crucibles and thoroughly mixed with $\text{NH}_4\text{F}\cdot\text{HF}$ in a 1:10 (sample:flux) ratio. The mixtures were fused at 200 °C for 60 min in the high temperature oven. The fusion melts were then cooled to ambient temperature and then dissolved with ultra-pure water. Visual inspection indicated that some of the sample did not dissolve. The mixtures were filtered and the filtrate solutions were quantitatively transferred to 100.0 mL PTFE volumetric flasks and filled to the mark with ultra-pure water. A 10.0 mL aliquot of each of the solutions was transferred to another 100.0 mL volumetric flask and the acidity of the solutions were adjusted with of 95 - 97% H_2SO_4 , cooled and then filled to the mark with ultra-pure water. The solutions were analysed using ICP-OES and the results are presented in **Tables 5.38** and **5.39**. The content (in percentage) present in the samples after magnetic separation is shown in **Figures 5.17** and **5.18** for Sample A and B respectively.

Table 5.38: ICP-OES results for the elements contained in the magnetic and the non-magnetic portions of Sample A

Analyte	Sample A: magnetic Quantity (%) Found*	Sample A: non-magnetic Quantity (%) Found*	Expected
Nb_2O_5	11.81	26.73	43.74
Fe_2O_3	9.32	17.58	29.49
TiO_2	3.57	6.14	10.63
Mn_3O_4	0.51	0.99	2.10
SnO_2	0.07	0.30	1.42
U_3O_8	0.00	0.00	<0.05
ThO_2	0.00	0.00	<0.055
WO_3	0.25	0.52	0.81
Ta_2O_5	1.35	2.99	4.51
ZrO_2	0.02	0.03	0.64
Y_2O_3	0.02	0.03	0.15
Sc_2O_3	0.06	0.09	0.135

* - Average of two analyses

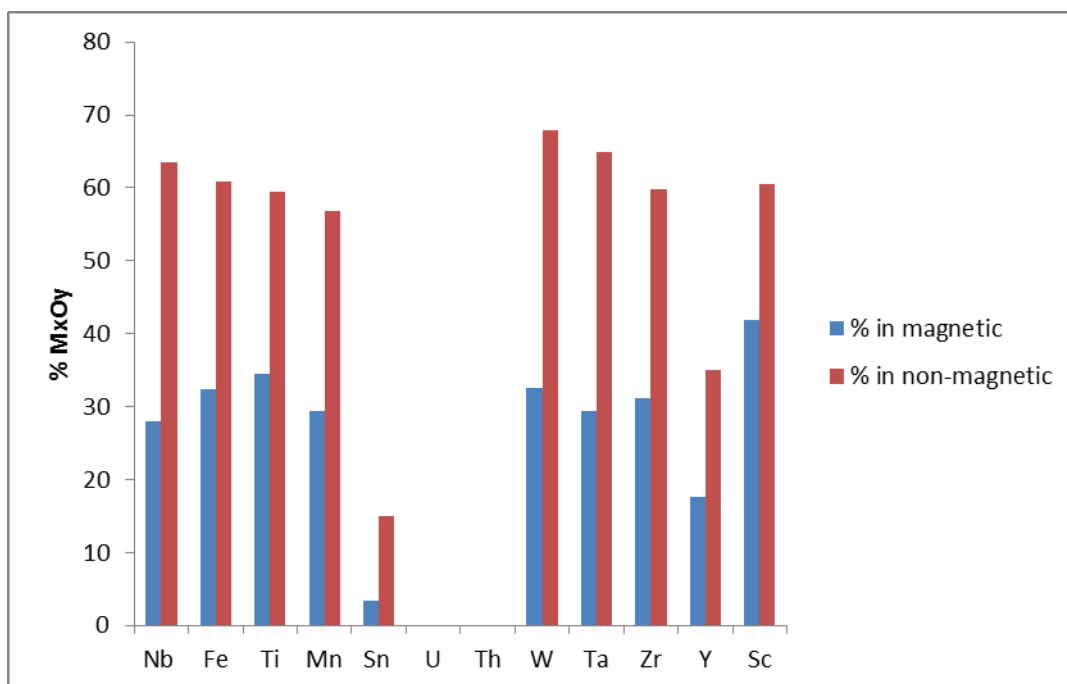


Figure 5.17: The % analytes present in Sample A after magnetic separation

Table 5.39: ICP-OES results for the elements contained in the magnetic and the non-magnetic portions of Sample B

Analyte	Sample B: magnetic Quantity (%) Found*	Sample B: non-magnetic Quantity (%) Found*	Expected
Nb ₂ O ₅	1.18	2.15	3.89
Fe ₂ O ₃	11.32	20.63	39.93
TiO ₂	0.40	0.42	1.58
Mn ₃ O ₄	0.20	0.10	0.26
SnO ₂	0.07	0.14	2.45
U ₃ O ₈	0.00	0.00	0.19
ThO ₂	0.00	0.00	0.18
WO ₃	0.02	0.02	0.31
Ta ₂ O ₅	0.22	0.23	0.35
ZrO ₂	0.01	0.13	1.38
Y ₂ O ₃	0.02	0.01	0.38
Sc ₂ O ₃	0.23	0.24	0.795

* - Average of two analyses

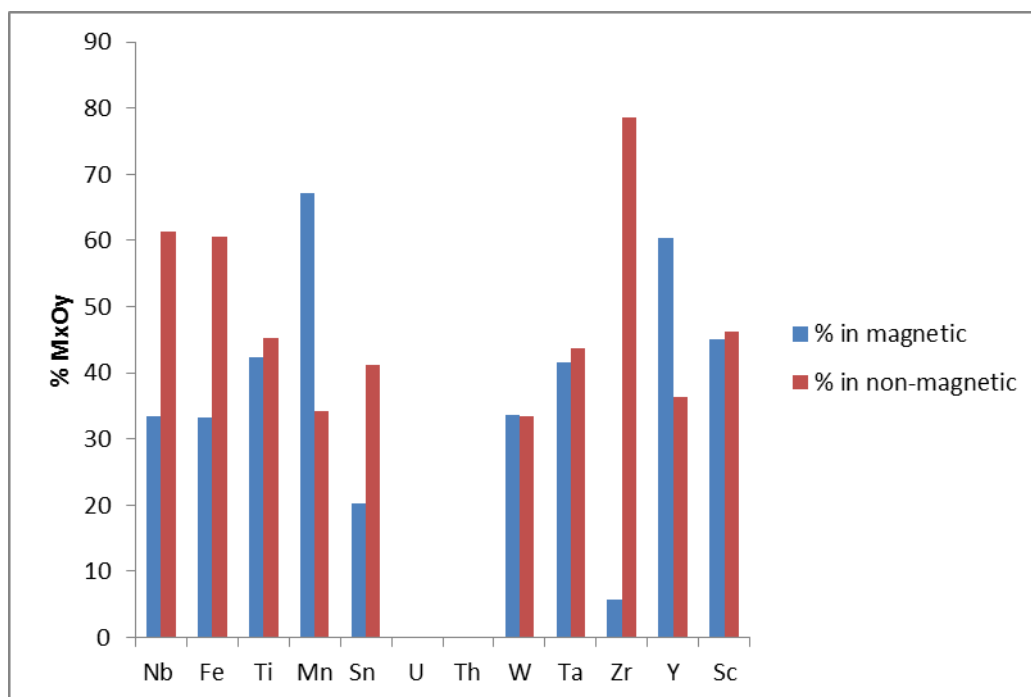


Figure 5.18: The % analytes present in Sample B after magnetic separation

5.7.5 Solvent extraction of tantalum in a columbite mineral (Sample A)

The next step in this process involved the removal of Ta, as one of the major elements in the samples, from the rest of the sample solution using solvent extraction. 5.0 mL of the bulk solution of sample A obtained from **Section 5.7.3** was transferred to a separating funnel and 5.0 mL H_2SO_4 of desired acid concentration (2.0 M to 8.0 M) was added to this solution as indicated in the study by Nete⁶⁹. The solution was thoroughly mixed for 5 min and the Ta was then extracted with two successive portions of 10.0 mL of MIBK. Each time the solution was allowed to stand for 5 min to allow for the complete separation of the two immiscible liquid phases. The aqueous solution (the bottom layer) was then collected in a 100 mL beaker. This aqueous solution was stirred for 10 min on a hot plate set at 60 °C to evaporate any dissolved organic solvent and transferred to 100.0 mL volumetric flasks. The two organic portions were combined and back extracted with two portions of 20 mL water. The solution was allowed to stand for 5 min for the complete separation of the liquid phases. The water solutions were then combined in a 100.0 mL beaker and heated to evaporate any dissolved organic solvent before it was quantitatively transferred to a 100.0 mL volumetric flask. The acidity of the solutions was adjusted with H_2SO_4 to match the 1.848 M H_2SO_4 of the blank, as well as that of the standard solutions. The

solutions were again allowed to cool to room temperature and the volumetric flasks were then filled to mark with ultra-pure water and subsequently analyzed using ICP-OES. The results obtained in this study are presented in **Table 5.40** and the average percentages obtained are graphically presented in **Figures 5.19** and **5.20**.

Table 5.40: Solvent extraction of Ta in Sample A using MIBK after $\text{NH}_4\text{F}\cdot\text{HF}$ fusion. $[\text{H}_2\text{SO}_4]$ varied at 2, 4 and 8 M.

M_xO_y (%)	$[\text{H}_2\text{SO}_4]$ (M)						Expected (%)
	Aqueous			Organic			
	2.0	4.0	8.0	2.0	4.0	8.0	
Nb_2O_5	40.38	41.62	38.29	2.38	2.82	2.23	43.74
Fe_2O_3	27.11	27.73	27.41	1.43	1.63	1.25	29.49
TiO_2	10.93	11.06	10.65	0.43	0.52	0.38	10.63
Mn_3O_4	1.90	1.90	1.91	0.17	0.18	0.16	2.10
SnO_2	0.52	0.49	0.49	0.13	0.06	0.13	1.42
U_3O_8	0.00	0.00	0.00	0.00	0.00	0.00	<0.05
ThO_2	0.00	0.00	0.00	0.01	0.00	0.00	<0.055
WO_3	1.13	1.10	1.01	0.16	0.09	0.08	0.81
Ta_2O_5	0.89	0.91	0.88	4.51	4.08	4.25	4.51
ZrO_2	0.08	0.08	0.08	0.03	0.03	0.03	0.64
Y_2O_3	0.08	0.08	0.08	0.05	0.05	0.05	0.15
Sc_2O_3	0.15	0.15	0.15	0.00	0.00	0.00	0.135

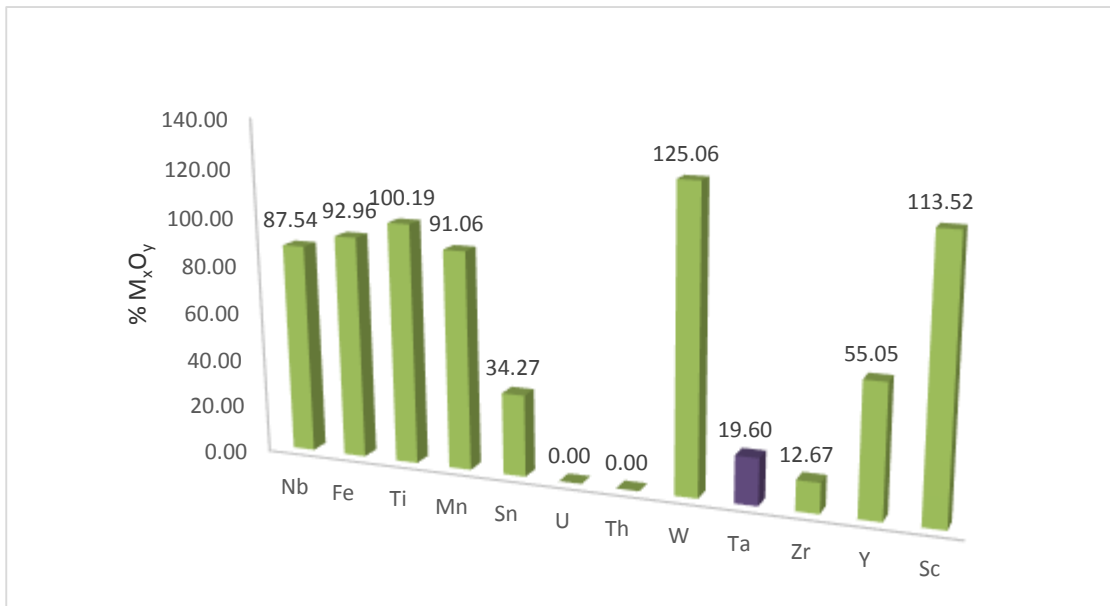


Figure 5.19: Elemental analysis in the aqueous solution after solvent extraction separation of elements at $[H_2SO_4] = 8\text{ M}$ in Sample A

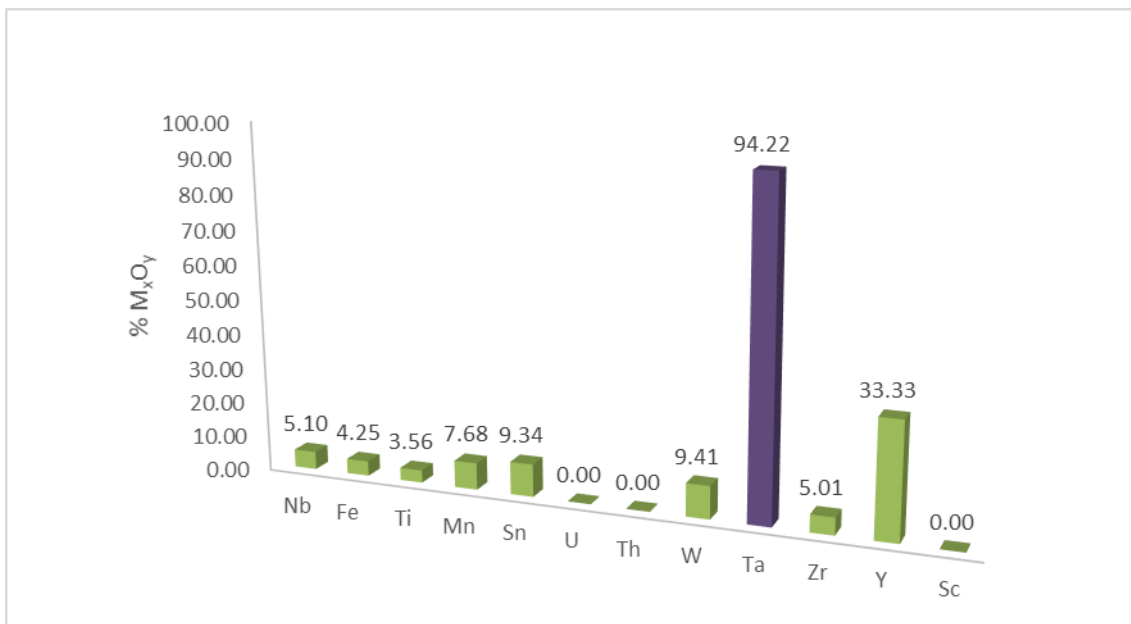


Figure 5.20: Elemental analysis in the organic solution after two times solvent extraction separation steps at $[H_2SO_4] = 8\text{ M}$ in Sample A using MIBK

The results in **Table 5.40** indicate that some of Nb has been extracted with Ta to the organic phase. This proposed the attempt to extract Nb by increasing acid concentration as part of Sc beneficiation process.

5.7.6 Solvent extraction of tantalum and niobium in the non-magnetic portion of Sample A with MIBK

Aliquots (5.0 mL) of the non-magnetic portion of Sample A as described in **Section 5.7.4.3** were transferred to separating funnels and 5 mL H₂SO₄ of desired concentration (4.0 - 16 M) was added to each solution. Each solution was thoroughly mixed for 5 min and Ta and Nb were then extracted with two successive portions of 10.0 mL of MIBK. The aqueous solution was collected in a 100 mL beaker and heated up to remove any dissolved organic solvent, then transferred to a 100.0 mL volumetric flask. The organic phase was back extracted with two portions of 20 mL water and the water solutions were collected and combined in a 100 mL beaker and heated to remove any dissolved organic solvent. The aqueous portions were then quantitatively transferred to a 100.0 mL volumetric flask. The acidity of the solution was adjusted with H₂SO₄ to match the blank as well as the standard solutions matrices. The solutions were then filled to the mark with ultra-pure water and subsequently analysed using ICP-OES. The results obtained are presented in **Tables 5.41** and **5.42**. **Figure 5.21** shows the relationship between the acid concentration and the Nb extracted.

Table 5.41: Elemental analysis of the aqueous solution of the non-magnetic portion of Sample A with MIBK at [H₂SO₄] between 4 and 16 M

M _x O _y (%)	[H ₂ SO ₄] (M)						Expected
	Aqueous						
	4.0	8.0	10.0	12.0	14.0	16.0	
Nb ₂ O ₅	25.66	24.43	24.66	17.69	17.50	15.20	43.74
Fe ₂ O ₃	16.76	16.85	16.24	14.28	15.48	15.11	29.49
TiO ₂	5.43	5.01	5.59	4.89	4.09	5.27	10.63
Mn ₃ O ₄	1.05	1.74	1.30	1.23	1.19	1.27	2.10
SnO ₂	0.33	0.30	0.30	0.31	0.29	0.36	1.42
U ₃ O ₈	0.29	0.30	0.00	0.00	0.26	0.18	<0.05
ThO ₂	0.02	0.04	0.00	0.01	0.02	0.00	<0.055
WO ₃	0.30	0.56	0.51	0.50	0.46	0.51	0.81
Ta ₂ O ₅	0.99	0.75	0.69	0.65	0.56	0.71	4.51
ZrO ₂	0.10	0.12	0.09	0.07	0.07	0.08	0.64
Y ₂ O ₃	0.03	0.05	0.02	0.03	0.05	0.03	0.15
Sc ₂ O ₃	0.09	0.11	0.11	0.13	0.07	0.06	0.135

Table 5.42: Elemental analysis of the organic solution of the non-magnetic portion of Sample A with MIBK at $[H_2SO_4]$ between 4 and 16 M

M_xO_y (%)	$[H_2SO_4]$ (M)						Expected
	Organic						
	4.0	8.0	10.0	12.0	14.0	16.0	
Nb_2O_5	1.37	1.38	1.50	4.38	5.68	6.23	43.74
Fe_2O_3	0.23	0.79	0.85	0.71	0.47	0.52	29.49
TiO_2	0.29	0.26	0.38	0.38	1.48	0.44	10.63
Mn_3O_4	0.13	0.00	0.19	0.18	0.40	0.17	2.10
SnO_2	0.00	0.05	0.00	0.05	0.09	0.06	1.42
U_3O_8	0.00	0.07	0.00	0.03	0.00	0.00	<0.05
ThO_2	0.03	0.10	0.14	0.11	0.09	0.08	<0.055
WO_3	0.00	0.00	0.12	0.12	0.19	0.09	0.81
Ta_2O_5	2.10	2.16	2.22	2.19	2.23	2.18	4.51
ZrO_2	0.00	0.00	0.00	0.00	0.01	0.01	0.64
Y_2O_3	0.00	0.01	0.01	0.00	0.00	0.03	0.15
Sc_2O_3	0.01	0.01	0.01	0.04	0.06	0.08	0.135

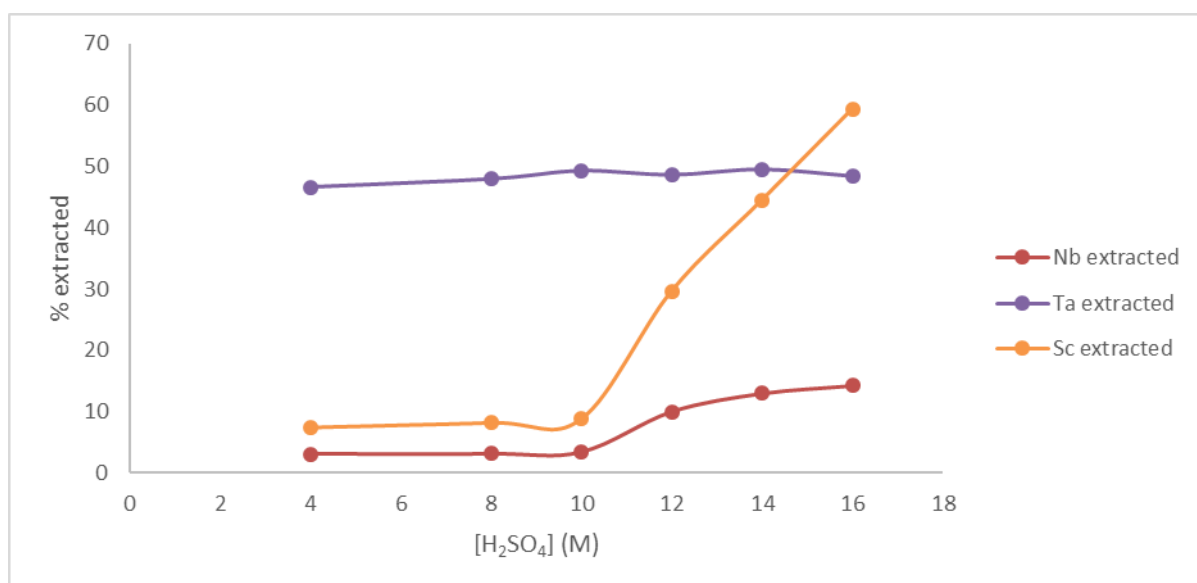


Figure 5.21: % Nb, Ta and Sc extracted with MIBK at different H_2SO_4 concentrations

Since the main objective of this study is to pre-concentrate scandium by trying to remove dominating or major elements in the columbite, it was then decided to extend the study by investigating other potential organic solvents that can collectively extract both Ta and Nb. From **Table 5.42** it can be seen that MIBK as solvent can be used for both collective and selective extraction of Ta and Nb. However, results indicate

that as the acid concentration increases, Sc is also being extracted into the organic layer which results in a substantial loss of Sc from the aqueous layer and that is huge a loss in beneficiation process. Despite its success as extractant, MIBK has disadvantages which include a relatively high solubility (1.91%) in aqueous solutions as well as a low flash point (14 °C). The high solubility of MIBK in aqueous solution necessitates the evaporating of any dissolved organic solvent before ICP-OES analyses. Octan-1-ol and methyl isoamyl ketone (MIAK) with solubilities of 1.0×10^{-6} and 0.50 % in water respectively and flash points of 81 and 43 °C respectively⁶⁹ were also investigated for the collective extraction of Ta and Nb.

5.7.7 Solvent extraction of tantalum and niobium in the non-magnetic portion of Sample A with octan-1-ol and MIAK

A 5.0 mL aliquot of the Sample A solution obtained in **Section 5.7.4.3** was mixed with 5 mL H₂SO₄ of desired concentration (4.0 - 16 M) in a separating funnel. Extraction of Ta and Nb was performed with two successive portions of 10.0 mL of each solvent and back extraction (from the organic phase) was done with two portions of 20 mL distilled water. All the aqueous solutions were heated to about 60 °C for 10 min in glass beakers to ensure that all the organic solvents were removed, then transferred to 100.0 mL volumetric flasks. The acidity of the solutions was adjusted to 1.848 M H₂SO₄ to match the blank as well as the standard solutions. The solutions were allowed to cool to room temperature and then filled to the mark with ultra-pure water. The results for each solvent are given in **Tables 5.43 - 5.45**. Niobium extracted at different [H₂SO₄] is illustrated in **Figure 5.22**.

Tables 5.43: Elemental analysis of the aqueous solution of the non-magnetic portion of Sample A with octan-1-ol at [H₂SO₄] between 4 and 16 M

M _x O _y (%)	[H ₂ SO ₄] (M)						Expected
	Aqueous						
	4.0	8.0	10.0	12.0	14.0	16.0	
Nb ₂ O ₅	19.15	17.83	16.53	14.62	14.28	10.94	43.74
Fe ₂ O ₃	17.85	16.53	16.86	15.58	15.27	15.31	29.49
TiO ₂	5.26	5.11	5.29	4.79	4.93	4.99	10.63
Mn ₃ O ₄	1.05	1.24	1.10	1.25	1.29	1.28	2.10
SnO ₂	0.44	0.51	0.38	0.33	0.25	0.30	1.42
U ₃ O ₈	0.31	0.30	0.29	0.09	0.23	0.20	<0.05
ThO ₂	0.01	0.05	0.06	0.00	0.00	0.00	<0.055
WO ₃	0.39	0.56	0.60	0.45	0.47	0.52	0.81
Ta ₂ O ₅	0.86	0.85	0.89	0.45	0.59	0.61	4.51
ZrO ₂	0.10	0.12	0.09	0.06	0.07	0.09	0.64
Y ₂ O ₃	0.04	0.06	0.04	0.04	0.04	0.03	0.15
Sc ₂ O ₃	0.10	0.10	0.11	0.11	0.09	0.06	0.135

Table 5.44: Elemental analysis of the organic solution of the non-magnetic portion of Sample A with octan-1-ol at [H₂SO₄] between 4 and 16 M

M _x O _y (%)	[H ₂ SO ₄] (M)						Expected
	Organic						
	4.0	8.0	10.0	12.0	14.0	16.0	
Nb ₂ O ₅	4.66	4.79	6.34	8.60	11.33	14.10	43.74
Fe ₂ O ₃	0.43	0.00	0.86	0.60	0.57	0.56	29.49
TiO ₂	0.54	0.86	0.38	1.02	0.99	0.67	10.63
Mn ₃ O ₄	0.13	0.12	0.20	0.35	0.36	0.20	2.10
SnO ₂	0.09	0.06	0.10	0.04	0.05	0.05	1.42
U ₃ O ₈	0.03	0.05	0.03	0.01	0.00	0.01	<0.05
ThO ₂	0.01	0.09	0.09	0.06	0.09	0.06	<0.055
WO ₃	0.02	0.05	0.02	0.12	0.18	0.09	0.81
Ta ₂ O ₅	2.12	2.08	2.09	2.28	2.23	2.22	4.51
ZrO ₂	0.00	0.00	0.00	0.03	0.00	0.05	0.64
Y ₂ O ₃	0.02	0.02	0.03	0.03	0.05	0.05	0.15
Sc ₂ O ₃	0.02	0.01	0.03	0.05	0.07	0.09	0.135

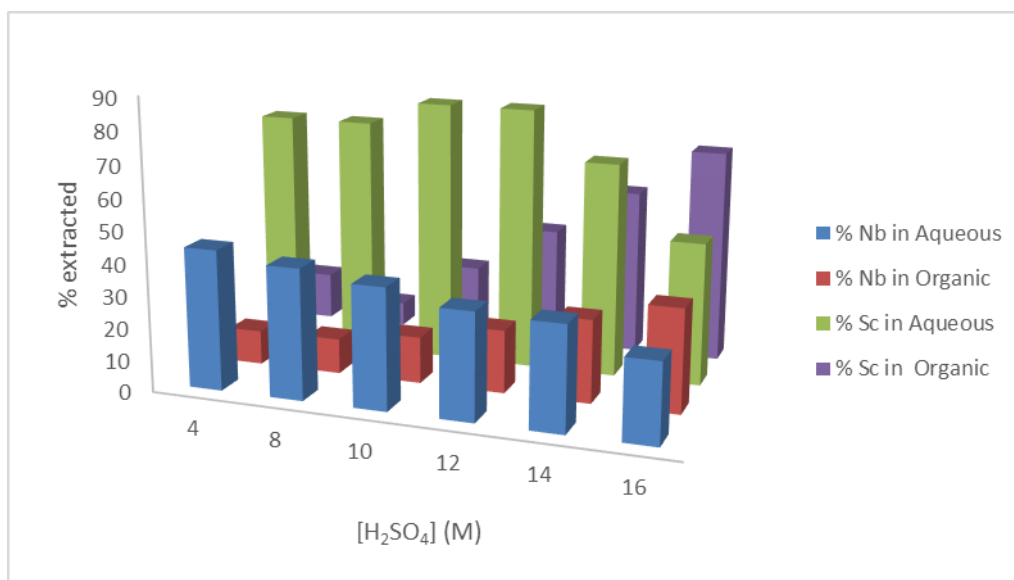


Figure 5.22: % Nb and % Sc in the aqueous and organic phase after solvent extraction with octan-1-ol at different [H₂SO₄]

Tables 5.45: Elemental analysis of the aqueous and organic solutions of the non-magnetic portion of Sample A with MIAK at [H₂SO₄] between 4 and 16 M

M _x O _y (%)	[H ₂ SO ₄] (M)										Expected
	Aqueous					Organic					
	4.0*	8.0*	12.0*	14.0*	16.0*	4.0*	8.0*	12.0*	14.0*	16.0*	
Nb ₂ O ₅	21.42	20.12	20.56	25.26	20.36	0.88	0.91	0.57	0.28	0.74	43.74
Fe ₂ O ₃	14.70	16.00	16.23	24.00	17.80	1.45	2.83	2.44	3.34	5.55	29.49
TiO ₂	6.07	6.51	5.53	6.73	6.29	0.88	0.88	0.77	0.71	0.81	10.63
Mn ₃ O ₄	1.41	1.50	1.54	1.78	1.63	0.44	0.47	0.41	0.41	0.41	2.10
SnO ₂	0.31	0.40	0.33	0.61	0.38	0.12	0.17	0.14	0.55	0.27	1.42
U ₃ O ₈	0.00	0.00	0.00	0.00	0.00	0.00	0.00	0.00	0.00	0.00	<0.05
ThO ₂	0.00	0.00	0.00	0.00	0.00	0.00	0.00	0.00	0.00	0.00	<0.055
WO ₃	0.34	0.25	0.44	0.89	0.25	0.08	0.19	0.26	0.42	0.05	0.81
Ta ₂ O ₅	1.11	0.83	0.83	0.68	0.19	3.12	3.32	2.77	3.25	2.56	4.51
ZrO ₂	0.11	0.11	0.12	0.15	0.12	0.02	0.02	0.02	0.02	0.01	0.64
Y ₂ O ₃	0.01	0.01	0.01	0.02	0.00	0.00	0.00	0.00	0.00	0.00	0.15
Sc ₂ O ₃	0.08	0.08	0.07	0.09	0.07	0.00	0.00	0.00	0.00	0.00	0.135

* - Average of two replicates

Octan-1-ol behaves like MIBK as extractant and an increase in Nb extraction is observed when an increase in acidity (**Figure 5.22**) which is good for concentrating

the Sc. However, the increase in acidity also increases the Sc extraction and subsequent loss from the aqueous layer. On the other hand, MIAK does not extract Nb even at high acidity. MIAK is only good for Ta separation from Nb and not for the collective extraction of these two elements. Results in **Table 5.40** indicate that at least 2.23 % Nb₂O₅ was extracted at 8 M H₂SO₄ with MIBK and since Sample B contains smaller amounts of Nb and Ta, this method was chosen for the removal of these two elements in Sample B.

5.7.8 Solvent extraction of Ta and Nb in the non-magnetic portion of Sample B with MIBK

A 5.0 mL aliquot of the bulk solution of the non-magnetic portion of Sample B obtained from **Section 5.7.4.3** was transferred to a separating funnel and 5 mL of 8.0 M H₂SO₄ was added to this solution. The solution was thoroughly mixed for 5 min and the Ta and Nb were then extracted with two successive portions of 10.0 mL of MIBK. The aqueous portion was collected in a 100 mL beaker and heated up to remove any dissolved organic solvent, then transferred to 100.0 mL volumetric flask. The organic phase was back extracted with two portions of 20 mL water and the water portions were combined and heated to about 60 °C for 10 min in a glass beaker to ensure that all the organic solvents were removed, then quantitatively transferred to a 100.0 mL volumetric flask. The acidity of the solution was adjusted with H₂SO₄ to match the blank as well as the standard solutions matrices. The solutions were then filled to the mark with ultra-pure water and analysed using ICP-OES. The results obtained in this study are presented in **Table 5.46**.

Table 5.46: Elemental analysis of the aqueous and organic solutions of the non-magnetic portion of Sample B with MIBK at $[H_2SO_4] = 8\text{ M}$

M_xO_y (%)	Aqueous	Organic
	8.0*	8.0*
Nb ₂ O ₅	0.03	2.10
Fe ₂ O ₃	18.16	2.95
TiO ₂	1.00	0.72
Mn ₃ O ₄	0.58	0.48
SnO ₂	0.07	0.001
U ₃ O ₈	0.00	0
ThO ₂	0.00	0
WO ₃	0.02	0.03
Ta ₂ O ₅	0.03	0.21
ZrO ₂	0.02	0.01
Y ₂ O ₃	0.00	0.00
Sc ₂ O ₃	0.23	0.00

* - Average of two replicates

5.8 Results and discussions

5.8.1 LOD and LOQ

The limits of detection and of quantification were determined with the ICP-OES to obtain the smallest amount of scandium the developed method (equipment performance, experimental conditions and analyst skills) can detect and quantify in the samples. The LOD for Sc was determined to range between 0.000991 - 0.00773 ppm while the LOQ was determined to range between 0.00991 - 0.0773 ppm in different acids, (**Table 5.4**) indicating that the equipment and method are capable to detect Sc concentrations in the trace and ultra-trace range. The Sc concentrations quantified in the different samples analysed in this study were higher than the LOD and LOQ values.

5.8.2 Dissolution and quantification of Sc in inorganic compounds

5.8.2.1 *ScCl₃·H₂O analyses*

ScCl₃ readily dissolves in water and Sc quantification was done using the ICP-OES. The results in **Table 5.5** indicated that excellent recoveries of Sc were achieved, in the range of 99.64 - 99.79 %, with a low RSD value of about 0.075 %. These results clearly indicate that there is coherence between the method, the equipment and the analyst which allow for the accurate determination of Sc in various samples.

5.8.2.2 *Sc₂O₃ analyses*

5.8.2.2.1 *Open-beaker dissolution of Sc₂O₃*

Three different mineral acids, namely HNO₃, HCl and H₂SO₄ were used to digest scandium oxide using the open-beaker dissolution method. Visual inspection indicated the complete digestion of Sc₂O₃ in both HNO₃ and HCl with Sc recoveries in the range of 98.69 - 99.52 and 98.69 - 99.19 % respectively. However, H₂SO₄ failed to completely digest the oxide even when the mixture was heated to higher temperatures (\approx 90 °C) for 40 min. This incomplete digestion led to recoveries in the 43.99 - 45.26 % range.

5.8.2.2.2 *Microwave-assisted dissolution of Sc₂O₃*

In order to improve the digestion of Sc₂O₃ in H₂SO₄, microwave-assisted digestion method was attempted. The three different mineral acids, HNO₃, HCl and H₂SO₄ were again used, applying the microwave conditions listed in **Table 5.1**. Visual inspection indicated that all the samples were completely dissolved. The Sc recoveries improved to 99.44 - 99.95 %, 99.75 - 100.3 % and 99.75 - 101.9 % range for HNO₃, HCl and H₂SO₄ respectively. The low RSD values for all three mineral acids indicate the good precision, see **Table 5.7**. These results clearly indicate and confirm the improved ability of microwave digestion to dissolve inert metal oxides such as Sc₂O₃.

5.8.3 Characterisation of organometallic compounds with melting point determination, IR and CHNS micro-element analysis and the quantification of Sc in organometallic compounds using ICP-OES

5.8.3.1 Melting point of organometallic compounds

The melting points for the synthesized Sc complexes were measured using a Gallenkamp melting point apparatus. Some of the results deviate slightly from the literature^{164,165} while some are very different from cited values, especially Sc(tfac)₃. These differences may be due to the fact that the synthesized compounds were not pure enough or it might be that the products obtained were not the desired or expected product. **Table 5.47** lists the melting points of the compounds synthesized and those from the literature.

Table 5.47: Melting points of the different scandium organometallic compounds

Complex name	Melting point (°C)	
	Experimental	Literature ^{164,165}
Sc(acac) ₃	183 - 184.7	187 – 187.5
Sc(tfac) ₃	97.3 - 98.3	106.5±1.0
Sc(btfac) ₃	107.2 - 108.1	-----
Sc(dbm) ₃	87.5 - 90	-----
Sc(hfac) ₃	99.2 - 99.9	96.9±0.8
Sc(sacac) ₃	172 – 173.8	-----

-----No references could be found

5.8.3.2 Characterisation and quantification of Sc in Sc(acac)₃

5.8.3.2.1 Infrared spectrum of Sc(acac)₃

Figure 5.9 shows the spectra of the ligand acacH and that of Sc(acac)₃. The important absorption band frequencies of acacH and that of Sc(acac)₃ are presented in **Table 5.9**. The stretching frequency at 1708.5 cm⁻¹ is attributed to $\nu(\text{C}=\text{O})$

¹⁶⁴ Morgan G.T., and Moss H.W., Researches on residual affinity and co-ordination. Part I. Metallic acetylacetonates and their absorption spectra, **Journal of Chemical Society**, p. 189, (1914)

¹⁶⁵ Zherikova, K. V., Zelenina, L. N., Chusova, T. P., Morozova, N. B., Trubin, S. V., Vikulova, E. S., Scandium(III) Beta-diketonate derivatives as precursors for oxide film deposition by CVD. *Physics Procedia*, Volume 46, pp. 200-208, (2013)

stretching of the keto form for the acacH ligand while that at 1610.3 cm^{-1} is assigned to the $\nu(\text{C}=\text{O})$ enol form.¹⁶⁶ The absorption bands at 1570.7 and 1519.0 cm^{-1} for $\text{Sc}(\text{acac})_3$ are assigned to chelated carbonyl $\nu(\text{C}=\text{O})$ and $\nu(\text{C}=\text{C})$ stretching respectively. The shift of the carbonyl stretching frequency to lower value in the spectrum of $\text{Sc}(\text{acac})_3$ relative to the spectrum of pure acacH proved that the coordination took place through the carbonyl oxygen instead of other possible coordination sites of the molecule. The lowering of the carbonyl stretching frequency can be attributed to the fact that in the free acetylacetonate anion, the oxygen atoms have a considerable negative charge originating from the π electron cloud and due to coordination, the excess negative charge will transfer to the metal and reduces the $\text{C}=\text{O}$ bond order leading to a decrease of the $\text{C}=\text{O}$ stretching vibration position.¹⁶⁷

5.8.3.2.2 CHNS micro-elemental analysis of $\text{Sc}(\text{acac})_3$

The $\text{Sc}(\text{acac})_3$ complex was analysed for C and H and results are given in **Table 5.10**. Literature²⁰ reveals that many researchers have studied this complex and based on their results as well as this study it was proved that the complex synthesized was $\text{Sc}(\text{acac})_3$, **Figure 5.23**. Three deprotonated acacH ligands are needed to complete the octahedral coordination about the central metal ion, giving formula $[\text{Sc}(\text{acac})_3]$.

¹⁶⁶ Sohn J.R. and Lee S., An infrared spectroscopic study of acetylacetonate adsorbed on layer silicates containing various interlayer cations, **Journal of Industrial and Engineering Chemistry**, Volume 3, No. 3, pp. 198 – 202, (1997)

¹⁶⁷ Kerim F.M.A, Aly H.F. and El-Agramy A., Infrared absorption spectra of some lanthanide acetylacetonate complexes. In: *Proceedings of the Indian Academy of Sciences*, Volume 85 A, No. 6, pp. 559 – 566, (1977)

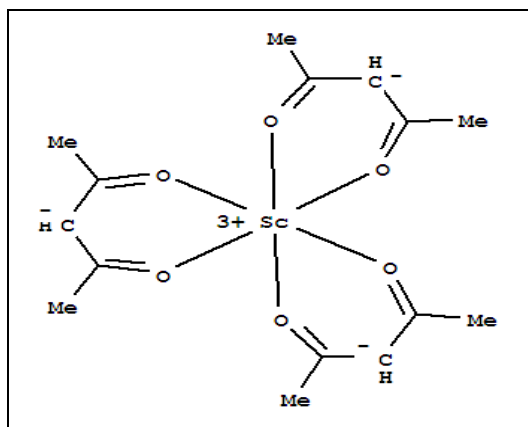


Figure 5.23: A proposed structure for $\text{Sc}(\text{acac})_3$ ¹⁶⁸

5.8.3.2.3 ICP-OES results of $\text{Sc}(\text{acac})_3$

Table 5.11 presents the Sc recovery from the $\text{Sc}(\text{acac})_3$ complex after open-beaker dissolution with HNO_3 . The results indicate excellent recovery of Sc of 99.4 % with RSD value of 0.56 %.

5.8.3.3 Characterisation and quantification of Sc in $\text{Sc}(\text{tfac})_3$

5.8.3.3.1 Infrared spectrum of $\text{Sc}(\text{tfac})_3$

Table 5.12 lists the most important IR stretching frequencies of trifluoroacetylacetonate (tfacH) and $\text{Sc}(\text{tfac})_3$. The strong peak at 1600.9 cm^{-1} for tfacH can be attributed to $\nu(\text{C}=\text{O})$ stretching. In the $\text{Sc}(\text{tfac})_3$ spectrum two strong peaks are observed in the C=O and C=C regions, these at 1614.5 cm^{-1} and 1534.7 cm^{-1} and are assigned to $\nu(\text{C}=\text{O})$ and $\nu(\text{C}=\text{C})$ stretching respectively. The carbonyl stretching frequency for the pure tfacH is shifted to lower values in the $\text{Sc}(\text{tfac})_3$ spectrum (**Figure 5.10**) which indicates that the ligand is coordinated via O atom to the Sc^{3+} metal ion. Kazuo Nakamoto¹⁶⁹ mentioned the observed frequencies for metals reacted with acetylacetonate. Nakamoto further mentioned that when a methyl group is substituted with CF_3 groups (electron withdrawing) in normal acetylacetonate, it causes marked

¹⁶⁸ Scandium(III) 2,4-pentanedionate, [Accessed 24-10-2015]. Available from:

<http://weiyuanchems.lookchem.com/products/CasNo-14284-94-7-Scandium-III-2-4-pentanedionate-11913691.html>

¹⁶⁹ Kazuo Nakamoto, Infrared Spectra of Inorganic and Coordination compounds, 1st Edition, 1962, 216 - 225

shifts in the delocalised C=C and C=O stretching bands to higher frequencies due to strong positive inductive and electron withdrawing properties of CF₃. This is clearly observed when comparing $\nu(\text{C}=\text{O})$ and $\nu(\text{C}=\text{C})$ of Sc(acac)₃ with that of Sc(tfac)₃, (Tables 5.9 and 5.12).

5.8.3.3.2 CHNS micro-elemental analysis of Sc(tfac)₃

Good C and H percentages for Sc(tfac)₃ complex were obtained (Table 5.13) confirming that the complex also poses the 1:3 metal:ligand ratio as was shown by Bennett *et al.*¹⁷⁰

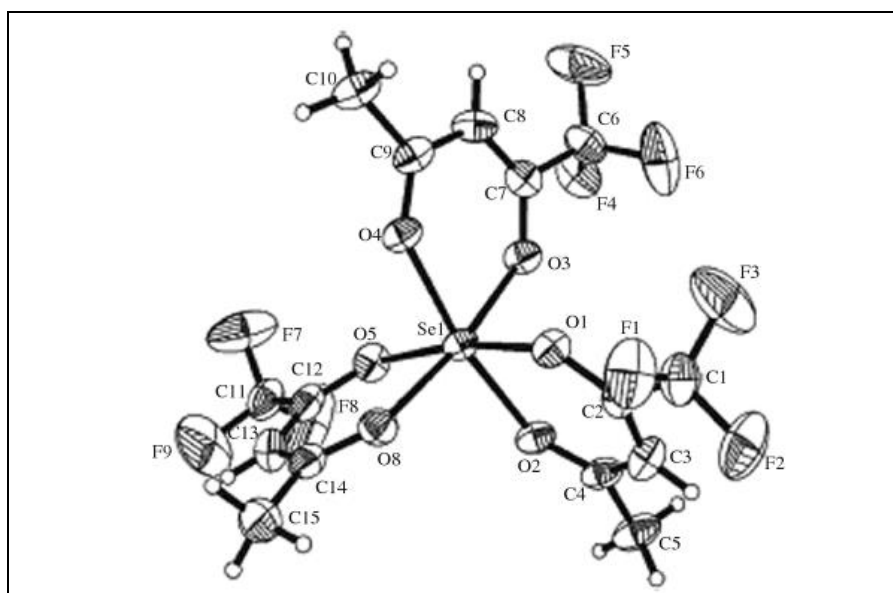


Figure 5.24: Molecular structure of Sc(tfac)₃¹⁷¹

5.8.3.3.3 Open-beaker and microwave dissolution of Sc(tfac)₃

Open-beaker digestion led to low Sc recoveries as shown in Table 5.14 are attributed to the incomplete dissolution of the complex as indicated by the oily substance that floated on top of the aqueous solution. Only 58.0 % Sc was recovered in this process. The microwave dissolution method was then attempted and visual inspection indicated complete dissolution. Sc recoveries improved to 96.5 % with an RSD of 0.55 % (Table 5.15). Interestingly, all these results clearly indicate that the

¹⁷⁰ Bennett D.W, Siddiquee T.A, Haworth D.T and Lindeman S.V, **Journal of Chemical Crystallography**, Volume 37, p. 207, (2007)

correct product was isolated, however the melting point in **Table 5.47** clearly differ from previously reported results begging the question if the previously reported melting point is correct. Further research on this complex may shed light on this discrepancy.

5.8.3.4 Characterisation and quantification of Sc in Sc(btfac)₃

5.8.3.4.1 Sc(btfac)₃ and btfacH infrared spectra

The infrared spectrum of the btfacH ligand was compared with that of Sc(btfac)₃ (**Figure 5.11**) in order to determine if the ligand reacted with the metal and chelation occurred. From **Table 5.16** the $\nu(\text{C}=\text{O})$ at 1598.0 cm^{-1} for btfacH is shifted to 1592.5 cm^{-1} in the spectrum for Sc(btfac)₃. The appearance of a new stretching band at 1567.6 cm^{-1} for Sc(btfac)₃ is attributed to $\nu(\text{C}=\text{C})$. As mentioned in **Section 5.8.3.2.3**, CF₃ substitution on the acac backbone increases the stretching frequency of the carbonyl and C=C for metal acetylacetonates compared to normal acacH the metal complexes.

5.8.3.4.2 CHNS micro-elemental analysis of Sc(btfac)₃

The percentage C and H calculated and experimentally obtained for Sc(btfac)₃ as reported in **Table 5.17** is in good agreement with each other suggesting that the isolated and predicted chemical formula compatible is with a 1:3 metal:ligand ratio. However, a 100 % recovery was not obtained due to impurities that may be present in the complex.

5.8.3.4.3 Sc recoveries from Sc(btfac)₃ after open-beaker and microwave dissolution

Poor Sc recoveries were obtained after open-beaker dissolution of Sc(btfac)₃, which is possible due to the incomplete dissolution of the complex that was observed and only 26.7 % was recovered. However, microwave dissolution (**Table 5.19**) improved the recovery to 95.3 % with the RSD value of 3.22 %. This deviation from 100 % may be attributed to two possibilities namely, i) the isolated product was not pure, with some of the starting materials also isolated and ii) the molar mass from the empirical formula known is not completely correct, with possibly inclusions of solvent molecules

or other adducts. The RSD value is a bit higher which shows that the precision was less than satisfactory.

5.8.3.5 Sc(dbm)₃ characterisation and quantification of Sc

5.8.3.5.1 Infrared of dbmH and Sc(dbm)₃

A slight shift in the $\nu(\text{C}=\text{O})$ and $\nu(\text{C}=\text{C})$ stretching frequencies is observed when the dbmH ligand and Sc(dbm)₃ is compared (**Figure 5.12** and **Table 5.20**). The $\nu(\text{C}=\text{O})$ and $\nu(\text{C}=\text{C})$ stretching frequencies shift from 1590.9 and 1523.9 cm⁻¹ for dbmH to 1586.9 and 1517.5 cm⁻¹ for the Sc(dbm)₃ complex and is attributed to the chelation process that occur when the dbmH ligand coordinates to the Sc metal ion. In a study done by Nakamoto *et al.*¹⁷¹ it was mentioned that phenyl substitution in a normal acacH slightly increases the delocalised C=C stretching band and slightly decreases the delocalised C=O band of metal acetylacetonates. This is clearly observed when comparing $\nu(\text{C}=\text{O})$ and $\nu(\text{C}=\text{C})$ stretching frequencies of Sc(acac)₃ with that of Sc(dbm)₃, (**Tables 5.9** and **5.20**).

5.8.3.5.2 CHNS micro-element analysis of Sc(dbm)₃

Results in **Table 5.21** shows highly inaccurate C content in Sc(dbm)₃ compared to what was expected. This percentage recovery may be due to that it is possible that the product isolated was highly contaminated with starting material or the empirical formula known is incorrect. A further possible explanation is that extra carbon observed in the analysis may originate from the benzene that was used for recrystallisation, provided the sample was not completely dry or that the benzene crystallised as a solvent molecule in the crystal lattice of the final product.

5.8.3.5.3 Open-beaker and microwave dissolution of Sc(dbm)₃

Open-beaker digestion of Sc(dbm)₃ in HNO₃ resulted in incomplete dissolution and resulted in low Sc recoveries (**Table 5.22**). It was then decided to employ the

¹⁷¹ Nakamoto K., Morimoto Y. and Martell A.E., Infrared spectra of metal chelate compounds. V. Effect of substituents on the infrared spectra of metal acetylacetonates, **Journal of Physical Chemistry**, Volume 66, pp. 346 - 348, (1962)

microwave dissolution method which led to improved Sc recoveries from 67 % to 95 % (**Table 5.23**). The inability to recover 100 % Sc correlate with the C, H analysis, and indicate contamination or incorrect molecular mass (presence of adducts). Recrystallisation of the product or even crystal structure determination may shed light on this discrepancy.

5.8.3.6 *Sc(hfac)₃ characterisation and quantification of Sc*

5.8.3.6.1 *Infrared of hfacH and Sc(hfac)₃*

The most important IR stretching frequencies of hexafluoroacetylacetone (hfacH) and Sc(hfac)₃ are listed in **Table 5.24**. The stretching frequencies appearing at 1718.2 and 1669.0 cm⁻¹ are assignable to the C=O and C=C stretching modes for hfacH. In Sc(hfac)₃ spectrum two strong stretching frequencies are observed in the C=O and C=C regions. The two stretching frequencies at 1672.8 cm⁻¹ and 1646.2 cm⁻¹ are assigned to $\nu(\text{C=O})$ and $\nu(\text{C=C})$ respectively. The carbonyl stretching frequency for the pure hfacH is shifted to lower frequency in the Sc(hfac)₃ spectrum (**Figure 5.13**) which indicates that the ligand is coordinated via O atom to Sc³⁺. The strong positive inductive effect of CF₃, by substituting CH₃ with CF₃ in normal acetylacetone, shifts the delocalised C=C and C=O stretching bands to higher frequencies which is clearly the case in this comparison (**Tables 5.9 and 5.24**).¹⁷² The $\nu(\text{C=O})$ and $\nu(\text{C=C})$ shifted from 1570.7 and 1519.0 cm⁻¹ to 1672.8 and 1646.2 cm⁻¹ respectively.

5.8.3.6.2 *CHNS micro-elemental analysis of Sc(hfac)₃*

The C, H elemental analysis results for Sc(hfac)₃ (**Table 5.25**) also yielded inaccurate C and H content found, compared to the calculated or expected value. This may be due to an impure isolated product or that the empirical formula known is incorrect. As previously indicated, recrystallisation and/or crystal structure determination may explain these differences that were observed.

5.8.3.6.3 *Open-beaker dissolution of Sc(hfac)₃*

The poor Sc recoveries (**Table 5.26**) obtained after open-beaker dissolution of Sc(hfac)₃ only yielded 80.4 % with an RSD of 0.35 %. This low percentage recovery

also correlate with the C and H analysis and may be attributed to the possibility that the molar mass from the empirical formula known is incorrect and maybe to impure product isolation.

5.8.3.7 Characterisation and quantification of Sc in Sc(sacac)₃

5.8.3.7.1 Infrared of sacacH and Sc(sacac)₃

The IR spectra of the sacacH ligand and that of Sc(sacac)₃ are reported in **Figure 5.14**. The most important stretching frequencies of sacacH and that of Sc(sacac)₃ are presented in **Table 5.27**. The $\nu(\text{C}=\text{O})$ stretching vibration band at 1703.5 cm⁻¹ is attributed to the keto form of the sacacH ligand and that at 1615.0 cm⁻¹ is assigned to the $\nu(\text{C}=\text{O})$ of the enol form. In the IR spectrum for Sc(sacac)₃, the absorption bands at 1570.5 and 1517.2 cm⁻¹ are assigned to the chelated carbonyl $\nu(\text{C}=\text{O})$ and the $\nu(\text{C}=\text{C})$ stretch respectively. The slight shift of the carbonyl stretching frequency to lower value in the spectrum for Sc(sacac)₃, relative to the spectrum of pure sacacH, is a proof that coordination occurred. At this time it is important to note that these stretching frequencies are very similar to that of Sc(acac)₃ reported in **Paragraph 5.8.3.2** and the biggest difference between the two isolated compounds are the melting points (**Table 5.47**) (173.8 vs. 184.7 °C) and the colour of the isolated products (light orange vs. light yellow). It is also important to note that the successful synthesis and coordination of sacacH has been established with the isolation of [Ir(sacac)(cod)].¹⁷²

5.8.3.7.2 CHNS micro-elemental analysis of Sc(sacac)₃

from the C, H and S analysis reported in **Table 5.28** shows highly inaccurate S content (1.61 %) in Sc(sacac)₃ relative to what was expected (24.64 %) and prompted the question whether the ligand used for synthesis was 100 % pure. The thio-acac ligand is not commercially available but was prepared (synthesized) in the laboratory using the normal acetylacetone as a starting material.

¹⁷² Purcell W., Conradie J., Kumar S., Venter J.A., Characterisation and mechanistic study of the oxidative addition reactions of [Ir(cod)(sacac)], **Journal of Organometallic Chemistry**, Volume 801, 1 January 2016, pp. 80–86



There is a high possibility that during the synthesis of the sacacH ligand, the product isolated is not 100 % pure (reaction equilibrium exists) with some of the starting material remaining in the final product, hence the percentage C and H in $\text{Sc}(\text{sacac})_3$ nearly matched that of $\text{Sc}(\text{acac})_3$ (see **Table 5.10**).

5.8.3.7.3 X-ray crystallography of isolated complex

The crystal and molecular structure of the newly synthesized and isolated product was determined with single crystal X-ray diffraction. **Table 5.29** presents the crystal data obtained for this complex and from the results (empirical formula and molar mass) it can clearly be seen that the product was actually $\text{Sc}(\text{acac})_3$. The crystal structure is shown in **Figure 5.25** and the crystal packing along the a-axis is shown in **Figure 5.26**. The compound crystallises in the orthorhombic space group $Pbca$, with cell constants $a = 13.535$ (3), $b = 15.292$ (3), $c = 16.576$ (3) Å and all angles equal to 90 °. The results obtained are in agreement with the literature where the compound prepared crystallised in the space group $Pbca$, with cell constants $a = 13.73$ (3), $b = 15.38$ (3), $c = 16.72$ (4) Å.¹⁷³ Refinement of the data gave a final R_{int} factor of 0.0389 % for 3889 significant reflections. The coordination environment about the scandium ion is a distorted octahedron and is surrounded by 3 acac⁻ anions. The scandium-oxygen bond lengths range from 2.0598 - 2.1654 Å (**Table 5.43**).

¹⁷³ Anderson T.J., Neuman M.A. and Melson G.A., Coordination chemistry of scandium. V. Crystal and molecular structure of tris(acetylacetonato)scandium(III), **Inorganic Chemistry**, Volume 12, No. 4, pp. 927 – 930, (1973)

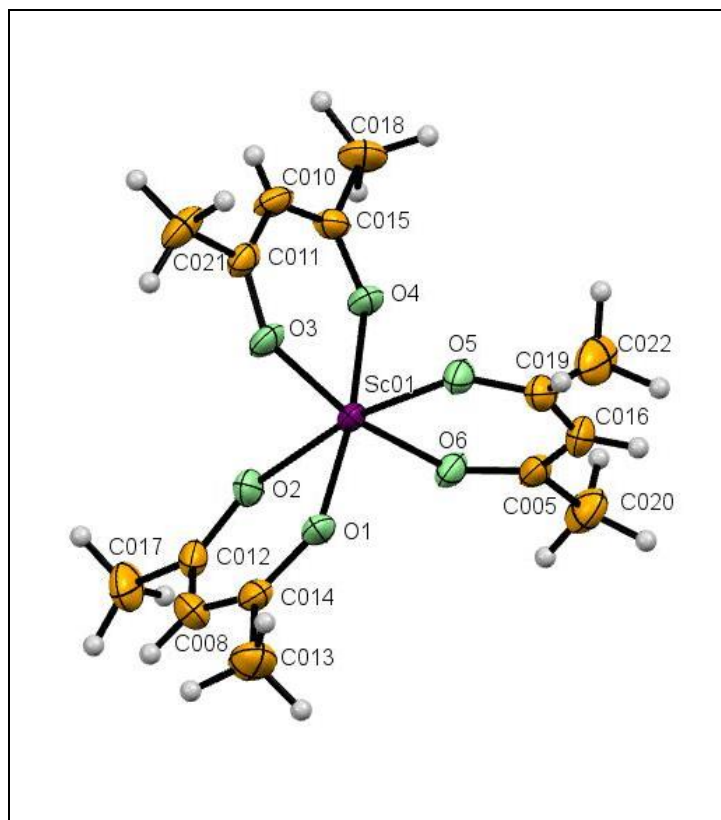


Figure 5.25: The crystal structure of Sc(acac)₃

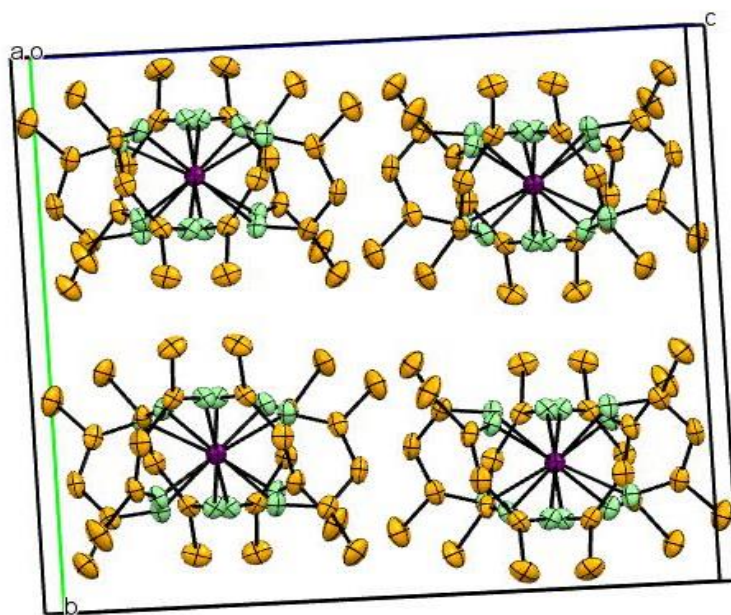


Figure 5.26: Packed unit cell of Sc(acac)₃ along the a-axis

A summary of the general crystal data of $\text{Sc}(\text{acac})_3$ is given in **Table 5.29**. Selected bond distances and bond angles are reported in **Table 5.48**.

Table 5.48: Selected bond distances and angles for $\text{Sc}(\text{acac})_3$ and those of other complexes in the literature.

Bond	Distance (Å)			Bond	Distance (Å)		
	Sc ^a	Al _{0.09} Cr _{0.91} ^b	Al ^c		Sc ^a	Al _{0.09} Cr _{0.91} ^b	Al ^c
O1-M	2.165(13)	1.948(3)	1.876(10)	O4-M	2.093(12)	1.944(3)	1.885(10)
O2-M	2.118(13)	1.951(3)	1.882(10)	O5-M	2.081(12)	1.935(3)	1.887(10)
O3-M	2.059(13)	1.957(3)	1.885(10)	O6-M	2.082(13)	1.948(3)	1.891(10)
Bond angle	Angle (°)			Bond angle	Angle (°)		
	Sc ^a	Al _{0.09} Cr _{0.91} ^b	Al ^c		Sc ^a	Al _{0.09} Cr _{0.91} ^b	Al ^c
O3-M-O5	82.24(5)	91.3(1)	91.82(4)	O6-M-O2	84.87(5)	89.3(1)	91.21(4)
O3-M-O6	168.81(5)	177.7(1)	177.9(5)	O4-M-O2	93.53(5)	90.4(1)	89.00(4)
O5-M-O6	92.21(5)	90.1(1)	90.40(4)	O3-M-O1	80.50(5)	89.3(1)	88.33(5)
O3-M-O4	92.77(5)	88.9(1)	88.85(5)	O5-M-O1	85.86(5)	90.5(1)	90.03(4)
O5-M-O4	97.14(5)	89.9(1)	91.00(5)	O6-M-O1	108.90(5)	91.2(1)	91.44(4)
O6-M-O4	78.22(5)	89.8(1)	88.13(4)	O4-M-O1	172.23(5)	179.4(1)	179.55(5)
O3-M-O2	102.47(5)	89.4(1)	90.22(4)	O2-M-O1	84.23(5)	90.9(1)	89.64(5)
O5-M-O2	168.14(5)	178.6(1)	178.5(4)				

^a - $\text{Sc}(\text{acac})_3$ synthesized in this study.

^b - The end members and seven isotopic members of the series $\text{Al}_{1-x}\text{Cr}_x(\text{acac})_3$, with x varying from 0.02 to 0.91 were prepared by dissolving appropriate amounts of $\text{Al}(\text{acac})_3$ and $\text{Cr}(\text{acac})_3$ (ca. 2.0 g total) in acetone (ca. 30 mL) and heated slightly. Crystals suitable for X-ray crystallography were formed upon cooling (25 °C) overnight. Reported here, are the results for $x = 0.91$.¹⁷⁴

^c - $\text{Al}(\text{acac})_3$ prepared Shirodker *et al.*¹⁷⁵

The isolation of the acac instead of the sacac complex is significant from a Sc isolation point of view. The +3 oxidation state of Sc is regarded as a high oxidation state and would preferably coordinate with hard bases (strong σ and π coordination) as highlighted by the large amount of oxygen related compounds known or isolated for Sc. The substitution of the oxygen by a sulphur change the acac from a hard base

¹⁷⁴ Bott S.G., Fahlman B.D., Pierson M.L. and Barron A.R., An accuracy assessment of the refinement of partial metal disorder in solid solutions of $\text{Al}(\text{acac})_3$ and $\text{Cr}(\text{acac})_3$, **Journal of chemical society, Dalton trans.**, pp. 2148 – 2152, (2001)

¹⁷⁵ Shirodker M., Borker V., Nather C, Bensch W and Rane K.S., Synthesis and structure of tris (acetylacetonato) aluminium(III), **Indian Journal of Chemistry**, Volume 49, pp. 1607 – 1611, (2010)

ligand to a borderline or soft base ligand¹⁷⁶ and this change is enough for the Sc^{3+} to selectively react with the small amount of acac that remained in solution (sacac ligand mixture). Isolation or separation of Sc from other elements in solution may be directed or controlled along this line of thinking in future.

5.8.3.7.4 Quantification of Sc in $\text{Sc}(\text{sacac})_3$

The Sc recovery in $\text{Sc}(\text{acac})_3$ (isolated product instead of $\text{Sc}(\text{sacac})_3$) after open-beaker dissolution method with H_2SO_4 is reported in **Table 5.30**. The results indicated the good recovery of Sc of 99.3 % with RSD value of 0.81 %.

5.8.4 Columbite and Ta/Nb residue or tailings processing

The overarching aim of this study is to isolate Sc as minor element from a complex elemental matrix such as columbite. The mineral sample as well as the Ta/Nb residue or tailings were sources from a niobium processing plant in Brazil. The original dark coloured sample, Sample A (**Figure 5.15**) was processed, most probably with HF or a mixture of HF and other acids and the majority of Nb and Ta was removed, leaving the light coloured residue or tailings, Sample B, behind (see **Figure 5.27**).

The chemical analysis (**Table 5.31**) of two typical samples from this plant indicates that about 90 % of the Nb_2O_5 , Ta_2O_5 , TiO_2 and Mn_3O_4 are removed from the original columbite ore. The remaining elements present in the columbite tailings is Fe_2O_3 as major element (39.03 %), Al_2O_3 (4.91 %), Nb_2O_5 (3.89 %) and smaller amounts of ZrO_2 (1.38%), Ta_2O_5 (0.35 %), TiO_2 (1.58 %) and notably Sc_2O_3 (0.795 %). It is clear that the original extraction process does not remove any Sc from the mineral and that the Sc content is concentrated from 0.135 to 0.795 %.

¹⁷⁶ Hard and soft acids and bases, [Accessed 29-11-2015]. Available from:

http://chemwiki.ucdavis.edu/Inorganic_Chemistry/Coordination_Chemistry/Hard_and_Soft_Acids_and_Bases

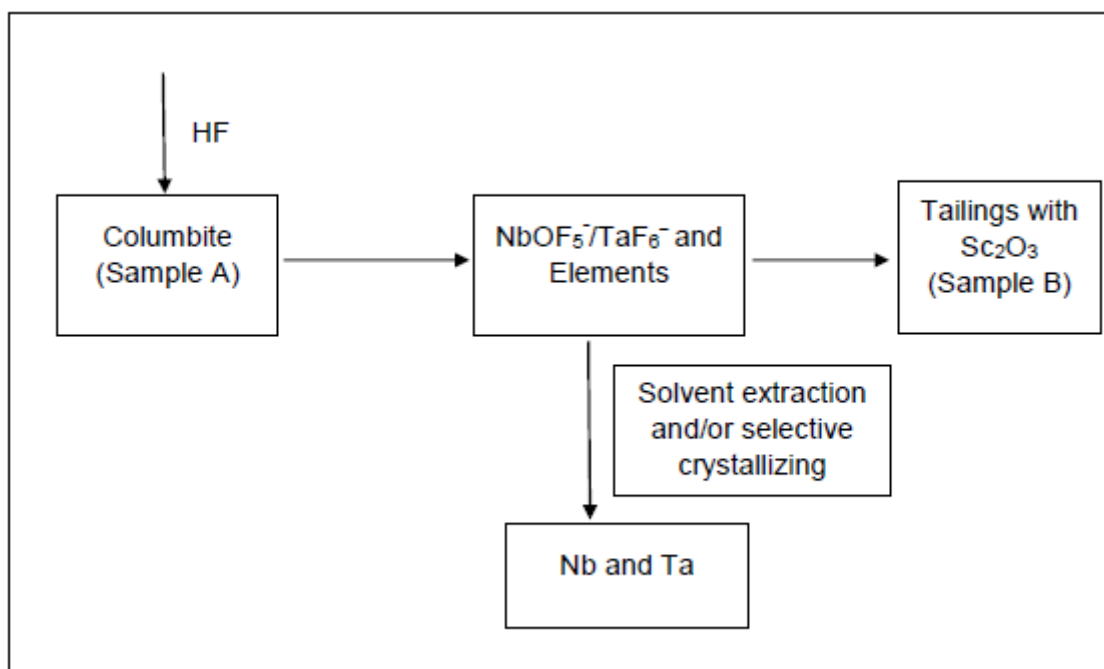


Figure 5.27: Columbite (sample A) processing

Two possible ways exist to try and isolate Sc from either or both the two samples (A and B). The most ideal process should involve the selective isolation of Sc in the presence of all these different elements in one or two steps. For this to happen, a reagent or process is needed to discriminate between Sc and the rest of the elements and either by precipitation, selective crystallisation, solvent extraction or ion exchange (to name a few) remove it from the reaction mixture. However, Sc has also been classified as a rare earth element which put the element in a bracket with 16 other elements which have very similar chemical properties and hence, difficult to separate.

The second possibility is to try a selectively method to remove the major elements in solution by the careful manipulation/application of its unique chemical properties and remove it from solution to leave Sc as the only or one of a few elements in solution.

The second option was followed in this part of the study with the possible removal of Fe via magnetic separation (as major impurity in both samples and the removal of Ta and Nb via processes previously identified and evaluated.⁶⁹

The first step in the current process is to evaluate flux fusion with $\text{NH}_4\text{F}\cdot\text{HF}$ as dissolution agent, then the evaluation of the magnetic removal of Fe from both samples and finally the evaluation of Ta and Nb removal with solvent extraction. Sc was chemically followed in each step to evaluate its loss or movement through the different separation steps.

5.8.4.1 Dissolution of columbite and the Ta/Nb residue

5.8.4.1.1 Dissolution of columbite mineral and Ta/Nb residue samples using the $\text{NH}_4\text{F}\cdot\text{HF}$ fusion method

The columbite mineral (Sample A) was dissolved by flux fusion with $\text{NH}_4\text{F}\cdot\text{HF}$ and the melt easily dissolved in water. Incomplete dissolution (visual inspection indicated small amounts of solid remaining in solution) of the mineral sample was obtained with the initial conditions used. The analytical results obtained with ICP-OES were compared to the concentrations of the metal ions in **Table 5.31** to evaluate the extent of dissolution. About 83 % of the Nb_2O_5 , 89 % of the Fe_2O_3 and 91 % of the TiO_2 (dominating elements in the sample) (**Table 5.33**) were recovered. Only about 49 % of the Sc_2O_3 (the element of interest) was recovered. The analytical results for Al and Si indicated quantities which were much higher than expected. It was decided to investigate various experimental parameters such as sample to flux ratio and the fusion time to try and optimise this digestion method to effect the complete dissolution and total elemental recoveries, especially Sc.

5.8.4.1.2 Influence of sample:flux ratio and the fusion time on dissolution of columbite ore

The next part of the study involved the investigation of the effect of sample:flux ratio and the digestion time on the dissolution of the columbite mineral. The results obtained (**Table 5.34**) in this study showed that the 60 min digestion time at a sample:flux ratio of 1:10 is sufficient for dissolution of the main elements in the columbite mineral as indicated by recoveries of 96.30 % Nb_2O_5 , 99.12 % Fe_2O_3 and 99.26 % Sc_2O_3 . It was decided to use these experimental conditions for the evaluation of the study.

5.8.4.1.3 Application of the optimum conditions for the dissolution of Samples A and B

The results obtained in **Sections 5.7.2.1** and **5.7.2.2** for the dissolution of the columbite mineral indicated that a 60 min digestion time with a 1:10 ratio (sample:flux) at 200 °C is the optimum condition using $\text{NH}_4\text{F}\cdot\text{HF}$ as flux. The recoveries of 96(3) % Nb_2O_5 , 97.9(9) % Fe_2O_3 , 97.3(2) % TiO_2 , 103.70(1) % Sc_2O_3 and 102.2(2) % Ta_2O_5 were obtained from the dissolution of Sample A while 90.23(6) % Nb_2O_5 , 85(2) % Fe_2O_3 and 64.15(2) % Sc_2O_3 were recovered for Sample B (see **Table 5.35**). Most of the other elements were inaccurate (using **Table 5.31** as reference). The good recoveries obtained for the main elements in Sample B were regarded as sufficient to continue with the rest of the magnetic separation and solvent extraction studies.

5.8.4.2 Magnetic separation of magnetic materials

From the elemental composition of the samples (A and B) in **Table 5.31**, Sample B would be expected to be magnetically more active with its major Fe content compared to Sample A. The magnetism in these samples were quantified in this study by the determination of the mass magnetic susceptibility (χ_g) of these samples. The results (**Table 5.36**) indicated that Sample A contains a much higher amount of magnetic (magnetic susceptibility χ_g is large) particles than Sample B, hence there were some difficulties when separating the Fe in Sample B. These results are surprising since the Fe content increases from 28.86 % in Sample A to about 40 % in Sample B and yet its magnetic susceptibility decreased by a factor 100. In practice it implies that the chemical treatment of the original columbite ore also changes the type of Fe compound in the final tailings which render it less ferromagnetic (change in oxidation state possibly). This was underlined by the results presented in **Figures 5.17** and **5.18** which indicate that poor separation or removal of the Fe from both samples were achieved, while the rest of the other elements are present in more or less 50/50 quantities in both portions. The magnetic susceptibility in this columbite and tailings samples is much lower than the values obtained for the tantalite samples which were investigated by Nete.⁶⁹ The two tantalite samples had magnetic susceptibility values of 2.8 and 29.3 x 10⁻⁶ cm³g⁻¹ compared to the 1.3 x 10⁻⁶ cm³g⁻¹ of the original columbite ore sample. Magnetic separation of Fe was successfully

applied to tantalite samples with the high susceptibility values, while poor separation was also obtained for the tantalite sample with low susceptibility value. The experimental results for the magnetic separation not only indicated the unsuccessful removal of Fe from the samples, but also indicated a substantial loss of Sc (**Tables 5.38 and 5.39**). The results indicated that 40.00 % of Sc_2O_3 in Sample A was lost and 45.01 % Sc_2O_3 was lost in Sample B after the magnetic separation process.

5.8.4.3 Solvent extraction of tantalum in Sample A with MIBK as solvent

MIBK was used as solvent extractant for Sample A at different H_2SO_4 concentrations ranging from 2.0 M to 8.0 M. The results obtained (**Table 5.40**) from this part of the study confirmed that the digestion of the columbite using $\text{NH}_4\text{F}\cdot\text{HF}$ as a flux produced a chemical compound which is suitable for selective Ta extraction from the dissolved mineral matrix (see also **Figures 5.19 and 5.20**). The analytical results showed that 92.84 % of the Ta was recovered from the organic portion while 4.88 Nb and 4.99 % Fe were also extracted into the organic portion. The results also indicated that the majority of Sc (≈ 100 %) remained in the aqueous solution which favors possible beneficiation of Sc. Poor extraction of the other elements (see **Figure 5.20**) also confirmed the possible isolation of a Ta compound from the columbite matrix.

The extent of extraction of each metal in a columbite mineral sample by MIBK as solvent at 8 M H_2SO_4 was determined by calculating its extraction ratio (D), which was calculated as the ratio of concentration of the solute in the organic phase and in the aqueous phase using **Equation 4.5**. The results are presented in **Table 5.49**. It can be noted that the extraction ratio (D) of Ta greatly exceeds that of all other elements in solution.

Table 5.49: Distribution ratios for elements present in columbite mineral after extraction with MIBK solvent at 8.0 M H₂SO₄

Metal	Extraction ratio (D)
Nb	0.058
Fe	0.046
Ti	0.036
Mn	0.084
Sn	0.272
U	–
Th	–
W	0.075
Ta	4.808
Zr	0.395
Y	0.605
Sc	0.000

5.8.4.4 Solvent extraction of tantalum and niobium in the non-magnetic portion of Sample A with MIBK

From **Section 5.7.5** it was clear that Ta can be selectively removed and isolated from the columbite sample by solvent extraction using MIBK as solvent at H₂SO₄ ~ 8 M. It was decided to apply the same process step in the non-magnetic portion of Sample A. In this solvent extraction step it is clear that Ta also successfully extracted from the Sample A solution using MIBK. The results presented in **Tables 5.41** and **5.42** clearly indicate that an increase in [H₂SO₄] also increases the extent of Nb extraction into MIBK (**Figure 5.21**) as 23.31 % Nb was extracted at 16 M H₂SO₄. However, 53.33 % of Sc is also extracted into the organic solvent and this is a large amount of Sc that has been lost. Increasing [H₂SO₄] may be good for Nb extraction but not so good for the Sc beneficiation process.

5.8.4.5 Evaluation of different extractants on the metal separation process

Two more organic solvents (octan-1-ol and MIAK) were also evaluated for their ability to extract Ta and Nb collectively from the columbite mineral. The results obtained from this study indicated that octan-1-ol behaves like MIBK, at low [H₂SO₄] only Ta is extracted into the organic phase and at high [H₂SO₄] Nb also tends to be extracted with Ta into the organic solvent. About 52.75 % Nb (**Figure 5.22**) is extracted with

octan-1-ol at $[\text{H}_2\text{SO}_4]$ of 16 M but again about 53.33 % of Sc is also extracted into the organic solvent (**Tables 5.43** and **5.44**). On the other hand, MIAK only extracts Ta selectively even at high acid concentrations. An average of 100.4 % Ta was extracted with MIAK and only 2.77 % Nb was extracted at 16 M H_2SO_4 (**Table 5.45**). There is no notable amount of Sc that was extracted into the organic solvent with the MIAK process. In terms of selectivity towards the Sc isolation, the MIBK process was selected to be used to extract small contents of Nb and Ta in the non-magnetic portion of Sample B.

5.8.4.6 Solvent extraction of Ta and Nb in the non-magnetic portion of Sample B with MIBK

The results in **Table 5.46** clearly indicated that tantalum and niobium can be successfully extracted from the $\text{NH}_4\text{F}\cdot\text{HF}$ solution of the non-magnetic portion of Sample B from **Section 5.7.4.3** with MIBK at 8M H_2SO_4 . An average of 97.67 % Nb and 91.30 % Ta were extracted while 95.86 % Sc was recovered from the aqueous solution. The results indicate the successful extraction of both Nb and Ta in Sample B. However there is still a large amount of Fe in the solution that needs to be removed prior to the extraction of Sc from the sample.

5.9 Conclusion

Excellent results (99.0 % +) were obtained for the scandium quantification in inorganic samples, namely scandium chloride and scandium oxide. Quantitative determination of scandium from the newly synthesized organometallic complexes revealed overall good scandium recovery in most samples, except for the $\text{Sc}(\text{hfac})_3$ complex. The low recovery of scandium in $\text{Sc}(\text{hfac})_3$ can most probably be attributed to impure product synthesis or an incorrect formula. Most samples investigated were dissolved by the open-beaker dissolution method prior to analyses and only Sc_2O_3 , $\text{Sc}(\text{tfac})_3$, $\text{Sc}(\text{btfac})_3$ and $\text{Sc}(\text{dbm})_3$ compounds were dissolved with the microwave dissolution method which improved the Sc recoveries.

Characterisation of synthesized organometallic complexes with IR was used to confirm the coordination of the different bidentate ligands to the Sc metal center. Elemental analyses using the CHNS-micro element analyzer also played an important role in identifying the newly synthesized complexes. However, in some complexes such as $\text{Sc}(\text{hfac})_3$ and $\text{Sc}(\text{dbm})_3$, less than satisfactory results were obtained and this can be attributed to impure products and unreacted starting material as was the case with the sacac complex which was correctly characterised with X-ray crystallography to be the $\text{Sc}(\text{acac})_3$ complex.

Interesting results were obtained for the columbite ore and the Ta/Nb residue samples with the newly developed dissolution method which corresponded well with that obtained for columbite by other researchers. The magnetic separation of both samples, Sample A and Sample B was not very successful in removing the majority of the Fe from the solid samples, possibly due to low ferromagnetic properties of the Fe in both samples. The same procedure confirmed that a large amount of Sc is removed in this step. Solvent extraction was very successful to isolate and remove Ta from the reaction mixture and that a small amount of Sc is lost when the $[\text{H}_2\text{SO}_4]$ was increased to extract Nb in Sample A using MIBK. The two other extractants were also successful to remove Ta from the solution, however they also extracted Sc in the same process. A summary of the degree of the success achieved with the Sc isolation process is given in **Table 5.50**.

Table 5.50: Evaluation of various steps involved in the Sc beneficiation process investigated in this study

Process	Evaluated by looking at:	Evaluation
Dissolution of the mineral samples by $\text{NH}_4\text{F}\cdot\text{HF}$	Complete dissolution of the samples	90 – 95 %
	Complete recovery of Sc	√√
Magnetic Separation	Removal of Fe and/or Ti without losing Sc	××
Solvent Extraction	Removal of Ta without losing Sc with MIBK	√
	Removal of Nb without losing Sc with MIAK/Octanol	××

√√- Successful to above 95%

√- Successful to about 90%, ××- Not successful

5.10 Method validation

5.10.1 Introduction

The final step in the analytical method development is method validation which is used to confirm whether the newly developed analytical procedures employed in this study were suitable for the scandium determination. The validation of the methods that were developed to determine Sc in inorganic compounds and in the synthesized organometallic compounds will be discussed in the following sections. Method validation is essential for any analytical laboratory and forms part of quality assurance which makes sure that analytical results from laboratories are of a high standard. Organisations such as the International Organisation for Standards (ISO) have sets of standards by which the quality of results are judged and the widely applied standard in chemical analytical laboratories is the so-called ISO 17025 standard. The validation results will be used to determine the quality and the reliability of the developed method. As discussed in **Chapter 4**, method validation can be performed by evaluating certain parameters such as precision, accuracy, range, linearity, specificity, limit of detection and limit of quantitation which will be evaluated for each scandium analysis performed in this study and these parameters will be evaluated in this section.

Statistical tests will also be used to determine whether the experimental results obtained should be accepted or rejected at 95 % confidence interval using hypothesis testing criteria. One of these statistical values is called the student t-test. The t-value determines if an experimentally obtained value is in fact the same, or different, as the true or accepted value. This is done using the null hypothesis which either states that the obtained results are equal to the accepted value or not, *i.e.* $H_0: \bar{x} = \mu_0$ or alternative hypothesis $H_a: \bar{x} \neq \mu_0$. The formula for the statistical t-test is given in **Equation 5.2**.

$$t = \frac{\bar{x} - \mu_0}{s/\sqrt{N}} \quad 5.2$$

where \bar{x} is the experimental mean, s is the standard deviation of the set of results, μ_0 is the true/accepted value and N is the number of replicates. The calculated t -value is then compared to theoretically t_{crit} values tabulated according to confidence intervals and the degrees of freedom. If the t -value falls within the range ($- t_{crit} < t < t_{crit}$), the alternative hypothesis is accepted while t -values that fall outside this range are statistically not considered to be accurate.

Table 5.51: Validation of Sc determination in ScCl₃·H₂O

Validation Criteria	Parameter	Value
Recovery	Mean % (s)	99.71(8)
Precision	RSD (%)	0.075
Working Range	Calibration curve	0.5 – 10 ppm
Linearity	R ²	0.9997
Sensitivity	Slope	14.751
Selectivity	s _m	0.1408
Error of the Slope	y-intercept	0.6393
Specificity	s _c	0.7185
t _{crit} at 95 % confidence interval		4.30
t-value		-0.3025
Decision		Accepted

s_m – Standard deviation of the slope

s_c - Standard deviation of the y-intercept

Table 5.52: Validation of Sc determination in Sc₂O₃ dissolved by open-beaker digestion with different acids

Validation Criteria	Parameter	HNO ₃	HCl	H ₂ SO ₄
Recovery	Mean % (s)	99.2(4)	98.9(3)	44.7(7)
Precision	RSD (%)	0.43	0.25	1.46
Working Range	Calibration curve	0.5 – 10 ppm	0.5 – 10 ppm	0.5 – 10 ppm
Linearity	R ²	0.9963	1.0000	0.9998
Sensitivity	Slope	8.6184	9.8852	14.6917
Selectivity	s _m	0.3019	0.0361	0.1312
Error of the Slope	y-intercept	2.0618	0.1907	0.9766
Specificity	s _c	1.5408	0.1841	0.6695
t _{crit} at 95 % confidence interval	4.30			
t-value		-0.2224	-0.4974	-9.7973
Decision		Accepted	Accepted	Rejected

s_m – Standard deviation of the slope

s_c - Standard deviation of the y-intercept

Table 5.53: Validation of Sc determination in Sc₂O₃ dissolved by microwave digestion with different acids

Validation Criteria	Parameter	HNO ₃	HCl	H ₂ SO ₄
Recovery	Mean % (s)	99.8(3)	100.1(3)	101(1)
Precision	RSD (%)	0.32	0.27	1.16
Working Range	Calibration curve	0.5 – 10 ppm	0.5 – 10 ppm	0.5 – 10 ppm
Linearity	R ²	0.9963	1.0000	0.9998
Sensitivity	Slope	8.6184	9.8852	14.6917
Selectivity	s _m	0.3019	0.0361	0.1312
Error of the Slope	y-intercept	2.0618	0.1907	0.9766
Specificity	s _c	1.5408	0.1841	0.6695
t _{crit} at 95 % confidence interval	4.30			
t-value		-0.0309	0.0068	0.0192
Decision		Accepted	Accepted	Accepted

s_m – Standard deviation of the slope

s_c - Standard deviation of the y-intercept

Table 5.54: Validation of S_c in $S_c(\text{acac})_3$

Validation Criteria	Parameter	Value
Recovery	Mean % (s)	99.4(6)
Precision	RSD (%)	0.56
Working Range	Calibration curve	0.5 – 10 ppm
Linearity	R^2	1.0000
Sensitivity	Slope	14.3913
Selectivity	s_m	0.0547
Error of the Slope	y-intercept	-0.3507
Specificity	s_c	0.2792
t_{crit} at 95 % confidence interval	4.30	
t-value	-0.2598	
Decision	Accepted	

s_m – Standard deviation of the slope

s_c - Standard deviation of the y-intercept

Table 5.55: Validation of S_c in $S_c(\text{tfac})_3$ dissolved by open-beaker and microwave digestion

Validation Criteria	Parameter	Open-beaker digestion	Microwave digestion
Recovery	Mean % (s)	58.0(8)	96.5(6)
Precision	RSD (%)	1.45	0.57
Working Range	Calibration curve	0.5 – 10 ppm	0.5 – 10 ppm
Linearity	R^2	1.0000	1.0000
Sensitivity	Slope	20.0246	20.0246
Selectivity	s_m	0.0176	0.0176
Error of the Slope	y-intercept	0.1036	0.1036
Specificity	s_c	0.0898	0.0898
t_{crit} at 95 % confidence interval	4.30		
t-value		-7.9881	-1.0131
Decision		Rejected	Accepted

s_m – Standard deviation of the slope

s_c - Standard deviation of the y-intercept

Table 5.56: Validation of S_c in $S_c(\text{btfac})_3$ dissolved by open-beaker and microwave digestion

Validation Criteria	Parameter	Open-beaker digestion	Microwave digestion
Recovery	Mean % (s)	26.7(7)	95(3)
Precision	RSD (%)	2.56	3.38
Working Range	Calibration curve	0.5 – 10 ppm	0.5 – 10 ppm
Linearity	R ²	1.0000	1.0000
Sensitivity	Slope	20.0246	20.0246
Selectivity	s_m	0.0176	0.0176
Error of the Slope	y-intercept	0.1036	0.1036
Specificity	s_c	0.0898	0.0898
t_{crit} at 95 % confidence interval		4.30	
t-value		-7.3009	-0.1678
Decision		Rejected	Accepted

s_m – Standard deviation of the slope

s_c - Standard deviation of the y-intercept

Table 5.57: Validation of S_c in $S_c(\text{dbm})_3$ dissolved by open-beaker and microwave digestion

Validation Criteria	Parameter	Open-beaker digestion	Microwave digestion
Recovery	Mean % (s)	67(2)	95(3)
Precision	RSD (%)	2.82	2.77
Working Range	Calibration curve	0.5 – 10 ppm	0.5 – 10 ppm
Linearity	R ²	0.9998	0.9998
Sensitivity	Slope	19.7156	19.7156
Selectivity	s_m	0.1604	0.1604
Error of the Slope	y-intercept	0.8495	0.8495
Specificity	s_c	0.8189	0.8189
t_{crit} at 95 % confidence interval		4.30	
t-value		-1.7501	-0.2750
Decision		Accepted	Accepted

s_m – Standard deviation of the slope

s_c - Standard deviation of the y-intercept

Table 5.58: Validation of S_c in $S_c(\text{hfac})_3$

Validation Criteria	Parameter	Value
Recovery	Mean % (s)	80.4(4)
Precision	RSD (%)	0.44
Working Range	Calibration curve	0.5 – 10 ppm
Linearity	R^2	1.0000
Sensitivity	Slope	20.0246
Selectivity	s_m	0.0176
Error of the Slope	y-intercept	0.1036
Specificity	s_c	0.0898
t_{crit} at 95 % confidence interval		4.30
t-value		-6.6115
Decision		Rejected

s_m – Standard deviation of the slope

s_c - Standard deviation of the y-intercept

Table 5.59: Validation of S_c in $S_c(\text{sacac})_3/ S_c(\text{acac})_3$

Validation Criteria	Parameter	Value
Recovery	Mean % (s)	99.2(9)
Precision	RSD (%)	0.82
Working Range	Calibration curve	0.5 – 10 ppm
Linearity	R^2	1.0000
Sensitivity	Slope	7.7933
Selectivity	s_m	0.0803
Error of the Slope	y-intercept	-0.3030
Specificity	s_c	0.4175
t_{crit} at 95 % confidence interval		4.30
t-value		-0.0212
Decision		Accepted

s_m – Standard deviation of the slope

s_c - Standard deviation of the y-intercept

Table 5.60: Validation of Sc in columbite and in Ta/Nb residue

Validation Criteria	Parameter	Columbite ore (Sample A)	Ta/Nb residue (Sample B)
Recovery	Mean % (s)	105.98(1)	64.66(2)
Precision	RSD (%)	0.006	0.03
Working Range	Calibration curve	0.1 – 1.0 ppm	0.1 – 1.0 ppm
Linearity	R ²	0.9994	0.9994
Sensitivity	Slope	6.8113	6.8113
Selectivity	s _m	0.0933	0.0933
Error of the Slope	y-intercept	0.0724	0.0724
Specificity	s _c	0.0566	0.0566
t _{crit} at 95 % confidence interval		4.30	
t-value		0.8660	-24.6817
Decision		Accepted	Rejected

s_m – Standard deviation of the slope

s_c - Standard deviation of the y-intercept

5.10.2 Conclusion

The method validation done above was considered satisfactory. All calibration curves showed good linearity as can be seen from the excellent R²-values. Precision and accuracy were considered to be relatively good, but still left some room for improvement. Many of the developed methods of which the null hypothesis was rejected, was because of incomplete dissolution and the rejection of the hypotheses was expected. The results obtained by the methods of which the null hypothesis was accepted, are regarded as true and accurate because of the thorough method validation process.

6 Evaluation of the study and future research

6.1 Introduction

The aim of this chapter is to evaluate the achievements of this study against the aims/objectives that were set out in the beginning of the study in **Chapter 1** and also to identify possible future research projects that may complement the study.

6.2 Degree of success with regard to the set objectives

The objectives as it was outlined in **Chapter 1, Section 1.3** were to:

- Perform an in-depth literature study of the analytical techniques used in the analysis of scandium compounds
- Develop an analytical procedure that can accurately determine and quantify scandium in synthetic scandium containing matrices.
- Find an alternative, but effective dissolution method for columbite-tantalite mineral ore and the residue that is friendlier to the environment.
- Develop a method to recover scandium from low grade mineral ores (columbite-tantalite in this case) and residues.
- Study the coordination behaviour of O-O'/O-S bidentate ligands for the possible selective separation of scandium from low grade ores and residues.
- Characterisation of the scandium compounds using different analytical techniques such as ICP-OES, IR and CHNS-micro analysis.
- Validation of the above mentioned methods in accordance with the criteria of the International Standards Organisation (ISO 17025).

In terms of the above-mentioned objectives of this study it has been successful concluding from the previous chapters. The literature study revealed that few methods to analyze scandium exist but mostly old techniques such as

spectrophotometric techniques which are tedious and unable to analyze scandium in complex matrices. Most other techniques for analyzing scandium necessitate the need for pre-concentration of Sc before analysis in natural samples like mineral ores since it exists in minute quantities in most minerals. The results obtained during this study showed that the developed methods were capable to accurately quantify scandium in commercial supplied compounds such as inorganic compounds and also in the synthesized compounds studied.

The different samples studied were successfully dissolved by a range of dissolution techniques including open-beaker dissolution, microwave-assisted dissolution (using different mineral acids) and flux fusion dissolution methods. The efficiency of the dissolution methods was accessed by analysis with the ICP-OES. Columbite mineral and Ta/Nb residue samples were successfully dissolved with the flux fusion method using $\text{NH}_4\text{F}\cdot\text{HF}$ salt which is considered more friendly-environment relative to the use of HF. In the process of recovering Sc in the low grade mineral samples (columbite and Ta/Nb residue), magnetic separation and solvent extraction were used in the beneficiation process of Sc. Both these processes were somehow unsuccessful as a loss of Sc was observed during the beneficiation process.

The coordination behaviour of O-O'/S bidentate ligands with Sc was studied and it was successful. The results revealed the successful preparation of organometallic compounds and their characterisation proved to be feasible for the possible selective separation of scandium from low grade ores and residues although the pre-concentration of Sc is required first. Characterisation of all the scandium compounds studied was successful as the anticipated results were obtained. Validation of the methods developed revealed the remarkable performance of ICP-OES as indicated by the validation parameters in **Chapter 5, Section 5.10**. Most of the results from the inorganic and organometallic compounds were in the acceptable range of the null hypothesis tests at 95 % confidence interval.

6.3 Future research

The potential projects which could be further investigated following the current study could be:

- Synthesis of more Sc organometallic complexes using different ligands to gain understanding of the chemistry to identify unique or highly selective extraction reagents for Sc in complex matrices.
- Investigating suitable and feasible methods to extract dominating metals in the complex prior to extraction of Sc without losing any amount of Sc in the samples. Columbite-tantalite minerals contain more Nb, Ta, Fe and Ti that needs to be eliminated to pre-concentrate Sc prior to extraction with suitable agents.
- Extraction of scandium from low grade mineral ores or residues and subsequently wastes by using other techniques such as gas phase extraction by using a volatile organic reagent which passes through the feed material and reacts selectively with Sc.
- Separation of scandium from other components in low-grade ores by solvent based membrane extraction process and investigating characteristics of a membrane (porosity, selectivity, electric charge, etc.) to selective separate Sc from other components. Membrane separation process has an advantage of that it does not require heating.
- Separation of scandium in the complex matrices by electrophoresis technique.
- A comparative study on scandium quantitative analysis using other analytical techniques such as ICP-MS, AAS and UV-Vis as well as for the characterisation of the isolated products.

Summary

The main objective of this study was to develop an analytical method to accurately quantify scandium in different Sc-containing matrices including inorganic compounds, organometallic complexes and finally low grade Sc mineral ores and residues. The organometallic complexes ($\text{Sc}(\text{acac})_3$, $\text{Sc}(\text{tfac})_3$, $\text{Sc}(\text{btfac})_3$, $\text{Sc}(\text{dbm})_3$, $\text{Sc}(\text{hfac})_3$ and $\text{Sc}(\text{sacac})_3$) were synthesized and characterised using melting point, IR, CHNS-micro element analysis and X-ray crystallography techniques. The study involved the use of different mineral acids such as HNO_3 , HCl and H_2SO_4 for the dissolution of the different samples using both open-beaker and microwave-assisted dissolution techniques. Flux fusion using $\text{NH}_4\text{F}\cdot\text{HF}$ flux was used for the dissolution of columbite mineral and Ta/Nb residue samples. ICP-OES was used for quantification of Sc in all samples as well as some of the other metals in the mineral samples. The wavelengths were carefully selected to minimise any spectral interferences and the matrix matching was also ensured throughout the study for accurate measurements.

$\text{ScCl}_3\cdot\text{H}_2\text{O}$ was dissolved in water and recoveries ranging from 99.64 - 99.79 % were obtained. Open-beaker dissolution of Sc_2O_3 with HNO_3 , HCl or H_2SO_4 yielded Sc recoveries ranging from 44(7) - 99.2(4) % and these recoveries were improved with the microwave dissolution method to recoveries between 99.8(3) and 101(1) %. Excellent Sc recoveries from the most of the organometallic complexes ($\text{Sc}(\text{acac})_3$, $\text{Sc}(\text{tfac})_3$, $\text{Sc}(\text{btfac})_3$, $\text{Sc}(\text{dbm})_3$ and $\text{Sc}(\text{sacac})_3$) ranging from 95(3) - 99.4(6) % were obtained while $\text{Sc}(\text{hfac})_3$ yielded a lower than expected recovery of 80.4(4) % due to the possibility that the molar mass from the empirical formula known is incorrect or that an impure product was isolated.

Excellent results were obtained for the columbite ore and the Ta/Nb residue samples (Sample A and B respectively) after the $\text{NH}_4\text{F}\cdot\text{HF}$ fusion dissolution. In the process of the beneficiation of Sc, magnetic separation was attempted for the removal of Fe and Ti from the rest of the sample (both Sample A and Sample B) but was

considered unsatisfactory since a large portion of the Fe in the sample did not exhibit ferromagnetic properties and hence remained with the original portion (non-magnetic) of the samples. Results also indicated the loss of a relatively significant portion of Sc in both samples. Solvent extraction with MIBK was also attempted for the possible extraction of Ta and Nb and the results indicated that this process was only successful to eliminate the Ta in large quantities and that both the Ta and Nb can be extracted with MIBK at high [H₂SO₄] with relatively insignificant losses of Sc, especially from Sample B.

The experimental results for the scandium analysis were validated for a large number of validation parameters, which included accuracy, precision, sensitivity, specificity, linearity, *etc.* to confirm whether the newly developed analytical procedures were suitable for the scandium determination in terms of internationally required standards (ISO 17025). The limit of detection (LOD) and limit of quantitation (LOQ) for Sc were determined to be 0.000991 and 0.00991 ppm respectively, which is sufficient to measure trace amounts of scandium. The linearity of the calibration curves was determined from the regression coefficient (R^2) and ranged from 0.996 to 1.00. Statistical tests of the experimental results were calculated using the hypothesis test of the *t*-statistical at 95 % confidence interval (C.I) to determine whether the results were acceptable as recommended by ISO 17025.

Opsomming

Die primêre doel van hierdie studie was om 'n analitiese metode te ontwikkel om skandium akkuraat in verskillende Sc-bevattende matrikse, insluitend anorganiese verbindings, organometaalkomplekse en uiteindelik lae graad Sc minerale erts en prosesafval-materiaal te kwantifiseer. 'n Aantal organometaalkomplekse, naamlik $\text{Sc}(\text{acac})_3$, $\text{Sc}(\text{tfac})_3$, $\text{Sc}(\text{btfac})_3$, $\text{Sc}(\text{dbm})_3$, $\text{Sc}(\text{hfac})_3$ en $\text{Sc}(\text{sacac})_3$ is tydens die studie berei en met behulp van smeltpunt, IR, CHNS mikro-element analise en X-straalkristallografie tegnieke gekarakteriseer. Verder is die vertering van die verskillende monsters met behulp van beide gewone oop beker en mikrogolfvertering in die teenwoordigheid van 'n aantal HNO_3 , HCl en H_2SO_4 ondersoek. Die vertering en oplos van die kolumbiet minerale monster en die Ta/Nb prosesafval monsters is ook met gesmelte sout of vloeimiddelsmelting ondersoek en $\text{NH}_4\text{F}\cdot\text{HF}$ is hoofsaaklik as smeltmiddel gebruik. In alle gevalle is IGP-OES is vir die akkurate bepaling van die hoeveelheid Sc en ander elemente in al die anorganiese verbindings, organometaalkomplekse asook in die minerale monsters gebruik. Die golflengtes vir hierdie bepalings is sorgvuldig gekies om enige spektrale steurings te verhoed en in alle gevalle is matriksparing toegepas om die moontlike invloed van al die bygevoegde chemikalië in die Sc-bepaling uit te skakel.

Die $\text{ScCl}_3\cdot\text{H}_2\text{O}$ los maklik op in water en Sc-opbrengste wat tussen 99.64 - 99.79 % wissel, is verkry. Die natvertering van Sc_2O_3 in HNO_3 , HCl of H_2SO_4 het Sc-opbrengste wat wissel tussen 44(7) - 99.2(4) % gelewer. Die gebruik van mikrogolfvertering in die teenwoordigheid van dieselfde sure het die Sc-opbrengste tot 99.8(3) en 101(1) % verbeter. Uitstekende Sc-opbrengste is vir die meerderheid organometaalkomplekse ($\text{Sc}(\text{acac})_3$, $\text{Sc}(\text{tfac})_3$, $\text{Sc}(\text{btfac})_3$, $\text{Sc}(\text{dbm})_3$ en $\text{Sc}(\text{sacac})_3$) verkry met Sc-waardes wat tussen 95(3) en 99.4(6) % gewissel het, terwyl heelwat laer Sc-opbrengste (80.4(4) %) vir $\text{Sc}(\text{hfac})_3$ verkry is. Moontlike redes vir hierdie laer opbrengste kan moontlik aan die gebruik van 'n verkeerdelike molêre massa of empiriese formule of dat 'n onsuivere produk geïsoleer is, toegeskryf word.

Die magnetiese skeiding van Fe en Ti in beide die kolumbiet erts en die Ta/Nb prosesafval-materiaal was onbevredigend met 'n groot hoeveelheid van die yster wat in die nie-magnetiese gedeelte agtergebly het asook betekenisvolle Sc-hoeveelhede wat in die magnetiese gedeelte verlore geraak het. Uitstekende Sc-resultate is na die $\text{NH}_4\text{F}\cdot\text{HF}$ vloeimiddelsmelting vertering vir die beide die kolumbiet erts en die Ta/Nb prosesafval-materiaal verkry. Resultate het ook die verlies van 'n relatief beduidende gedeelte van Sc in beide monsters aangedui. Die skeiding van Ta en Nb in beide die kolumbiet erts en die Ta/Nb prosesafval-materiaal met behulp van MIBK oplosmiddel-ekstraksie ondersoek. Die resultate het aangedui dat hierdie proses suksesvol is om al die Ta in beide monsters te verwyder, met relatief onbeduidende verliese van Sc.

Die eksperimentele resultate vir die Sc- analise is vir 'n groot aantal valideringsparameters volgens ISO 17025 kriteria, wat onder andere akkuraatheid, presisie, sensitiwiteit, spesifisiteit, lineariteit ens. insluit, geëvalueer. Die beperking/grens van die opsporing (LOD) en laagste vlak van kwantifisering (LOQ) vir Sc was 0.000991 en 0.00991 dpm onderskeidelik bepaal. Die lineariteit van al die kalibrasie kurwes (regressie-koëffisiënt, R^2) het tussen 0.996 - 1.00. gevarieer. Verdere statistiese toetse vir al die eksperimentele resultate is met behulp van 'n hipotese toets (t -toets met 'n op 95 % betroubaarheidsinterval) geëvalueer.